CHARACTERIZATION OF CETA AND CETB, ENERGY TAXIS REGULATORS IN *CAMPYLOBACTER JEJUNI*

by

Kathryn T. Young

A dissertation submitted in partial fulfillment
of the requirements for the degree of
Doctor of Philosophy
(Microbiology and Immunology)
in The University of Michigan
2008

Doctoral Committee:

Professor Victor J. DiRita, Chair
Professor N. Cary Engleberg
Professor Robert S. Fuller
Associate Professor Philip C. Hanna
Assistant Professor Melody N. Neely, Wayne State University

To Mom, Dad, Drew and Valerie.
With thanks for your unwavering love
and support. Without you, I would
never have made it here.

ACKNOWLEDGEMENTS

I would like to thank my parents for their love and encouragement. They have always believed in me and supported me in my goals in every way that they could. I can never thank them enough for all they have done to help me achieve my dreams. I would also like to thank my fiancé Drew. I couldn't have asked for a more supportive, caring, considerate partner in life. He has helped me to laugh when I wanted to cry, to keep going when I wasn't sure I could, to achieve what so often seemed elusive. His patience has been limitless. His presence makes each day brighter.

I would also like to express my deep gratitude to my thesis advisor Vic DiRita. Vic has guided my scientific development with great care. He has taught me a tremendous amount about experimental design, data analysis and scientific communication. He provided guidance when I needed it and left me to my own devices when I needed to solve problems myself. He has also been a role model for balancing career and family. He quite obviously cares for the people in his lab on a personal level, which makes his lab a very positive place to study. I am extremely thankful to him for all he has done to promote my scientific and personal growth.

I would like to thank my committee: Cary Engleberg, Bob Fuller, Phil Hanna and Melody Neely. They have provided invaluable suggestions and advice throughout my graduate career. I am grateful to all of them for my making my committee meetings so positive, encouraging and fruitful.

I want to particularly thank David Friedman and Eric Krukonis. Our labs have had joint lab meetings for many years and their insights have always been helpful. David in particular has made a point of asking after my progress whenever I see him. He always knows what experiments are in progress and is ready with suggestions and advice.

I have to thank all of the current and former members of the DiRita lab for providing such a fun place to work every day and for always being willing to teach me a technique, help me troubleshoot or brainstorm. I am particularly indebted to Dave Hendrixson who developed most of the tools we use to work with Campy. Dave initially identified CetA and CetB and was always willing to help as I got my thesis project up and running. Even now that he's left the lab, he's been a continued resource for me. He is also a great friend. Becky Erfurt and George Fogg were also instrumental in teaching me the ways of Campy. Becky was a joy to work with in the back lab and I still miss working with her. Jyl Matson has been a true friend in the lab, always ready to commiserate or encourage and I can't imagine the last few years without her. Lindsay Davis joined Team Campy and the back lab when Becky graduated and has made sure I laugh every day since. I would also like to thank Jeff Withey, Eric Krukonis, Aimee Richard, Nancy Beck, Tsutomu Kakuda, Luz Blanco, Jian-guo Zhu, Kerrie Notman, Kara Levinson, and Becca Anthouard.

I have been blessed with many good friends during graduate school: Valerie Hardy, Kevin and Jess Holler, Becky and Rob Erfurt, Jyl Matson, Jeff Withey, Dave Hendrixson, Erin Rees, Bethany King, Beth and Dan Ernst, Jess and Ryan Tyler, Neal Hammer, Kelsey Sivick, Lindsay Davis, Aimee Richard, Eric Krukonis, George and Vanessa Fogg, Karen Beeri, Helen Lau, Malinda Schaefer, Lee Shaughnessy, Toby

Rodriguez, Andrew Bryan and Nancy Beck. I thank each of you for your friendship and for dragging me out of lab every once in a while and insisting that I have a good time. I want to particularly thank Valerie for her love and friendship. I miss her each and every day.

I would also like to thank several people who instilled in me a love of science and were instrumental in my path to graduate school: Jeff Elhai, Deb Wohl, David Phoebus, Ray Cho and Dennis Kim.

Acknowledgements on text and figures

I also owe thanks to several collaborators. Dave Hendrixson created several of the strains and plasmids I used in Chapters II and III. He was aided in the construction of pECO101 (Chapter II) by Erin O'Rourke. Igor Zhulin at the University of Tennessee and Oak Ridge National Laboratory identified the CetA HAMP domain and the initial members of the bipartite family in Chapter III. Jeanne Stuckey in the Life Sciences Institute created the CetA HAMP domain structural model presented in Chapter III and aided us in its interpretation. Nick Dorrell, Abdi Elmi and Ozan Gundogdu in Brendan Wren's lab at the London School of Tropical Hygiene and Medicine performed the microarray experiments in the Appendix. Andrew Bryan, a rotation student, performed the qRT-PCR analysis in the Appendix.

Finally, I would like to acknowledge that selected text and figures in Chapter I were previously published in:

Young KT, Davis LD, DiRita VJ. (2007) *Campylobacter jejuni*: molecular biology and pathogenesis. *Nature Reviews Microbiolology*. 5:665-79.

TABLE OF CONTENTS

LIST OF FIGURES

FIGURE

LIST OF TABLES

TABLE

CHAPTER I

INTRODUCTION

Campylobacter jejuni Biology

Infections and sequelae

Campylobacter jejuni is a small, Gram-negative, spiral-shaped, microaerophilic bacterium in the epsilon class of proteobacteria. *C. jejuni* is one of the most common causes of food borne gastroenteritis in the United States (Foodnet, 2007). Infection most commonly occurs by consumption of contaminated poultry products, as *C. jejuni* is found at high levels in poultry gastrointestinal tracts. *C. jejuni* can also colonize other animals with few or no symptoms and human infection can occur from other livestock, family pets, contaminated drinking water and unpasteurized milk (Fig. 1).

C. jejuni gastroenteritis is usually self-limiting and is characterized in the U.S. and other developed countries by bloody diarrhea, abdominal pain and fever (reviewed in (Blaser *et al.*, 1983)). In the developing world, however, *C. jejuni* infection usually manifests as a watery diarrhea (reviewed in (Blaser *et al.*, 1983)). *C. jejuni* infection, while usually resolving within a week, can lead to serious neurological sequelae. These include Guillain-Barré syndrome (GBS), characterized by ascending muscle weakness or paralysis, and the less common GBS variant, Miller-Fisher syndrome (MFS), characterized by weakness or paralysis of the ocular muscles (reviewed in (Yuki and Koga, 2006; Yuki, 2007b)).

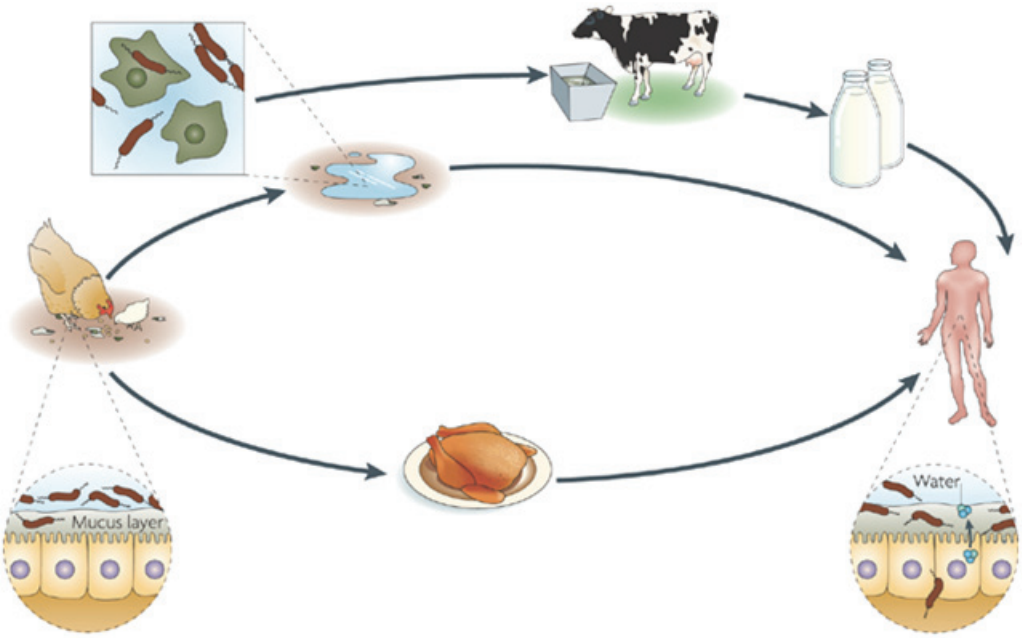

Figure 1. The sources and outcomes of *C. jejuni* infection. Several environmental reservoirs can lead to human infection by *C. jejuni*. It colonizes the chicken gastrointestinal tract in high numbers, primarily in the mucosal layer, and is passed between chicks within a flock through the fecal–oral route. *C. jejuni* can enter the water supply, where it can associate with protozoans, such as freshwater amoebae, and possibly form biofilms. *C. jejuni* can infect humans directly through the drinking water or through the consumption of contaminated animal products, such as unpasteurized milk or meat, particularly poultry. In humans, *C. jejuni* can invade the intestinal epithelial layer, resulting in inflammation and diarrhea.

Genetic and genomic tools

Despite the frequency of *C. jejuni* infection and potential for neurological sequelae, our understanding of *C. jejuni* pathogenesis lags far behind that of many other pathogens. However, the determination of the complete genome sequence of several *C. jejuni* strains and plasmids has heralded the beginning of a new era of *C. jejuni* research (Bacon *et al.*, 2002; Fouts *et al.*, 2005; Gundogdu *et al.*, 2007; Hofreuter *et al.*, 2006; Parkhill *et al.*, 2000). These projects have revealed the potential mechanisms by which *C. jejuni* associates with the host; for example, the complete sequencing of pVir, a plasmid that is found in some isolates of *C. jejuni*, has led to the identification of a type IV secretion system that has been demonstrated to have a role in cell invasion and pathogenicity in ferrets (Bacon *et al.*, 2000; Bacon *et al.*, 2002). Along with the publication of the genome sequence, progress has been spurred by the development of multiple genetic and genomic tools for use in *C. jejuni*, including microarrays, transposons for efficient random mutagenesis, signature-tagged mutagenesis, new reporter constructs and vectors for constructing in-frame deletion mutants and chromosomal point mutations (Carrillo *et al.*, 2004; Colegio *et al.*, 2001; Dorrell *et al.*, 2001; Gaynor *et al.*, 2005; Golden *et al.*, 2000; Grant *et al.*, 2005; Hendrixson *et al.*, 2001; Hendrixson and DiRita, 2003, 2004).

Genetic variation and natural transformation

C. jejuni displays extensive genetic variation, which has arisen from intragenomic mechanisms as well as genetic exchange between strains. Sequencing the genome of *C. jejuni* has revealed the presence of hypervariable sequences that consist of homopolymeric tracts (Parkhill *et al.*, 2000). Genome sequence data has also indicated

that the frequency of variation within these sequences is high, which may be partly due to the lack of clear homologues of many *E. coli* DNA-repair genes (Parkhill *et al.*, 2000). Most of the hypervariable sequences that have been found are in regions that encode proteins involved in the biosynthesis or modification of surface-accessible carbohydrate structures, such as the capsule, lipooligosaccharide (LOS) and flagellum (Parkhill *et al.*, 2000) (Fig. 2). Variation in these structures arises from mechanisms such as phase variation, gene duplication and deletion, frameshifts and point mutations (Gilbert *et al.*, 2002; Guerry *et al.*, 2002; Karlyshev *et al.*, 2002; Karlyshev *et al.*, 2005b; Linton *et al.*, 2000; Parkhill *et al.*, 2000).

C. jejuni is naturally competent, meaning that it can take up DNA from the environment. This leads to recombination between strains, which allows the generation of even more genetic diversity. The horizontal transfer of both plasmid and chromosomal DNA occurs both *in vitro* and during chick colonization, which indicates that natural transformation could have an important role in genome plasticity and in the spread of new factors such as antibiotic resistance, even in the absence of selective pressure (Avrain *et al.*, 2004; de Boer *et al.*, 2002; Wilson *et al.*, 2003). *In vitro*, *C. jejuni* displays a marked preference for DNA from *C. jejuni* strains, as opposed to DNA from other species (Wilson *et al.*, 2003). In addition, the frequency of natural transformation is affected by carbon dioxide and bacterial cell density, which indicates that horizontal exchange is probably environmentally regulated *in vivo* (Wilson *et al.*, 2003).

Transposon mutagenesis of *C. jejuni* has identified several genes that are required for natural transformation, including some components of a type II secretion system

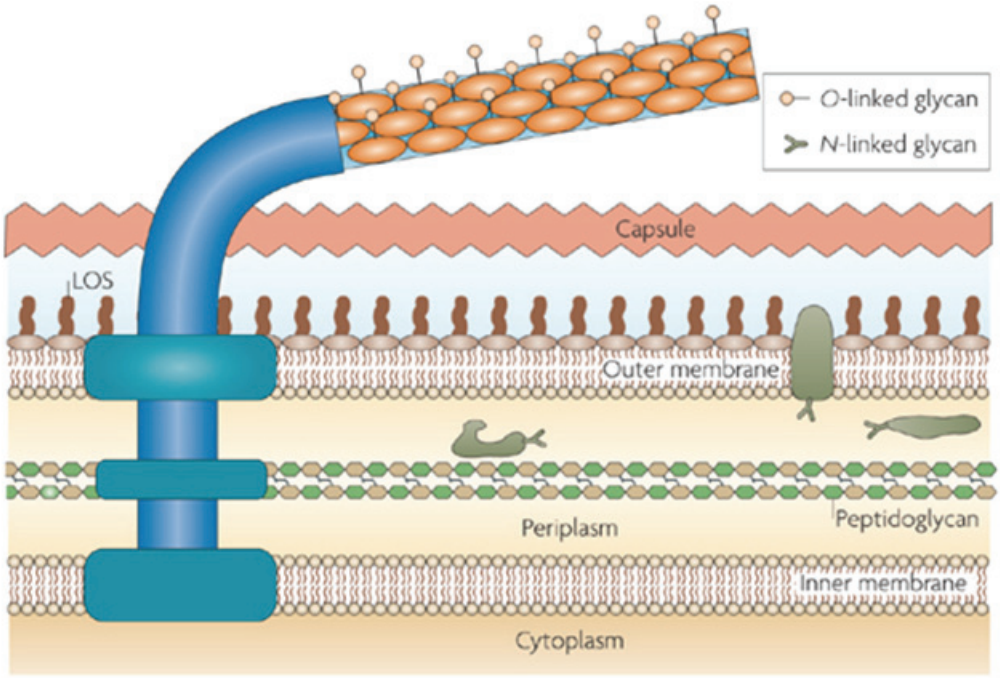

Figure 2. The *C. jejuni* glycome and surface structures. The *C. jejuni* cell surface displays several structures, including many polysaccharides, that have vital roles in *C. jejuni* biology, particularly host–bacterium interactions. The capsule, a highly variable polysaccharide, is important for virulence, epithelial cell adherence and invasion. The lipooligosaccharide (LOS) is also highly variable and has a role in serum resistance, epithelial cell adherence and invasion. LOS structures of *C. jejuni* can display molecular mimicry of neuronal gangliosides, which is linked to Guillain-Barré syndrome and Miller-Fisher syndrome. The flagellum is required for colonization, virulence and epithelial cell invasion and also acts as a secretion apparatus for invasion antigens. The flagellin is modified by *O*-linked glycosylation. This modification is required for flagellar assembly and is, therefore, important for motility, virulence and epithelial cell adherence and invasion. The *N*-linked-glycosylation system modifies some periplasmic and outer-membrane proteins. The *N*-linked glycan is also important for colonization and epithelial cell adherence and invasion, but the role of this glycan in these processes is unclear.

(Wiesner *et al.*, 2003). A candidate-gene approach to identify competence genes has implicated elements of a plasmid-encoded type IV secretion system as well as genes for *N*-linked glycosylation, LOS biosynthesis and a homologue of *H. pylori* DprA, a putative DNA-processing enzyme, as being necessary for wild-type levels of natural transformation (Bacon et al., 2000; Fry et al., 2000; Larsen et al., 2004; Takata et al., 2005). In addition, a recent search for proteins binding to a specific promoter identified the protein Cj0011c, which binds DNA non-specifically and appears to be a periplasmic DNA receptor involved in transformation (Jeon and Zhang, 2007). Mutants lacking *cj0011c*, while less competent than wildtype, retain high levels of competence compared to other transformation mutants (Jeon and Zhang, 2007). This indicates that other DNA receptors may be involved, and these may provide the specificity for *C. jejuni* DNA that it is not inherent in Cj0011c (Jeon and Zhang, 2007). However, other than the identification of these genes, no specific mechanism has yet been elucidated that explains how extracellular DNA is recognized and taken up by *C. jejuni*.

Lipooligosaccharide and capsule

Consistent with a role in immune avoidance, the LOS of *C. jejuni* is highly variable. Various *C. jejuni* LOS structures resemble human neuronal gangliosides. This molecular mimicry is thought to lead to autoimmune disorders, including GBS, a paralytic neuropathy that occurs following approximately 1 in every 1,000 cases of campylobacteriosis, and MFS, a variant of GBS (reviewed in (Hughes, 2004; Komagamine and Yuki, 2006; Nachamkin, 2002; Yuki and Koga, 2006; Yuki, 2007a, b)). The type of sequelae (GBS, MFS, or other variants), if one occurs, is determined by the particular ganglioside mimicked by the *C. jejuni* LOS (reviewed in (Yuki, 2007a, b)). In

addition, genes involved in LOS biosynthesis have been implicated in serum resistance, as well as adherence to, and the invasion of, INT 407 cells (Fry *et al.*, 2000).

Until recently, many strains of *C. jejuni* were thought to produce both LOS and a high molecular weight lipopolysaccharide (HMW LPS). In fact, the HMW LPS is now known to be a highly variable capsular polysaccharide, rather than an LPS (Karlyshev *et al.*, 2000). The structures of the capsules of several *C. jejuni* strains have been determined. The capsule structure of *C. jejuni* strain 11168 includes 6-methyl-D-glycero-α-L-glucoheptose, β-D-glucouronic acid modified with 2-amino-2-deoxyglycerol, β-D-Gal*f*NAc and β-D-ribose (St Michael *et al.*, 2002), and contains a novel modification on the Gal*f*NAc (Szymanski *et al.*, 2003). The capsule structure of *C. jejuni* strain RM1221 has also been determined and includes 6-deoxy-D-manno-heptose and D-xylose (Gilbert *et al.*, 2007), which are two sugars that are not often detected in bacterial polysaccharides. Other strains possess teichoic acid-like or hyaluronic acid-like capsules (McNally *et al.*, 2005; McNally *et al.*, 2006b). The extensive variation in the capsule structure has been attributed to multiple mechanisms that include phase variation of structural genes and an O-methyl phosphoramidate modification (Karlyshev *et al.*, 2000; Karlyshev *et al.*, 2005a; St Michael *et al.*, 2002; Szymanski *et al.*, 2003).

The *C. jejuni* capsule is important for serum resistance, the adherence and invasion of epithelial cells, chick colonization and virulence in a ferret model (Bachtiar *et al.*, 2007; Bacon *et al.*, 2001; Jones *et al.*, 2004). An historical scheme for serotyping *C. jejuni* strains is now known to be based on differences in capsule structure (Karlyshev *et al.*, 2000), which indicates that the capsular polysaccharide is accessible to the immune system and that the extensive variation in its structure probably has a key role in the

evasion of the host immune response. Additionally, the capsule might have a role beyond host colonization, such as protection against desiccation or phage infection, although these possibilities have not yet been explored.

Protein glycosylation

C. jejuni expresses two protein glycosylation systems: one modifies serine or threonine residues on flagellin (*O*-linked glycosylation) and the other modifies asparagine residues on many proteins (*N*-linked glycosylation). Prior to the discovery of the *N*-linked modification system in *C. jejuni*, *N*-linked glycosylation had been observed only in eukaryotes and archaea (Szymanski *et al.*, 1999). Mutant analysis indicates that some enzymes might be capable of functioning in both *O*-linked glycosylation or *N*-linked glycosylation pathways (Guerry *et al.*, 2007), but whether this normally occurs *in vivo* is unclear.

Proteins of the *O*-linked glycosylation system, as well as many of their biochemical functions and a hypothetical biosynthetic pathway, have been elucidated by a combination of sequence analysis, targeted mutation and chemical analysis (Chou *et al.*, 2005; Guerry *et al.*, 2006; McNally *et al.*, 2006a; Thibault *et al.*, 2001). The flagellin in *C. jejuni* strain 81-176 is glycosylated with pseudaminic acid at up to 19 sites, which accounts for approximately 10% of its observed mass (Thibault *et al.*, 2001). The flagellin of *Campylobacter coli* strain VC167 is modified with legionaminic acid, and the genes that encode the proteins that are involved in the biosynthesis of this glycan are shared by many strains of *C. jejuni* (not including strain 81-176) (McNally *et al.*, 2007). This indicates that this modification might also occur in these strains (McNally *et al.*, 2007). A specific recognition sequence for *O*-linked glycosylation has not been

identified, although the addition of the glycan is thought to require surface exposure and hydrophobicity (Thibault *et al.*, 2001). *O*-linked glycosylation of flagellin is necessary for the proper assembly of the flagellar filament (Goon *et al.*, 2003), which has led to the hypothesis that the *O*-glycan might have a role in the interactions of flagellin subunits with one another or with other elements of the flagellar apparatus. In keeping with the importance of flagella and motility to many aspects of *C. jejuni* biology, defects in *O*-linked glycosylation result in a loss of motility, a decrease in the adherence to and invasion of host cells and decreased virulence in ferrets (Guerry *et al.*, 2006). It is unknown whether *O*-linked glycosylation has any role in immune avoidance or the host-cell interaction.

Unlike other surface carbohydrate structures of *C. jejuni* (such as LOS, the capsule and the *O*-linked glycan), the *N*-linked glycan is conserved in all *C. jejuni* strains that have been examined, as well as in *C. coli* (Dorrell *et al.*, 2001; Szymanski *et al.*, 1999; Szymanski *et al.*, 2003). The conservation of *N*-linked glycosylation, compared with the variability of other surface carbohydrate traits, suggests that *N*-linked glycosylation might play a more fundamental role in the biology of *C. jejuni*. The *N*-linked glycosylation system, which is encoded by the *pgl* genes (Szymanski *et al.*, 1999), has been extensively studied since its discovery, both for a better understanding of its role in *C. jejuni* pathogenicity and for its potential importance in biotechnological applications (Glover *et al.*, 2005a; Glover *et al.*, 2005b; Glover *et al.*, 2006; Kowarik *et al.*, 2006a; Olivier *et al.*, 2006; Weerapana *et al.*, 2005). The *N*-linked glycan that is assembled by the Pgl system consists of a heptasaccharide, unlike the tetradecasaccharide that is transferred by the eukaryotic *N*-linked glycosylation machinery (Wacker *et al.*, 2002;

Young *et al.*, 2002). In contrast to the *O*-linked glycosylation system, a consensus sequence element (sequon) for *N*-linked glycosylation – D/E-X_1-N-X_2-S/T (where X_1 and X_2 can be any amino acid except proline) (Kowarik *et al.*, 2006b; Nita-Lazar *et al.*, 2005) – has been identified. The glycosylation sequon is necessary, but not sufficient, for glycosylation, which indicates that other sequences or factors, such as tertiary or quaternary structure, also have a role (Kowarik *et al.*, 2006b).

The specific effect of a sequon mutation was tested with the periplasmic protein Cj1496c (Kakuda and DiRita, 2006). A strain that lacked Cj1496c was defective for both chick colonization and adherence to INT 407 human intestinal epithelial cells *in vitro*. However, a strain that expressed a Cj1496c sequon mutant, which expressed wild-type levels of protein that could not be glycosylated, colonized chicks to levels equivalent to wildtype and was not defective for INT 407 cell association (Kakuda and DiRita, 2006). By contrast, VirB10, a competence protein that is *N*-glycosylated by the Pgl system, might require glycosylation for its function. A mutant allele that lacked one of its two functional glycosylation sequons (*virB10*N87A) was unable to complement a *virB10* mutant to wild-type levels of competence (Larsen *et al.*, 2004).

The role of *N*-linked glycosylation in the biology of *C. jejuni* is not clear. Strains with *pgl* mutations exhibit reduced adherence and invasion in the INT 407 intestinal cell line as well as defects in natural competence (Larsen *et al.*, 2004) and colonization in mouse and chick models (Hendrixson and DiRita, 2004; Kakuda and DiRita, 2006; Karlyshev *et al.*, 2004; Kelly *et al.*, 2006; Szymanski *et al.*, 2002). *N*-linked glycosylation changes the immunoreactivity of at least some glycosylated proteins (Szymanski *et al.*, 1999), which suggests that *N*-linked glycosylation might be involved

in the evasion of the immune system. However, most proteins that are modified by the Pgl system are predicted to be periplasmic, rather than surface exposed (Young *et al.*, 2002), and therefore it is unclear how modifying these proteins would enhance immune avoidance. Lectin-binding studies have identified numerous glycosylated proteins that are located mostly in the periplasm or membrane (Kowarik *et al.*, 2006b; Linton *et al.*, 2002; Nita-Lazar *et al.*, 2005; Young *et al.*, 2002), but no obvious hypothesis for the role of *N*-linked glycosylation has arisen from the knowledge of which proteins are glycosylated.

In summary, although our knowledge of these two post-translational modifications, *O*-linked and *N*-linked glycosylation, has greatly increased in recent years, there are still many gaps in our understanding. We have a good understanding of the mechanisms that are involved in *N*-linked glycosylation, but the biological function of this glycan is poorly understood. Conversely, although less is known about the mechanisms that are involved in *O*-linked glycosylation, its role in *Campylobacter* biology, particularly its importance in flagella assembly and, consequently, host-cell interactions, is better appreciated.

Secretion

The secretion mechanisms of *C. jejuni* are poorly characterized relative to those of other bacterial pathogens. *C. jejuni* secretes a protein, called CiaB, that is required for the invasion of cultured epithelial cells (Konkel *et al.*, 1999a, b). *ciaB* expression, but not secretion, is induced by exposure to the bile salt deoxycholate (Malik-Kale *et al.*, 2008), which would likely be encountered during host colonization. Mutants that lack *ciaB*

exhibit reduced chick colonization levels (Ziprin *et al.*, 2001), which implies that cell invasion might be an underappreciated factor in chick colonization.

The mechanism of CiaB secretion and its role in invasion has been likened to the model of type III secretion systems, in which effectors are injected directly into host cells (Konkel *et al.*, 1999a; Rivera-Amill *et al.*, 2001). However, *C. jejuni* does not encode a type III secretion system and evidence for the direct injection of CiaB is lacking. Rather, CiaB and other secreted Cia proteins (CiaA–H) require a functional flagellar export apparatus for their secretion (Konkel *et al.*, 2004), which is similar to the secretion of some proteins from *Yersinia* spp. (Young *et al.*, 1999). In addition to Cia proteins, the flagellar export apparatus of *C. jejuni* secretes FlaC, which is required for adherence to and invasion of HEp-2 cells and shares limited homology with the major and minor flagellins (FlaA and FlaB) (Song *et al.*, 2004). Additionally, the small protein FspA requires the flagellum for secretion (Poly *et al.*, 2007). Two variants of FspA are expressed by different *C. jejuni* strains, one of which binds INT 407 cells and induces apoptosis (Poly *et al.*, 2007). Thus, the flagellar export apparatus is an important secretion mechanism in *C. jejuni* and is required for host-cell invasion and possibly for strain-specific apoptosis affects.

Cytolethal distending toxin

C. jejuni produces cytolethal distending toxin (CDT), which is also produced by a diverse group of other bacterial species, including *E. coli*, *Actinobacillus actinomycetemcomitans*, *Haemophilus ducreyi* and *Helicobacter hepaticus*. The toxin causes arrest at the G_1/S or G_2/M transition of the cell cycle, depending on the cell type (Hassane *et al.*, 2001; Hassane *et al.*, 2003; Lara-Tejero and Galan, 2000, 2001;

Whitehouse *et al.*, 1998). The active holotoxin is a tripartite complex of CdtA, CdtB and CdtC (Lara-Tejero and Galan, 2001) (Fig. 3), although one study has indicated that CdtB and CdtC combined have some cytotoxicity without CdtA (Lee *et al.*, 2003).

The role of CDT in *C. jejuni* pathogenesis remains unclear, but its mechanism of action is becoming understood. CdtB is known to be the toxic component, as microinjection or transfection of this subunit alone into host cells leads to the effects that are observed with the holotoxin (Lara-Tejero and Galan, 2000). CdtB is thought to act as a DNase, as it shares similarity with a family of DNase I-like proteins. CdtB localizes to the nucleus of host cells, causes DNA damage and, ultimately, phosphorylation of the histone protein H2AX, thereby recruiting the DNA-repair protein Rad50 to double-strand breaks (Hassane *et al.*, 2003). These activities require residues of CdtB that are shared with members of the DNase I family (Elwell and Dreyfus, 2000; Lara-Tejero and Galan, 2000). However, these residues are conserved within the larger phosphodiesterase family to which CdtB belongs and will therefore be required for catalytic activity even if CdtB is not a DNase (Hassane *et al.*, 2001). CdtB has weak DNase activity *in vitro* (Lara-Tejero and Galan, 2000), and studies that have attempted to determine whether DNA damage *in vivo* is a direct or indirect result of CdtB activity have produced conflicting results (Hassane *et al.*, 2001; Li *et al.*, 2002; Mao and DiRienzo, 2002; Sert *et al.*, 1999; Whitehouse *et al.*, 1998).

CdtB nuclear localization has been evident for several years (Lara-Tejero and Galan, 2000), and the mechanism behind this localization was recently established. CdtB sequences from several species contain putative bipartite nuclear-localization signals

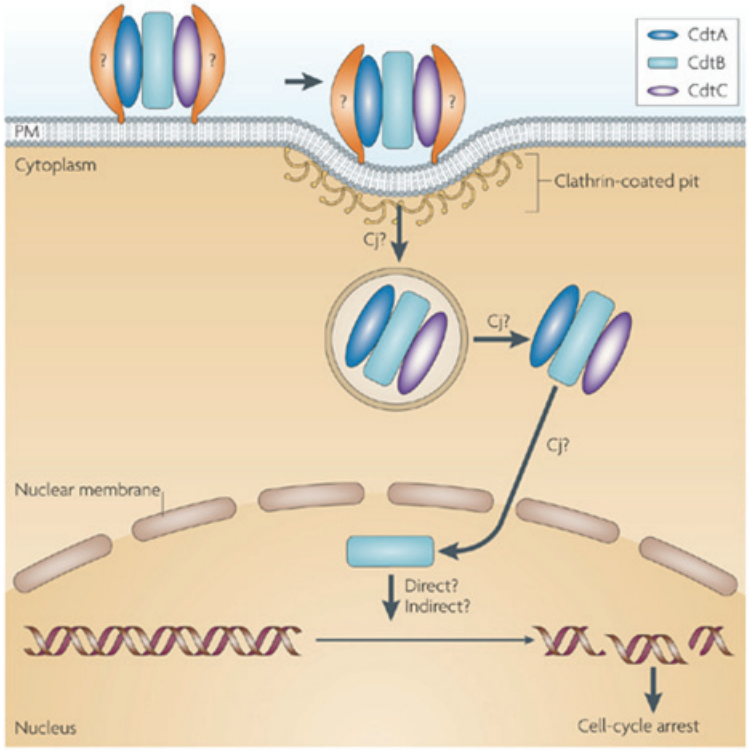

Figure 3. Uptake and activity of cytolethal distending toxin. The cytolethal distending toxin (CDT) holotoxin consists of three subunits, CdtA, CdtB and CdtC. CdtA and CdtC are thought to bind to an unknown receptor on the host cell surface. CDT is taken up into host cells by way of clathrin-coated pits. Following internalization, nuclear localization signals on CdtB probably lead to its active transport into the nucleus through the classical nuclear-import cycle. Once in the nucleus, the toxin leads to double-strand DNA breaks and cell-cycle arrest. Whether or not CdtB acts as a DNase to cause the DNA damage directly, as opposed to this being an indirect effect of some other CdtB enzymatic activity, has yet to be definitely established. The arrows marked Cj? indicate the aspects of CDT uptake or activity that have only been studied using CDT from species other than *Campylobacter jejuni*.

(NLSs), most of which are in the carboxy half of the protein (McSweeney and Dreyfus, 2004). At least one of the two putative NLSs in *E. coli* CdtB-II is definitely required for nuclear localization and cytotoxicity (McSweeney and Dreyfus, 2004). An amino-terminal region of *A. actinomycetemcomitans* CdtB is also required for nuclear localization, and this domain is necessary for cellular distension and cell-cycle arrest by *A. actinomycetemcomitans* CDT (Nishikubo et al., 2003). This region of *A. actinomycetemcomitans* CdtB contains one complete and one partial bipartite NLS, which potentially explains the affect on nuclear localization (McSweeney and Dreyfus, 2004). Together, these studies emphasize the importance of the active transport of the toxin to the nucleus. A formal demonstration of the role of the NLS in *C. jejuni* CdtB has not been reported.

The functions of CdtA and CdtC in this family of toxins are unclear, but one or both might mediate binding to host cells. CdtA and CdtC have some similarity to the B chain of the ricin toxin, which is responsible for receptor-mediated endocytosis of ricin (Lara-Tejero and Galan, 2001). Additionally, CdtA and CdtC bind HeLa cells with specificity, probably using the same receptor (Lee *et al.*, 2003). As *H. ducreyi* CDT is taken up into cells by clathrin-coated pits, it seems likely that CdtA and CdtC mediate binding and subsequent internalization through this pathway (Cortes-Bratti *et al.*, 2000) (Fig. 3).

The fact that a microorganism such as *C. jejuni*, which establishes long-term, asymptomatic associations with many hosts, has retained a toxin such as CDT is intriguing. CDT is responsible for some of the secretion of interleukin (IL)-8, a hallmark of *C. jejuni* pathogenesis, but there are also CDT-independent mechanisms of IL-8

stimulation (Hickey *et al.*, 2000). CDT might have a role in asymptomatic, commensal infections, which would provide a way to either avoid host immune-response mechanisms or redirect them towards tolerance. *In vitro*, *C. jejuni* CDT induces apoptosis in monocytic cell lines (Hickey *et al.*, 2005). Experiments that used a mouse model of *H. hepaticus* colonization suggest that CDT has a function in immune modulation and persistent colonization (Ge *et al.*, 2005; Pratt *et al.*, 2006). In addition, the persistent *C. jejuni* colonization of wild-type mice, but not mice that are deficient for nuclear factor (NF)-κB, requires CdtB, which indicates that CDT might allow *C. jejuni* to escape immune surveillance in an NF-κB-dependent manner (Fox *et al.*, 2004). In chickens, which are the more natural hosts for *C. jejuni*, CDT is expressed by bacteria in the ceca, a site of heavy colonization, although colonized chicks do not generate CDT-neutralizing antibodies (AbuOun *et al.*, 2005). Furthermore, mutants that lack CDT colonize chicks with wild-type efficiency (Biswas *et al.*, 2006).

Adherence mechanisms

To colonize hosts, microorganisms typically require adherence factors, which are often surface appendages such as the pili that are found on the surface of many Gram-negative and Gram-positive species. Genome annotations of several *C. jejuni* strains do not include obvious pilus or pilus-like open reading frames (Fouts *et al.*, 2005; Parkhill *et al.*, 2000). A multi-protein type II-like secretion system of a type that is associated with pilus assembly in *Vibrio cholerae* and *Neisseria gonorrhoeae* was identified as part of the competence machinery, but an actual pilus-like structure has not been identified (Wiesner *et al.*, 2003).

Despite the lack of identifiable adherence organelles, several proteins contribute to *C. jejuni* adherence to eukaryotic cells. CadF binds specifically to fibronectin, which is located basolaterally on epithelial cells *in situ* (Konkel *et al.*, 1997; Monteville and Konkel, 2002; Monteville *et al.*, 2003). The fibronectin-binding domain of CadF consists of amino acids 134–137 (FRLS), which represents a novel fibronectin-binding motif (Konkel *et al.*, 2005). CadF is required for maximal binding and invasion by *C. jejuni in vitro*, and *cadF* mutants are greatly reduced in chick colonization compared with the wild type (Monteville *et al.*, 2003; Ziprin *et al.*, 1999). CadF is similar to *E. coli* OmpA and forms membrane channels, but the role of this activity, if any, has not been established (Mamelli *et al.*, 2006).

Another characterized adhesion, JlpA, is a surface-exposed lipoprotein that is crucial for HEp-2 cell binding (Jin *et al.*, 2001). JlpA binds to Hsp90α, some of which is surface localized in these cells (Jin *et al.*, 2003). Binding to Hsp90α by JlpA activates NF-κB and p38 mitogen-activated protein (MAP) kinase, both of which contribute to proinflammatory responses (Jin *et al.*, 2003). This indicates that some of the inflammation that is observed during *C. jejuni* pathogenesis might be related to JlpA-dependent adherence. Another lipoprotein, CapA, was implicated as a possible adhesion (Ashgar *et al.*, 2007). CapA is an autotransporter that is homologous to an autotransporter adhesin, and CapA-deficient mutants have decreased adherence to Caco-2 cells and decreased colonization and persistence in a chick model (Ashgar *et al.*, 2007).

Paradoxically, some putative adhesins of *C. jejuni* are located in the periplasm. The Peb1 adhesin, also known as CBF1, is one such adhesin. Although crucial for adherence to HeLa cells (Kervella *et al.*, 1993; Pei *et al.*, 1998), Peb1 is periplasmic and

shares homology to the periplasmic-binding proteins of amino acid ATP-binding cassette (ABC) transporters (Leon-Kempis Mdel *et al.*, 2006; Pei and Blaser, 1993). In fact, Peb1 binds to both aspartate and glutamate with high affinity, and *peb1*-deficient mutants cannot grow if these amino acids are the major carbon source (Leon-Kempis Mdel *et al.*, 2006). Although Peb1 has not been localized to the inner or outer membrane, some has been observed in culture supernatants (Leon-Kempis Mdel *et al.*, 2006). Furthermore, Peb1 contains a predicted signal peptidase II recognition site, a common motif in surface-localized lipoproteins, and so there is a possibility that some Peb1 is surface accessible, despite the failure of fractionation techniques to demonstrate this (Leon-Kempis Mdel *et al.*, 2006; Pei and Blaser, 1993). Mutants that lack *peb1* colonize mice poorly, but this could be attributed to the loss of either the adhesion or the amino-acid-transport functions, or both (Leon-Kempis Mdel *et al.*, 2006; Pei *et al.*, 1998). Another periplasmic protein, the glycoprotein Cj1496c, which has homology to a magnesium transporter, is also required for wild-type levels of adherence (see above) (Kakuda and DiRita, 2006). The mechanism by which these periplasmic proteins contribute to host-cell adherence by *C. jejuni* is unclear.

Invasion mechanisms

Campylobacter invades intestinal epithelial cells, albeit at much lower levels than other invasive pathogens such as *Shigella* and *Salmonella*. The mechanism that controls this invasion is being dissected experimentally, but complete understanding is complicated by differences between strains. Studies of the events involved in initiation of invasion by *C. jejuni* have demonstrated that *C. jejuni* interaction with caveolae is required for invasion (Hu *et al.*, 2006; Watson and Galan, 2008). However, the

observation that *C. jejuni* invasion does not require dynamin, which facilitates caveolae-mediated endocytosis, indicates that the role of caveolae in invasion is not to facilitate endocytosis, but rather signal transduction (Watson and Galan, 2008). There is evidence that *C. jejuni* initiates multiple signal transduction cascades in host cells involving host protein kinases and small Rho GTPases (Hu *et al.*, 2006; Krause-Gruszczynska *et al.*, 2007; Watson and Galan, 2008) and this may be accomplished at least in part by interactions with caveolae-localized receptors (Watson and Galan, 2008).

It is clear that all strains require microtubule polymerization for maximal invasion, although some also require microfilament polymerization (Biswas *et al.*, 2000, 2003; Hu and Kopecko, 1999; Monteville *et al.*, 2003; Oelschlaeger *et al.*, 1993). This is different from the microfilament-dependent mechanism of entry that is used by many other invasive bacteria, in which the disruption and subversion of actin-based processes has been well described (reviewed in (Finlay, 2005; Selbach and Backert, 2005)). Scanning electron microscopy has captured epithelial cell membrane pseudopods extending towards and enveloping *C. jejuni* (Biswas *et al.*, 2000), and immunofluorescence experiments have indicated that these pseudopods contain microtubules (Hu and Kopecko, 1999). *C. jejuni* invasion of primary chick intestinal epithelial cells has been reported (Byrne *et al.*, 2007; Van Deun *et al.*, 2007), and also appears to be predominantly microtubule-dependent (Van Deun *et al.*, 2007).

Additional efforts are being made to understand the long-term fate of intracellular *C. jejuni*. *C. jejuni*-containing vacuoles (CCV) appear to move along microtubules to the perinuclear region of the cell by interactions with dynein (Hu and Kopecko, 1999). The CCV deviates from the endocytic pathway and apparently avoids fusion with lysosomes

(Watson and Galan, 2008). If *C. jejuni* is delivered to the lysosomes by Fc-mediated endocytosis, intracellular survival dramatically decreases (Watson and Galan, 2008). There is evidence that long-term survival by *C. jejuni* is accompanied by physiological changes including oxygen sensitivity (Watson and Galan, 2008). Further evidence that the CCV environment requires adaptation by *C. jejuni* comes from the observation that *C. jejuni* that lack polyphosphate kinase (Ppk1), which have survival defects during various environmental stresses, are also defective in long-term intracellular survival (Candon *et al.*, 2007). The role of invasion and intracellular survival in *C. jejuni* colonization and pathogenesis, possibly in immune evasion or establishment of a protected reservoir, has not yet been definitively established.

A recent addition to the *C. jejuni* invasion literature is the somewhat controversial finding that invasion is preceded by subcellular migration, termed "subvasion" (van Alphen *et al.*, 2008). This study found that *C. jejuni* first localizes beneath host cells, then invades them. This behavior, however, was studied with non-confluent, non-polarized cells (van Alphen *et al.*, 2008), so the relevance of subcellular invasion in this assay or *in vivo* remains unclear. Further, this study did not include non-*C. jejuni* controls (van Alphen *et al.*, 2008) to determine if such subvasion is observed with other invasive pathogens and may be, perhaps, an artifact of the invasion assay as opposed to a novel invasion mechanism. Finally, the authors suggest that the loss (or dramatic decrease) of CheW, a chemotaxis protein, in a strain with increased subvasion indicates that this behavior is accomplished by chemotaxis (van Alphen *et al.*, 2008). CheW is a critical protein in the chemotactic machinery and is required for chemotaxis in *E. coli* (reviewed in (Wadhams and Armitage, 2004)). The loss of detectable CheW would be

expected to greatly diminish, if not completely abrogate, chemotaxis by *C. jejuni*. The logic behind the assertion that less CheW leads to more efficient chemotaxis-mediated migration beneath cells is difficult to follow. Much more information is needed to assess the relevance of and mechanism underlying this phenotype.

C. jejuni factors required for chick colonization

Studies using genetic screens and/or targeted mutagenesis of candidate genes have led to a growing understanding of which *C. jejuni* traits are important in chicken colonization. A common emerging theme from this work is the importance of flagella and flagellar motility. Signature-tagged mutagenesis of *C. jejuni* in a chick model of infection resulted in the identification of two methyl-accepting chemotaxis receptors and other elements of the flagellar and chemotactic machinery as being important for wild-type chick colonization (Hendrixson and DiRita, 2004). Additionally, mutants in the genes that encode the flagellins and flagellar biosynthesis regulators FlgR, σ^{54} and σ^{28} all display defects in chick colonization (Fernando *et al.*, 2007; Hendrixson and DiRita, 2004; Hendrixson, 2006; Nachamkin *et al.*, 1993; Wassenaar *et al.*, 1993; Wosten *et al.*, 2004) .

Other regulators that are not associated with flagellar motility are also important for efficient chick colonization. These include CbrR, which regulates deoxycholate resistance and contains two response-regulator domains and a GGDEF domain, thereby implicating this protein in regulating production of the second messenger cyclic diguanylate (c-di-GMP) (Raphael *et al.*, 2005). Deoxycholate has been found to induce *ciaB* expression, as well as other virulence factors (Malik-Kale *et al.*, 2008). In addition, deoxycholate may affect gene expression directly via the TetR-like regulator CmeR,

which is required for wildtype levels of chick colonization (Gu *et al.*, 2007; Guo *et al.*, 2008). Mutants in the DccRS two-component system, for which an activating signal is unknown, are also poor colonizers of chicks compared with wild type (MacKichan *et al.*, 2004). The DccRS-regulated genes that have been identified have no known or predicted functions, but one appears to be essential for growth and mutants in two others lead to chick colonization defects (MacKichan *et al.*, 2004).

One trait of chickens that is different from humans and other mammals and could contribute to the different outcomes of infection with *C. jejuni* is body temperature. Chickens have a body temperature that ranges from 41 to 45°C, as opposed to the 37°C that is normal in humans, making temperature a potential signal for host-specific infection. Transcription profiles of *C. jejuni* cultures that were shifted from 37°C to 42°C showed evidence of potential alterations in membrane structure by the upregulation of genes for transport and binding proteins, as well as cell wall and envelope constituents (Stintzi, 2003). *In vitro* growth at 42°C, but not 37°C, requires the Clp protease complex (Cohn *et al.*, 2007), indicating that this complex likely plays a key role in chick colonization, although this has not been tested directly. Additionally, there is a regulatory system that might contribute to survival at the higher temperatures. RacRS is a two-component system that is required for wildtype chick colonization, and mutants that lack RacRS have a growth defect at 42°C (Bras *et al.*, 1999). The RacRS system can act as both an activator and repressor to regulate gene expression, sometimes in a temperature-dependent manner (Bras *et al.*, 1999). Expression of *cj0414* and *cj0415* is upregulated at 42°C (Pajaniappan *et al.*, 2008), although it is not known if this requires RacRS. These genes encode gluconate dehydrogenase, which is required for use of

gluconate as an electron donor (Pajaniappan *et al.*, 2008). A *cj0415* mutant was impaired in chick colonization, indicating that gluconate is an important electron donor during colonization (Pajaniappan *et al.*, 2008).

Several genes that control mechanisms other than motility and gene regulation are also required for chick colonization. These include genes encoding the *N*-linked glycosylation system, as well as proteins modified by this system (Hendrixson and DiRita, 2004; Kakuda and DiRita, 2006; Karlyshev *et al.*, 2004) and various adherence and invasion factors, such as *cadF* and *ciaB* (Ziprin *et al.*, 1999; Ziprin *et al.*, 2001). Stress adaptations appears to be important in chick colonization, as a *ppk1* mutant, with defects in stress survival, has a dose-dependent chick colonization defect (Candon *et al.*, 2007). γ-glutamyl transpeptidase (GGT) is required for long term persistence in, but not initial colonization of chicks (Barnes *et al.*, 2007). It is unclear, however, what role GGT plays during chick colonization as it could contribute to oxidative stress resistance, to biosynthesis of amino acids or to both (Barnes *et al.*, 2007). Finally, antimicrobial resistance mechanisms, reduction of nitrate and nitrite, and elements of metabolism that are related to low iron, low oxygen (but not anaerobic) and high serine or other amino-acid environments might have significant effects on chick colonization (Lin *et al.*, 2003; Luo *et al.*, 2003; Palyada *et al.*, 2004; Purdy *et al.*, 1999; Velayudhan *et al.*, 2004; Weingarten *et al.*, 2008; Woodall *et al.*, 2005).

Chemotaxis and Methyl-accepting Chemotaxis Proteins

Flagella-mediated motility

While other mechanisms of motility exist, flagella-mediated motility is the most well-studied in bacteria and archaea. Flagella, which are helical in nature, propel microbes forward by rotating, and are powered by the proton motive force or, less frequently, a sodium motive force (reviewed in (Armitage, 2006)). Different numbers and distributions of flagella have been found, including a single flagella at or near one or both poles, several flagella at one or both poles, and flagella distributed randomly over the cell surface (peritrichous flagella) (reviewed in (Armitage, 2006)).

Differing distributions of flagella clearly lead to different swimming behaviors and necessitate different control mechanisms, all of which are mediated by changes in the direction of flagellar rotation (reviewed in (Armitage, 2006)). In the case of *E. coli*, which has peritrichous flagella, the flagella form a bundle and move together when rotating counter-clockwise (CCW). Thus, CCW rotation leads to forward motion or smooth-swimming. When some of these flagella change to clockwise rotation (CW), the bundled flagella separate resulting in a tumbling motion of the bacterium. Once the flagella return to a CCW rotation, the flagella again form a bundle and lead to smooth-swimming, but now in a new direction. Chemotaxis, the ability to swim toward attractants and away from repellents, is mediated by changes in the frequency of runs (smooth-swimming) to tumbles. In the absence of an attractant or repellent gradient, the bacteria will engage in a random walk of runs and tumbles. In the presence of such a gradient, however, this "random walk" becomes biased. The frequency of direction changes (tumbles) increase if the bacteria move toward a repellent or away from an

attractant. On the other hand, direction changes decrease if the bacteria move away from a repellent or toward an attractant (i.e. smooth-swimming predominates).

In other bacteria, direction changes do not necessarily occur as a result of tumbles (reviewed in (Armitage, 2006)). The flagellum of *Rhodobacter spaeroides*, for example, normally rotates CW, leading to smooth-swimming (reviewed in (Armitage, 2006)). At some frequency, this rotation stops and the flagellum forms a tight coil (reviewed in (Armitage, 2006)). As bacteria are too small to experience significant inertia, the bacteria come to a rest. They are buffeted by Brownian motion, resulting in a new direction when CW rotation resumes (reviewed in (Armitage, 2006)). The flagellum of *Psuedomonas aeruginosa* normally rotates CCW (reviewed in (Armitage, 2006)). Upon switching to CW, the flagella very briefly reverse the movement of the bacteria (reviewed in (Armitage, 2006)). The flagella of *Sinorhizobium meliloti*, which are peritrichous like those of *E. coli*, don't change their direction of rotation (reviewed in (Armitage, 2006)). Rather, some of the flagella slow down, leading the bundle to come apart and the bacterium to change direction (reviewed in (Armitage, 2006)). The polar bundles of flagella found on *Rhodospirillum rubrum*, however, rotate in opposite directions to propel the bacterium forward (reviewed in (Armitage, 2006)). The bacterial direction of swimming is altered when both polar bundles change their direction of rotation (reviewed in (Armitage, 2006)). An alternative swimming pattern has been observed in marine vibroid bacteria with single bipolar flagella (Thar and Kuhl, 2003). These bacteria swim by a combination of translation along and rotation around the short axis of the cell and it is proposed that changes in the rotational speed of one of the two flagella leads to direction changes (Thar and Kuhl, 2003). Another variation is seen in *Vibrio*

alginolyticus, which utilizes two types of flagella: sodium motive force powered polar flagella for swimming in liquid and proton motive force powered lateral flagella for swarming on surfaces (reviewed in (Armitage, 2006)). Both of these flagella are regulated by the same chemotaxis machinery, but the output is quite different. While the polar flagellum switches between CCW (runs) and CW (tumbles), the lateral flagella only rotate CCW and the direction of movement is altered by changes in rotational speed (Kojima *et al.*, 2007). In light of so many swimming patterns and methods of direction changes, the ability of very similar signal transduction pathways to regulate chemotaxis in such diverse organisms is somewhat astounding.

Chemotaxis signal transduction in *E. coli*

The signal transduction machinery responsible for chemotaxis is best characterized in *E. coli* (Fig. 4). Other microbes use core elements of the *E. coli* paradigm, with some variations that are discussed below (Table 1). Chemotaxis responses occur in four steps (adapted from (Szurmant and Ordal, 2004)): signal recognition, excitation, adaptation, and signal termination. The first step, signal recognition, is carried out by chemotaxis receptors (methyl-accepting chemotaxis proteins or MCPs) (discussed below). MCPs and MCP-like proteins interact with CheW and CheA, which signal to CheY, to stimulate excitation of the chemotaxis system. Adaptation involves CheB and CheR and signal termination requires CheZ.

CheA is a histidine kinase that trans-autophosphorylates within a dimer (reviewed in (Wadhams and Armitage, 2004)). The phosphate group can subsequently be transferred to one of two response regulator domain-containing proteins, CheY or CheB (reviewed in (Armitage, 2006; Wadhams and Armitage, 2004)). In *E. coli*, CheA kinase

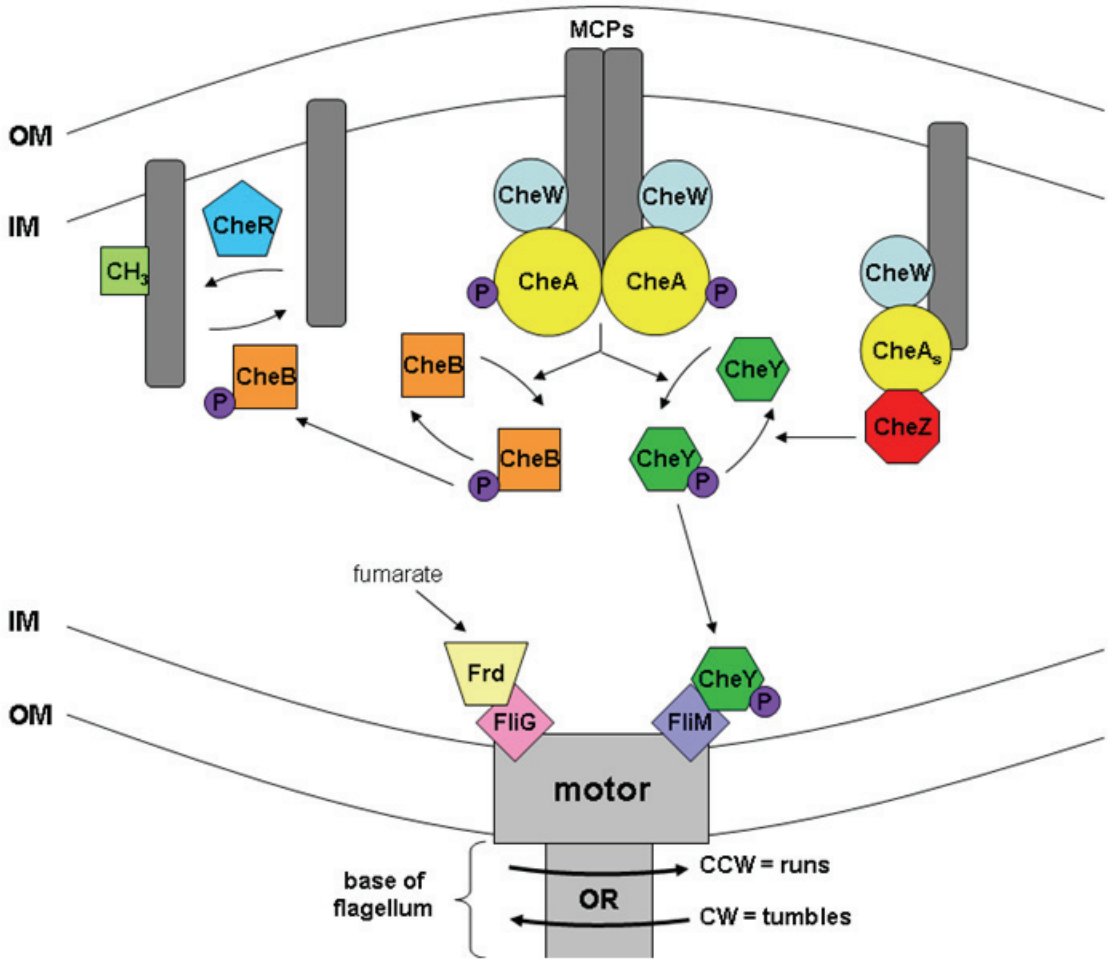

Figure 4. *E. coli* proteins involved in chemotaxis signal transduction. Signals sensed by MCPs are translated to changes in flagellar rotation by a signal transduction cascade. Proteins involved in this cascade include the scaffold protein CheW, the histidine kinase CheA, and the response regulator CheY, which interacts with the motor switch protein FliM when phosphorylated. CheZ interacts with a small variant of CheA and acts as a phosphatase to terminate signal transduction. The methyltransferase CheR and methylesterase CheB (which is also a response regulator) are involved in adaptation. Finally, fumarate is not sensed by MCPs, but binds to Frd, which in turns interacts with the motor switch protein FliG.

Table 1. Proteins involved in chemotaxis signal transduction.

Protein Name	Class of Protein	Role in Chemotaxis
methyl-accepting chemotaxis protein (MCP)$^{Ec, Bs, Cj}$	Chemoreceptor	Receptor for chemotaxis stimulus.
CheA$^{Ec, Bs, Cj}$	Histidine protein kinase	Autophosphorylates in response to MCPs. Phosphorylates CheY and CheB.
CheW$^{Ec, Bs, Cj}$	Adaptor protein	Required for formation of MCP-CheA-CheW complex.
CheY$^{Ec, Bs, Cj}$	Response regulator	Binds FliM when phosphorylated to alter flagellar rotation. Multiple CheYs may act as phosphate sinks.
FliM$^{Ec, Bs, Cj}$	motor switch protein	Alters flagellar rotation in response to CheY-P binding.
FliG$^{Ec, Bs, Cj}$	motor switch protein	Alters flagellar rotation in response to fumarate-Frd.
CheB$^{Ec, Bs, Cj}$	Response regulator, methylesterase	Removes methyl groups from MCPs. Activated upon phosphorylation.
CheR$^{Ec, Bs, Cj}$	Methyltransferase	Constitutively methylates MCPs.
CheZ^{Ec}	Phosphatase	Stimulates dephosphorylation of CheY, leading to signal termination.
Frd$^{Ec, Cj}$	Fumarate reductase	Binds FliG to alter flagellar rotation in response to fumarate.
HP0170^{Cj}	Phosphatase?	Appears to be a distant CheZ homolog and possible CheY-phosphatase.
CheV$^{Bs, Cj}$	CheW-CheY fusion	May function as a phosphate sink, leading to signal termination. Alternatively, may function in adaptation.
FliY^{Bs}	Switch protein	Has some CheY-P phosphatase activity.
CheC^{Bs}	FliY-like protein	Has low CheY-P phosphatase activity. Inhibits CheD activity.
CheX	CheC-truncation	Has strong CheY-P phosphatase activity.
CheD^{Bs}	Methylesterase	Removes methyl groups from MCPs. Inhibited by CheC. CheC-CheD complex stabilized by CheY-P.
FrzE	CheA-CheY fusion	Similar role as CheA. Role of CheY domain unknown.
FrzZ	CheY-CheY fusion	One CheY domain binds FliM, the other acts as phosphate sink.

This table summarizes the chemotaxis proteins discussed in the text, as well as their function and role in chemotaxis. Superscripts Ec, Bs and Cj indicate that a homologue is found in *E. coli*, *B. subtilis* or *C. jejuni*, respectively.

activity is inhibited by an increase in attractant binding or a decrease in repellent binding to MCPs (reviewed in (Szurmant and Ordal, 2004; Wadhams and Armitage, 2004)).

The CheW structure revealed that this protein contains two Src-homology 3 (SH3) domains, although there is no sequence homology to eukaryotic SH3 domains (reviewed in (Baker *et al.*, 2006; Wadhams and Armitage, 2004)). CheW possesses no known enzymatic activity. Rather, CheW is thought of as a scaffolding protein, transmitting the MCP signal to CheA (reviewed in (Armitage, 2006; Wadhams and Armitage, 2004)). Specifically, CheW is thought to stabilize CheA in an active conformation (reviewed in (Baker *et al.*, 2006)).

Once CheA autophosphorylates, the phosphate group can be transferred to CheY, giving rise to CheY-P (reviewed in (Armitage, 2006; Wadhams and Armitage, 2004)). CheY-P, but not CheY, interacts with FliM in the flagellar switch and increases the probability of CW rotation of the flagella (tumbles) (reviewed in (Armitage, 2006; Wadhams and Armitage, 2004)). Thus, CheY/CheY-P is the ultimate output of the chemotaxis signal transduction pathway. The phospho-relay from CheA (histidine kinase) to CheY (response regulator) is similar to other pairs of regulatory proteins known as two-component systems (TCS), many of which regulate transcription. The ~10-20s half-life of CheY-P is much shorter than that of other TCS response regulators, which may be on the order of several minutes (reviewed in (Armitage, 2006)). This is consistent with the fact that CheA/CheY regulate a behavior (chemotaxis) that operates on a much faster time-scale than the changes in transcription mediated by other TCS proteins. A less understood characteristic of CheY is its ability to be acetylated by acetyl-CoA-synthetase as well as its ability to autoacetylate (reviewed in (Wadhams and

Armitage, 2004)). CheY acetylation levels are quite high *in vivo* and appear to be mainly attributable to autoacetylation (Yan *et al.*, 2008). CheY acetylation appears to contribute to chemotaxis, particularly the response to addition of a repellent, but the mechanism underlying this effect has not been elucidated (Barak *et al.*, 2006).

Once the chemotaxis system is excited, resulting in production of CheY-P, the system must undergo adaptation. Adaptation is a type of "memory" mechanism, by which bacteria can sense changes in their environment relative to what they have recently experienced (reviewed in (Armitage, 2006; Wadhams and Armitage, 2004)). Adaptation resets the signaling state of the MCP, and consequently CheA, to prestimulus levels (reviewed in (Armitage, 2006; Wadhams and Armitage, 2004)). This allows temporal gradient sensing, where a further increase or decrease in the MCP stimulus is required to alter CheA activity, and therefore CheY-P levels (reviewed in (Armitage, 2006; Wadhams and Armitage, 2004)). *E. coli* adaptation is accomplished by a methylation scheme involving CheB and CheR.

Like CheY, CheB contains a response regulator domain and can be phosphorylated following CheA autophosphorylation (reviewed in (Armitage, 2006; Wadhams and Armitage, 2004)). CheB is also a methylesterase, and this activity is stimulated ~10-fold by CheB phosphorylation (reviewed in (Armitage, 2006; Szurmant and Ordal, 2004)). CheB removes methyl groups that have been added to conserved glutamates by CheR (reviewed in (Armitage, 2006; Wadhams and Armitage, 2004)). These glutamates can also be glutamines, which are post-translationally deamidated by CheB, resulting in glutamate (reviewed in (Armitage, 2006; Wadhams and Armitage, 2004)). The affect of methylation/demethylation appears to be a change in the charge of

methylation sites on MCPs, resulting in a change in conformation that reduces signaling to CheA (reviewed in (Baker *et al.*, 2006)). CheB phosphorylation occurs less rapidly than CheY phosphorylation, which ensures that excitation precedes adaptation (reviewed in (Wadhams and Armitage, 2004)).

CheR is a constitutively active methyltransferase that adds methyl groups to the conserved glutamates of MCPs (reviewed in (Armitage, 2006; Wadhams and Armitage, 2004)). CheR interacts with a C-terminal pentapeptide, NWETF, on some MCPs, and it is interactions with pentapeptide-containing MCPs which primarily localizes CheR to MCP clusters (reviewed in (Armitage, 2006; Wadhams and Armitage, 2004)). CheR levels are much lower than those of MCPs; CheR moves through MCP clusters methylating the MCPs to which it is bound, as well as neighboring MCPs lacking the pentapeptide (reviewed in (Armitage, 2006; Wadhams and Armitage, 2004)).

Signal termination in *E. coli* is accomplished by the activity of CheZ, a phosphatase that increases the auto-dephosphorylation rate of CheY-P (reviewed in (Armitage, 2006; Wadhams and Armitage, 2004)). This further decreases the half-life of CheY-P to ~200ms (reviewed in (Wadhams and Armitage, 2004)). CheZ binds a truncated form of CheA ($CheA_s$) that results from an alternative transcriptional start site for *cheA* (reviewed in (Baker *et al.*, 2006)). CheZ, in complex with $CheA_s$, binds and destabilizes CheY-P (reviewed in (Baker *et al.*, 2006)).

In a departure from the above signal transduction cascade, fumarate has been shown to impact the switching frequency and bias of flagellar rotation in *E. coli* directly. This behavior is mediated by fumarate reductase (Frd) which binds the switch protein FliG and switches the direction of flagellar rotation (Cohen-Ben-Lulu *et al.*, 2008). The

mechanism of fumarate-Frd switching is unclear at present, but is CheY-independent, indicating that it does occur independently of the chemotaxis signal transduction pathway described above (Cohen-Ben-Lulu *et al.*, 2008; Prasad *et al.*, 1998). It has been postulated that fumarate binding by Frd may alter the interaction between Frd and FliG, but this has not yet been shown (Cohen-Ben-Lulu *et al.*, 2008). It remains to be seen whether other examples of MCP-independent effects on chemotaxis exist.

Variations on chemotaxis signal transduction in other microbes

Elements of the *E. coli* chemotaxis machinery are found in all other chemotactic bacteria and archaea, most of which have added layers of complexity compared to *E. coli*. The *Bacillus subtilis* chemotaxis system has also been fairly well characterized and, while similar to that of *E. coli*, contains significant differences. For example, the effect of attractant on CheA activity is reversed in *B. subtilis* relative to *E. coli*. In *B. subtilis*, attractant binding increases CheA activity and repellent binding inhibits CheA activity (reviewed in (Armitage, 2006; Szurmant and Ordal, 2004)). Consistent with this reversal, CheY-P still interacts with FliM, but that interaction results in CCW rotation of the flagella leading to smooth-swimming (reviewed in (Armitage, 2006; Szurmant and Ordal, 2004)).

Significant differences exist between *E. coli* and other microbes in their mechanisms of signal termination. Until recently, it was thought that the CheZ phosphatase that decreases the CheY-P half-life was only found in γ-proteobacteria, which include *E. coli*, and β-proteobacteria (reviewed in (Szurmant and Ordal, 2004)). However, a gene (HP0170) has been identified in the ε-proteobacterium *H. pylori* that appears to be a distant CheZ homologue (Terry *et al.*, 2006). While CheY-P phosphatase

activity has not been definitely demonstrated for HP0170, the protein does contain several conserved residues in the CheZ active site (Terry *et al.*, 2006). Potential HP0170 homologues were subsequently identified in all Proteobacteria groups, as well as in the Firmicute group, indicating that CheZ may be more widespread than previously believed (Terry *et al.*, 2006). As HP0170 homologues diverge significantly from CheZ, it remains to be seen whether they have CheY-P phosphatase activity and whether there are any functional differences between this family of CheZ-like proteins and those resembling *E. coli* CheZ.

Other bacteria and archaea that lack CheZ must have an alternate mechanism for signal transduction. Many bacterial genomes encode two or more CheY proteins and the reigning hypothesis is that one of these functions as a phosphate sink, as has been shown for *Sinorhizobium meliloti* (reviewed in (Wadhams and Armitage, 2004)). Alternatively, several bacterial genomes encode a CheW-CheY fusion protein, named CheV, which has also been postulated to function as a potential phosphate sink (reviewed in (Wadhams and Armitage, 2004)). This role of CheV is somewhat controversial, as experiments have shown that CheV is instead important for adaptation in *B. subtilis* (Karatan *et al.*, 2001). *B. subtilis* CheV is phosphorylated relatively slowly and CheV-P is relatively stable, making it an unlikely candidate for a phosphate sink (Karatan *et al.*, 2001). Whether these characteristics are shared by other CheV proteins is not clear.

B. subtilis also expresses two proteins that decrease the CheY-P half-life, the flagellar switch protein FliY and CheC, which has some homology to FliY. Other species express CheX, an apparent truncation of CheC that is a stronger CheY-P phosphatase than either CheC or FliY and may play a role in signal termination (Muff *et*

al., 2007). Although CheC does have CheY-P phosphatase activity, the rate of CheY-P dephosphorylation is much slower than CheX or FliY and this activity appears to be dispensible for *B. subtilis* chemotaxis *in vivo* (Muff and Ordal, 2007). Rather, a role for CheC in adaptation has been suggested (discussed below) (Muff and Ordal, 2007). In the case of *R. sphaeroides*, which expresses six CheY proteins, some have argued that these may act as phosphate sinks (reviewed in (Szurmant and Ordal, 2004)). Others have argued that this species may not have need of a signal termination mechanism as all six CheY proteins in this species have very short CheY-P half-lives (reviewed in (Wadhams and Armitage, 2004)). One study indicated that some *R. sphaeroides* make two kinds of flagella, a single subpolar flagellum and multiple polar flagella and that each type of flagellum is regulated by 3 of the 6 CheY proteins (del Campo *et al.*, 2007). Whether all of these CheYs function as response regulators or some act as phosphate sinks remains undetermined.

An alternative set of domain fusions are present in the Frz chemotaxis system of *Myxococcus xanthus* (Inclan *et al.*, 2007). *M. xanthus* has a protein, FrzE that consists of a CheA-CheY fusion. The FrzE CheA domain autophosphorylates and in turn facilitates phosphotransfer to its own CheY domain, as well as to either of two CheY domains fused together in the protein FrzZ (Inclan *et al.*, 2007). FrzZ is the output response regulator and it appears one of its two CheY domains may act as a phosphate sink, but only under certain growth conditions (Inclan *et al.*, 2007).

A complex variant on the CheA-CheY fusion, FrzE, is seen in *Pseudomonas aeruginosa*. This protein, ChpA is the histidine kinase in the Chp-Pil chemotaxis system regulating type IV pili twitching motility (Whitchurch *et al.*, 2004). ChpA contains nine

potential phosphorylation sites: six that contain histidine as the phospho-acceptor, one containing a serine as the phospho-acceptor, one containing a threonine phospho-acceptor and a CheY domain (Whitchurch *et al.*, 2004). The function of each of these alternative phosphorylation sites has not been elucidated, but it is interesting to note that ChpA homologues containing multiple histidine and either serine or threonine phospho-acceptors have been identified in other species, each of which contain type IV pili (Whitchurch *et al.*, 2004).

Other bacteria also differ from *E. coli* in their adaptation mechanisms. In *B. subtilis* deamidation is performed by CheD, not CheB (reviewed in (Szurmant and Ordal, 2004)). In addition, unlike *E. coli* where methylation at each site has the same effect on MCP status and CheA activity, different sites seem to play different roles in *B. subtilis*. In the *B. subtilis* chemoreceptor McpB, one methylation site is important for adaptation following either the addition or removal of an attractant, while another methylation site is important for adaptation only following addition of an attractant (reviewed in (Szurmant and Ordal, 2004; Wadhams and Armitage, 2004)). A third methylation site in McpB may be required for regulation of methylation, as opposed to returning the MCP to prestimulus activity levels (reviewed in (Szurmant and Ordal, 2004)). An additional difference in adaptation mechanisms was elucidated in *Thermotoga maritima*. While *T. maritima* expresses a CheR homologue capable of methylating MCPs, this methylation is independent of the pentapeptide motif to which *E. coli* CheR binds (Perez and Stock, 2007). Further analysis indicated that only approximately 10% of all bacterial MCPs contain the pentapeptide and there are many bacteria that do not express any MCPs

containing the pentapeptide (Perez and Stock, 2007). Clearly, pentapeptide-independent methylation by CheR is a widespread alternative to the *E. coli* CheR activity.

The proteins CheC and CheD appear to function in methylation-dependent adaptation. The CheD of *T. maritima* has been shown to possess methylesterase activity, in addition to the previously mentioned deamidase activity (Chao *et al.*, 2006). CheB and CheD of *T. maritima* demethylate overlapping subsets of MCPs (Chao *et al.*, 2006). Further, CheC inhibits CheD activity and the CheC-CheD interaction is stabilized by CheY-P, leading to adaptation of CheD-demethylated MCPs (Chao *et al.*, 2006; Muff and Ordal, 2007). Whether there is an intrinsic advantage to having separable adaptation systems (CheB-dependent and CheD-dependent) for different subsets of MCPs is not yet clear.

When levels of an attractant are low, a methylation-independent system of adaptation involving CheV seems to be effective. CheV-mediated adaptation appears to require phosphorylation of the response regulator (CheY-like) domain of CheV (reviewed in (Szurmant and Ordal, 2004)). In *Helicobacter pylori*, which lacks CheR and CheB, three CheV homologues are present and may serve as the only mechanism of adaptation (reviewed in (Szurmant and Ordal, 2004)).

In another departure from *E. coli*, many species contain multiple sets of chemoreceptors and chemotaxis genes the expression of which is regulated (reviewed in (Armitage, 2006)). Whereas *E. coli* always expresses the same MCPs, other species vary their MCP contingents depending on their current environment. This may allow these species to respond to changes in a stimulus only when that stimulus is limiting (reviewed in (Armitage, 2006)).

All of the above mechanisms of chemotaxis support the biased random walk means of chemotaxis where the bacteria are guided by temporal sensing of a gradient. It has long been argued that bacteria are too small to engage in the spatial sensing of gradients employed by eukaryotes, where differences in the concentration of an attractant (or repellent) at different positions in the cell are used to sense gradients. However, there is preliminary evidence that larger bacteria (≥5μm) may be able to engage in spatial sensing of gradients (Thar and Kuhl, 2003). Although spatial gradient sensing by bacteria has not been definitively established, it would provide a potential explanation for the widespread observation of bipolar localization of MCPs (Thar and Kuhl, 2003).

Known types of MCPs and stimuli

The prototypical MCPs of *E. coli* sense stimuli including amino acids, sugars, dipeptides, pyrimidines, pH, temperature and blue-light (Liu and Parales, 2008; Wright *et al.*, 2006) (reviewed in (Armitage, 2006; Wadhams and Armitage, 2004)). Each of these MCPs has a periplasmic domain that (except in the cases of pH, temperature and blue-light) bind their respective stimuli directly or indirectly via periplasmic binding proteins (reviewed in (Armitage, 2006; Baker *et al.*, 2006; Wadhams and Armitage, 2004)). In those MCPs where it has been studied, the stimulus or periplasmic binding protein binds at the interface of two monomers in a dimer (reviewed in (Armitage, 2006; Wadhams and Armitage, 2004)). This periplasmic domain is flanked by two transmembrane domains.

C-terminal to the second transmembrane domain is a HAMP domain. HAMP domains (named for their presence in histidine kinases, adenylyl cyclases, methyl-accepting chemotaxis proteins and phosphatases) (Aravind and Ponting, 1999) represent a common motif in numerous bacterial signal transduction proteins. Most HAMP

domain-containing proteins are bacterial, but they have also been identified in archaea and lower eukaryotic organisms. HAMP domains are thought to play a role in intramolecular communication between input and output domains of a single protein (Appleman *et al.*, 2003; Appleman and Stewart, 2003; Aravind and Ponting, 1999). In the case of MCPs, the HAMP domain is thought to be involved in transmitting the MCP signal from the periplasmic domain to the C-terminus of the MCP, the highly conserved domain (so-called because it is well conserved in all MCPs) (reviewed in (Armitage, 2006; Baker *et al.*, 2006; Wadhams and Armitage, 2004). This highly conserved domain consists of the flexible bundle (Alexander and Zhulin, 2007), methylation helices and the signaling domain, which interacts with CheA and CheW (reviewed in (Armitage, 2006; Baker *et al.*, 2006; Wadhams and Armitage, 2004).

MCPs containing variations on this architecture have been identified in a number of microbes. In addition to the four MCPs with the previously described topology, *E. coli* expresses an energy taxis transducer with a cytoplasmic input domain. This protein, Aer, and other energy taxis transducers are discussed below. Many bacteria and archaea also express MCPs with no apparent transmembrane region (reviewed in (Wadhams and Armitage, 2004)). Several archaea also express two proteins that function together in phototaxis. These phototaxis receptors consist of a transmembrane sensory rhodopsin and an associated transducer, which has two transmembrane helices, a HAMP domain and an HCD (reviewed in (Klare *et al.*, 2004; Oprian, 2003)).

Signal transduction within MCPs

The signal provided by receptor binding site occupation must be translated across the membrane to the signaling domains located in the cytoplasmic C-terminus of MCPs.

This is accomplished by a small ~1-2Å piston-like shift in one transmembrane helix relative to another (reviewed in (Falke and Hazelbauer, 2001)). Modeling studies based on cross-linking analysis indicate that this shift may be larger, perhaps on the order of 4-6Å (Peach *et al.*, 2002). These modeling studies, as well as further structural studies, suggest that this piston-like shift of the transmembrane helix may also be accompanied by a rotational movement of this helix or MCP monomer (Moukhametzianov *et al.*, 2006; Peach *et al.*, 2002).

This piston-like shift in transmembrane helices must be transmitted to the HCD of the MCP by the HAMP domain. Our knowledge about HAMP domains has been limited by a dearth of structural information until very recently. HAMP domains share very limited sequence conservation, and no single residue is absolutely conserved in all HAMP domains. Recently, the structure of the HAMP domain from the *Archaeoglobus fulgidus* protein Af1503 was solved (Hulko *et al.*, 2006). This structure consisted of two amphipathic helices (AS-1 and AS-2) that come together in the only known occurrence of a parallel coiled-coil (Hulko *et al.*, 2006). These helices form a four-helix bundle in a HAMP domain dimer, which adopts an unusual knobs-to-knobs conformation (Hulko *et al.*, 2006). A rotation of the HAMP domain helices relative to one another could potentially bring them into the more common knobs-into-holes conformation (Hulko *et al.*, 2006). These findings gave rise to a model where the transmembrane helix shift is translated into a gear-like 26° rotation of the helices relative to one another within the HAMP dimer four-helix bundle (Hulko *et al.*, 2006).

Af1503 is atypical of HAMP domain-containing proteins in that it lacks an output signal transduction domain (Hulko *et al.*, 2006), so it was unknown whether this HAMP

structure would be representative of other HAMP domains. However, cysteine-scanning mutagenesis combined with *in vivo* disulfide cross-linking analysis of Tar and Aer, two chemoreceptors in *E. coli*, are consistent with the Af1503 structure (Swain and Falke, 2007; Watts *et al.*, 2008b).

The HAMP domain signal, possibly the rotation of the HAMP helices in the four-helix bundle, must then be translated to the HCD. There is some evidence that this occurs via a newly defined region of the HCD, termed the flexible bundle region (Alexander and Zhulin, 2007). The flexible bundle contains a previously identified glycine hinge and it is proposed that bending at this glycine hinge is a key signaling mechanism (Alexander and Zhulin, 2007). A mechanical model suggests that rotation can be converted into bending in the presence of such a hinge (personal communication in (Watts *et al.*, 2008b)).

One model asserts that this bending results in an increased distance between signaling domains (Parkinson, 2007). The signaling domain is the portion of the HCD that interacts directly with CheW and CheA (reviewed in (Armitage, 2006)). Supporting this bending model, distances between receptors have been found to increase upon attractant binding and decrease upon repellent binding *in vivo* (reviewed in (Hazelbauer *et al.*, 2008)). The distance between signaling domains is also affected by the methylation state of the methylation domain within the HCD, presumably due to the difference in charge resulting from the presence or absence of a methyl group (reviewed in (Baker *et al.*, 2006)). In fact, there is evidence that methylation reverses the piston-like shift of MCP transmembrane helices (reviewed in (Hazelbauer *et al.*, 2008)). This implies that the HAMP domain, in addition to converting transmembrane shifts into

bending of the signaling domain, must also convert methylation-induced "unbending" into a reversal of the transmembrane shift. This is the first indication that HAMP domains may function in two directions (reviewed in (Hazelbauer *et al.*, 2008)).

The overall model of signal transduction presented here explains signaling in transmembrane MCPs. However, cytoplasmic MCPs lacking transmembrane helices remain poorly understood. What signal does the HAMP domain of these MCPs sense, and does the HAMP domain transmit that signal to the HCD in the same way as in transmembrane MCPs? Additionally, in MCPs that contain a membrane anchor, but both the input and output domains are cytoplasmic, does the path of signal transduction include the transmembrane domains? Or is the signal transmitted directly from the input domain to the HAMP domain? If the latter, could the HAMP domains of transmembrane MCPs interact with alternative, cytoplasmic input domains to transmit additional signals? Clearly, while these studies and models provide a framework for understanding transmembrane MCPs, many questions remain about how other MCPs might function.

MCP interactions

Accumulating evidence indicates that MCP homodimers do not function in a vacuum, but instead interact in higher order arrays (reviewed in (Hazelbauer *et al.*, 2008; Kentner and Sourjik, 2006)). Further, modeling and experimental evidence both suggest that these higher order arrays of MCPs and associated chemotaxis proteins are responsible for several aspects of chemotactic signaling, including signal gain, large signal ranges, receptor cooperativity, signal integration and adaptation (reviewed in (Hazelbauer *et al.*, 2008; Kentner and Sourjik, 2006)).

MCP homodimers can participate in most of the signal transduction outlined above, but they are incapable of activating the CheA kinase (reviewed in (Hazelbauer *et al.*, 2008)). Rather, CheA activation requires multiple homodimers, likely a trimer of dimers (reviewed in (Hazelbauer *et al.*, 2008)). Such trimers of dimers appear to form *in vivo* and can form without the assistance of other chemotaxis proteins (reviewed in (Hazelbauer *et al.*, 2008; Kentner and Sourjik, 2006)). However, trimers of dimers are stabilized by CheW and CheA (reviewed in (Hazelbauer *et al.*, 2008)).

Even these trimers of dimers do not appear to be the *in vivo* functional unit. Rather, patches containing thousands of receptors and associated chemotaxis proteins are found in cells and within these, several dozen receptors appear to form a cooperative unit (reviewed in (Hazelbauer *et al.*, 2008)). These patches likely consist of arrays of trimers of dimers, but this is not the only possibility. *T. maritima* MCPs form "hedgerows," long lines of receptors, as opposed to trimers of dimers, and it is postulated that these may come together to form larger lattices (reviewed in (Hazelbauer *et al.*, 2008; Kentner and Sourjik, 2006)). While residues important for trimerization are well-conserved, trimer of dimer formation has not been well-studied beyond *E. coli* (reviewed in (Hazelbauer *et al.*, 2008)).

These patches of MCPs are frequently localized to the poles and those that are non-polar tend to occur at future sites of cell division; more specifically, lateral clusters of MCPs occur at intervals corresponding to approximately $1/8^{th}$ the length of the cell, marking division sites of the next two generations (Thiem *et al.*, 2007). Polar localization and cluster formation are closely related, with the same region of MCPs being required for both (reviewed in (Kentner and Sourjik, 2006)). The role of polar

localization remains unclear, but several possibilities have been suggested. As mentioned above, although not well-accepted, it is possible that these polar arrays could function as a "nose" of sorts, allowing spatial gradient sensing, as opposed to, or in additional to, temporal gradient sensing (Thar and Kuhl, 2003) (reviewed in (Armitage, 2006)). Alternatively, polar localization may be required for receptor methylation or facilitate formation of higher order clusters of MCPs, which is in turn responsible for proper chemotactic responses (reviewed in (Armitage, 2006)). Finally, polar localization may simply be energetically favored by the shape of the higher order clusters/arrays (reviewed in (Kentner and Sourjik, 2006)).

In some bacteria, with multiple sets of chemotaxis proteins, differential localization may aid the separation of signaling from different chemotaxis systems. In particular, *R. sphaeroides* expresses multiple transmembrane MCPs, localized to poles, and non-membrane bound MCPs, termed transducer like proteins (Tlps), localized to discrete regions of the cytoplasm (reviewed in (Armitage, 2006)). Different subsets of chemotaxis proteins co-localize with either polar/MCP or cytoplasmic/Tlp arrays, indicating that their signaling is not integrated (reviewed in (Armitage, 2006)). An additional example of discrete patch formation occurs in *P. aeruginosa*. In *P. aeruginosa*, *che* genes are expressed throughout growth, while *che2* genes are only expressed during stationary phase (Guvener *et al.*, 2006). While a stationary phase-specific MCP, McpA, can be incorporated into the polar Che patches, Che2 patches remain distinct from Che patches (Guvener *et al.*, 2006). This occurs despite the fact that both Che and Che2 patches are polarly localized, frequently occurring at the same pole in

a given cell (Guvener *et al.*, 2006). The potential advantages of non-integration of signaling by subsets of chemotaxis proteins are unclear and demand further study.

MCPs and nonchemotaxis responses

Many bacteria other than *E. coli* express multiple sets of *che* genes (reviewed in (Szurmant and Ordal, 2004)). Some of these Che systems are not involved in chemotaxis, but in regulation of other phenotypes. The most studied cases of this occur in *Myxococcus xanthus*, a Gram-negative bacterium with a complex developmental life cycle. The *M. xanthus* genome encodes eight sets of *che* genes and several of these regulate chemotaxis via non-flagellar motility (using Type IV pili and adhesion complexes) (reviewed in (Zusman *et al.*, 2007)). The Che3 system, on the other hand, appears to regulate developmental gene expression based on nutrient availability via CrdA, a σ^{54} activator (reviewed in (Zusman *et al.*, 2007)). Additionally, the Che7 system is involved in regulating fatty acid composition during different developmental states (reviewed in (Zusman *et al.*, 2007)). In another variation on Che system functions, the Che6 system is involved in Type IV pilus assembly, but does not affect expression of Type IV pili genes (reviewed in (Zusman *et al.*, 2007)). The mechanisms underlying the regulatory activity of the Che6 and Che7 systems have not yet been described.

A set of *che* genes in *P. aeruginosa* encode the Wsp proteins involved in biofilm formation (reviewed in (Zusman *et al.*, 2007)). The Wsp response regulator, WspR, contains a GGDEF domain, which is involved in generation of the second messenger c-di-GMP, increased levels of which are associated with biofilm formation in many bacteria (Hickman *et al.*, 2005). A system with homology to Wsp regulates cellulose

production in *Pseudomonas fluorescens*, potentially via a similar mechanism (Hickman *et al.*, 2005).

Rhodospirillum centenum contains three Che systems, only one of which, Che1, is involved in chemotaxis (reviewed in (Zusman *et al.*, 2007)). The activity of Che2 has some similarity to Che6 of *M. xanthus*, as Che2 is required for flagellar assembly, but has no effect on flagellar gene expression, indicating that it acts post-transcriptionally (Berleman and Bauer, 2005). Che3, on the other hand, regulates *R. centenum* development (Berleman *et al.*, 2004). *R. centenum* forms cysts, a cell type that is resistant to several environmental stresses, in response to decreased nutrient availability. *che3* mutants, however, form cysts in rich media, where they would not ordinarily be formed (Berleman *et al.*, 2004).

E. coli chemotaxis genes are also apparently involved in development, as the chemotaxis system is required for swarming motility, but this motility does not involve chemotaxis (Burkart *et al.*, 1998). The mechanism behind this is unknown and it may be that flagellar mediated chemotactic movement affects swarming cell development, as opposed to the chemotaxis system playing a direct role in gene regulation (reviewed in (Harshey, 2003)). If the *E. coli* chemotaxis system does have a direct impact on gene regulation, it would be the only known instance of a chemotaxis system involved in both chemotaxis and gene regulation. In all other cases discussed here, chemotaxis systems are dedicated to regulating one or the other, but not both.

There are clear functional consequences of gene regulation and regulation of macromolecular structure assembly by chemotaxis systems stemming from the presence of adaptation mechanisms. In chemotaxis, various adaptation systems (discussed above)

allow a response to be triggered by a stimulus and then dampened in the presence of continued stimulation. Similarly, with gene regulation by Che systems one would expect changes in gene expression to be transitory, occurring with the initiation of signaling and falling off once signaling is attenuated by adaptation (reviewed in (Armitage, 2003; Zusman *et al.*, 2007). Using such a mechanism to control development of *M. xanthus* fruiting bodies and *R. centenum* cysts in response to high cell density or starvation would allow the initiation of development to occur for a brief period and be suppressed when genes involved in later stages of development are expressed, despite the fact that high cell density or starvation continues (reviewed in (Zusman *et al.*, 2007)).

Energy Taxis

Energy taxis behaviors

Energy taxis is the ability of microbes to alter their direction of motility in response to changes in the local environment affecting energy-generating processes (Alexandre *et al.*, 2004; Taylor and Zhulin, 1998). In this behavior, receptors sense changes in the redox state of components of the electron transport system (ETS) or in the closely coupled proton motive force (reviewed in (Taylor and Zhulin, 1998)). Energy taxis behaviors include some forms of aerotaxis, phototaxis, taxis to electron acceptors, and even chemotaxis in those cases where the bacteria sense chemicals based on changes in energy generation resulting from their metabolism (reviewed in (Alexandre and Zhulin, 2001; Alexandre *et al.*, 2004; Taylor and Zhulin, 1998; Taylor *et al.*, 1999)).

Discerning energy taxis behaviors from other kinds of taxis can be difficult and requires knowledge regarding the sensory mechanism involved. For example, both *E.*

coli and *B. subtilis* engage in aerotaxis, but *E. coli* senses changes in environmental oxygen indirectly through changes in the ETS (see below), whereas *B. subtilis* senses changes in oxygen directly via a myoglobin-like oxygen sensor (Hou *et al.*, 2000). Additionally, while energy taxis is necessarily metabolism-dependent, not all metabolism-dependent taxis is energy taxis. Some bacteria sense and respond to secondary metabolites, as opposed to responding to the original signal or changes in energy generation resulting from its metabolism (reviewed in (Alexandre *et al.*, 2004)).

Energy taxis transducers

Aer and Tsr, the *E. coli* energy taxis transducers discussed below, are the most well-understood energy taxis transducers to date. However, other energy taxis transducers that employ different energy sensing mechanisms have been identified. A phototaxis transducer, Ptr, has been identified in *R. centenum* (Jiang and Bauer, 2001). Ptr has a classical MCP topology, with two transmembrane domains, a periplasmic domain and a cytoplasmic HCD (Jiang and Bauer, 2001). The periplasmic domain contains a sequence motif resembling the b-type heme-binding sequence in cytochrome b_6, leading to the hypothesis that Ptr senses changes in photosynthesis associated electron transport via a heme cofactor (Jiang and Bauer, 2001).

An apparent aerotaxis transducer in *Desulfovibrio vulgaris* has been identified and shown to undergo methylation upon the addition of oxygen or a reducing agent indicating that it is an energy taxis transducer (Fu *et al.*, 1994). As a *dcrA* mutation does not have a significant impact on aerotaxis, it is assumed that there are additional aerotaxis/energy taxis transducers in this species (Fu and Voordouw, 1997). DcrA has a periplasmic region with a consensus c-type heme binding site and has been demonstrated to bind

heme (Fu *et al.*, 1994). Biophysical studies of DcrA-heme indicate that this protein may sense oxygen, redox and/or CO (Yoshioka *et al.*, 2005). It has been noted, however, that DcrA also possesses a cytoplasmic PAS domain (Ponting and Aravind, 1997), which does not bind a cofactor (unpublished data in (Yoshioka *et al.*, 2005)). Thus, DcrA may have two sensory modules and mediate responses to multiple redox signals.

Energy taxis, the dominant behavior in *Azospirillum brasilense* (Alexandre *et al.*, 2000), is mediated in part by the MCP-like protein Tlp1, although another unidentified energy taxis transducer is also postulated (Greer-Phillips *et al.*, 2004). Tlp1, like Ptr of *R. centenum*, has the topology of a classical MCP (Greer-Phillips *et al.*, 2004). The periplasmic region of Tlp1 has no homology to known functional domains or motifs, but similar periplasmic domains have been identified in a large number of predicted MCPs and histidine kinases in a diverse group of bacteria (Greer-Phillips *et al.*, 2004). Thus, this uncharacterized periplasmic domain may represent a novel and well-conserved energy sensing mechanism. Tlp1 was found to play a key role in root colonization by *A. brasilense*, a necessary step in the contribution of this bacterium to the growth of many agriculturally important crops (Greer-Phillips *et al.*, 2004).

In *H. pylori*, an energy taxis transducer, TlpD, was recently identified (Schweinitzer *et al.*, 2008). TlpD lacks any predicted transmembrane domains and does not possess homology to any known oxygen or redox sensing domains, leaving open the question of signal and sensory mechanism within this protein (Schweinitzer *et al.*, 2008).

Aer: An Energy Taxis Transducer in *E. coli*

Identification of energy taxis transducers in *E. coli*

A mechanism to alter motility based on the energy level of the cell had long been postulated prior to identification of any energy taxis receptors (reviewed in (Taylor, 1983; Taylor *et al.*, 1999)). Early studies led to the Links-Clayton hypothesis which proposed that the behaviors we now term energy taxis would be mediated by an ATP-sensor (Clayton, 1958). This hypothesis has since been discarded, as defects in ATP-synthesis have no effect on energy taxis behaviors. Rather, a collection of studies pointed to the more rapid changes in either the ETS or the closely coupled proton motive force as likely energy taxis signals (Bespalov *et al.*, 1996; Clancy *et al.*, 1981; Laszlo and Taylor, 1981; Miller and Koshland, 1977; Shioi *et al.*, 1988; Taylor *et al.*, 1979; Zhulin *et al.*, 1997). A comparison of the requirements for energy taxis with those of conventional chemotaxis indicated that these behaviors were both mediated by Che proteins (Laszlo and Taylor, 1981; Rowsell *et al.*, 1995). Energy taxis behaviors, however, did not require any known MCPs (Bespalov *et al.*, 1996; Laszlo and Taylor, 1981; Zhulin *et al.*, 1997), indicating that there may be another MCP-like protein responsible for transducing an energy taxis signal.

Aer, unlike the other *E. coli* MCPs, was identified as a likely aerotaxis/energy taxis transducer on the basis of sequence homology upon completion of the *E. coli* genome sequence (Bibikov *et al.*, 1997; Rebbapragada *et al.*, 1997). The N-terminus of Aer has similarity to other known oxygen sensors, including FixL, NifL and Bat, as well as the blue light sensor Wc-1 (Bibikov *et al.*, 1997; Rebbapragada *et al.*, 1997). This region is now known to contain a PAS domain that binds an FAD cofactor (Bibikov *et*

al., 1997; Bibikov *et al.*, 2000). Sequence analysis also indicated that Aer had a helical hairpin membrane anchor and a C-terminal HCD (Bibikov *et al.*, 1997; Rebbapragada *et al.*, 1997). An amphipathic sequence immediately following the membrane anchor was also noted (Rebbapragada *et al.*, 1997) and is now known to be a HAMP domain (Bibikov *et al.*, 2000). (See Fig. 5 for a schematic of Aer domains and topology.)

Behavioral assays with insertion and deletion mutants of *aer* demonstrated that this strain has altered – not abrogated – aerotaxis and energy taxis responses (Bibikov *et al.*, 1997; Rebbapragada *et al.*, 1997). An *aer tsr* double mutant, however, had no residual aerotaxis/energy taxis behavior (Rebbapragada *et al.*, 1997). Aerotaxis in this double mutant could be recovered by expression of either Aer or Tsr (Rebbapragada *et al.*, 1997). Together, these data indicate that Aer (Bibikov *et al.*, 1997; Rebbapragada *et al.*, 1997) and Tsr (Rebbapragada *et al.*, 1997) are the long sought after energy taxis transducers of *E. coli*.

Aer and Tsr could conceivably sense either electron transport or proton motive force. These proteins differ, however, in the strength of their responses to different oxidizable substrates in a manner consistent with the hypothesis that Aer senses redox changes and Tsr senses changes in proton motive force (Greer-Phillips *et al.*, 2003). To differentiate between these closely related processes, strains were designed that expressed one of two NADH dehydrogenase enzymes and one of two cytochrome oxidases (Edwards *et al.*, 2006). Pairwise combinations of different NADH dehydrogenases and cytochrome oxidases result in different H^+/e^- ratios (i.e. different numbers of protons exported per electron flowing through the ETS), giving rise to differing changes in proton motive force in response to oxygen (Edwards *et al.*, 2006). These mutants were

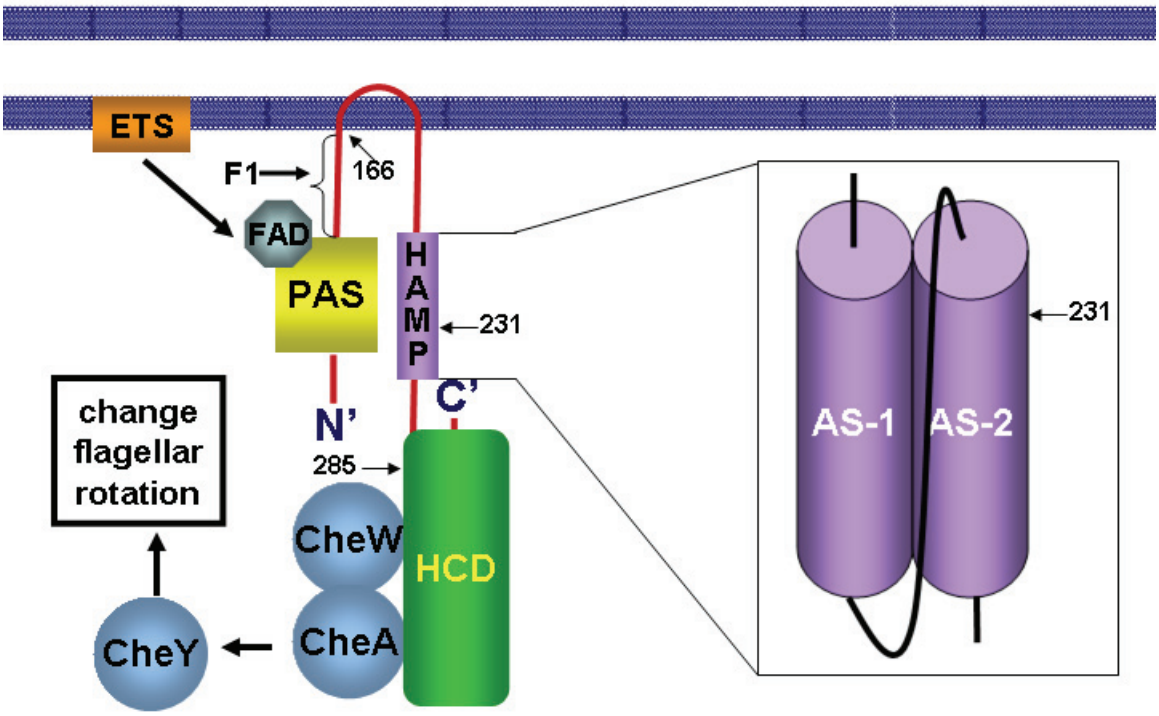

Figure 5. Schematic of Aer domains and topology. Aer contains an N-terminal PAS domain with an FAD cofactor thought to senses changes in electron transport. The PAS domain is linked to a transmembrane helical hairpin by the F1 segment. The HAMP domain, which consists of two helices (AS-1 and AS-2) resides between the membrane anchor and the C-terminal highly conserved signaling domain (HCD), which interacts with CheW and CheA to transmit a signal to the chemotaxis machinery. The locations of truncations discussed in the text are indicated.

combined with *aer* and/or *tsr* mutations in an attempt to correlate aerotactic responses to either proton motive force or electron transport. Tsr-mediated aerotaxis correlated well with the proton motive force (Edwards *et al.*, 2006).

Aer-mediated aerotaxis, on the other hand, did not correlate with either the proton motive force or respiration (Edwards *et al.*, 2006). Rather, Aer function was strongly affected by the presence or absence of NADH dehydrogenase I (NDH-1) (Edwards *et al.*, 2006). NDH-1 was not absolutely required for aerotaxis under all conditions, however (Edwards *et al.*, 2006). Specifically, NDH-1 was required for aerotaxis in temporal and plate assays, but not in capillary assays (Edwards *et al.*, 2006). Temporal assays assess the time required to return to prestimulus tumbling frequency after exposure to a change in oxygen concentration in a gas flow chamber (Edwards *et al.*, 2006). Plate assays involve the inoculation of a culture into a semi-solid agar plate. As the bacteria use up the available nutrients, they swim through to agar toward optimal concentrations of a carbon source or energy source forming rings of differing diameters (Edwards *et al.*, 2006). In capillary assays, liquid cultures are drawn into a capillary tube and an oxygen gradient results from the combination of bacterial metabolism and oxygen diffusion from the air in the capillary. The bacteria form a band at the position relative to the air-liquid interface where the optimal oxygen concentration occurs (Edwards *et al.*, 2006). The mechanism underlying the discrepancy in requirement of NDH-1 based on the assay method remains unclear. Nevertheless, this evidence suggests that Aer is a redox sensor and that NDH-1 is one potential source of the signal sensed by Aer, but cannot be the sole contributor (Edwards *et al.*, 2006).

Further information arises from studies of NADH-dependent flavin reductase (Fre). Fre affects, but is not required for, Aer-mediated aerotaxis (personal communication in (Taylor, 2007)). Fre reduces approximately 80% of the free cytoplasmic FAD, but might also interact with some proteins to provide FADH directly (Woodmansee and Imlay, 2002).

A detailed understanding of the source(s) of the Aer signal is one of the most significant unanswered questions regarding this protein (Taylor, 2007). It is clear that the Aer signal is closely related to the redox status of the ETS. Efforts using two-hybrid techniques to identify an Aer interaction partner that could link Aer to the ETS have been unsuccessful (personal communication in (Taylor, 2007)). It is possible that NDH-1 can reduce the Aer FAD cofactor directly, but in that case there must be another factor that can substitute for NDH-1 under some conditions (Edwards *et al.*, 2006), perhaps a quinone, NADH or free FAD(H_2) from the ETS (Taylor, 2007). As the Aer PAS domain has a relatively low affinity for FAD (discussed below) another possibility is that the Aer FAD cofactor exchanges with cytoplasmic FAD(H_2) pools, in which case the Aer FAD cofactor's redox state would reflect the cytoplasmic FAD/$FADH_2$ ratio (Taylor, 2007). Further studies are needed to differentiate between all of these possibilities.

Aer topology and dimerization

Aer localized to the membrane in subcellular fractionation experiments (Bibikov *et al.*, 1997). Sequence analysis indicates a hydrophobic segment approximately 40 residues in length occurring between the PAS and HAMP domains of Aer (Bibikov *et al.*, 1997). Although most transmembrane prediction programs suggest this region consists of a single transmembrane helix, placing the PAS domain in the periplasm, the length of

this segment and rarity of periplasmic PAS domains led to the prediction that this region instead forms two transmembrane helices in a hairpin conformation (Rebbapragada *et al.*, 1997). Such a membrane anchor would place the PAS domain and the HAMP and HCD domains in the cytoplasm (Rebbapragada *et al.*, 1997).

The topology of Aer has been probed with cysteine-scanning mutagenesis in the hydrophobic segment combined with *in vivo* disulfide cross-linking and accessibility studies (Amin *et al.*, 2006). These studies confirmed that Aer contains two transmembrane helices (TM1 and TM2) separated by a rigid four residue periplasmic loop (Amin *et al.*, 2006, 2007). Although the intervening periplasmic loop contains a proline, known to induce helical hairpins in transmembrane regions, many substitutions and insertions can be accommodated at this position while maintaining wildtype topology and function (Amin *et al.*, 2006). These results are consistent with an absence of a role of this periplasmic loop in signaling (Amin *et al.*, 2006).

Using native cysteines for *in vivo* disulfide cross-linking analysis, Aer was shown to form homodimers, with residues in the membrane anchor and HAMP domain present at the dimer interface (Ma *et al.*, 2004). Point mutations in the AS-2 of the HAMP domain that abrogate FAD binding (see below) had no effect on dimerization (Ma *et al.*, 2004). Additionally, Aer fragments Aer_{2-231} and Aer_{2-285} both dimerize, indicating that the HAMP domain (residues 206-258), although at the dimerization interface, is not required for dimerization (Ma *et al.*, 2004). Together these data demonstrate that the HCD domain, the HAMP domain and FAD binding are all dispensible for formation of the Aer homodimer (Ma *et al.*, 2004). Cysteine-scanning/cross-linking analysis also

indicated that the periplasmic loops of Aer monomers are in close proximity to one another within Aer homodimers and trimers of dimers (Amin *et al.*, 2007).

Aer PAS domain and FAD binding

PAS domains, named for the first three proteins in which they were found (Per, Arnt, Sim) (Nambu *et al.*, 1991) have been identified in eubacteria, archaea and eukaryotes. In eukaryotes, PAS domains are involved in such diverse phenotypes as Drosophila and mammalian development, mammalian oxygen homeostasis, mammalian circadian rhythm, human obesity, learning disabilities, and cardiac arrhythmia (reviewed in (Crews, 2003)). Most bacterial PAS domains are found in sensor kinases of two component systems, but they have also been found in other kinases, in transcriptional regulators and in proteins synthesizing the second messenger c-di-GMP (reviewed in (Taylor and Zhulin, 1999; Taylor *et al.*, 2003)). Bacterial PAS domains sense signals such as oxygen, cellular redox status and various wavelengths of light to regulate behaviors including nitrogen fixation and metabolism, root nodulation during plant symbiosis, photosystem biosynthesis, degradation of aromatic hydrocarbons, sporulation and virulence gene expression (reviewed in (Taylor and Zhulin, 1999; Taylor *et al.*, 2003)).

PAS domains sense changes in the environment via a wide variety of cofactors including FAD, FMN, heme, the 4-hydroxycinnamyl chromophore, iron-sulfur clusters or with no associated cofactor (reviewed in (Taylor and Zhulin, 1999; Taylor *et al.*, 2001)). Those PAS domains structures that have been solved share a glove-like fold, with variation in the central pocket that would presumably account for the ability of different

PAS domains to accommodate such different cofactors (reviewed in (Zhong *et al.*, 2003)).

The Aer PAS domain binds an FAD cofactor. Overexpression of Aer led to the accumulation of a chromophore at the membrane (Bibikov *et al.*, 1997). Fluorescence spectra and various chromatography techniques determined that this chromophore was likely FAD (Bibikov *et al.*, 1997). To definitively establish that Aer binds FAD, the protein was purified and denatured, which led to the release of a compound with the same mass (Bibikov *et al.*, 2000), HPLC retention time and fluorescence spectrum as FAD (personal communication in (Repik *et al.*, 2000)). The FAD cofactor was easily dissociated from Aer and could be extracted by overnight dialysis, indicating that Aer binds FAD less avidly than other flavoproteins do (personal communications in (Bibikov *et al.*, 2000; Repik *et al.*, 2000)). Once the mature Aer protein is folded, FAD binding is apparently not necessary for protein stability, as FAD can be removed by dialysis without ensuing degradation (personal communication in (Taylor, 2007)). FAD was isolated from Aer up to a ratio of one FAD per Aer monomer (personal communication in (Repik *et al.*, 2000)). Together with the easy dissociation of FAD from Aer, this suggests that one FAD cofactor participates in a reversible association with each Aer monomer. As discussed above, the accepted hypothesis is that the redox state of this FAD cofactor reflects the status of the ETS and that this is the signal sensed by Aer.

PAS domain regions and residues important for FAD binding and/or Aer function have been identified in screens of random and cysteine-scanning mutants, as well as truncations of Aer, for defects in aerotaxis (Bibikov *et al.*, 2000; Repik *et al.*, 2000; Watts *et al.*, 2006b). Most point mutants that abrogate FAD binding fall into the Aer PAS

domain (others are discussed below) and these point mutations are found in all predicted structural features of the PAS domain (Bibikov *et al.*, 2000). Mutation of one residue (Tyr111) predicted to be in the proximity of the FAD binding site gave rise to an intriguing phenotype. The Y111C point mutation led to an inverted aerotactic response; it caused tumbling (CW signal) in response to an oxygen increase where wildtype cells swim smoothly (CCW signal) (Repik *et al.*, 2000).

The N-terminal cap (Aer residues 1-19) is the least conserved region within PAS domains (Taylor *et al.*, 2001). Truncations in the N-terminal cap and an M21P substitution led to greatly diminished levels of Aer, while other substitutions in and near the N-terminal cap led to less severe reductions in Aer levels (Watts *et al.*, 2006b). This indicates that the N-terminal cap is critical for the stability of Aer. In addition, the junction of the N-terminal cap and the PAS core seems critical for Aer signaling, as this was a "hot spot" for null aerotactic mutants (Watts *et al.*, 2006b).

The N-terminal cap participates in the dimer interface of the *E. coli* direct oxygen sensor (DOS) protein PAS domain (Kurokawa *et al.*, 2004), raising the hypothesis that the N-terminal cap of Aer could be contributing to Aer function by aiding dimerization. The position of the N-terminal cap in a homodimer was explored using cysteine substitution and *in vivo* disulfide cross-linking experiments (Watts *et al.*, 2006b). These experiments indicated that N-terminal cap is not a dimerization interface, but rather faces outward from the Aer homodimer, requiring lateral diffusion in the membrane to collide with the N-terminal cap of other homodimers (Watts *et al.*, 2006b). In fact, although PAS domains often form homodimers, there is no evidence to date that the PAS domain of Aer dimerizes (Taylor, 2007). That being said, $Aer_{2\text{-}231}$ dimerizes despite an inability

to bind FAD, indicating that the PAS domain, F1 segment and membrane anchor are sufficient for dimerization (Ma *et al.*, 2004). As there is no significant homology between Aer homologues in the membrane anchor or F1 regions, it seems likely that the PAS domain does mediate dimerization. Additional studies are necessary to test this hypothesis.

The current model of the Aer FAD redox signal is as follows (Repik *et al.*, 2000; Taylor, 2007; Watts *et al.*, 2006b). During maximal electron transport, the semi-quinone form of FAD ($FADH^{\cdot}$) predominates. Sub-maximal electron transport may be detected by increased levels of the fully oxidized (FAD) and fully reduced ($FADH_2$) forms. Either FAD or $FADH_2$ lead to a CW signal (tumbling), whereas $FADH^{\cdot}$ leads to a CCW signal (smooth swimming). In this model, the inverted response of the Y111C mutant can be explained if the wildtype tyrosine is in close proximity to the FAD moiety and the presence of a cysteine residue in the mutant shifts the redox potential of the FAD cofactor such that FAD, rather than $FADH^{\cdot}$, predominates during maximal electron transport, leading to an inappropriate CW signal (tumbling) (Repik *et al.*, 2000; Taylor, 2007).

Evidence for a HAMP-PAS interaction

As discussed above, conventional MCPs transmit a signal from the periplasm to the cytoplasmic HCD via a shift of their transmembrane helices relative to one another. Due to the unique topology of Aer, where both the input (PAS) and output (HAMP, HCD) domains are located in the cytoplasm, a different route of signal transduction seems likely within this protein. Rather than traversing the inner membrane, the Aer signal has been proposed to move parallel to the membrane by direct interaction of the PAS and HAMP domains (reviewed in (Taylor, 2007)). More than 1200 proteins are

predicted by SMART analysis to include both PAS and HAMP domains. Thus, there is significant interest in the possibility that these domains have functional interactions in signal transduction and in Aer as a model for these proposed interactions.

The Aer HAMP domain appears to be required for proper maturation of the protein and FAD binding by the PAS domain. Analysis of Aer fragments created by nonsense mutations indicated that both the PAS domain and the HAMP domain are required to bind FAD (Bibikov *et al.*, 2000). Further experiments indicated that a fragment consisting solely of the PAS domain and F1 segment of Aer (Aer_{2-166}) was predominantly insoluble, residing in inclusion bodies or a non-dissociable complex with the chaperone protein GroEL (Herrmann *et al.*, 2004). These data indicate that this fragment cannot fold in an aqueous environment, leading to the hypothesis that the folding of the Aer PAS domain requires regions of Aer outside of the PAS domain itself (Herrmann *et al.*, 2004). Fragments consisting of Aer residues 2-231 and 2-285, which include the membrane anchor, both insert into the membrane, however, Aer_{2-285} binds FAD and Aer_{2-231} does not (Herrmann *et al.*, 2004). These data suggest that residues 231-285, which includes much of the Aer HAMP domain (residues 206-258) and proximal signaling domain, are required for binding of FAD by the PAS domain (Herrmann *et al.*, 2004).

Several point mutations in the Aer HAMP and proximal signaling domains have been found to abrogate FAD binding (Bibikov *et al.*, 2000; Buron-Barral *et al.*, 2006; Ma *et al.*, 2005; Watts *et al.*, 2004; Watts *et al.*, 2008b). Point mutations that affected FAD binding predominantly clustered in the HAMP domain AS-2 (see below) (Ma *et al.*, 2005; Watts *et al.*, 2004). HAMP domain mutants that eliminate FAD binding were used

to screen for psuedorevertants. Several second site mutations in the PAS domain restored FAD binding in the HAMP mutant backgrounds (Watts *et al.*, 2004). Most of these were non-specific, with three point mutants (S28G, A65V and A99V) restoring FAD binding to a large number of HAMP point mutants (Watts *et al.*, 2004).

The interpretation of these point mutation results, however, has recently been called into question by the finding that many of these point mutants affect the stability of Aer, and this may be responsible for the lower levels of FAD-binding observed (Buron-Barral *et al.*, 2006). This conclusion is supported by the fact that the "general suppressor" of these mutations, S28G, dramatically increases the stability of Aer (Buron-Barral *et al.*, 2006). This would provide a mechanism for counteracting the effects of HAMP mutations that does not necessarily require direct interaction between the domains.

More definitive evidence of a HAMP-PAS interaction arises from the discovery of allele specific second site suppressors in each domain. One HAMP point mutant (C253R) was not complemented by the aforementioned non-specific suppressors and was used to screen for specific suppressors (Watts *et al.*, 2004). Such a pseudorevertant was identified (N34D), which was specific to C253R (i.e. it did not restore FAD binding to other HAMP point mutants (Watts *et al.*, 2004)). N34 is not predicted to be located near the predicted FAD binding pocket (Watts *et al.*, 2004). A reverse screen for suppressors of the N34D point mutant yielded only C253R (Watts *et al.*, 2004). This specific pair of suppressor mutations is strong, albeit indirect, evidence of a direct interaction between the PAS and HAMP domains of Aer.

Aer HAMP domain structure

The identity of the HAMP domain of Aer was confirmed by PSI-BLAST (Ma *et al.*, 2005). However, the predicted secondary structure of the Aer HAMP domain differs significantly from that of other HAMP domains. While most HAMP domains consist of two amphipathic helices separated by a connector, the Aer HAMP domain is predicted to contain one amphipathic helix (AS-1) and one hydrophobic, or buried, helix (AS-2) separated by the connector (Ma *et al.*, 2005). Based on the genetic evidence discussed above, it appears that AS-2 may mediate HAMP-PAS interactions, in addition to participating in HAMP-HAMP interactions within a dimer (Ma *et al.*, 2005; Watts *et al.*, 2004), possibly explaining why this helix is predicted to be buried.

Cysteine-scanning/cross-linking analysis was combined with *in silico* modeling of the Aer HAMP and proximal signaling domains to test their predicted secondary and tertiary structures (Watts *et al.*, 2008b). The results of this analysis were consistent with a HAMP domain containing two α-helices in a coiled-coil separated by a structured loop (Watts *et al.*, 2008b). In the case of both helices (AS-1 and AS-2), the rate of dimerization was inversely correlated with the β-carbon distances in the *in silico* model (Watts *et al.*, 2008b). As this model was constructed using the coordinates of the Af1503 HAMP domain structure (Hulko *et al.*, 2006), it appears that both HAMP domains share the same structure. There is no such correlation between dimerization rates and predicted β-carbon distances in the connector region between AS-1 and AS-2, indicating that either this region is flexible or the structure of the connector differs between Aer and Af1503 (Watts *et al.*, 2008b).

When mapped onto the *in silico* model of the Aer HAMP domain, several previously identified CW-biased point mutations clustered together at the base of the HAMP domain four-helix bundle (Watts *et al.*, 2008b). These point mutations may alter signal input to the HAMP domain, locking the HAMP domain in the CW-signal conformation (Taylor, 2007; Watts *et al.*, 2008b). Thus, this cluster of residues may represent a PAS domain interaction surface (Taylor, 2007; Watts *et al.*, 2008b). Such a surface would have direct bearing on the hypothesis that the Aer signal is transmitted directly from the PAS domain to the HAMP domain.

Analysis of the Aer proximal signaling domain by cysteine-scanning mutagenesis and *in vivo* disulfide cross-linking supported a coiled-coil α-helical structure for this region as well (Watts *et al.*, 2008b). However, the helix is not continuous as there is evidence for a loop in the middle of the proximal signaling domain, indicating that this domain actually consists of extensions of the AS-2 helix and signaling domain helix, both separated by a loop (Watts *et al.*, 2008b). Although the position is slightly different from that within other MCPs, this loop likely corresponds to the hinge with the flexible bundle which is postulated to translate HAMP rotation into bending of the signaling domain (Alexander and Zhulin, 2007; Watts *et al.*, 2008b).

Role of membrane anchor and F1 segment

The membrane anchor of Aer appears to contribute to proper folding of the protein. Aer_{2-166}, which terminates immediately prior to the membrane anchor (residues 167-205), is found in inclusion bodies and in a non-dissociable complex with GroEL (Herrmann *et al.*, 2004). In contrast, Aer_{2-231} inserts in the membrane, indicating that it is released from the GroEL complex (Herrmann *et al.*, 2004). These data indicate that the

membrane domain may be required for Aer folding. However, Aer_{2-231} does not bind FAD (Herrmann *et al.*, 2004), indicating that elements beyond the membrane anchor, specifically the HAMP domain, are required for complete maturation of the protein.

There is no apparent conservation in the membrane anchor region among Aer homologues (Bibikov *et al.*, 2000), and mutations affecting aerotaxis have not been identified in this region to date. Therefore, it is likely that the membrane anchor affects Aer folding indirectly, perhaps by maintaining proper orientation of the PAS and HAMP domains. The membrane anchor may also serve to bring the PAS domain of Aer in close proximity to the ETS (Bibikov *et al.*, 2000). An Aer mutant with the membrane anchor deleted, but all other functional domains intact, neither associated with the membrane nor bound FAD (Bibikov *et al.*, 2000). Whether this membrane anchor deletion is in inclusion bodies or in complex with GroEL was not determined, so it is not yet possible to differentiate between potential roles of this region in Aer folding and function. However, a functional Aer homologue lacking a membrane anchor has been characterized (see below), confirming that this region should be not critical for signal transduction.

The region between the PAS domain and membrane anchor of Aer has been designated the F1 segment (Bibikov *et al.*, 2000). Point mutations in the F1 segment that lead to an aerotaxis defect have been identified (Bibikov *et al.*, 2000; Buron-Barral *et al.*, 2006), albeit with much lower frequency than HAMP point mutations (Buron-Barral *et al.*, 2006). As with the membrane anchor, there is no significant homology among Aer homologues in the F1 segment (Bibikov *et al.*, 2000). However, both monomers in an Aer homodimer need to possess the F1 segment to be functional (Watts *et al.*, 2006a).

Together, these data suggest that the F1 segment may contribute indirectly to Aer function, perhaps playing a role in proper folding or orientation of the protein.

Route of signal transduction within an Aer dimer

The HAMP-PAS interaction required for FAD binding and the signaling pathway in Aer could each conceivably be either intra- or inter-subunit within an Aer homodimer. Using intragenic complementation experiments, combining multiple point mutations and/or truncations within monomers or mixed dimers, it was established that HAMP-PAS interaction between cognate subunits in an Aer dimer is required for FAD binding (Watts *et al.*, 2006a). In contrast, the signaling pathway involved the PAS domain and HCD within a single subunit (Watts *et al.*, 2006a). Signaling required only one PAS domain and one HCD in each dimer, and these had to be in the same monomer (Watts *et al.*, 2006a). Two full-length HAMP domains were required for aerotaxis, but a HAMP point mutation that abrogates FAD binding could be tolerated if present on the subunit possessing both functional PAS and HCD domains (Watts *et al.*, 2006a).

These data are consistent with three models of signal transduction within Aer (Watts *et al.*, 2006a): 1) The signal is transduced from a PAS domain to the HAMP domain on the same dimer, via interactions that are different from those between cognate subunits supporting FAD binding. 2) The signal is transduced from a PAS domain to the cognate HAMP domain and back to the HCD of the original subunit. 3) The signal is transmitted directly from a PAS domain to the proximal signaling domain of the same monomer, and the HAMP domain is not involved in signaling. The evidence for a role of HAMP domains in signal transduction within other proteins argues against this last possibility, but it cannot yet be ruled out.

Interactions with other MCPs

There are approximately 300 copies of Aer per *E. coli* cell (personal communication in (Taylor *et al.*, 2001)), making Aer a low-abundance chemoreceptor (Li and Hazelbauer, 2004). Based on these estimates, if MCP dimers are randomly incorporated into trimers of dimers, Aer would be predicted to exist almost exclusively in mixed trimers of dimers (i.e. trimers containing one Aer homodimer and two homodimers of other MCPs) (Gosink *et al.*, 2006). If Aer is expressed to high levels in the absence of other MCPs, it can form Aer-exclusive trimers of dimers (Gosink *et al.*, 2006). However, when the high-abundance MCP Tar is present, Aer forms mixed trimers of dimers and shows no preference for unmixed (Aer-exclusive) trimers of dimers (Gosink *et al.*, 2006). The ability of Aer to form mixed trimers of dimers indicates that the absence of a large periplasmic sensory domain and the presence of the cytoplasmic PAS domain in Aer do not interfere with trimer of dimer formation (Amin *et al.*, 2007). As with other trimers of dimers in a complex including CheA and CheW (Studdert and Parkinson, 2005), these associations are quite stable and do not exchange neighbors over time (Amin *et al.*, 2007). As Aer is a low abundance chemoreceptor, it would be expected to have minimal impact on the steady-state activity of CheA in wildtype *E. coli* (Gosink *et al.*, 2006). In fact, in the absence of other MCPs, Aer must be expressed to levels approximately equivalent to the total number of MCPs in a wildtype cell to promote optimal energy taxis (Gosink *et al.*, 2006).

Adaptation

Prior to the identification of Aer, it was established that aerotaxis by *E. coli* did not require the methylation/adaptation elements of the chemotactic machinery (Bespalov

et al., 1996; Niwano and Taylor, 1982; Zhulin *et al.*, 1997). The Aer HCD lacks the consensus methylation sites present in the other *E. coli* MCPs (Bibikov *et al.*, 2004). HCD methylation in MCPs can be detected by SDS-PAGE, as CheR and CheB modifications lead to changes in their gel mobility of MCPs. However, no CheR or CheB dependent mobility shifts are seen with Aer (Bibikov *et al.*, 2004). Moreover, CheR, CheB, the other MCPs and the noncanonical sites corresponding to normally methylated regions of the HCD are all dispensible for Aer-mediated aerotaxis (Bibikov *et al.*, 2004). Further, a chimera consisting of the PAS-TM-HAMP regions of Aer fused to the HCD of Tar is capable of both methylation-dependent and methylation-independent aerotaxis (Bibikov *et al.*, 2004). This result was surprising in that it indicated that the PAS-TM-HAMP portion of Aer, rather than the HCD, was sufficient for methylation-independence (Bibikov *et al.*, 2004; Taylor, 2004). This observation led to the suggestion that the methylation-independence of Aer may be attributable to the signal that Aer senses. If the redox signal sensed by the PAS domain FAD cofactor is transient, then the Aer response may also be inherently transitory and adaptation would not be necessary (Bibikov *et al.*, 2004; Taylor, 2004).

Evidence from other energy taxis systems indicates, however, that some are methylation-independent. Aerotaxis by an Aer homologue in *Pseudomonas aeruginosa* appears to be methylation dependent (Hong *et al.*, 2004b). Energy taxis in *Azospirillum brasilense*, which is not mediated by an Aer-homologue, is methylation-independent (Stephens *et al.*, 2006). The *D. vulgaris* energy taxis receptor DcrA, also not an Aer homologue, is methylated upon exposure to oxygen or a reducing agent, but whether methylation is necessary for energy taxis has not been determined (Fu *et al.*, 1994). It

may be that different energy taxis transducers and various stimuli lead to differing requirements for methylation.

Effect on gene expression

A study examining the effect of mutations in the master flagellar transcriptional activators, FlhC and FlhD, on gene expression in *E. coli* suggested a role for Aer in gene regulation (Pruss *et al.*, 2003). Aer was upregulated by FlhC and FlhD (Pruss *et al.*, 2003), presumably via the sigma factor, σ^{28}, as sequence analysis indicates that Aer has a σ^{28}-dependent promoter (Park *et al.*, 2001). Microarray and transcriptional fusion analysis indicated that Aer is involved in activating transcription of several genes encoding enzymes involved in anaerobic respiration, as well as the Entner-Doudoroff pathway, the major route of degradation of sugar acids (Pruss *et al.*, 2003). The authors of this study indicated preliminary evidence, involving a *cheY* mutant, that this regulation by Aer is independent of its role in chemotaxis, however this data has not yet been published (Pruss *et al.*, 2003). While other MCPs have been implicated in gene regulation, those systems usually involve alternate sets of chemotaxis proteins that are involved strictly in gene regulation, as opposed to chemotaxis (discussed above). As there is only one set of chemotaxis proteins in *E. coli*, the mechanism of gene regulation by Aer remains to be elucidated. Without publication of the data showing that Aer-mediated regulation is independent of its function in chemotaxis, it is impossible to discount the possibility that this apparent gene regulation is instead due to the altered environment encountered by bacteria incapable of energy taxis.

Aer homologues in other organisms

Aer homologues were originally identified on the basis of sequence homology in *Pseudomonas putida*, *Yersinia pestis*, *V. cholerae* (three orfs), *Shewanella putrifaciens*, *Salmonella typhimurium* and the transposon Tn1721 (Bibikov *et al.*, 2000). To identify other potential Aer homologues, I used the SMART architecture analysis tool (Letunic *et al.*, 2004). This analysis identified proteins with domain architecture similar to that of Aer in 45 Gram-negative genera. A SMART search for proteins that contain a PAS domain and HCD (or MA, for methyl-accepting domain), without regard for domain order or the presence or absence of transmembrane regions or other functional domains, currently identifies 587 eubacterial proteins including some in Gram-positives, 34 archaeal proteins and one protein in the eukaryote *Oryza sativa* (rice).

Clearly, Aer-like proteins are quite common and widespread. However, only a handful of Aer homologues have been characterized. Of three apparent Aer homologues in *V. cholerae*, only one functions in aerotaxis *in vitro* (Boin and Hase, 2007). Several Aer homologues have been identified in *P. putida*, including one lacking a transmembrane region (Nichols and Harwood, 2000; Sarand *et al.*, 2008). Two of the membrane-bound Aer homologues, in different strains, have been found to contribute to aerotaxis (Nichols and Harwood, 2000) and metabolism-dependent taxis to (methyl)phenols (Sarand *et al.*, 2008).

In *P. aeruginosa*, two Aer homologues were identified, including one lacking a transmembrane region (Hong *et al.*, 2004b). Both of these contribute to aerotaxis, as single mutants have altered aerotaxis, and a double mutant lacks an aerotactic response (Hong *et al.*, 2004b). This is the only evidence to date that an Aer protein lacking a

membrane anchor can transduce an energy taxis signal, although such proteins are identified by SMART and comprise an uncharacterized family of proteins, termed McpA homologues, identified in several bacteria on the basis of sequence alone (Minerdi *et al.*, 2002). Oddly, an apparent Aer homologue lacking a membrane anchor was identified and found to be important for various forms of chemotaxis in *Sinorhizobium meliloti*, but the PAS domain was dispensible for this phenotype (Meier *et al.*, 2007).

Recently, two Aer homologues were identified and demonstrated to function in aerotaxis of the plant pathogen *Ralstonia solanacearum* (Yao and Allen, 2007). Both Aer homologues are required for wildtype levels of localization to and aggregation on tomato roots (Yao and Allen, 2007). Additionally, mutants in both *aer* genes appear to overproduce biofilm compared to wildtype and to levels similar to nonmotile and nontactic mutants, indicating that aerotaxis is a key regulator of biofilm formation in this species (Yao and Allen, 2007).

An additional link between an Aer homologue and biofilm formation can be found in *P. aeruginosa*. Recently, another Aer homologue was identified in *P. aeruoginosa*, containing two PAS domains and an HCD (Morgan *et al.*, 2006). This protein, BldA, was important in biofilm dispersal in response to sudden changes in a variety of stimuli (Morgan *et al.*, 2006). Surprisingly, biofilm dispersal required neither flagella-mediated swimming or pili-mediated twitching motility, indicating that the affect of BldA on biofilm dispersal was not mediated by an affect on energy taxis or chemotaxis (Morgan *et al.*, 2006). Rather, it appears that BldA has a dramatic affect on c-di-GMP levels, which in turn regulate the adhesive nature of the bacterium (Morgan *et al.*, 2006). The nature of the link between BldA and c-di-GMP levels is not clear, but BldA does not

appear to affect c-di-GMP directly, as it does not possess GGDEF or EAL domains (Morgan *et al.*, 2006).

While Aer homologues in *E. coli* and *Salmonella* appear to be regulated in a σ^{28}-dependent manner (Frye *et al.*, 2006; Park *et al.*, 2001), there is evidence of additional layers of regulation of Aer homologues in other bacteria. In *P. aeruginosa*, the anaerobic regulator ANR upregulates expression of one Aer homologue, but not the other Aer homologue which lacks a membrane anchor (Hong *et al.*, 2004a). Conversely, the Aer homologue lacking a membrane anchor is upregulated by the stationary phase σ-factor RpoS, but the other Aer homologue is not (Hong *et al.*, 2005). In *Shewanella oneidensis*, the transcript encoding an Aer homologue is upregulated in the presence of metal terminal electron acceptors (Beliaev *et al.*, 2005), but the mechanism underlying this regulation remains unclear. Three Aer homologues in one strain of *P. putida*, one lacking a membrane anchor, were differentially regulated over the course of the growth curve and in response to different carbon sources (Sarand *et al.*, 2008). Differential regulation may explain why only some Aer homologues in strains harboring multiple homologues have been seen to affect aerotaxis *in vitro*.

Motility and Taxis in *C. jejuni*

C. jejuni flagella and flagellar regulation

C. jejuni flagella and flagellar motility are vital to many aspects of *C. jejuni* biology, including host colonization, virulence in ferret models, secretion and host-cell invasion. Consequently, the regulation of flagella biogenesis and motility is an active area of research. Various studies have elucidated a flagellar regulatory hierarchy that

includes σ^{54} (encoded by *rpoN*) and σ^{28} (encoded by *fliA*) as the flagellar σ-factors and the two-component system FlgRS (which is phase variable) (Carrillo *et al.*, 2004; Colegio *et al.*, 2001; Hendrixson and DiRita, 2003; Hendrixson, 2006; Jagannathan *et al.*, 2001; Wosten *et al.*, 2004). FlgR apparently represents a new class of NtrC-like regulators that lack a DNA-binding motif (Joslin and Hendrixson, 2008). Homologues of the flagellar master regulators FlhC and FlhD, which are crucial for flagellar gene expression in other species, have not been identified in the *C. jejuni* genome (Parkhill *et al.*, 2000). Two proteins, FlgP and FlgQ, that are required for flagellar motility have recently been identified, but their roles are unclear; no homologues of these proteins are found in *E. coli* and only uncharacterized homologues have been identified in other species (Sommerlad and Hendrixson, 2007).

C. jejuni flagella contribute to more than just motility. As mentioned above, the flagellum is the only identified secretion mechanism in *C. jejuni*. Additionally, there is accumulating evidence that the *C. jejuni* flagellum contributes to biofilm formation (Kalmokoff *et al.*, 2006; Reeser *et al.*, 2007). Finally, *C. jejuni* flagellin does not stimulate TLR-5, due to deviations from the more common residues at the locations recognized by this innate immune receptor (Andersen-Nissen *et al.*, 2005).

C. jejuni **chemotaxis mechanisms**

Chemotaxis probably has an important role in both the commensal and pathogenic lifestyles of *C. jejuni*. *C. jejuni* has a flagellum at one or both poles and apparently swims by alternating runs and tumbles, but in high viscosity this changes to runs and pauses (Szymanski *et al.*, 1995), presumably due to the lessened impact of Brownian motion. *C. jejuni* motility in high viscosity is highly relevant, as the bacterium is often

found in the mucous layer of the gastrointestinal tract. In fact, *C. jejuni* motility appears well-suited to this environment, as its swimming velocity, which is already much higher than many other bacteria, increases with increasing viscosity (Szymanski *et al.*, 1995). *C. jejuni* displays chemotactic motility towards amino acids that are found in high levels in the chick gastrointestinal tract, organic acid intermediates of the TCA cycle and components of mucus including fucose (Hugdahl *et al.*, 1988). Non-mucin bile components are chemorepellents (Hugdahl *et al.*, 1988). Mutants that lack either *cj0019c* (DocB) or *cj0262c*, which are both methyl-accepting chemotaxis receptors (there are ten in total), show decreased chick colonization, but the attractants or repellents to which these proteins respond are unknown (Hendrixson and DiRita, 2004). Strains that either lack or overexpress CheY show decreased virulence in the ferret model (Yao *et al.*, 1997). All of these data demonstrate the central role of motility and chemotaxis in *C. jejuni* commensalism and pathogenesis.

Genome sequence analysis has shown that the *C. jejuni* genome encodes most features of the *E. coli* chemotaxis system (Marchant *et al.*, 2002; Parkhill *et al.*, 2000). However, *C. jejuni* lacks a homologue of the *E. coli* phosphatase CheZ, but does possess a homologue of CheV (Marchant *et al.*, 2002; Parkhill *et al.*, 2000) which may act as a phosphate sink. *C. jejuni* also encodes a homologue of HP0170 (discussed above) which may be a CheY-P phosphatase, although that has not been tested (Terry *et al.*, 2006).

C. jejuni adaptation systems have not been studied, but sequence analysis raises some interesting possibilities. *C. jejuni* CheR falls in the pentapeptide-independent class by sequence analysis and all of *C. jejuni* MCPs lack pentapeptide sequences (Perez and Stock, 2007). In addition, only some *C. jejuni* MCPs possess methylation sites

(Marchant *et al.*, 2002). *C. jejuni* CheB is unique in that it does not contain a response regulator domain (Marchant *et al.*, 2002). This leads to the hypothesis that both methylation and demethylation of MCPs might both be constitutive in *C. jejuni* and leaves open the question of how adaptation occurs in this bacterium (Marchant *et al.*, 2002). Perhaps CheV-mediated adaptation (discussed above) is the only means of adaptation necessary for *C. jejuni*, as appears to be the case with the close relative *H. pylori* (Marchant *et al.*, 2002). The presence of both CheR and CheB as well as methylation sites on some MCPs, however, suggests that there may be a role for methylation-dependent adaptation in chemotaxis to some stimuli.

Clearly, *C. jejuni* chemotaxis combines elements of the signal transduction pathways of *E. coli*, *B. subtilis* and others. While understanding these model systems will aid our study of *C. jejuni* chemotaxis, much remains to be understood in terms of how these elements combine to control *C. jejuni* motility.

C. jejuni energy taxis

An energy taxis system identified in *Campylobacter jejuni* consists of a variation on the domain arrangement found in Aer (Fig. 6). A transposon screen of mutants with defects in motility identified insertions in *cetA* and *cetB*, which are encoded by adjacent genes on the *C. jejuni* genome (Hendrixson *et al.*, 2001). CetB contains a predicted PAS domain and no other functional domains. CetA is predicted to contain a transmembrane region, a HAMP domain and the HCD. Mutants lacking *cetA* or *cetB* are deficient in energy taxis (Hendrixson *et al.*, 2001). A gene upstream of *cetA*, *cj1191c*, was also noted to have high levels of similarity to *cetB*, although no role for this gene in energy taxis is known.

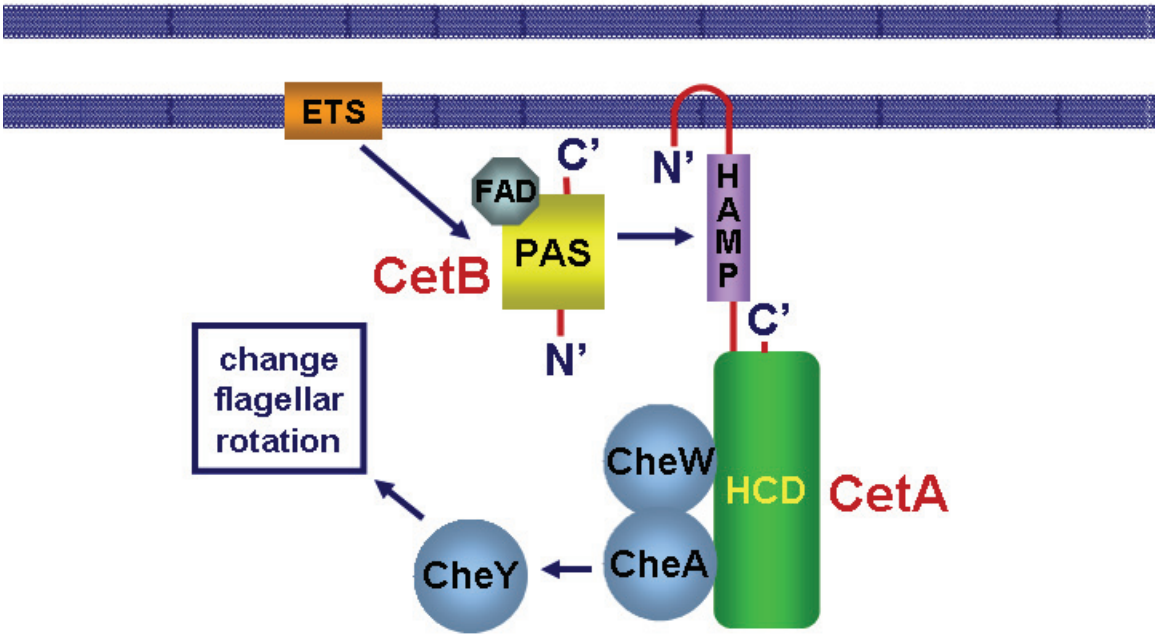

Figure 6. Schematic of predicted domains, topology and interactions of CetA and CetB. CetB contains a predicted PAS domain. CetA contains a predicted transmembrane region, HAMP domain and HCD. We hypothesize that CetB interacts with CetA to transduce an energy taxis signal.

These studies led to the hypothesis that CetA and CetB interact to transduce an energy taxis signal via a similar mechanism as that proposed for the single protein Aer. Specifically, we predict that CetB interacts with the HAMP domain of CetA, as is suggested of the PAS and HAMP domains of Aer. An additional hypothesis arises from the division of the domains of Aer into two proteins. We hypothesize that CetA and/or CetB may be able to interact with other proteins to regulate phenotypes other than energy taxis. This dissertation aims to test these hypotheses. Chapter II contains the molecular and biochemical characterization of CetA and CetB and includes experiments aimed at determining whether these proteins interact with each other. Chapter III tests whether the domain architecture of CetA and CetB are unique to *Campylobacter* and whether these proteins may be involved in separate cellular processes other than energy taxis.

CHAPTER II

CHARACTERIZATION OF CETA AND CETB, A BIPARTITE ENERGY TAXIS SYSTEM IN *CAMPYLOBACTER JEJUNI*

Summary

The energy taxis receptor Aer, in *Escherichia coli*, senses changes in the redox state of the electron transport system via an FAD cofactor bound to a PAS domain. The PAS domain is thought to interact directly with the Aer HAMP domain to transmit this signal to the highly conserved domain (HCD) found in chemotaxis receptors. An energy taxis system in *Campylobacter jejuni* is composed of two proteins, CetA and CetB, that have the domains of Aer divided between them. CetB has a PAS domain, while CetA has a predicted transmembrane region, HAMP domain and the HCD. In this study, we examined the expression of *cetA* and *cetB*, as well as the biochemical properties of the proteins they encode. *cetA* and *cetB* are co-transcribed independently of the flagellar regulon. CetA has two transmembrane helices in a helical hairpin, while CetB is a peripheral membrane protein very tightly associated with the membrane. CetB levels are CetA-dependent. Additionally, we demonstrated that both CetA and CetB participate in complexes, including a likely CetB dimer and a complex that may include both CetA and CetB. This study provides a foundation for further characterization of the signal transduction mechanisms within CetA/CetB.

Introduction

Motile bacteria alter the direction in which they swim based on changes in the local environment. These changes can be sensed directly in classical chemotaxis, where changes in the local concentration of a stimulus (i.e. an amino acid or sugar) are sensed in a metabolism-independent fashion, often by transmembrane methyl-accepting chemotaxis proteins (MCPs). Changes in the local environment can also be sensed indirectly by monitoring energy-generating processes within the cell. In this behavior, termed energy taxis, receptors sense changes in the redox state of components of the electron transport system (ETS) or in the closely coupled proton motive force (Taylor and Zhulin, 1998). Energy taxis behaviors include some forms of aerotaxis, phototaxis, taxis to electron acceptors, and even chemotaxis in those cases where the bacteria sense chemicals based on changes in energy generation resulting from their metabolism (Alexandre *et al.*, 2004; Taylor and Zhulin, 1998; Taylor *et al.*, 1999).

Energy taxis receptors and their signal transduction mechanisms have been well-characterized in *Escherichia coli*. *E. coli* contains two energy taxis receptors: Tsr, a classic serine-responsive MCP that also senses changes in the proton motive force, and Aer, which senses changes in the redox state of element(s) of the ETS (Rebbapragada *et al.*, 1997). Aer has been suggested to sense these changes via the redox state of an FAD cofactor bound to the N-terminal PAS domain (Taylor, 2007). This signal is thought to be transmitted to the HAMP domain of Aer (named for its presence in histidine kinases, adenylyl cyclases, MCPs and phosphatases) (Aravind and Ponting, 1999) by a direct PAS-HAMP interaction (Taylor, 2007). Finally, the HAMP domain relays the signal to the highly conserved domain (HCD) (named for its prevalence in MCPs) (Taylor, 2007).

Aer also possesses two transmembrane domains with a small intervening periplasmic loop, but there is, as yet, no evidence for the involvement of this region in signal transduction (Amin *et al.*, 2006). This differs from classical MCPs which are thought to transmit signals sensed by a periplasmic domain to the HAMP and HCD domains by a shift in their transmembrane helices (Chervitz and Falke, 1996; Moukhametzianov *et al.*, 2006).

Flagellar motility plays a vital role in the pathogenicity of *C. jejuni*, one of the most common causes of gastroenteritis in the United States, as well as in its colonization of livestock reservoirs, most commonly poultry (Guerry, 2007; Young *et al.*, 2007). An energy taxis system identified in *Campylobacter jejuni* consists of a variation on the domain arrangement found in Aer. A transposon screen of mutants with defects in motility identified insertions in *cetA* and *cetB*, which are adjacent genes on the *C. jejuni* genome (Hendrixson *et al.*, 2001). CetB contains a predicted PAS domain and no other functional domains. CetA is predicted to contain a transmembrane region, a HAMP domain and the HCD. Mutants lacking *cetA* or *cetB* are deficient in energy taxis (Hendrixson *et al.*, 2001). These studies led to the hypothesis that CetA and CetB interact to transduce an energy taxis signal via a similar mechanism as that proposed for the single protein Aer. Specifically, we predict that CetB interacts with the HAMP domain of CetA, as is suggested of the PAS and HAMP domains of Aer. However, significant divergence between the HAMP domains of Aer and CetA suggest that the molecular nature of these interactions likely differ (see Chapter III). In addition, the separation of the domains of Aer between CetA and CetB implies that these proteins may also be able to function independently of each other to participate in other signaling

processes. We have determined that CetA and CetB define a new family of HAMP/PAS containing proteins, with pairs of similar proteins identified in 22 species thus far (see Chapter III).

In this study, we initiated the molecular and biochemical characterization of CetA and CetB, testing predictions about their transcription, topology, localization and interaction. We found that *cetA* and *cetB* are co-transcribed independently of the flagellar regulon. We demonstrated that CetA and CetB are both membrane-associated; CetA by two transmembrane helices in a helical hairpin; CetB in a peripheral manner, likely via protein-protein interactions. In addition, we uncovered evidence of a likely protein-protein interaction between CetA and CetB, including low levels of CetB in the absence of CetA, and the existence of high molecular weight complexes that appear to include both proteins.

Materials and Methods

Bacterial strains and culture conditions. All bacterial strains and plasmids used in this study are listed in Table 2. DRH212, a spontaneous streptomycin resistant mutant of the clinical isolate *C. jejuni* 81-176, was the background strain for all mutants studied and is referred to as wildtype (Hendrixson *et al.*, 2001). *C. jejuni* was routinely grown on Mueller-Hinton (MH) agar with 10 μg/ml trimethoprim under microaerophilic conditions (85% N_2, 10% CO_2, 5% O_2) in a tri-gas incubator. Biphasic cultures were grown in 20mL MH broth overlaid on 20mL MH agar under microaerophilic conditions. For *C. jejuni*, the following antibiotic concentrations were used: 10 μg/ml trimethoprim, 30 μg/ml cefaperazone, 50 μg/ml kanamycin, 20 μg/ml chloramphenicol and 0.1 or 2 mg/ml

Table 2. Bacterial strains and plasmids used in Chapter II.

Strain or plasmid	Relevant characteristics	Reference
Bacteria		
E. coli		
JM101	F′ *traD36 proA*$^+$*B*$^+$ *lacI*^{q} Δ*(lacZ)M15/* Δ*(lac-proAB) glnV thi*	New England Biolabs
DH5α/ pRK212.1	contains conjugative plasmid for transfer of plasmid into *C. jejuni*	(Figurski and Helinski, 1979)
TG1	Δ*hsdS Δ(lac-proAB) supE thi F' [traD36 proAB*$^+$ *lacI*^{q} *ΔlacZM15]*	(Sambrook *et al.*, 1989)
C. jejuni		
DRH212	81-176 Sm^R, spontaneous mutant	(Hendrixson *et al.*, 2001)
DRH307	Δ*cetB*	(Hendrixson *et al.*, 2001)
DRH311	Δ*fliA*	(Hendrixson *et al.*, 2001)
DRH321	Δ*rpoN*	(Hendrixson *et al.*, 2001)
DRH333	Δ*cetA*	(Hendrixson *et al.*, 2001)
KYCj172	Δ*cetAB*	This study
Plasmids		
pRY108	Km^R, *E. coli*/*C. jejuni* shuttle vector	(Yao *et al.*, 1993)
pECO102	*C. jejuni* plasmid for gene expression from cat promoter, Cm^R	(Wiesner *et al.*, 2003)
pECO101	pRY108 derivative with *cat* promoter in *Xho*I-*Bam*HI site, Km^R	This study
pTrcphoA	pTrc99a containing *'phoA* (lacks *phoA* codons 1-26)	(Blank and Donnenberg, 2001)
pTrclacZ	pTrc99a containing *'lacZ* (lacks *lacZ* codons 1-7)	(Blank and Donnenberg, 2001)
pKTY295	pECO101 with *cj1191c-flag* cloned into EcoRI and XhoI sites	This study
pKTY360	pRY108 with 2.4 kb fragment containing *cetA* and *cetB* coding sequence cloned into the XmnI site	Chapter III
pKTY367	pKTY360 with the Y116A mutation in the *cetA* coding sequence	Chapter III
pKTY213	pECO101 with *cetB* cloned into the BamHI and XhoI sites	This study
pKTY300	pECO101 with *cetAB* cloned into BamHI and XhoI sites	This study
pKTY333	pTrcphoA with *cetA* codons 1-5 cloned into NcoI and XmaI sites	This study
pKTY349	pTrcphoA with *cetA* codons 1-24 cloned into NcoI and XmaI sites	This study
pKTY344	pTrcphoA with *cetA* codons 1-50 cloned into NcoI and XmaI sites	This study
pKTY343	pTrcphoA with *cetA* codons 1-140 cloned into NcoI and XmaI sites	This study
pKTY334	pTrcphoA with *cetA* (full length) cloned into NcoI and XmaI sites	This study
pKTY331	pTrcphoA with *cetB* (full length) cloned into NcoI and XmaI sites	This study
pKTY332	pTrclacZ with *cetA* codons 1-5 cloned into NcoI and XmaI sites	This study
pKTY328	pTrclacZ with *cetA* codons 1-24 cloned into NcoI and	This study

	XmaI sites	
pKTY327	pTrclacZ with *cetA* codons 1-50 cloned into NcoI and XmaI sites	This study
pKTY329	pTrclacZ with *cetA* codons 1-140 cloned into NcoI and XmaI sites	This study
pKTY326	pTrclacZ with *cetA* (full length) cloned into NcoI and XmaI sites	This study
pKTY330	pTrclacZ with *cetB* (full length) cloned into NcoI and XmaI sites	This study
pBW208	pECO102 with *ctsP* and C-terminal FLAG tag	Wiesner and DiRita, in preparation

streptomycin. *E. coli* was grown in Luria-Bertani (LB) agar or broth. For *E. coli*, the following antibiotic concentrations were used: 50 μg/ml kanamycin, 30 μg/ml chloramphenicol or 100 μg/ml ampicillin.

Construction of plasmids for gene expression in *C. jejuni*. To construct a kanamycin selectable plasmid for gene expression in *C. jejuni*, an 82-bp fragment containing the promoter for the *C. jejuni* chloramphenicol acetyltransferase (*cat*) gene from pRY109 (Yao *et al.*, 1993) was amplified by PCR using primers containing 5' XbaI and BamHI sites. These primers were used to amplify the 82-bp fragment, and the resulting fragment cloned into pRY108 (Yao *et al.*, 1993) giving rise to the plasmid pECO101. Except for antibiotic selection, pECO101 functions similarly to the previously constructed plasmid pECO102 (Wiesner *et al.*, 2003). To construct a plasmid expressing a FLAG-tagged Cj1191c from the *cat* promoter, the *cj1191c* coding sequence was amplified by PCR with primers containing restriction sites so that an EcoRI site was added immediately 5' to *cj1191c* and the FLAG coding sequence followed by an XhoI site immediately 3' to *cj1191c* for cloning into pECO101. To construct a plasmid expressing *cetB* from the *cat* promoter, the *cetB* coding sequence was amplified by PCR with primers containing restriction sites so that a BamHI site was added immediately 5' to *cetB* and an XhoI site immediately 3' to *cetB* for cloning into pECO101. To construct a plasmid expressing both *cetA* and *cetB* from the *cat* promoter, the *cetA* and *cetB* coding sequences and intergenic region were amplified by PCR with primers containing restriction sites so that a BclI site was added immediately 5' to *cetA* and an XhoI site immediately 3' to *cetB*. The resulting fragment was digested with BclI and XhoI and

cloned into the BamHI and XhoI sites of pECO101. All plasmids were confirmed by DNA sequencing.

Conjugation of plasmids into *C. jejuni*. Plasmids were conjugated into *C. jejuni* as described by Guerry *et al* (Guerry *et al.*, 1994). Briefly, *C. jejuni* was grown on MH agar with 10 μg/ml trimethoprim for 16-20 hours and resuspended in MH broth to an OD_{600} of 1.0. Overnight cultures of the *E. coli* donor strain (DH5α[pRK212.1] containing the plasmid to be conjugated into *C. jejuni*) were diluted into fresh LB broth and grown to an OD_{600} of 0.5. 500 μl of the donor culture was centrifuged and the pellet washed twice with MH broth, then resuspended in 1 ml of the *C. jejuni* recipient culture. This mixture was spotted onto MH agar with no antibiotics. After 5 hours at 37°C in microaerophilic conditions, the bacteria were resuspended and spread onto MH agar containing 10 μg/ml trimethoprim, 30 μg/ml cefaperazone, 2 mg/ml streptomycin and 50 μg/ml kanamycin. PCR was used to verify transfer of the plasmid to the recipient *C. jejuni* strain.

RNA extractions and RT-PCR. *C. jejuni* strains were grown in biphasic cultures for 48 hours. RNA extractions were performed using Qiagen RNAprotect and Qiagen RNeasy according to manufacturer's instructions, without the use of on-column DNase treatment. To eliminate contaminating DNA, 10x DNase buffer (200mM sodium acetate pH 4.5, 100mM $MgCl_2$, 100mM NaCl) and 10 units of DNase I (RNase-free, Roche) were added to each RNA sample and incubated at room temperature for 1 hour. DNase was removed by sequential phenol and chloroform extractions, followed by ethanol precipitation. The final concentration of RNA in each sample was quantified by OD_{260}.

Qualitative RT-PCR was performed as follows. 2.5μg of RNA was mixed with 3μg random primers (Invitrogen) and cDNA synthesized using MMLV reverse transcriptase (Invitrogen) according to manufacturer's instructions. Control reactions with MMLV reverse transcriptase omitted were performed simultaneously to detect any contaminating DNA. Equal amounts of cDNA products were then used as a template for PCR using either 2 primers within *rpoA* or one primer within *cetA* and one primer within *cetB*. Control reactions using genomic DNA as a template were also performed. RT-PCR products were separated on a 0.8% agarose gel and visualized with ethidium bromide.

SDS-PAGE and Western blots. For SDS-PAGE of whole cell lysates, *C. jejuni* strains were grown on MH agar for 16-20 hours, then resuspended in MH broth to an OD_{600} of 0.8. The bacteria were pelleted by centrifugation and the pellet resuspended in 100μL 2x sample buffer. All other samples were normalized by protein concentration or OD_{600} as indicated below. Samples were boiled then separated on 10% or 12.5% polyacrylamide gels (as indicated). Proteins were transferred to nitrocellulose membranes and probed with rabbit anti-CetA (1:10,000-1:75,000, generated against an internal peptide by Open Biosystems) or rabbit anti-CetB (1:500-1:5000, generated against an internal peptide by Open Biosystems) followed by either goat anti-rabbit alkaline phosphatase-conjugated secondary antibody (1:10,000, Zymed) or goat anti-rabbit peroxidase-conjugated secondary antibody (1:20,000, Pierce). For detection of Cj1191c-FLAG and CtsP-FLAG, membranes were probed with anti-FLAG peroxidase-conjugated antibody (1:1000, Sigma). Alkaline phosphatase probed Western blots were developed using the chromogenic substrate 5-bromo-4-chloro-3-indolyl phosphate/nitro

blue tetrazolium as previously described (Sambrook *et al.*, 1989). Peroxidase probed Western blots were developed using the Western Lightning kit (PerkinElmer).

Topology predictions. Transmembrane domain predictions were preformed using DAS (http://www.sbc.su.se/~miklos/DAS). Signal sequence predictions were performed using LipoP (http://www.cbs.dtu.dk/services/LipoP). Hydrophobicity of individual residues within the predicted CetA transmembrane region was assessed by plotting the Kyte-Doolittle value of each residue in this region. This approach resembles that used recently to analyze the attributes of individual HAMP domain residues (Hulko *et al.*, 2006) and differs from the usual Kyte-Doolittle analysis, which gives the average hydrophobicity of 19 residues centered at each position.

Topology analysis using PhoA and LacZ fusions. The plasmids pTrcphoA and pTrclacZ were used to construct plasmids containing C-terminal PhoA or LacZ fusions to full-length or truncated CetA. pTrcphoA consists of the coding sequence for *phoA* without codons 1-26 (the signal sequence), denoted *'phoA*, cloned into pTrc99a (Blank and Donnenberg, 2001). pTrclacZ consists of the coding sequence of *lacZ* without codons 1-7, denoted *'lacZ*, cloned into pTrc99a (Blank and Donnenberg, 2001). Truncations of *cetA* consisting of the first 24, first 50 or first 140 codons and full-length *cetA* were amplified using primers that added an NcoI site immediately 5' and an XmaI site immediately 3' to the coding sequence for cloning into the NcoI and XmaI sites of pTrcphoA and pTrclacZ. The first 5 codons of *cetA* were inserted between the NcoI and XmaI sites of pTrcphoA and pTrclacZ using Pfu mutagenesis (Weiner *et al.*, 1994). All resulting plasmids were confirmed by DNA sequencing.

Each of the above plamids, including the original vectors, was transformed into *E. coli* strain TG1, which lacks *phoA* and *lacZ*. Alkaline phosphatase and β-galactosidase activities of each strain were assessed as previously described (Manoil, 1991; Miller, 1972). Assays were performed in triplicate and the average and standard deviation calculated for each strain.

Subcellular fractionation. *C. jejuni* strains were grown on MH agar for 16-20 hours and resuspended in 10mM HEPES pH 7.4. Cells were lysed by one freeze-thaw cycle, followed by sonication 3-6 times for 10 seconds. Cellular debris was removed by centrifugation at 10,000 x g for 10 minutes. Soluble and membrane fractions were separated by ultracentrifugation at 100,000 x g for 1 hour. Following ultracentrifugation, the supernatant contained soluble (cytoplasmic and periplasmic proteins) and the pellet contained insoluble (membrane) proteins. Protein concentrations were quantitated using the Bio-Rad Protein Assay. Equal amounts of protein from each sample were run on SDS-PAGE for Western analysis.

Isocitrate dehydrogenase assays. Subcellular fractions were assayed for isocitrate dehydrogenase activity as previously described (Myers and Kelly, 2005). Briefly, equal amounts of protein from each fraction were incubated with 5mM Tris pH 8.0, 1mM nicotinamide adenine dinucleotide phosphate (NADP), 1mM $MgCl_2$ and 5mM sodium isocitrate at room temperature. Isocitrate dehydrogenase activity was monitored by measuring the rate of increase of OD_{340}, which represents the rate of NADPH production. The percent of isocitrate dehydrogenase specific activity within each fraction was determined. For all fractionation experiments, at least 90% of the isocitrate dehydrogenase specific activity was found in the soluble fraction.

Membrane extraction. *C. jejuni* strains were grown and fractionated into soluble and membrane fractions as described above. The membrane fraction was then mixed 1:1 with 10mM HEPES pH 7.4 or 10mM HEPES pH 7.4 containing 3M urea, 5M urea, 12M urea, 1M NaCl, 3M NaCl, or 0.3% Triton X-100 (concentrations given are twice the final concentration). These mixtures were incubated at 4°C with rocking for 30 minutes to 1 hour, followed by ultracentrifugation at 100,000xg for 1 hour. Following ultracentrifugation, the supernatant contained soluble proteins and the pellet insoluble proteins. The soluble proteins were precipitated with cold acetone. Both soluble and insoluble samples were resuspended in an equal volume of 10mM HEPES pH 7.4 and mixed 1:1 with 2x sample buffer. Equal volumes of each sample were used for SDS-PAGE and Western analysis.

***in vivo* cross-linking.** *C. jejuni* strains were grown on MH agar for 16-20 hours then resuspended in MH broth to an OD_{600} of 8.0. 2.5mM dithiobis(succinimidyl)propionate (DSP) in DMSO was added to each culture, with additional DMSO added to bring the combined DSP and DMSO volume to $1/10^{th}$ of the final volume. Untreated samples received $1/10^{th}$ final volume of DMSO. Samples were incubated at room temperature in ambient atmosphere for 20 minutes. 50mM Tris pH 8.0 was added to each sample to quench any remaining DSP. Equal volumes of each samples were run on SDS-PAGE without β-mercaptoethanol or DTT added to the sample buffer, as these would cleave the DSP mediated cross-linking.

Results

***cetA* and *cetB* are co-transcribed independently of the flagellar regulon, and CetB levels are CetA-dependent.** Our hypothesis that CetA and CetB interact to transduce an energy taxis signal is based in part on the fact that they are encoded by adjacent genes on the *C. jejuni* chromosome. As there are 17bp between the *cetA* and *cetB* genes, we expected that they would be co-transcribed. We tested this prediction by performing RT-PCR using one primer within each gene (Fig. 7A). If both *cetA* and *cetB* are present on the same transcript, then a single product spanning both genes would arise from these primers. This predicted product was present when the wildtype RNA was used as the template for RT-PCR, but not when RNA from the Δ*cetA*, Δ*cetB* or Δ*cetAB* mutants was used or when reverse transcriptase was omitted from the reaction (Fig. 7B). A product of the same size was also visible when genomic DNA was used for the PCR template. As a control, we performed RT-PCR with primers within the *rpoA* gene, which encodes the housekeeping sigma factor, σ^{70}. The *rpoA* RT-PCR product was evident in all RT samples (Fig. 7C). These data support our hypothesis that *cetA* and *cetB* are co-transcribed.

C. jejuni has only three known sigma factors identified within its genome: σ^{70}, σ^{54} (encoded by *rpoN*) and σ^{28} (encoded by *fliA*). The latter two sigma factors are required for the flagellar transcriptional cascade in *C. jejuni* (Hendrixson and DiRita, 2003). Levels of CetA and CetB were unaffected in strains lacking σ^{54} or σ^{28}, indicating that *cetA* and *cetB* are likely expressed in a σ^{70}-dependent fashion (Fig. 8A).

Western blots also demonstrated that CetB levels are at or below our limit of detection in the Δ*cetA* mutant (Fig. 8A). This is true whether CetB is expressed from the

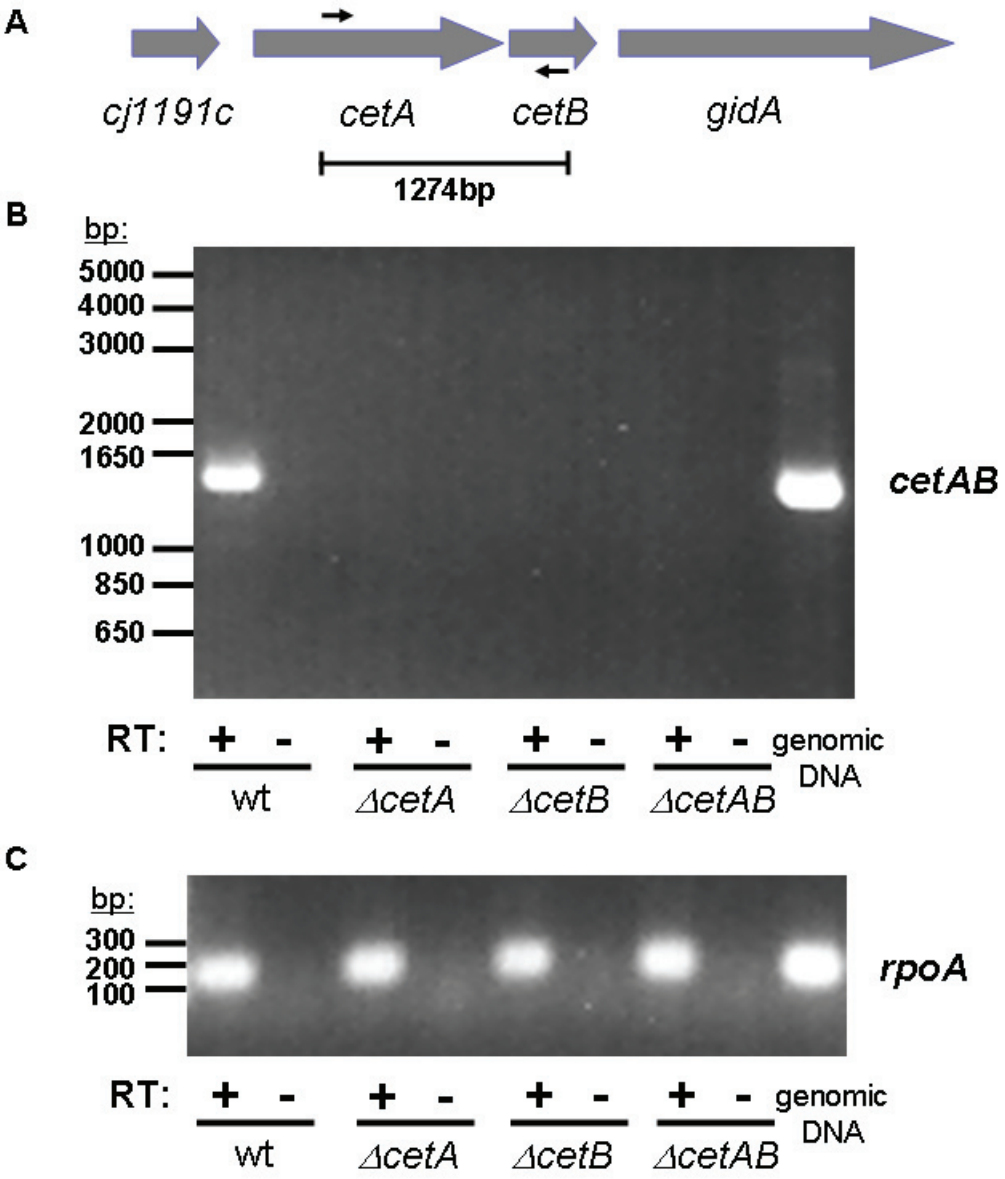

Figure 7. RT-PCR analysis of *cetAB* locus. A. Location of primers within *cetA* and *cetB* used to determine if both genes are present on one transcript. Expected PCR product size is given. **B.** RT-PCR results using primers shown in A. **C.** RT-PCR results using primers within *rpoA* that result in an 180bp product. In both B and C, results from RT-PCR using RNA from wildtype, Δ*cetA*, Δ*cetB* and Δ*cetAB* are shown. Control reactions were performed in which reverse transcriptase (RT) was omitted from the cDNA synthesis reaction, in order to rule out the presence of contaminating DNA. As a positive control, the PCR products resulting from use of genomic DNA as the template are also shown.

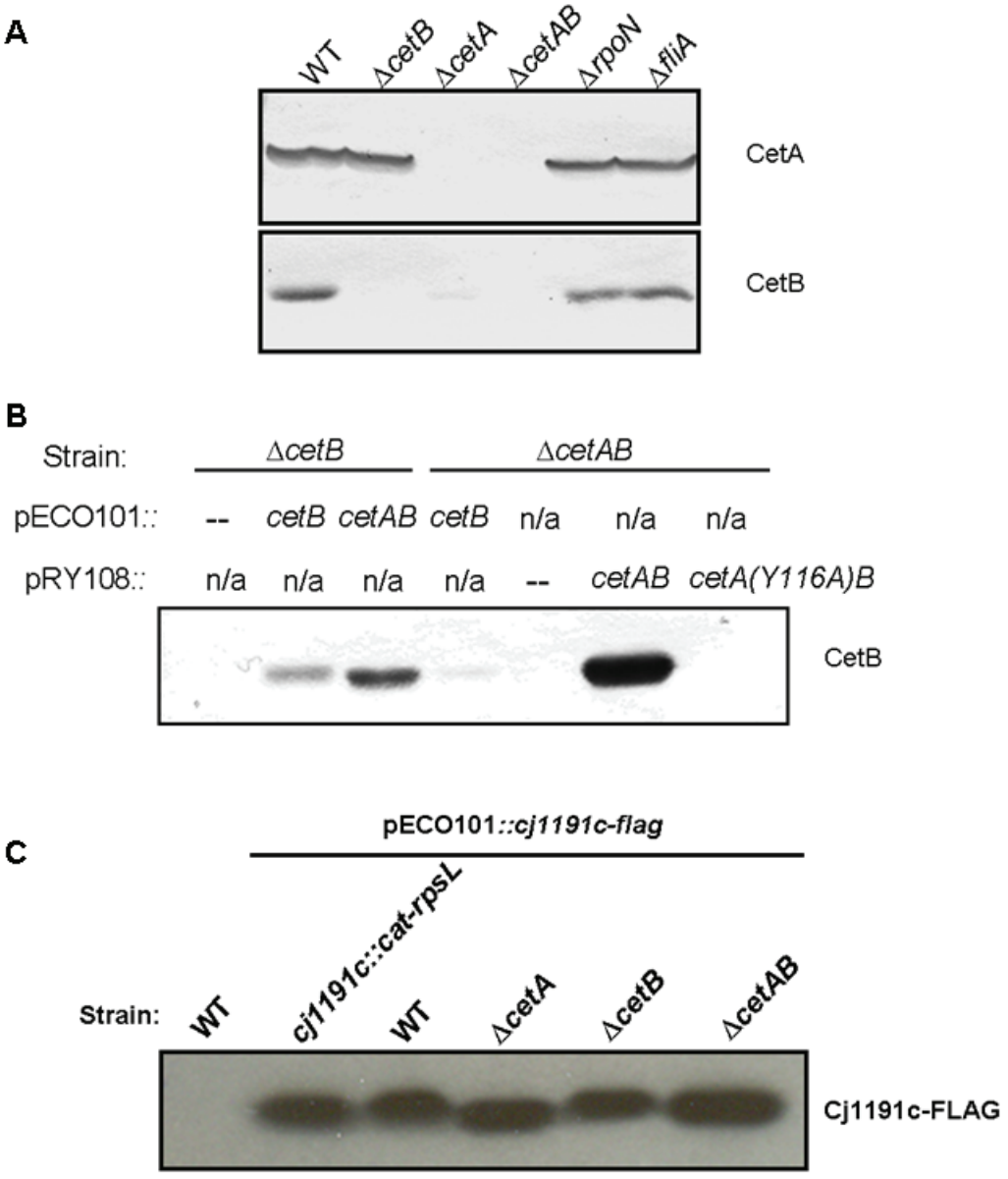

Figure 8. Expression of CetA and CetB in various genetic backgrounds. A. Whole cell extracts were prepared from wildtype, Δ*cetB*, Δ*cetA*, Δ*cetAB*, Δ*rpoN* and Δ*fliA*. These were separated by 12.5% SDS-PAGE and CetA and CetB detected by immunoblotting. **B.** Whole cell extracts were prepared from Δ*cetB* and Δ*cetAB* with pECO101, pECO101*::cetB*, pECO101*::cetAB*, pRY108, pRY108*::cetAB* or pRY108*::cetA(Y116A)cetB*. These samples were separated by 12.5% SDS-PAGE and CetA and CetB detected by immunoblotting. **C.** Whole cell extracts were prepared from the indicated strains containing either pECO101 or pECO101*::cj1191c-flag*. These samples were separated by 12.5% SDS-PAGE and Cj1191c-FLAG detected by immunoblotting.

chromosome (Fig. 8A) or from a plasmid under the control of a constitutive promoter (Fig. 8B), indicating that the low level of CetB expression in the Δ*cetA* mutant is not due to a polar effect of this in-frame deletion. Additionally, when both CetA and CetB are expressed from a plasmid bearing their native promoter, but CetA is rendered unstable by a HAMP domain point mutation (Y116A, see Chapter III), CetB levels are also quite low (Fig. 8B). The loss of stability of one protein in the absence of another is a frequent indication of a protein-protein interaction. Our data are consistent with CetB stability being CetA-dependent, however we cannot rule out a potential effect of CetA on CetB translation. Cj1191c, an apparent CetB paralogue encoded by the gene upstream of *cetA*, exhibits no role in energy taxis (Hendrixson *et al.*, 2001). Unlike those of CetB, Cj1191c levels are not CetA-dependent (Fig. 8C).

CetA has two transmembrane domains in a helical hairpin. We used the DAS algorithm to predict whether CetA and/or CetB possess transmembrane domains. According to this analysis, CetA has a transmembrane region of 36-38 amino acids in length from residues 6 to 43 or 7 to 42, depending on the cut-off used (Fig. 9A). DAS analysis indicates that CetB does not have any transmembrane domains (Fig. 9B). As the LipoP program indicates that CetB also does not possess a signal sequence (data not shown), we predict that CetB is located in the *C. jejuni* cytoplasm.

A dip in the DAS profile score is apparent at about the mid-point of the predicted transmembrane region in CetA. Closer examination of the hydrophobicity of each residue showed a strongly hydrophilic residue near the mid-point of this region (Fig. 9C). This residue is a histidine (His24) which is known to induce turns in transmembrane helices, giving rise to helical hairpins (Monne *et al.*, 1999a; Monne *et al.*, 1999b).

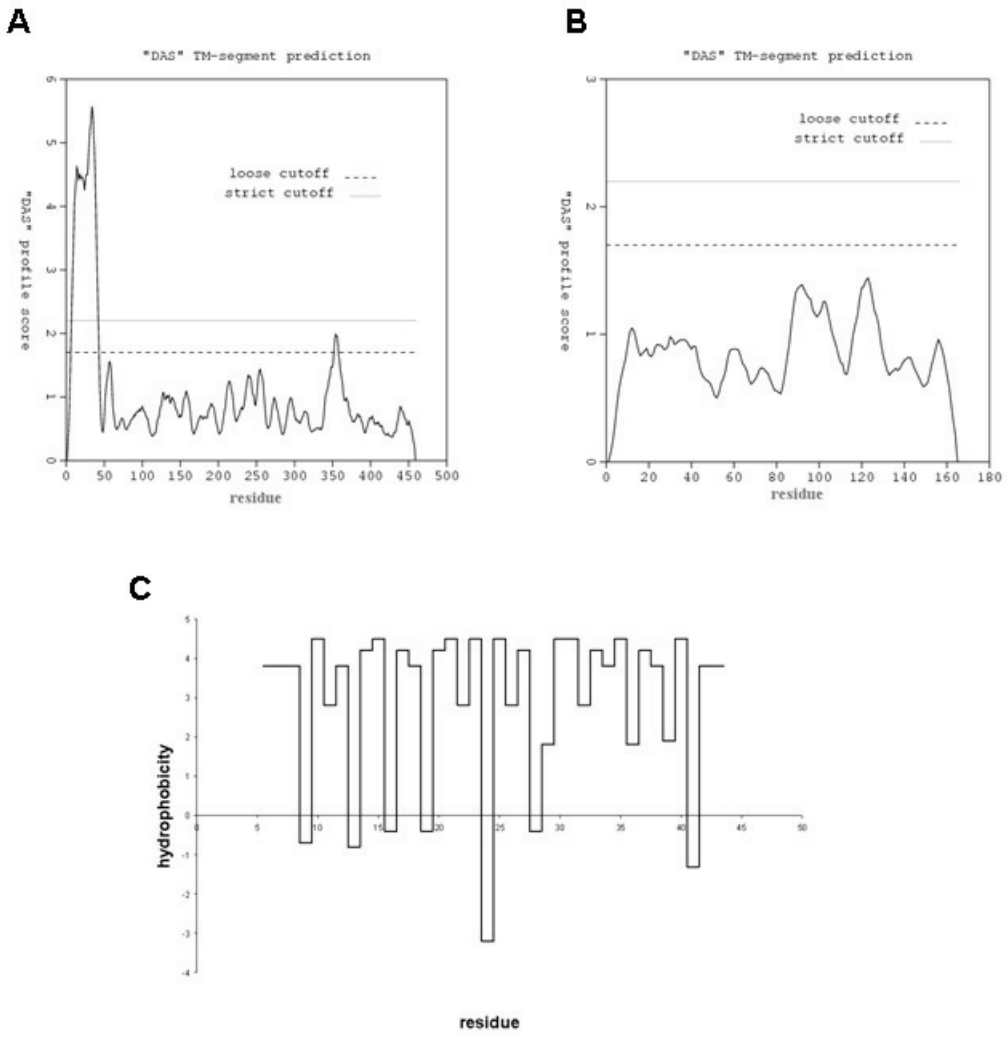

Figure 9. Prediction of transmembrane regions for CetA and CetB. A. DAS analysis results for CetA. **B.** DAS analysis results for CetB. **C.** Hydrophobicity (Kyte-Doolittle values) of each residue within the DAS-predicted transmembrane region of CetA.

Additionally, the predicted transmembrane region is flanked on either side by positively charged residues (K3, R44, H46, K47). Such residues near transmembrane helices have been proposed to act like the flukes of an anchor to moor the protein into the membrane, with the positive residues residing on the cytoplasmic surface of the protein (Boyd and Beckwith, 1989). These observations led us to hypothesize that CetA may contain two transmembrane helices in a helical hairpin confirmation, as opposed to the single transmembrane helix predicted by DAS analysis.

To differentiate between the single transmembrane helix predicted by the DAS algorithm and our prediction that CetA has two transmembrane helices, we performed topology analysis using *phoA* and *lacZ* fusions. *phoA* encodes alkaline phosphatase, which is active in the periplasm and inactive in the cytoplasm. *lacZ* encodes β-galactosidase, an enzyme that is active in the cytoplasm and too bulky to be transported to the periplasm. Fusion of β-galactosidase to periplasmic regions of a protein leads to the embedding of the fusion in the membrane, resulting in improper folding and a loss of enzymatic activity (Froshauer *et al.*, 1988). By comparing alkaline phosphatase and β-galactosidase activities resulting from fusions at various locations within a protein, we can develop a good prediction of the topology of that protein (Manoil and Beckwith, 1986; Manoil, 1990; Silhavy and Beckwith, 1985).

We made *phoA* and *lacZ* fusions such that alkaline phosphatase or β-galactosidase would be fused C-terminally to full-length CetA or to CetA that was truncated at residue 5, 24, 50 or 140 (Fig. 10A). These fusions were expressed in an *E. coli* strain lacking *lacZ* and *phoA* and assayed for alkaline phosphatase and β-galactosidase activity. The only alkaline phosphatase fusion construct with significant activity was that at His24 of

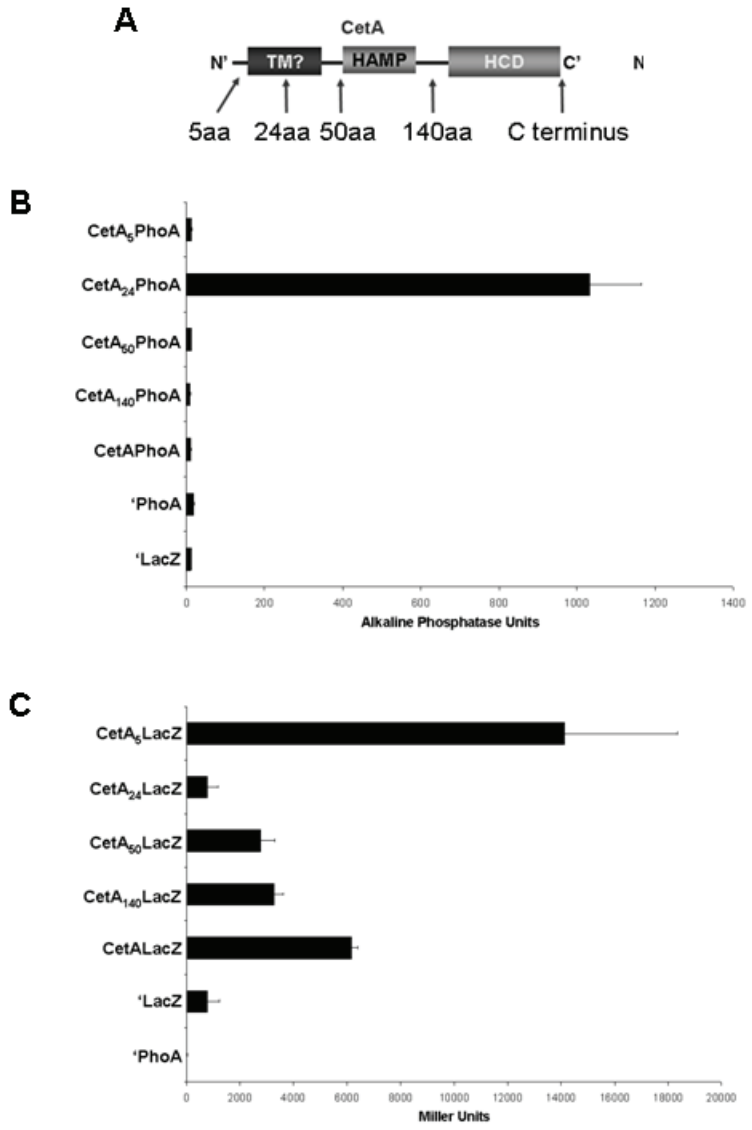

Figure 10. Location and activities of LacZ and PhoA fusions to CetA. A. Locations of PhoA and LacZ fusions to truncated or full-length CetA are indicated. LacZ or PhoA was fused C-terminally to the truncated or full-length protein. **B.** Alkaline phosphatase activity of PhoA fusions. **C.** β-galactosidase activity of LacZ fusions. In both B and C, 'PhoA and 'LacZ indicate the empty vectors pTrcphoA and pTrcLacZ, respectively.

CetA (Fig. 10B). The β-galactosidase fusion at this location (His24), was also the fusion with the lowest β-galactosidase activity (Fig. 10C). This fusion did have β-galactosidase activity above background levels, however. Work in other laboratories has indicated that β-galactosidase fusions to periplasmic regions, which do not lead to translocation of the fusion but rather embed the protein in the membrane, can sometimes lead to degradation of the fusion and release of native β-galactosidase, giving rise to activity (Georgiou *et al.*, 1988; Gott and Boos, 1988). These studies caution that use of β-galactosidase fusions must be complemented by an alternative topological probe, such as alkaline phosphatase, which is likely a more reliable indicator of subcellular localization. Together, our results indicate that His24 is accessible to the periplasm, whereas all of the other fusion locations are found in the cytoplasm. These data support our prediction that CetA has two transmembrane helices in a helical hairpin.

CetA is an integral membrane protein and CetB is a peripheral membrane protein. The above *phoA*/*lacZ* fusion experiments were performed in *E. coli*. We sought to determine the localization of CetA and CetB in *C. jejuni*. To do so, we prepared and analyzed subcellular fractions for localization of CetA and CetB. Wildtype *C. jejuni* was lysed as described in Materials and Methods. Soluble and membrane-associated proteins were then separated by ultracentrifugation. These samples were analyzed for the presence of CetA and CetB by Western blot. While some CetA is detectable in the soluble fraction, the majority of both CetA and CetB are in the membrane fraction (Fig. 11). Less than 10% of the isocitrate dehydrogenase specific activity (Myers and Kelly, 2005) was found in membrane fractions during these experiments. The presence of a minority of soluble CetA could be due to incomplete fractionation or the presence of

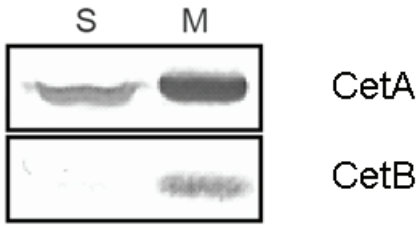

Figure 11. Subcellular fractionation of CetA and CetB. Whole cell lysates were separated into soluble and membrane fractions by ultracentrifugation. These fractions were separated by 12.5% SDS-PAGE. CetA and CetB were detected by immunoblotting. Membrane fractions contained <10% of the isocitrate dehydrogenase specific activity.

newly synthesized protein that has not yet localized to the membrane (Crawford *et al.*, 2003).

As DAS analysis indicated that CetB does not have a transmembrane region, the presence of CetB in the membrane fraction suggests that CetB is a peripheral membrane protein, associated with the membrane by protein-protein interactions or by direct interaction with the membrane. In order to determine the nature of the association of CetB with the membrane, we performed membrane extraction experiments. In these experiments, a *C. jejuni* strain was used that expressed a FLAG-tagged CtsP protein, which had been previously characterized by our lab as a peripheral membrane protein (Wiesner and DiRita, in preparation). The bacteria were lysed and separated into soluble and membrane fractions as described above. The membrane fraction was then treated with urea, NaCl or buffer alone. Urea denatures proteins and disrupts protein complexes, thereby releasing peripheral membrane proteins (Borel and Simon, 1996; Gilmore and Blobel, 1985). High salt treatment weakens ionic interactions between peripheral membrane proteins and other membrane proteins or the polar head groups of the lipid bilayer (Hugle *et al.*, 2001; Kretzschmar *et al.*, 1996). Integral membrane proteins should remain insoluble following treatment with urea or high salt. Peripheral membrane proteins may be soluble following urea and/or high salt treatment depending on the nature and strength of their membrane association.

After these treatments, the soluble and insoluble proteins were separated by ultracentrifugation and probed for the presence of CetA, CetB and CtsP-FLAG. Both CtsP and CetB could be solubilized in 6M urea, while CetA could not (Fig. 12A). CtsP was soluble in 1.5M NaCl, but both CetA and CetB remained insoluble following high

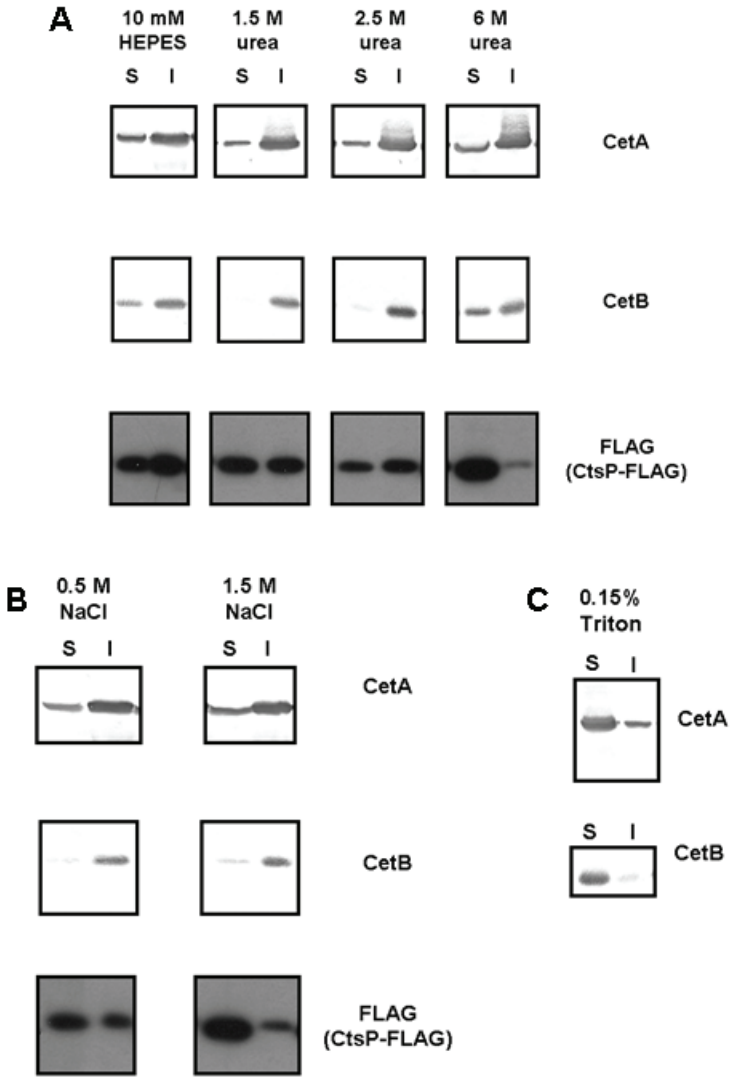

Figure 12. Membrane extractability of CetA and CetB. A. Membrane extractability in buffer alone or in urea. **B.** Membrane extractability in NaCl. **C.** Membrane extractability in Triton X-100. Membrane fractions following subcellular fractionation of wildtype cells expressing CtsP-FLAG (a peripheral membrane protein) were treated with buffer alone (10mM HEPES) or buffer containing the indicated concentrations of urea or NaCl. Soluble and insoluble proteins were separated by ultracentrifugation. Samples were separated on 12.5% SDS-PAGE and probed for the indicated protein by immunoblotting.

salt treatment (Fig. 12B). CetA and CetB are both soluble following treatment with 0.15% Triton X-100 (Fig. 12C), indicating that they are soluble when the membrane itself is disrupted. From these results, we conclude that CetA is an integral membrane protein and CetB is a peripheral membrane protein. The release of CetB from the membrane following treatment with urea, but not high salt, indicates that CetB has an avid association with the membrane, possibly as a result of protein-protein interactions.

CetA and CetB associate in larger complexes. In order to test further whether CetA and CetB interact with one another and/or other proteins, we performed *in vivo* cross-linking experiments. Cells were treated with 2.5mM of the membrane permeable primary amine cross-linker DSP in DMSO or with DMSO alone. DSP was inactivated by addition of 50mM Tris pH 8.0, these samples were analyzed by non-reducing SDS-PAGE and probed for CetA or CetB by Western blot.

When cross-linked wildtype samples were separated on 10% SDS-PAGE and immunoblotted with anti-CetA, several species with molecular weights between approximately 115.5 kD and 181.8 kD were apparent (Fig.13A). The largest of these species (arrow, Fig. 13A) was absent in the cross-linked sample from the Δ*cetB* strain. A CetA-containing species migrating between approximately 115.5 kD and 181.8 kD was observed in both wildtype and Δ*cetB* samples not subjected to cross-linking (Fig. 13A, 13B), although this band is much fainter in the wildtype sample.

When cross-linked wildtype samples were run on 12.5% SDS-PAGE, we detected two species on immunoblotting with anti-CetB (Fig. 13C). One was the predicted size of the CetB monomer (19.3 kD) and the other was the predicted size of a CetB homodimer (38.6 kD). In order to detect higher molecular weight CetB complexes, larger amounts of

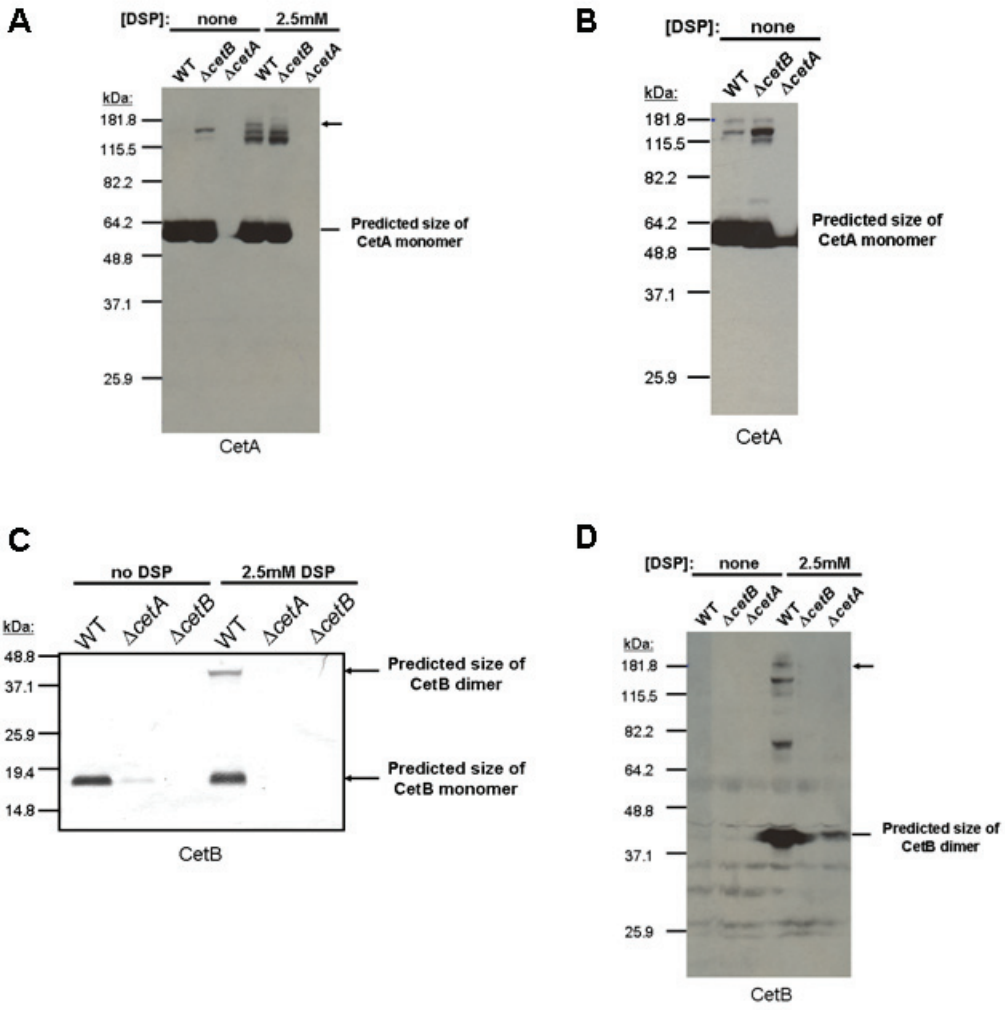

Figure 13. Cross-linking of CetA and CetB. A. anti-CetA Western blots of DSP cross-linked samples run on 10% SDS-PAGE. Arrow indicates a high molecular weight species present in the wildtype cross-linked sample, but not in the Δ*cetB* cross-linked sample. **B.** longer exposure of anti-CetA Western blots of samples not subjected to cross-linking run on 10% SDS-PAGE. **C.** anti-CetB Western blot of DSP cross-linked lysates run on 12.5% SDS-PAGE. **D.** anti-CetB Western blots of higher concentrations of DSP cross-linked samples run on 10% SDS-PAGE. In A, B, C and D, wildtype, Δ*cetB* and Δ*cetA* cells were treated with either 2.5mM DSP in DMSO or DMSO alone. The cross-linker (DSP) was quenched and the samples separated by SDS-PAGE (without β-mercaptoethanol or DTT added to the sample buffer) then probed for the presence of CetA and CetB by immunoblotting.

wildtype cross-linked samples were run on 10% SDS-PAGE and probed with anti-CetB (Fig. 13D). To obtain separation of larger complexes, the gel was run for a longer period of time, leading the CetB monomer to run off the gel. In this Western blot, the apparent homodimer was present, as were several species with higher molecular weights, including one between approximately 64.2 kD and 82.2 kD and two major species between approximately 115.5 kD and 181.8 kD (Fig. 13D). The largest of these species (arrow, Fig. 13D) was approximately the same size as the largest CetA species (arrow, Fig. 13A).

The identity of each of these CetA and CetB complexes has not been definitively determined, but some inferences can be made. In particular, the largest CetA and CetB complexes, approximately the same size, are consistent with a single complex containing both proteins. The molecular weight of this species is between approximately 115.5 kD and 181.8 kD, which would be consistent with a complex comprised of two CetA monomers (51.0 kD each) and two CetB monomers (19.3 kD each). We also hypothesize that CetA forms a homodimer, as do other MCPs, and this could be one of the CetB-independent species present in the blot shown in Figure 13A. Further, we expect CetA to interact with other elements of the chemotactic machinery, as discussed below.

Discussion

In this study, we carried out the molecular and biochemical characterization of CetA and CetB, the bipartite energy taxis system of *C. jejuni*. We found that *cetA* and *cetB* are co-transcribed, likely in a σ^{70}-dependent manner. We established that CetA is an integral membrane protein with two transmembrane helices in a helical hairpin

conformation. CetB, on the other hand, is a peripheral membrane protein, that is evidently capable of forming a homodimer. We determined that CetB levels are CetA-dependent and that CetA and CetB each participate in several high molecular weight complexes including one complex that appears to include both proteins. These data are consistent with a protein-protein interaction between CetA and CetB. Together these data support a model in which we hypothesize a membrane-associated CetB dimer senses changes in electron transport and relays that signal to the integral membrane protein CetA via a direct interaction (Fig. 14). This signal is then transduced to the chemotactic machinery, allowing a change in direction of motility based on changes in the local environment that impact electron transport.

CetA and CetB are encoded by adjacent genes 17bp apart on the *C. jejuni* chromosome. Based on the small intergenic distance, as well as the fact that both are required for energy taxis (Hendrixson *et al.*, 2001), we expected that *cetA* and *cetB* would be co-transcribed. RT-PCR analysis indicated that this is the case (Fig. 7). Additionally, wildtype levels of CetA and CetB were expressed in mutants lacking the sigma factors required for expression of genes involved in flagellar assembly and function, σ^{54} and σ^{28} (Hendrixson and DiRita, 2003) (Fig. 8A). This indicates that neither of these sigma factors is required for expression of the *cetAB* transcript. This differs from *E. coli* and *Salmonella typhimurium*, where *aer* expression appears to be σ^{28}-dependent (Frye *et al.*, 2006; Park *et al.*, 2001). We do not know whether other MCPs are expressed independently of the flagellar regulon in *C. jejuni* or whether *cetA* and *cetB* will prove to be unique in this respect.

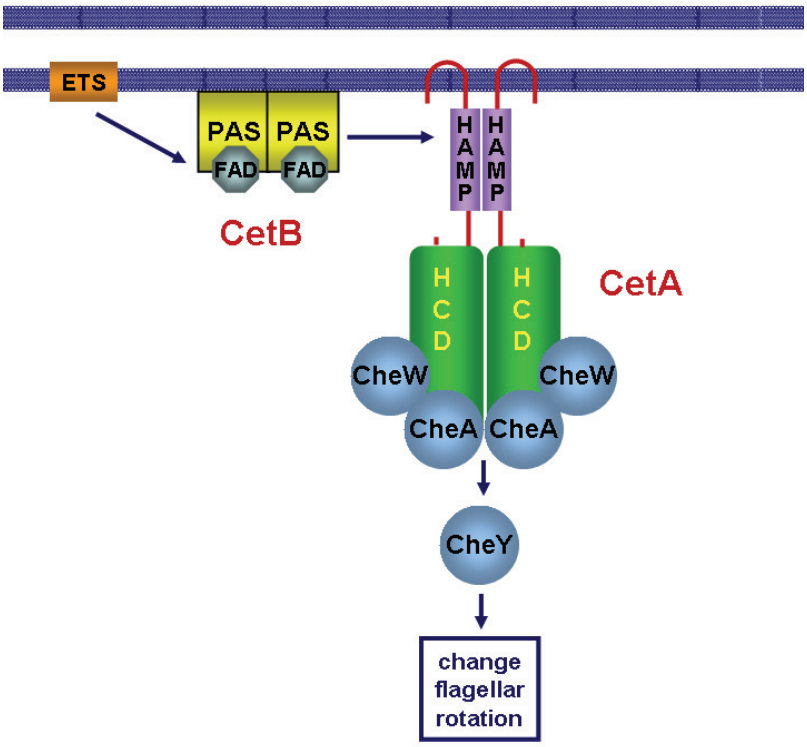

Figure 14. Current model of CetA and CetB localization, topology and function. CetB, which exists as a dimer, is peripherally associated with the membrane, possibly by protein-protein interactions. CetA is an integral membrane protein with two transmembrane domains in a helical hairpin. Our data are consistent with a CetB-CetA interaction, providing a mechanism for transduction of the energy taxis signal to the chemotactic machinery. (See discussion for more detail.)

Topology prediction programs indicated that CetA contains a single, fairly long transmembrane helix, and that CetB is entirely cytoplasmic (Fig. 9A, 9B). Closer examination of the predicted transmembrane helix of CetA led us to hypothesize that this protein instead contains two transmembrane helices separated by a short periplasmic loop, a so-called helical hairpin. We based this prediction on the presence of a histidine, His24, in the middle of this predicted transmembrane helix. Histidine has been shown to induce helical hairpin formation within transmembrane helices (Monne *et al.*, 1999a; Monne *et al.*, 1999b). We tested these topological predictions by making alkaline phosphatase and β-galactosidase fusions at multiple locations within CetA, including His24 (Fig. 10A). The enzyme activities of these fusions are consistent with CetA containing two transmembrane regions and a short periplasmic loop that includes His24 (Fig. 10B, 10C). Further studies are necessary to precisely define the ends of this loop. However, there are two glycines present 4-5 residues N-terminal and C-terminal to His24. Glycine also displays some turn-inducing tendencies in transmembrane helices and appears to predominate as the N-terminal residue in helical hairpin loops (Monne *et al.*, 1999b). Accordingly, we would predict that the periplasmic loop of CetA may extend from Gly19 to His24, potentially continuing on to Gly28. From our topology analysis with CetA, we arrive at a conclusion similar to the Aer topology model, which was derived biochemically (Amin *et al.*, 2006).

The sequence analysis and fusion data indicate that CetA is an integral membrane protein and CetB is cytoplasmic. We further examined the subcellular location of both CetA and CetB when expressed from the chromosome of *C. jejuni*. These experiments demonstrated that both CetA and CetB localize to the membrane of *C. jejuni* (Fig. 11).

Membrane extraction experiments, using various conditions to disrupt protein associations with the membrane, indicated that CetA is an integral membrane protein and CetB is a peripheral membrane protein (Fig. 12). As CetB is released from the membrane following urea treatment, but not high salt treatment, we conclude that CetB is membrane-associated via a strong interaction, likely with other proteins as opposed to the membrane itself. We predict that CetB associates with the membrane by interacting with either CetA or an unidentified element(s) of the ETS whose redox state CetB is predicted to sense. Attempts to determine whether or not the membrane-association of CetB is CetA-dependent have been confounded by the extremely low level of CetB expression in the absence of CetA.

Based on the fact that CetA and CetB possess all of the domains of the energy taxis receptor Aer and are required for energy taxis by *C. jejuni* (Hendrixson *et al.*, 2001), we predict that CetA and CetB interact directly to transduce an energy taxis signal. We observed that CetB levels are extremely low in the absence of CetA, whether CetB is expressed from the chromosome or from a multicopy plasmid (Fig. 8). Protein-protein interactions often manifest themselves in the loss of stability of one protein when the other is not present. This may be the case with CetA and CetB. However, at present we cannot rule out that CetA may instead have an effect on the levels of translation of CetB. If the latter scenario is true, then the *cis* element via which CetA affects translation must be strictly contained within the coding sequence of *cetB*, based on the maintenance of the CetA-dependent effect when the *cetB* orf is expressed constitutively from a multicopy plasmid. One could differentiate between an effect of CetA on stability or on translation of CetB using pulse-chase experiments. However, such experiments would require either

an inducible promoter system, which has not yet been developed for *C. jejuni*, or the ability to immunoprecipiate CetB, which we have been unable to do despite repeated attempts.

Evidence of an interaction between CetA and CetB was obtained from *in vivo* cross-linking experiments. In these experiments, whole cells were treated with the membrane permeable primary amine cross-linker DSP. When the cross-linked samples were probed for the presence of CetA by Western blot, a high molecular weight species was evident in the wildtype sample that was absent in the Δ*cetB* mutant sample (Fig. 13A). A high molecular weight species of similar size was also observed by anti-CetB Western blot (Fig. 13D). Due to the low levels of CetB in the Δ*cetA* mutant, we cannot be conclusive as to whether this species is present in the Δ*cetA* mutant sample. The size of this cross-linked species is consistent with a complex consisting of two CetA monomers and two CetB monomers. These data, together with the fact that CetB levels are CetA-dependent, are consistent with an interaction between CetA and CetB. Efforts to gather more direct evidence for such an interaction by yeast two-hybrid (Parrish *et al.*, 2007) and bacterial two-hybrid systems (data not shown) have been unsuccessful. Membrane proteins have often proved difficult to analyze using these methods. Additionally, CetB appears to form inclusion bodies when expressed at high levels in *E. coli* (data not shown), further confounding this approach and others involving expression in this background. While our results are consistent with an interaction between CetA and CetB, further studies are necessary to develop more direct evidence for or against such an interaction.

In other work, we determined that the HAMP domains of CetA and Aer differ significantly (see Chapter III). Based on similarity to the HAMP domain of CetA, we identified a family of 55 pairs of CetA- and CetB-like proteins (which we call HAMP/PAS pairs) in a diverse group of bacterial species (see Chapter III). The HAMP domains of this family contain nine conserved residues which we suggest may define a PAS-domain interaction surface (see Chapter III). Single alanine substitutions at these positions do not alter the localization of CetB to the membrane. If these conserved residues are involved in CetA-CetB interactions, we predict that substitutions at multiple positions within this region may lead to a change in CetB stability, CetB membrane localization and/or CetA-CetB complex formation.

Our *in vivo* cross-linking experiments also indicate that CetB forms a homodimer (Fig. 13C). PAS domains often form dimers, but it was not previously known if this was the case with CetB. In addition, whether or not the PAS domain of Aer dimerizes has yet to be established (Taylor, 2007). Further experiments aimed at defining the dimerization surface of CetB may provide genetic evidence for or against dimerization of the Aer PAS domain, based on similarity or dissimilarity in this region. The identification of CetB mutants deficient in dimerization would also allow us to test whether CetB dimer formation is required for energy taxis.

The *in vivo* cross-linking also demonstrated that CetA and CetB participate in several other high molecular weight complexes. Such complexes are expected, as interactions with the chemotaxis machinery would be necessary for CetA and CetB to transduce an energy taxis signal. Specifically, we expect that CetA would dimerize, as MCPs are known to function as homodimers. Additionally, we expect CetA to interact

with the adaptor protein, CheW (19.5 kD) facilitating an interaction with the histidine kinase CheA (85.3 kD). CetA may also interact with CheV (38.9 kD), which has a CheW-like domain as well as a C-terminal CheY-like response regulator domain. Although CetA methylation has not yet been demonstrated, CetA does possess an apparent methylation site (Marchant *et al.*, 2002), indicating that it may also interact with the adaptation proteins CheB (20.1 kD) and CheR (30.6 kD). In addition, MCP homodimers associate in large arrays with the basic unit being trimers of dimers, so CetA may also interact with other *C. jejuni* MCPs, but these complexes would likely be larger than those detected in our cross-linking experiments. The CetB complexes we observe could be higher order CetB oligomers. It is also possible that CetB interacts with other unidentified proteins. In particular, we might expect that CetB interacts with elements of the electron transport system as discussed above.

We can make some predictions about CetB based on sequence comparisons with the PAS domain of Aer. Three residues in the PAS domain of Aer (Arg57, His58 and Asp60) are required for FAD binding (Repik *et al.*, 2000), are located close to the predicted FAD binding site, and are conserved in Aer-like (FAD-binding) PAS domains (personal communication in (Taylor, 2007)). These residues align with identical or similar residues in CetB (Arg50, His51 and Glu53). Based on these similarities, we predict that CetB binds an FAD cofactor. Additionally, the HAMP domain of Aer is required for proper folding and FAD binding by the PAS domain. This requirement, however, can be subverted by non-specific suppressor mutations in the PAS domain (S28G, A65V and A99V) which allow FAD binding in the presence of HAMP domain point mutations that usually abrogate FAD binding (Buron-Barral *et al.*, 2006; Watts *et*

al., 2004). These suppressing residues (Gly28, Val65 and Val99) are the naturally occurring residues at the equivalent positions in CetB (Gly21, Val58 and Val92). This intriguing fact suggests that CetB may be able to fold and bind FAD without interacting with the CetA HAMP domain. Additionally, CetB does not contain homology to the N-terminal cap of the Aer PAS domain (Aer residues 1-19). This region was found to be critical for Aer protein stability (Watts *et al.*, 2006b). If the lack of this domain plays some role in the instability of CetB in the Δ*cetA* mutant, we would predict that fusion of the Aer N-terminal cap to CetB might lead to increased stability. More experiments are necessary to test these sequence based predictions.

These studies have allowed us to further refine our model of energy taxis signal transduction by CetA and CetB (Fig. 14) and make testable predictions about how this bipartite system works vis-à-vis what is known about the Aer single protein energy taxis receptor. Based on studies of both Aer and CetA/CetB, we predict that CetB binds an FAD cofactor whose redox state reflects that of element(s) of the ETS. CetB localizes to the membrane via avid associations consistent with a protein-protein interaction, which would place CetB in close proximity to the ETS. Whether CetB interacts directly with elements of the ETS or the FAD cofactor is exchanged between CetB and elements of this system remains unknown. Regardless, we suggest that this signal is transmitted to CetA by a direct interaction between CetB and CetA. Our data are consistent with such an interaction. We predict that this interaction occurs between the PAS domain of CetB and the HAMP domain of CetA, as is suggested for Aer. The molecular nature of this interaction likely differs significantly from that within Aer (see Chapter III). We have also identified several pairs of HAMP-containing and PAS-containing proteins which we

suggest may function analogously to CetA and CetB (see Chapter III), indicating that we may be able to extrapolate new knowledge about the properties of CetA and CetB to similar proteins in other organisms. The work presented here has provided information on the expression of and biochemical properties of CetA and CetB, allowing us to both further our understanding of these proteins as well as build a foundation for future studies aimed at elucidating the molecular mechanisms of signal transduction within this energy taxis system.

CHAPTER III

CONSERVED RESIDUES IN THE HAMP DOMAIN DEFINE A NEW FAMILY OF PROPOSED BIPARTITE ENERGY TAXIS RECEPTORS

Summary

HAMP domains, found in many bacterial signal transduction proteins, generally transmit an intramolecular signal between an extracellular sensory domain and an intracellular signaling domain. Studies of HAMP domains in proteins where both the input and output signals occur intracellularly are limited to those of the Aer energy taxis receptor of *Escherichia coli*, which has both a HAMP domain and a sensory PAS domain. *Campylobacter jejuni* has an energy taxis system consisting of the domains of Aer divided between two proteins, CetA (HAMP-containing) and CetB (PAS-containing). In this study, we found that the CetA HAMP domain differs significantly from that of Aer in predicted secondary structure. Using similarity searches, we identified 55 pairs of HAMP/PAS proteins encoded by adjacent genes in a diverse group of microorganisms. We propose that these HAMP/PAS pairs form a new family of bipartite energy taxis receptors. Within these proteins, we identified nine residues in the HAMP and a proximal signaling domain that are highly conserved, at least three of which are required for CetA function. Additionally, we demonstrated that CetA contributes to *C. jejuni* invasion of human epithelial cells, while CetB does not. This finding supports

the hypothesis that members of HAMP/PAS pairs possess the capacity to act independently of each other in cellular traits other than energy taxis.

Introduction

HAMP domains (named for their presence in histidine kinases, adenylyl cyclases, methyl-accepting chemotaxis proteins and phosphatases) (Aravind and Ponting, 1999) represent a common element in numerous bacterial signal transduction proteins. There are more than 11,700 known or predicted proteins containing HAMP domains identified in the SMART database (Letunic *et al.*, 2004). The vast majority of these proteins are bacterial, but HAMP domains have also been identified in archaea and lower eukaryotic organisms. HAMP domains are thought to play a role in intramolecular communication between input and output domains of a single protein (Appleman *et al.*, 2003; Appleman and Stewart, 2003; Aravind and Ponting, 1999). HAMP domains have predominantly been studied in transmembrane receptors that translate a signal originating extracellularly to an intracellular signal transduction domain.

Our understanding of how HAMP domains function has been hampered by considerable sequence divergence among these domains and a paucity of structural data. Sequence analysis and mutagenesis studies indicated that HAMP domains consist of two amphipathic helices (AS-1 and AS-2) which are joined by a flexible loop region to form a coiled-coil (Appleman and Stewart, 2003; Butler and Falke, 1998; Singh *et al.*, 1998). Recently, the structure of the HAMP domain from the *Archaeoglobus fulgidus* protein Af1503 was solved (Hulko *et al.*, 2006). Af1503 is atypical of HAMP domain-containing proteins in that it lacks an output signal transduction domain (Hulko *et al.*,

2006). This structure consisted of two amphipathic helices that come together in the only known occurrence of a parallel coiled-coil. These helices form a four-helix bundle in a HAMP domain dimer. This four-helix bundle adopts an unusual knobs-to-knobs conformation. These findings gave rise to a model where a shift in two transmembrane helices is translated into a gear-like 26° rotation of the helices relative to one another within the HAMP dimer four-helix bundle (Hulko *et al.*, 2006).

While many HAMP domains occur in transmembrane receptors with extracellular input and intracellular output domains, this is not true of all HAMP domains. Search of the SMART database reveals that there are more than 400 known or predicted proteins with a HAMP domain that lack a predicted transmembrane domain. The mechanism by which HAMP domains might function in such proteins has not been extensively probed. Studies of a HAMP domain-containing protein in which the input and output signals both occur in the cytoplasm are limited to Aer of *Escherichia coli*. Aer, the major energy taxis receptor of *E. coli*, possesses four major domains: i) a PAS domain (named after three proteins Per, ARNT and Sim, where it was first identified) (Taylor and Zhulin, 1999) that binds FAD, the redox state of which is thought to reflect the redox state of element(s) of the electron transport system; ii) two transmembrane domains separated by a short periplasmically accessible region; iii) a HAMP domain; and iv) a conserved signaling domain present in all methyl-accepting chemotaxis proteins (MCPs) (Alexander and Zhulin, 2007; Taylor, 2007). The PAS domain of Aer has been predicted to interact directly with the HAMP domain to transmit an energy taxis signal parallel to, rather than across, the inner membrane (Taylor, 2007).

An energy taxis system consisting of a variation on the domain arrangement of Aer was previously identified in *Campylobacter jejuni* (Hendrixson *et al.*, 2001). *C. jejuni*, a microaerophilic, Gram-negative bacterium commonly found in the gastrointestinal tract of chickens and other livestock, is one of the most common causes of food borne gastroenteritis in the U.S. The flagellum and motility of this bacterium has proven essential for both its commensal and pathogenic lifestyles (Guerry, 2007; Young *et al.*, 2007). An energy taxis system of *C. jejuni* was identified in a screen of a transposon library for mutants defective in flagellar motility (Hendrixson *et al.*, 2001). This system consists of two proteins, CetA and CetB, which together contain all of the domains of the single protein Aer. CetA, a predicted membrane bound protein, possesses a predicted HAMP domain and the signaling domain. CetB, a predicted cytoplasmic protein, possesses a predicted PAS domain (Hendrixson *et al.*, 2001).

CetA and CetB are proposed to interact with one another directly to transduce an energy taxis signal via a similar mechanism to the single protein Aer (Hendrixson *et al.*, 2001). As the HAMP domain of Aer is proposed to interact directly with the PAS domain, we hypothesize that the HAMP domain of CetA may mediate an interaction between CetA and CetB. Separation of these domains into distinct proteins may enable CetA and/or CetB to interact with other proteins and participate independently in alternate signaling pathways (Hendrixson *et al.*, 2001).

In this study, we determined that the HAMP domain of CetA differs from that of Aer in predicted secondary structure. Based upon similarity with the CetA HAMP domain, we identified other members of a new family of putative bipartite energy taxis transducers. We found that the CetA homologues in this family possess highly conserved

HAMP domain residues, at least three of which are required for wildtype function of CetA in energy taxis. Finally, we determined that the Δ*cetA* mutant, but not the Δ*cetB* mutant, has a defect in invasion of human epithelial cells, supporting the hypothesis that CetA and/or CetB may function independently of one another in cellular processes other than energy taxis.

Materials and Methods

Bacterial strains and culture conditions. All bacterial strains and plasmids used in this study are listed in Table 3. DRH212, a spontaneous streptomycin resistant mutant of the clinical isolate *C. jejuni* 81-176 (Hendrixson *et al.*, 2001), was the background strain for all mutants studied and is referred to as wildtype. *C. jejuni* was routinely grown on Mueller-Hinton (MH) agar with 10 μg/ml trimethoprim under microaerophilic conditions (85% N_2, 10% CO_2, 5% O_2) in a tri-gas incubator. For *C. jejuni*, the following antibiotic concentrations were used: 10 μg/ml trimethoprim, 30 μg/ml cefaperazone, 50 μg/ml kanamycin, 20 μg/ml chloramphenicol and 0.1 or 2 mg/ml streptomycin. *E. coli* was grown in Luria-Bertani (LB) agar or broth. For *E. coli*, the following antibiotic concentrations were used: 50 μg/ml kanamycin or 100 μg/ml ampicillin.

Bioinformatic analysis. The HAMP domain in CetA was identified by PSI-BLAST (Altschul *et al.*, 1997). Proteins that contained a HAMP domain and proximal signaling domain similar to those of CetA (residues 44-139) were identified by a BLAST search of the protein non-redundant database. Those proteins identified in this BLAST search that also possessed a neighboring open reading frame containing a PAS domain were further analyzed for the presence of other functional domains using the SMART

Table 3. Bacterial strains and plasmids used in Chapter III.

Strain or plasmid	Relevant characteristics	Reference
Bacteria		
E. coli		
JM101	F′ *traD36 proA*$^+$*B*$^+$ *lacI*^{q} Δ*(lacZ)M15/* Δ*(lac-proAB) glnV thi*	New England Biolabs
DH5α/ pRK212.1	contains conjugative plasmid for transfer of plasmid into *C. jejuni*	(Figurski and Helinski, 1979)
C. jejuni		
DRH212	81-176 Sm^R, spontaneous mutant	(Hendrixson *et al.*, 2001)
DRH304	*cetB::cat-rpsL*, intermediate strain for deletion mutagenesis	(Hendrixson *et al.*, 2001)
DRH307	Δ*cetB*	(Hendrixson *et al.*, 2001)
DRH321	Δ*rpoN*	(Hendrixson *et al.*, 2001)
DRH333	Δ*cetA*	(Hendrixson *et al.*, 2001)
KYCj172	Δ*cetAB*	This study
Plasmids		
pUC19	Amp^R	New England Biolabs
pRY108	Km^R, *E. coli*/*C. jejuni* shuttle vector	(Yao *et al.*, 1993)
pKTY60	pUC19 with 3.5kb fragment containing *cj1191c*, *cetA* and *cetB* region cloned into the KpnI site	This study
pKTY62	pKTY60 with a deletion from the first codon of *cetA* to the last codon of *cetB*	This study
pKTY152	pKTY60 with the D94A mutation in the *cetA* coding sequence	This study
pKTY153	pKTY60 with the E102A mutation in the *cetA* coding sequence	This study
pKTY154	pKTY60 with the E97A mutation in the *cetA* coding sequence	This study
pKTY155	pKTY60 with the K118A mutation in the *cetA* coding sequence	This study
pKTY156	pKTY60 with the R101A mutation in the *cetA* coding sequence	This study
pKTY157	pKTY60 with the R117A mutation in the *cetA* coding sequence	This study
pKTY158	pKTY60 with the R71A mutation in the *cetA* coding sequence	This study
pKTY159	pKTY60 with the Y116A mutation in the *cetA* coding sequence	This study
pKTY160	pKTY60 with the Y99A mutation in the *cetA* coding sequence	This study
pKTY360	pRY108 with 2.4 kb fragment containing *cetA* and *cetB* coding sequence cloned into the XmnI site	This study
pKTY361	pKTY360 with the R71A mutation in the *cetA* coding sequence	This study
pKTY362	pKTY360 with the D94A mutation in the *cetA* coding sequence	This study
pKTY363	pKTY360 with the E97A mutation in the *cetA* coding	This study

	sequence	
pKTY364	pKTY360 with the Y99A mutation in the *cetA* coding sequence	This study
pKTY365	pKTY360 with the R101A mutation in the *cetA* coding sequence	This study
pKTY366	pKTY360 with the E102A mutation in the *cetA* coding sequence	This study
pKTY367	pKTY360 with the Y116A mutation in the *cetA* coding sequence	This study
pKTY368	pKTY360 with the R117A mutation in the *cetA* coding sequence	This study
pKTY369	pKTY360 with the K118A mutation in the *cetA* coding sequence	This study

tool (Letunic *et al.*, 2004). These proteins were also assessed for the presence of transmembrane domains using the DAS (dense alignment surface) method (Cserzo *et al.*, 1997). Proteins predicted to contain one long transmembrane helix with a strong dip in hydrophobicity in the middle of this region, corresponding to helical hairpin residues (Monne *et al.*, 1999a; Monne *et al.*, 1999b), were designated as possessing two transmembrane domains on the basis of topology analysis of CetA (see Chapter II). The G+C % of each HAMP-containing bipartite family member gene was plotted against the G+C % of the genome in which it was found. Using Excel, a linear regression trendline and associated R^2 value were calculated. HAMP domains and adjacent regions from homologous proteins were aligned using CLUSTALX (Thompson *et al.*, 1997) with default parameters. Conserved residues were identified using Nigel Brown's consensus script (available at www.bork.embl-heidelberg.de/Alignment/consensus.html).

Modeling of CetA Structure. The structure of HAMP domain from *Archaeoglobus fulgidus* (PDB ID: 2ASW) was used as the foundation for modeling the structure of CetA. To model the HAMP domain of CetA, the amino acid sequence of 2ASW was mutated into that of CetA using the graphics program O (Jones *et al.*, 1991) and the single amino acid insertion was fit using the program's lego-loop option. The resulting CetA model was then placed into a box of waters containing a minimum of two shells of water, minimized and put through simulated annealing using torsion angle dynamics in CNS (Crystallography and NMR System) (Brunger *et al.*, 1998).

Construction of Δ*cetAB* deletion mutant. The Δ*cetAB* deletion mutant was constructed essentially as described by Hendrixson *et al* (Hendrixson *et al.*, 2001). The *cetA* and *cetB* coding sequences with 1036bp upstream and 595bp downstream were

amplified by PCR with primers designed with KpnI sites at their 5' ends for cloning into pUC19. The resulting plasmid was pKTY60. A deletion from the first codon of *cetA* to the last codon of *cetB* was created via Pfu mutagenesis (Weiner *et al.*, 1994). This plasmid, pKTY62, was electroporated into DRH304, which harbors the *cat-rpsL* cassette in the *cetB* coding sequence. Transformants were selected on 2 mg/ml streptomycin and screened for sensitivity on 20 μg/ml chloramphenicol. The deletion was confirmed by PCR analysis and chromosomal sequencing.

Construction of a plasmid to complement the Δ*cetAB* mutant. pKTY60 was digested with ApaLI and BsrBI. The resulting fragment containing the *cetA* and *cetB* coding sequences, along with 299 bases upstream and 202 bases downstream was blunted by T4 DNA polymerase. This fragment was then cloned into the XmnI site in the *E. coli*/*C. jejuni* shuttle vector pRY108 (Yao *et al.*, 1993).

Site-directed mutagenesis. Point mutations in the *cetA* coding sequence leading to alanine substitutions (R71A, D94A, E97A, Y99A, R101A, E102A, Y116A, R117A, K118A) were made in pKTY60 using Pfu mutagenesis (Weiner *et al.*, 1994). DNA sequence of the resulting plasmids was determined to confirm the presence of the point mutation and ensure the absence of additional mutations. These plasmids were then digested with ApaLI and BsrBI and the resulting fragment cloned into the XmnI site of pRY108 as described above. The orientation of the insertions into pRY108 was checked by multiple restriction digests to confirm that the resulting plasmids, pKTY361-pKTY369, are identical to pKTY360 except for the indicated point mutations.

Conjugation of plasmids into *C. jejuni*. Plasmids were conjugated into *C. jejuni* as described by Guerry *et al* (Guerry *et al.*, 1994). Briefly, *C. jejuni* was grown on MH

agar with 10 μg/ml trimethoprim for 16-20 hours and resuspended in MH broth to an OD_{600} of 1.0. Overnight cultures of the *E. coli* donor strain (DH5α[pRK212.1] containing the plasmid to be conjugated into *C. jejuni*) were diluted into fresh LB broth and grown to an OD_{600} of 0.5. 500 μl of the donor culture was centrifuged and the pellet washed twice with MH broth, then resuspended in 1 mL of the *C. jejuni* recipient culture. This mixture was spotted onto MH agar with no antibiotics. After 5 hours at 37°C in microaerophilic conditions, the bacteria were resuspended and spread onto MH agar containing 10 μg/ml trimethoprim, 30 μg/ml cefaperazone, 2 mg/ml streptomycin and 50 μg/ml kanamycin. PCR was used to verify transfer of the plasmid to the recipient *C. jejuni* strain.

SDS-PAGE and Western blots. For SDS-PAGE of whole cell lysates, *C. jejuni* strains were grown on MH agar for 16-20 hours, then resuspended in MH broth to an OD_{600} of 0.8. The bacteria were pelleted by centrifugation and the pellet resuspended in 100μL 2x sample buffer. Samples were boiled then separated on 12.5% polyacrylamide gels. Proteins were transferred to nitrocellulose membranes and probed with rabbit anti-CetA (1:10,000-1:75,000, generated against an internal peptide by Open Biosystems) or rabbit anti-CetB (1:500-1:5000, generated against an internal peptide by Open Biosystems) followed by goat anti-rabbit alkaline phosphatase-conjugated secondary antibody (1:10,000, Zymed). Western blots were developed using the chromogenic substrate 5-bromo-4-chloro-3-indolyl phosphate/nitro blue tetrazolium as previously described (Sambrook *et al.*, 1989).

Motility assays. *C. jejuni* was grown on MH agar containing 10 μg/ml trimethoprim and 50 μg/ml kanamycin for 16-20 h and resuspended in MH broth to an

OD_{600} of 0.4. 0.4 μl of each strain was injected into MH motility medium containing 0.4% agar. Plates were incubated for 28 h in microaerophilic conditions. The diameter of the outermost motility ring was measured with calipers. The average and standard deviation of six replicates was calculated and the assay was repeated three times.

Tissue culture. The human epithelial cell line INT 407 was used in invasion experiments. INT 407 cells were cultured in DMEM + 10% FBS supplemented with GIBCO MEM non-essential amino acids and 2mM glutamine (referred to as DMEM hereafter) in a 37°C, 5% CO_2 incubator. When cells were cultured in the absence of *C. jejuni*, the DMEM was supplemented with 10 units/ml penicillin and 10 μg/ml streptomycin.

Adherence and invasion assays. For invasion assays, INT 407 cells were seeded at approximately 10^5 cells/well in each well of a 24-well plate and incubated in the absence of antibiotics for an additional 12-18 h. For the inoculum, *C. jejuni* strains were grown on MH agar for 16-20 h and resuspended in DMEM. The INT 407 cells were rinsed twice with PBS and inoculated with *C. jejuni* at an MOI of ~200. The 24-well plates were centrifuged at 150 x g for 5 minutes, then incubated in a 37°C, 5% CO_2 incubator. To determine the number of total cell-associated bacteria, the cells were incubated for 2 h, rinsed twice with PBS, lysed in PBS + 0.1% Triton X-100, and serial dilutions were plated on MH agar to obtain colony forming units (cfu). To determine the number of intracellular bacteria, the cells were incubated for 2 h, rinsed twice with PBS and incubated for an additional 2.5h in DMEM + 100μg/ml gentamicin. The cells were then rinsed twice with PBS, lysed in PBS + 0.1% Triton X-100, and serial dilutions were plated on MH agar to obtain cfu. For invasion time course experiments, the cells were

infected with *C. jejuni* as described above. At 0.5 h, 1 h, 1.5 h, 2 h or 4 h post-infection, the numbers of total cell-associated and intracellular bacteria were determined as described above. To assess invasion, the percentage of total cell-associated bacteria that were intracellular was calculated. To assess adherence, the percentage of the inoculum that was cell-associated was calculated. The average and standard deviation of three replicates were obtained and each invasion assay and time course assay was repeated a minimum of three times.

Secretion assay. *C. jejuni* cultures were metabolically labeled with [^{35}S]-methionine as previously described elsewhere (Konkel and Cieplak, 1992). Supernatant fluids were concentrated four-fold by the addition of ice-cold 1 mM HCl-acetone. The pellets were air dried and resuspended in 100 µl of water and 100 µl of 2x sample buffer. Equal volumes of the concentrated samples were separated on 12.5% SDS-PAGE. Autoradiography was performed with Kodak BioMax MR film at -80°C.

Results

CetA and Aer differ in predicted HAMP domain secondary structure. Using PSI-BLAST, the CetA HAMP domain was identified as residues 47-101. This region was not identified as a HAMP domain by SMART analysis. This is not surprising because of a high degree of divergence between various HAMP domains. Current HAMP domain models miss more than 30% of HAMP homologues (Rekapalli and Zhulin, unpublished data). The CetA HAMP domain is significantly divergent from that of Aer.

The HAMP domain of Aer has an unusual predicted secondary structure (Ma *et al.*, 2005). While the canonical HAMP domain consists of two amphipathic helices (AS-

1 and AS-2), Aer possesses one amphipathic helix (AS-1) and one hydrophobic helix (AS-2) (Fig. 15A) (Ma *et al.*, 2005). In contrast to the unusual secondary structure of Aer, CetA is predicted to have the more common HAMP domain structure of two amphipathic helices (Fig. 15B).

CetA and CetB found a new family of proposed bipartite energy taxis receptors. Aer and CetA/CetB contain the same domains and are hypothesized to transduce energy taxis signals via a similar mechanism (Hendrixson *et al.*, 2001). However, the differences in HAMP domain primary and secondary structure between Aer and CetA led us to examine the CetA HAMP domain in more detail. Using the HAMP domain and proximal signaling domain (residues 44-139) of CetA in a BLASTP search of the non-redundant database, we identified 63 proteins with similar domain arrangements to that of CetA. 55 of them were encoded by genes with a neighboring open reading frame (orf) encoding a PAS domain and lacking other functional domains, similar to *cetA* and *cetB*, which are adjacent in the *C. jejuni* genome. We refer to these pairs of proteins encoded by adjacent genes as HAMP/PAS pairs (Table 4).

The CetA-like (HAMP-containing) members of this family can be divided into 8 classes, based on predicted topology and functional domains (Fig. 16). Most CetA homologues fall into Classes I-III, which contain a HAMP domain, a signaling domain and two, one or zero transmembrane domains, respectively. There are only two predicted proteins in Class II, with a single predicted transmembrane domain. It is possible that these genes contain a sequencing error leading to an incorrect predicted transcriptional start site. Variations on the domain arrangement of CetA containing additional domains or lacking the signaling and/or transmembrane domains were also identified (Classes IV-

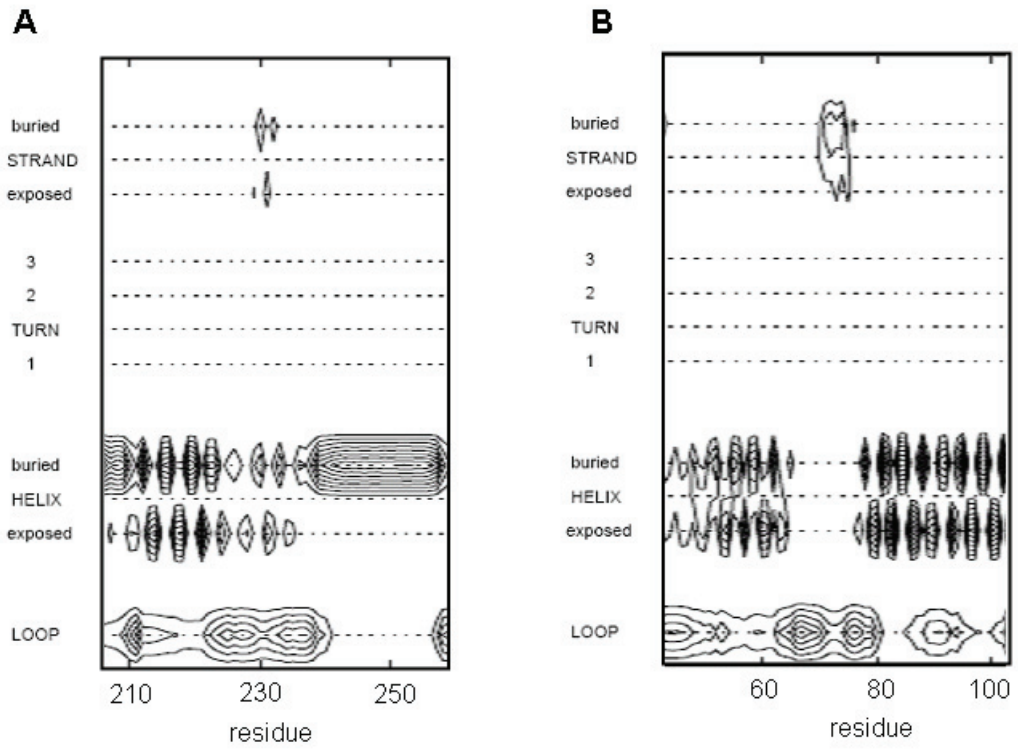

Figure 15. Secondary structure analysis of the Aer and CetA HAMP domains. A. Aer HAMP domain contour plot of secondary-structure probabilities at indicated residues (PSA server). **B.** CetA HAMP domain contour plot of secondary-structure probabilities at indicated residues (PSA server).

Table 4. Members of the bipartite family of energy taxis transducers identified by similarity to the CetA HAMP and proximal signaling domain.

Species/strain	Accession no.	e-value[a]	Class[b]	PAS neighbor accession no.[c]
Azoarcus sp. BH72	YP_934977	9.00E-04	I	YP_934978
Bradyrhizobium japonicum USDA 110	NP_769616	2.00E-06	I[d]	NP_769615
Caminibacter mediatlanticus TB-2	ZP_01871323 ZP_01870851	0.001 0.002	I I	ZP_01871324 ZP_01870852
Campylobacter coli RM2228	ZP_00367208	8.00E-51	I[d]	ZP_00367209, ZP_00367207
Campylobacter concisus 13826	YP_001466825	2.00E-06	III	YP_001466824
Campylobacter curvus 525.92	YP_001408340[e]	0.001	III	YP_001408339
Campylobacter jejuni 11168	NP_282337	7.00E-51	I[d]	NP_282336, NP_282338
Campylobacter jejuni 81-176	YP_001000865	7.00E-51	I[d]	YP_001000864, YP_001000866
Campylobacter jejuni HB93-13	ZP_01070888	7.00E-51	I	ZP_01070815, ZP_01071201
Campylobacter jejuni CG8486	ZP_01809879	7.00E-51	I[d]	ZP_01809880, ZP_01809878
Campylobacter jejuni 260.94	ZP_01069112	7.00E-51	I[d]	ZP_01069301, ZP_01069270
Campylobacter jejuni CF93-6	ZP_01068608	7.00E-51	I[d]	ZP_01068595, ZP_01068567
Campylobacter jejuni 81116	YP_001482710	7.00E-51	I[d]	YP_001482711, YP_001482709
Campylobacter jejuni RM1221	YP_179311	7.00E-51	I[d]	YP_179312, YP_179310
Campylobacter jejuni 84-25	ZP_01099629	8.00E-51	I[d]	ZP_01099329, ZP_01099967
Campylobacter jejuni doylei 269.97	YP_001397715	2.00E-49	I[d]	YP_001397716
Campylobacter lari RM2100	ZP_00368322	7.00E-34	I	ZP_00368323,

				ZP_00368324
Campylobacter upsaliensis RM3195	ZP_00371342	1.00E-38	I	ZP_00371343, ZP_00371341
Chromobacterium violaceum ATCC 12472	NP_900065	3.00E-04	I	NP_900066
Dechloromonas aromatica RCB	YP_287205	7	I	YP_287206
Kineococcus radiotolerans SRS30216	YP_001363132	0.009	III	YP_001363131
Magnetospirillum gryphiswaldense MSR-1	CAM75236	0.003	I[d]	CAM75237
	CAM75032	0.005	V	CAM75033
	CAM78133	0.065	VI	CAM78134, CAM78135[f]
Magnetospirillum magneticum AMB-1	YP_419949[g]	3.00E-04	I	YP_419948
	YP_423371	0.002	I	YP_423372
	YP_423064	0.06	I	YP_423063
	YP_420357	0.07	I	YP_420358
	YP_421559	0.13	I	YP_421560
	YP_419547	1.9	I	YP_419548
Magnetospirillum magneticum MS-1	ZP_00055894	4.00E-04	IV	ZP_00055893
	ZP_00207863	9.00E-04	I	ZP_00207862
	ZP_00208993	0.003	VIII	ZP_00208994, ZP_00051415 [f]
	ZP_00054945[h]	0.43	VII	ZP_00054944
Oceanobacter sp. RED65	ZP_01306652	0.32	I	ZP_01306653
Oceanospirillum sp. MED92	ZP_01166142	0.051	I	ZP_01166143
Reinekea sp. MED297	ZP_01113626	0.88	I	ZP_01113627
Rhodopseudomonas palustris BisA53	YP_783562	1.00E-04	I	YP_783563
Rhodopseudomonas palustris BisB5	YP_568532	4.00E-04	I	YP_568531
	YP_571029	0.26	I	YP_571030
Rhodopseudomonas palustris BisB18	YP_534502	2.00E-06	I	YP_534503
Rhodopseudomonas palustris CGA009	NP_949817[i]	8.00E-05	I	NP_949818[i]
	NP_949819[i]	1.00E-04	II	NP_949820[i]
	NP_949538	1.00E-04	I[d]	NP_949539
	NP_949647	0.45	I	NP_949648
Rhodopseudomonas palustris HaA2	YP_484693	3.00E-07	II	YP_484692
	YP_485035	8.00E-04	I	YP_485034
	YP_484934	0.16	I	YP_484933
Rhodospirillum rubrum ATCC 11170	YP_428546[j]	0.011	I	YP_428545
Stappia aggregata IAM 12614	ZP_01546232	2.00E-04	I[d]	ZP_01546231

Sulfurimonas denitrificans DSM 1251	YP_392559	1.00E-05	III	YP_392560
Wolinella succinogenes DSM 1740	NP_907800	1.00E-11	I	NP_907801
	NP_906923	6.00E-09	I[d]	NP_906922
	NP_907510	3.00E-05	I[d]	NP_907511

[a] e-value obtained from BLAST search with CetA HAMP and proximal signaling domain (amino acids 44-139).
[b] Class of HAMP domain-containing bipartite family member (see Fig. 2).
[c] Adjacent gene encoding a PAS domain, but no other domains unless so indicated.
[d] Transmembrane helix prediction programs predict one transmembrane helix, but we propose that there are two transmembrane helices present in a helical hairpin (see Materials and Methods).
[e] Misannotated as a DNA binding response regulator.
[f] PAS neighbor contains additional predicted functional domains.
[g] Misannotated as a sensory rhodopsin II transducer.
[h] Misannotated as MCP, but does not contain the HCD.
[i] These HAMP/PAS pairs are adjacent to one another.
[j] Misannotated as a response regulator.

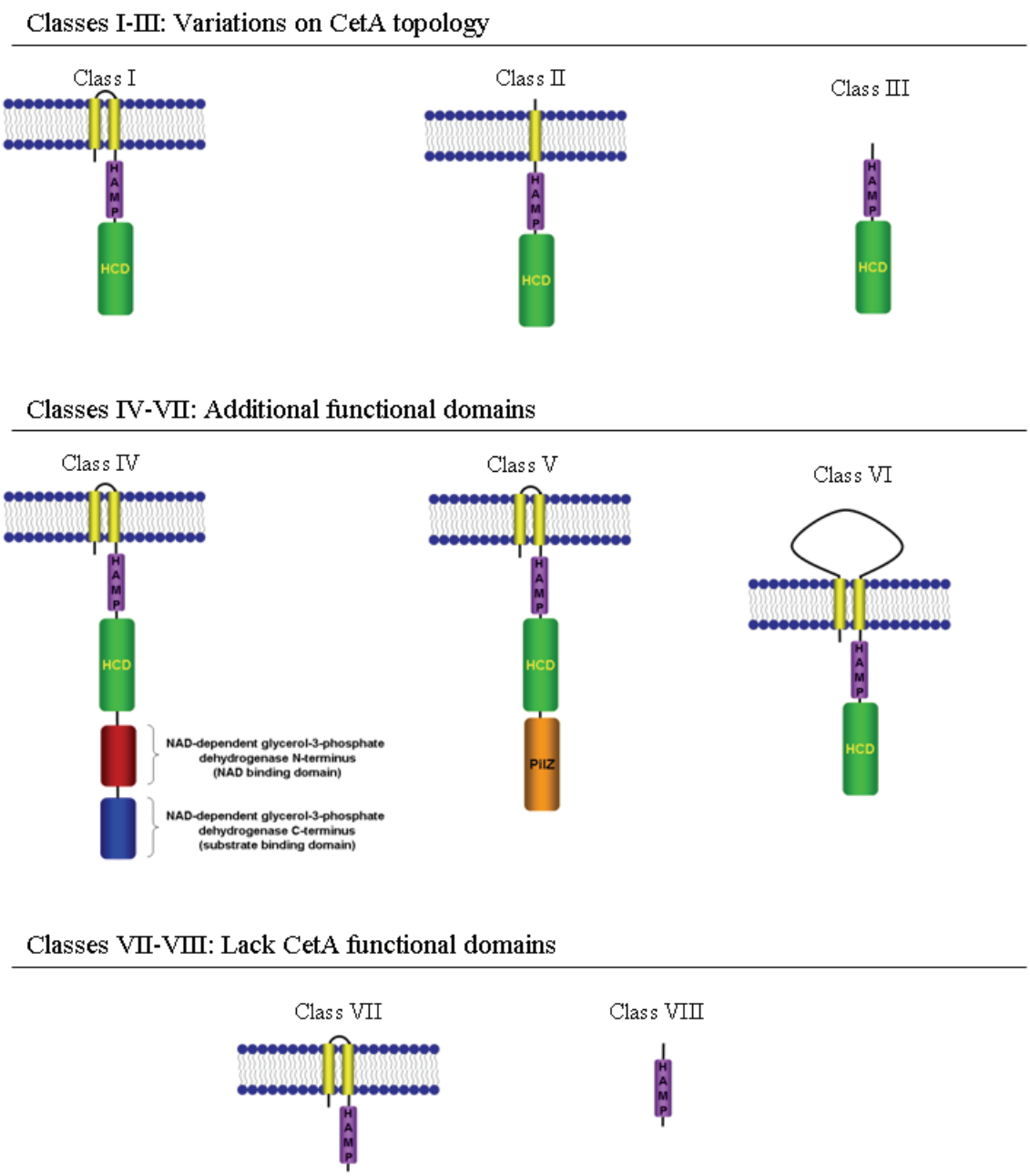

Figure 16. Classes of HAMP-containing bipartite family members. HAMP-containing proteins from Table 1 were analyzed by SMART and DAS and separated into different classes on the basis of predicted topology and functional domains.

VIII). In all, we identified 55 HAMP/PAS pairs, 40 of which are in genera other than *Campylobacter* (Table 4). The majority of organisms containing HAMP/PAS pairs belong to the epsilon class of proteobacteria, but HAMP/PAS pairs are also found in the alpha, beta, and gamma classes of proteobacteria as well as in one Gram-positive, the actinobacterium *Kineococcus radiotolerans* (Table 5). The GC content of the HAMP genes corresponds well to that of the genomes in which they are found (Fig. 17A). Several strains contain more than one HAMP/PAS pair (Fig. 17B). In those strains that contain multiple HAMP/PAS pairs, the HAMP members of different HAMP/PAS pairs may also fall into more than one class (Fig. 17C). We propose that these HAMP/PAS pairs comprise a new family of bipartite energy taxis receptors.

Bipartite family members contain conserved HAMP and proximal domain residues. The HAMP domain and proximal signaling domain of representative CetA-like bipartite family members were aligned using CLUSTALX (Fig. 18). Nine residues are highly conserved within this subfamily, but not within the HAMP consensus sequence. HAMP domains, in general, share very low levels of sequence conservation, so the presence of such highly conserved residues is notable. Interestingly, most of highly conserved residues are predicted to participate in protein-protein interactions (charged and aromatic).

To understand the placement of these conserved residues in the protein, a model of the CetA HAMP domain was created. The amino acid sequence of CetA was threaded onto the averaged NMR structure of *Archaeoglobus fulgidus* (2ASW), the only HAMP domain present in the Protein Data Bank, using the graphics program O (Jones *et al.*, 1991). Four of the five conserved residues that fall within the HAMP domain (R71, D94,

Table 5. Taxonomic distribution of bipartite family members

Taxonomic phylum	# strains with HAMP/PAS pairs
α-proteobacteria	11
β-proteobacteria	3
ε-proteobacteria	18
γ-proteobacteria	3
actinobacteria	1

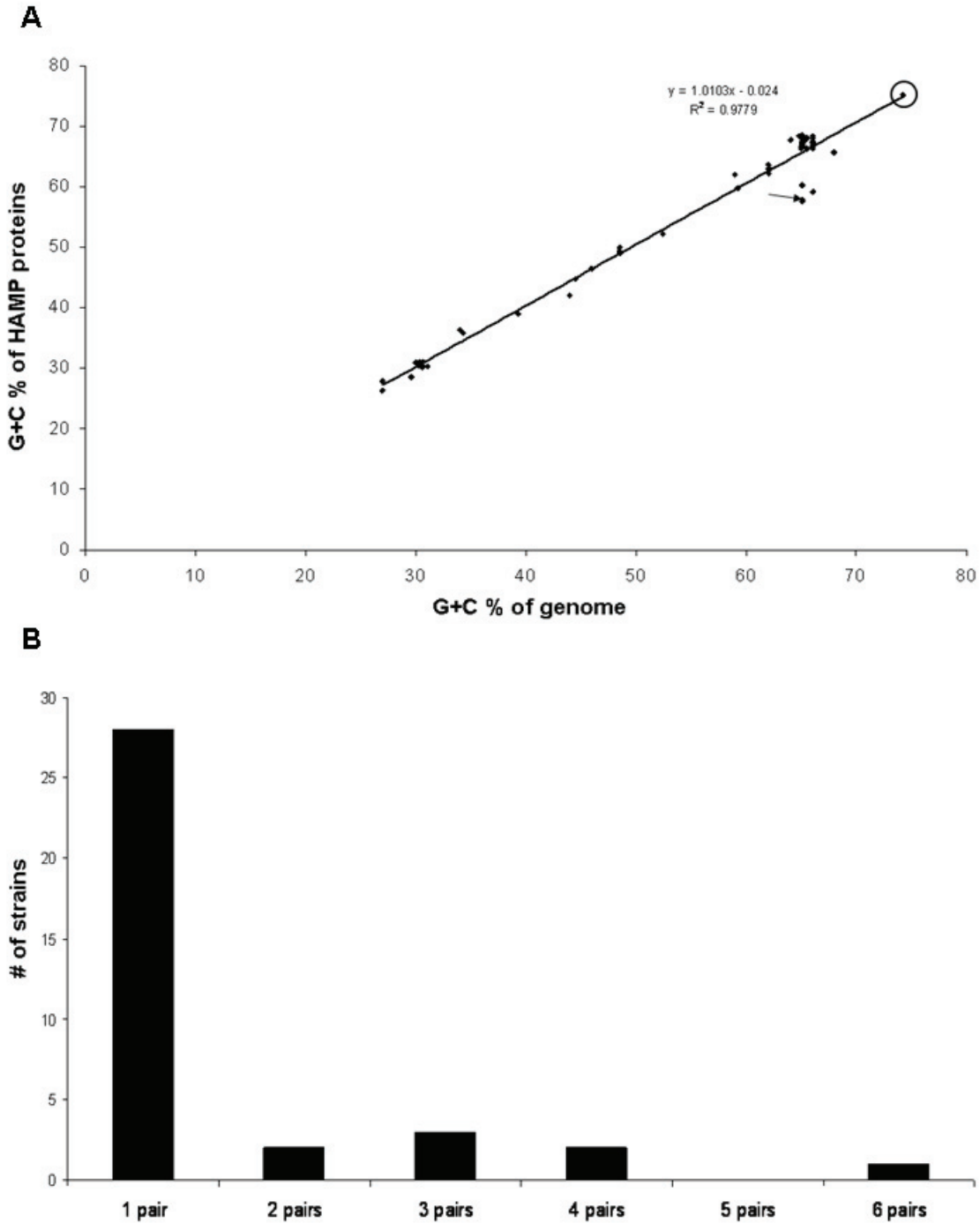
A
y = 1.0103x - 0.024
R² = 0.9779
G+C % of HAMP proteins
G+C % of genome
0
10
20
30
40
50
60
70
80
B
# of strains
0
5
10
15
20
25
30
1 pair
2 pairs
3 pairs
4 pairs
5 pairs
6 pairs

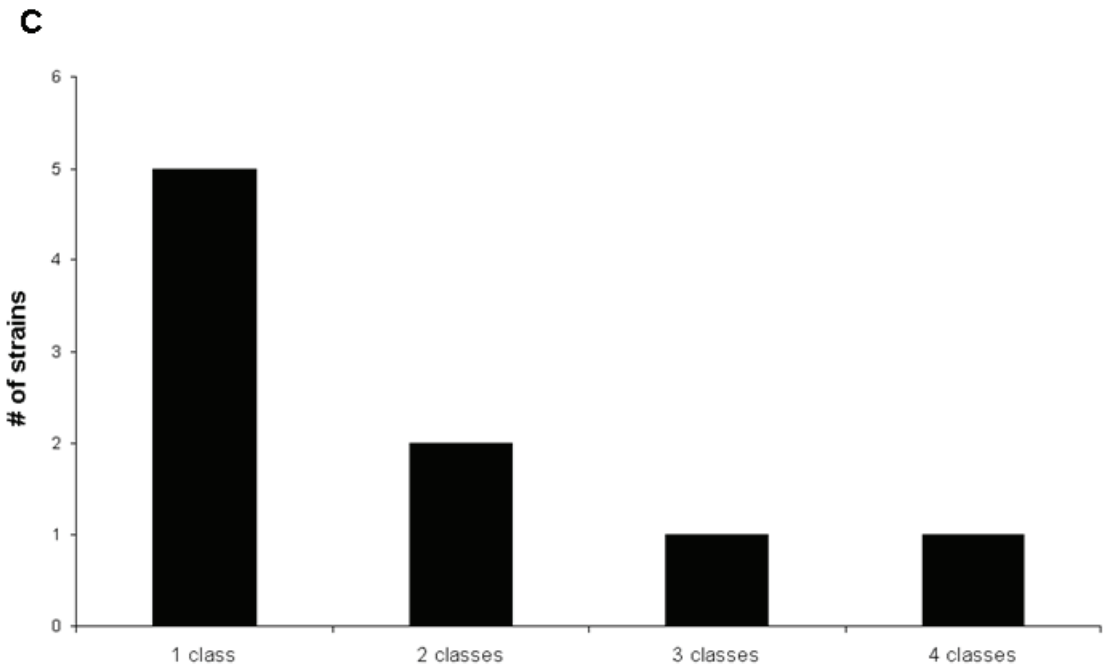

Figure 17. Distribution of bipartite family members. A. The G+C % of each gene encoding a HAMP protein in the bipartite family plotted vs. the G+C % of the genome in which it resides. A linear regression trendline and R^2 value are shown. The data point for the *Kineococcus radiotolerans* HAMP protein is circled. Arrow indicates the data point for the *Magnetospirillum magneticum* AMB-1 HAMP protein found in the magnetosome island (see Discussion). **B.** Histogram indicating the number of HAMP/PAS pairs per strain. **C.** Histogram indicating the number of classes represented by the HAMP member of HAMP/PAS pairs in strains harboring multiple HAMP/PAS pairs.

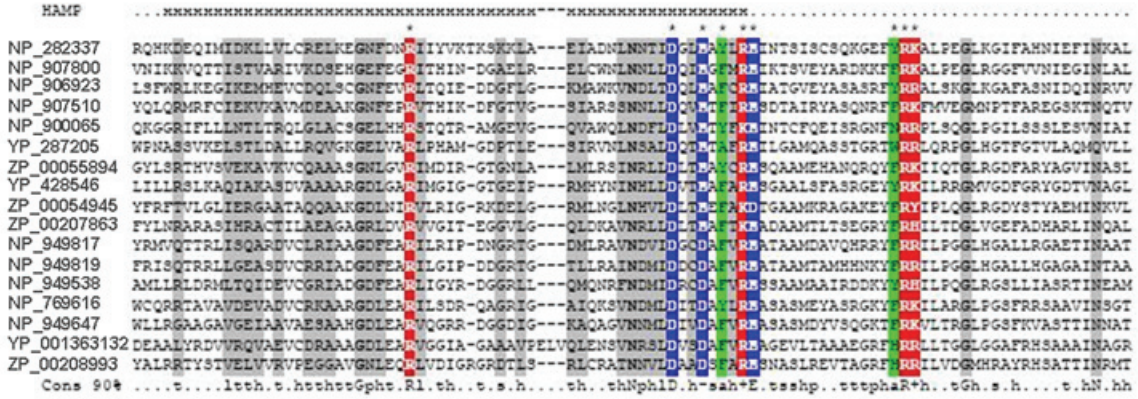

Figure 18. Distribution of conserved residues within the HAMP and proximal signaling domains of CetA homologues. Multiple alignment of the HAMP and proximal signaling domains of representative CetA homologues. Strongly conserved positions that are likely to contribute to protein-protein interactions are highlighted in blue (negative charge), red (positive charge) and green (aromatic). Strongly conserved positions that are likely to contribute primarily to structure and mildly conserved positions are highlighted in gray.

E97 and R101) appear to cluster near one another on the surface of the HAMP four-helix bundle (Fig. 19B). The fifth conserved residue in the HAMP domain (Y99), however, is located between the two monomers and is predicted to be involved in tyrosine stacking interactions between HAMP monomers at the base of the four-helix bundle (Fig. 19B). The four remaining conserved residues (E102, Y116, R117 and K118) fall outside of the Af1503 structure used to model the CetA HAMP domain and, therefore, their location within the protein cannot be predicted. This model of the CetA HAMP domain structure shows an overall dipole moment, as the N-terminal half of the structure has a net positive charge, while the C-terminal half of the structure has a net negative charge (Fig. 19C). When we calculated the electrostatic surface potentials for the Af1503 HAMP domain, an overall dipole moment was also apparent, although less pronounced than in the CetA HAMP domain structural model (Fig. 19D).

Conserved HAMP domain residues are important for CetA function.

Attempts to complement a Δ*cetA* mutant with a plasmid expressing *cetA* from a constitutive promoter were unsuccessful (data not shown), likely because the relative levels of CetA to CetB, as well as the levels of these proteins relative to other MCPs, are important for proper energy taxis signal transduction. A double deletion strain was constructed with the deletion extending from the first codon of *cetA* to the last codon of *cetB*. We also constructed a plasmid, pKTY360, consisting of the *cetA* and *cetB* genes, as well as 299 bases upstream and 202 bases downstream, cloned into the pRY108 *E. coli*/*C. jejuni* shuttle vector (Yao *et al.*, 1993). This plasmid does not contain a promoter to drive expression of the cloned region, so *cetAB* expression must originate from their

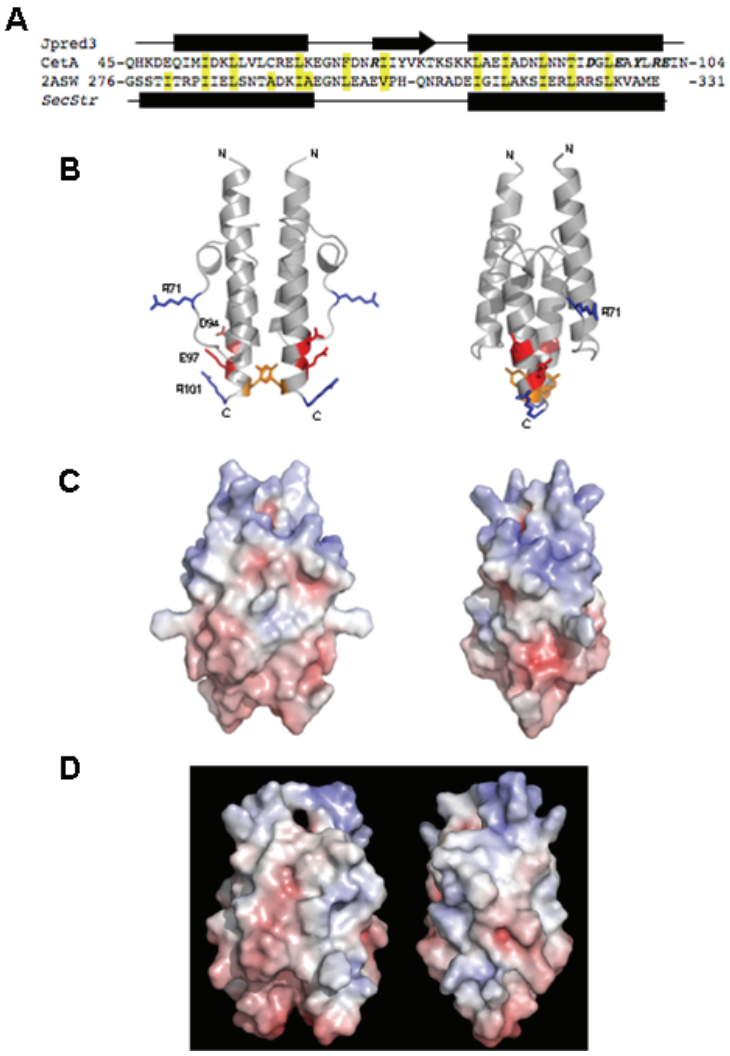

Figure 19. Model of CetA HAMP domain. A. The sequence alignment of CetA and AF1503 HAMP domains from ClustalW2 (Chenna *et al.*, 2003) (http://www.ebi.ac.uk/Tools/clustalw2/index.html) is shown with the hydrophobic residues of the heptad repeat and linker region boxed in yellow. The secondary structure prediction for CetA (Cuff and Barton, 2000) (http://www.compbio.dundee.ac.uk/~www-jpred/index.html) and the published secondary structure of AF1503 are shown above and below their amino acid sequences, respectively. Helices and β-strands are represented as black rectangles and arrows, respectively. Residues mutated in CetA are italicized. **B.** The model of a CetA HAMP domain dimer is depicted as a ribbon diagram with the mutated residues shown in ball-n-stick. The views for individual molecules are separated by a 90° rotation about the y-axis. **C.** Electrostatic surface potentials for the modeled structure of CetA were calculated using APBS (Baker *et al.*, 2001) and mapped onto their respective solvent accessible surfaces using Pymol (DeLano, 2002). Negative potentials (-10 kT/e) are shown in red, positive potentials (10 kT/e) in blue. The views are the same as in B. The proteins structures are shown at the same magnification for each view. **D.** Electrostatic surface potentials for the Af1503 HAMP domain structure were calculated as in C.

native promoter. pKTY360 (pRY108*::cetAB*) partially complements the motility defect of the Δ*cetAB* double mutant in MH motility agar (Fig. 20).

Alanine substitutions were made for each of the conserved residues in CetA in the context of pKTY360. Several of these substitutions led to a growth defect or loss of CetA stability (Fig. 21A, 21B), but three substitutions (R71A, Y99A and K118A; pKTY361, pKTY364 and pKTY369, respectively) retained growth kinetics and CetA expression levels at or near that of Δ*cetAB* [pKTY360] (Fig. 21A, 21C). Mutant proteins with these substitutions exhibited abrogated or reduced ability to rescue the motility defect of the Δ*cetAB* double deletion strain (Fig. 20). These results indicate that at least some of the conserved residues within the bipartite family HAMP and proximal signaling domains are required for wildtype function.

Δ*cetA* has an epithelial cell invasion defect, but Δ*cetB* does not. CetA and CetB are each required for energy taxis in *C. jejuni*, suggesting a functional interaction whose mechanism may be similar to that of Aer (Hendrixson *et al.*, 2001). However, the separation of Aer domains into two proteins in CetA and CetB, as well as other members of this family, raises the possibility that each member of a HAMP/PAS pair may contribute independently to different traits. As *C. jejuni* is a common commensal of chickens, we previously tested Δ*cetA* and Δ*cetB* mutants in a chick colonization model and both mutants colonized to wildtype levels (Hendrixson and DiRita, 2004).

C. jejuni actively invades human epithelial cells, a trait associated with its pathogenicity (Kopecko *et al.*, 2001). To determine whether or not CetA or CetB contribute to this phenotype, we tested mutants in a tissue culture model of invasion (Hu and Kopecko, 1999; Oelschlaeger *et al.*, 1993). INT 407 cells were infected with

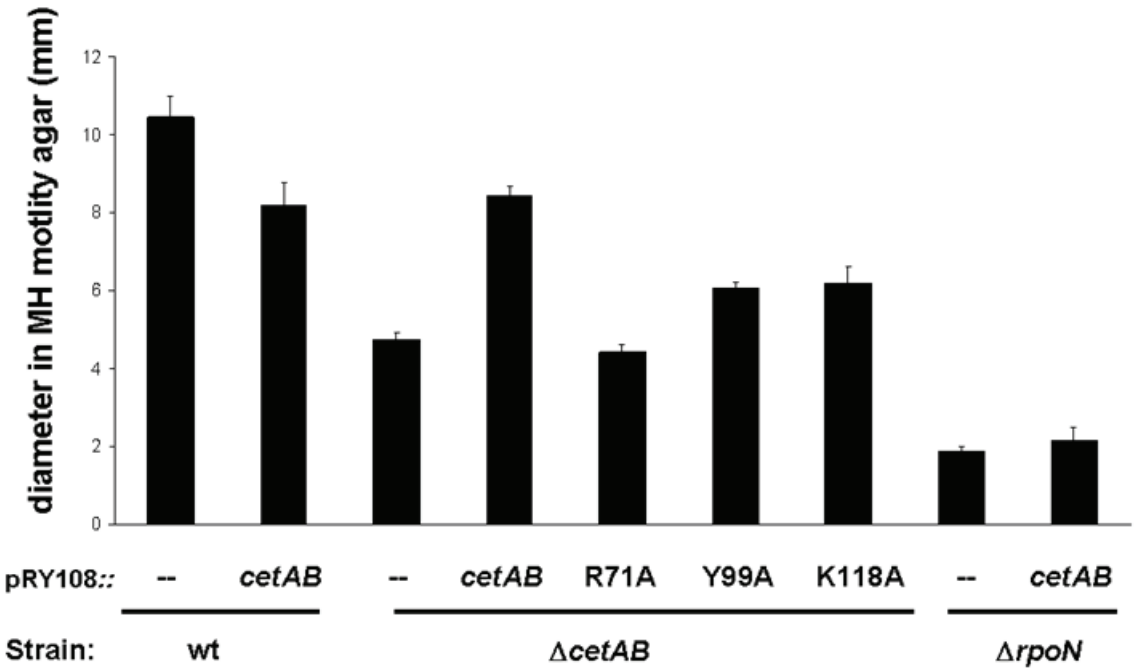

Figure 20. Influence of point mutations on CetA function in motility. Motility assays were performed on WT, Δ*cetAB* and Δ*rpoN* strains containing an empty vector, pRY108, or pRY108*::cetAB* (with and without the indicated HAMP and proximal signaling domain point mutations).

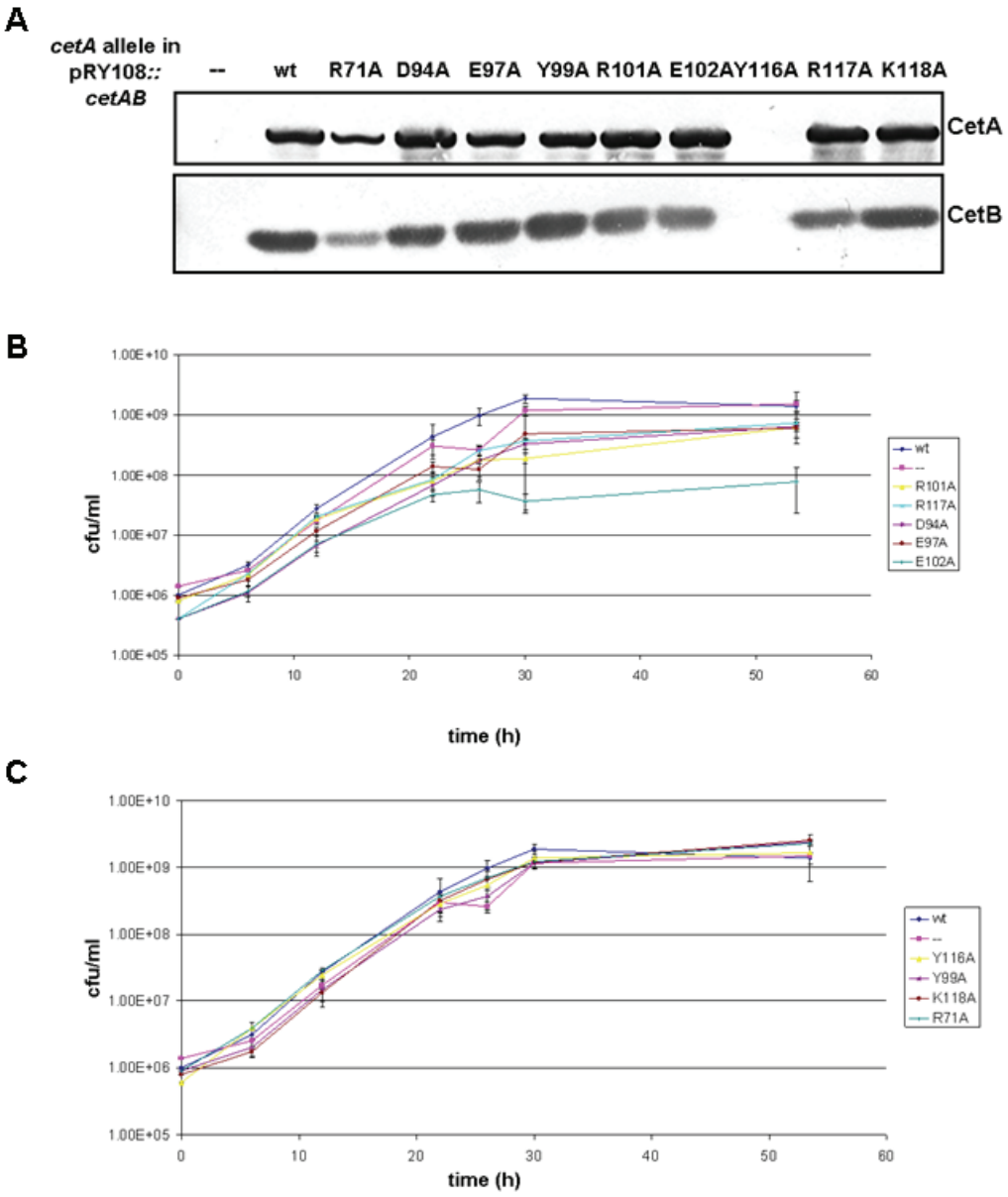

Figure 21. CetA and CetB expression levels and growth kinetics of CetA HAMP domain point mutants. A. Whole cell extracts were prepared from Δ*cetAB* with pRY108, pRY108*::cetAB* or pRY108*::cetAcetB* containing the indicated *cetA* point mutants. These samples were separated by 12.5% SDS-PAGE and CetA and CetB detected by immunoblotting. **B.** Growth curves of strains expressing CetA point mutants that slowed growth. **C.** Growth curves of strains expressing CetA point mutants that maintained wildtype growth.

wildtype (DRH212), Δ*cetA*, Δ*cetB* or Δ*cetAB* at a multiplicity of infection of ~200. Immediately upon infection, bacteria were centrifuged onto the INT 407 cells, in order to rule out any motility effects on the invasion assay. After two hours, the number of total cell-associated bacteria was determined in half of the wells (see Materials and Methods) and gentamicin was added to the remaining wells to kill extracellular bacteria. After a further 2.5 hours, the number of intracellular bacteria was determined as described in Materials and Methods and the percentage of total cell associated bacteria that were intracellular (invaded) was calculated. Strains lacking *cetA* alone, or both *cetA* and *cetB*, invaded INT 407 cells approximately 5-times less efficiently than wildtype, whereas a Δ*cetB* mutant invaded at wildtype levels (Fig. 22A).

Further investigation of the invasion defect exhibited by the Δ*cetA* mutant was done by performing a kinetic analysis of invasion. The percentage of total cell-associated bacteria that had invaded the INT 407 cells was determined at various times between 30 minutes and 4 hours post-infection (Fig. 22B). The level of invasion by the Δ*cetA* mutant remained lower than that of wildtype at all times. The rate of invasion by the Δ*cetA* mutant was initially much lower than that of wildtype. By 2 to 4 hours post-infection, however, the rate of invasion by the Δ*cetA* mutant reached near wildtype levels. These results indicate that the Δ*cetA* mutant lags in the initiation of invasion compared to wildtype.

While there is at present an incomplete understanding of *C. jejuni* invasion mechanisms, several factors are known to affect invasion in the tissue culture model we used here. We tested the affect of *cetA* and *cetB* mutations on these factors in an attempt to discern the root of the Δ*cetA* invasion defect (Fig. 23). While the Δ*cetA* mutant does

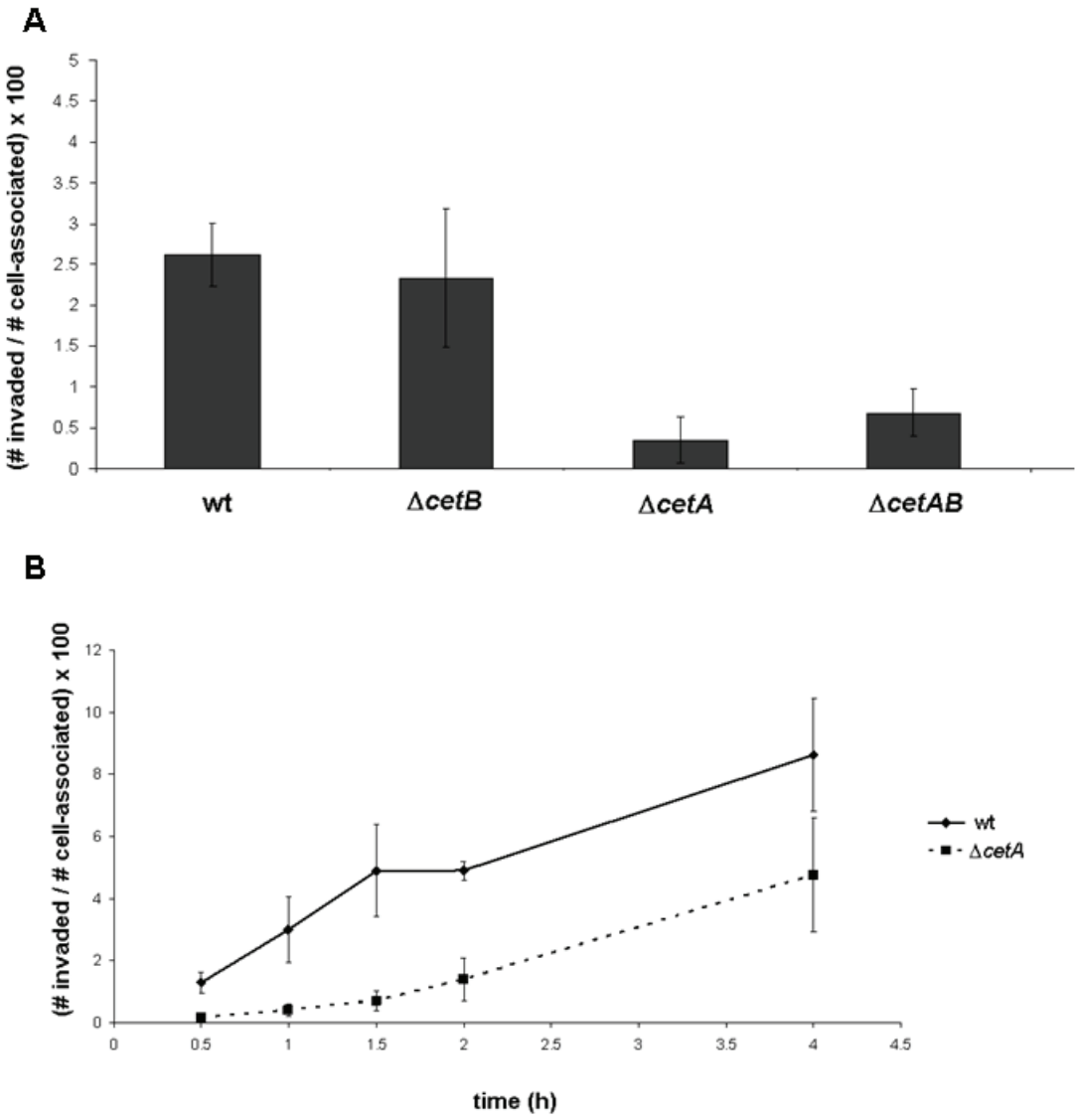

Figure 22. Effect of *cetA* and *cetB* mutations on epithelial cell invasion. A. INT 407 cells were infected with wildtype, the Δ*cetB* mutant, the Δ*cetA* mutant and the Δ*cetAB* mutant. The percent of total cell-associated bacteria that were intracellular following a 2 hour infection was calculated. **B.** INT 407 cells were infected with wildtype and the Δ*cetA* mutant. The percent of total cell-associated bacteria that were intracellular following a 30 minute, 1 hour, 1.5 hour, 2 hour, for 4 hour infection.

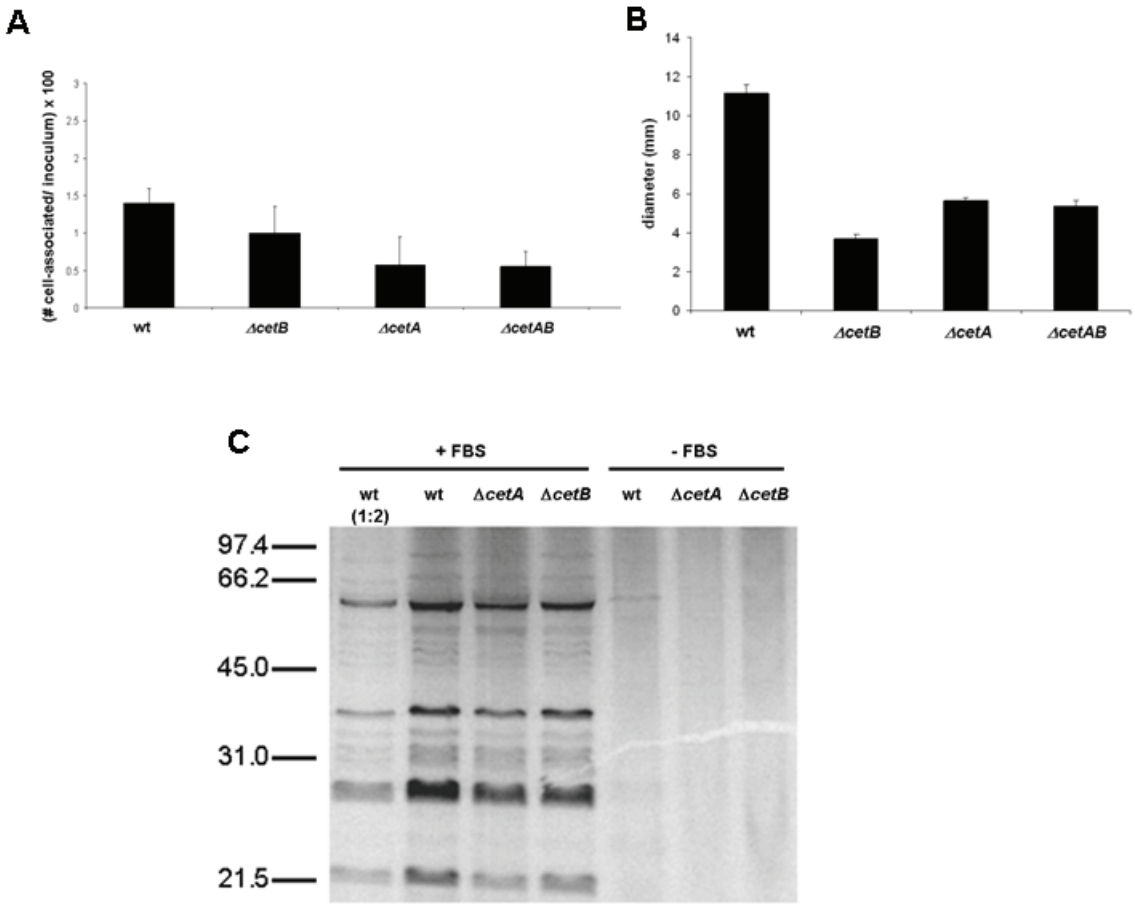

Figure 23. Effect of *cetA* and *cetB* mutations on factors impacting epithelial cell invasion. A. INT 407 cells were infected with wildtype, the Δ*cetB* mutant, the Δ*cetA* mutant and the Δ*cetAB* mutant. The percent of the inoculum that was cell-associated following a 2 hour infection was calculated. **B.** Motility assays were performed on wildtype, the Δ*cetB* mutant, the Δ*cetA* mutant and the Δ*cetAB* mutant. **C.** *C. jejuni* secretion assays were performed on cultures that were inoculated in RPMI 1640 medium supplemented with and without fetal bovine serum (FBS) for 3 hr. A 1:2 dilution of the wildtype sample following FBS stimulation is included for comparison.

have an adherence defect, this defect is quite small (Fig. 23A). In addition, adherence (total cell-associated cfu) was used to normalize the invasion data, so the invasion defect of the Δ*cetA* mutant cannot be accounted for by this slight decrease in adherence. While the Δ*cetA* mutant has a motility defect (Hendrixson *et al.*, 2001), the Δ*cetB* mutant has a slightly larger motility defect (Fig. 23B), indicating that this phenotype also does not likely explain the invasion defect of the Δ*cetA* mutant. Finally, *C. jejuni* secretes several proteins (Cia proteins) some of which may be involved in invasion. Secretion can be stimulated *in vitro* by the addition of fetal bovine serum (FBS) (Rivera-Amill *et al.*, 2001). The Δ*cetA* mutant secretes Cia proteins at levels similar to wildype (Fig. 23C), indicating that altered Cia secretion is not the reason for the invasion defect we observed. Further studies are necessary to reveal the mechanism underlying the contribution of CetA to epithelial cell invasion.

Discussion

In this study, we identified a new family of apparent bipartite energy taxis receptors that contain HAMP and proximal signaling domains homologous to CetA. These domains have several highly conserved residues, at least three of which are required for CetA function in *C. jejuni* motility. We propose that these conserved residues, several of which cluster on the exterior of the base of the HAMP domain four-helix bundle, make up the PAS-interaction surface.

In further studies of the CetA/CetB HAMP/PAS pair, we demonstrated that the Δ*cetA* mutant has a very different phenotype from that of the Δ*cetB* mutant in human epithelial cell invasion. These findings support the hypothesis that CetA and CetB, and

perhaps other members of the bipartite family, can act independently to regulate traits other than energy taxis, possibly via interactions with as yet unknown proteins (Fig. 24). Thus, we have both identified a new family of apparent bipartite energy taxis receptors and provided evidence of a functional consequence of having the domains of Aer separated into distinct proteins within this family.

The predicted secondary structures of Aer and CetA HAMP domains differ substantially from one another. Aer has previously been found to possess a hydrophobic helix (AS-2) where most HAMP domains have a second amphipathic helix (Fig. 15A) (Ma *et al.*, 2005). The hydrophobic nature of the Aer AS-2 is proposed to reflect the fact that this helix is involved both in HAMP-HAMP interactions (between Aer monomers in a dimer), and in HAMP-PAS interactions (Ma *et al.*, 2005). As Aer and CetA/CetB are proposed to transduce an energy taxis signal via similar mechanisms, we predict that the HAMP domain of CetA would also be involved in both HAMP-HAMP and HAMP-PAS interactions. If so, then the fact that the CetA HAMP domain, in contrast to Aer, contains two amphipathic helices (Fig. 15B) is unexpected. We propose that the amphipathic nature of AS-2 allows the CetA HAMP domain to exist in two states: one in which it interacts with the CetB PAS domain and one in which it is not associated with CetB and the PAS-interaction surface is exposed. If the CetA HAMP AS-2 were hydrophobic, like that of Aer, this latter state would be energetically unfavorable. Assuming that the CetA AS-2 does interact directly with CetB, the molecular nature of this interaction must differ substantially from that between the HAMP and PAS domains of Aer.

Based on similarity with the CetA HAMP and proximal signaling domain and genome context, numerous HAMP/PAS pairs homologous to CetA and CetB were

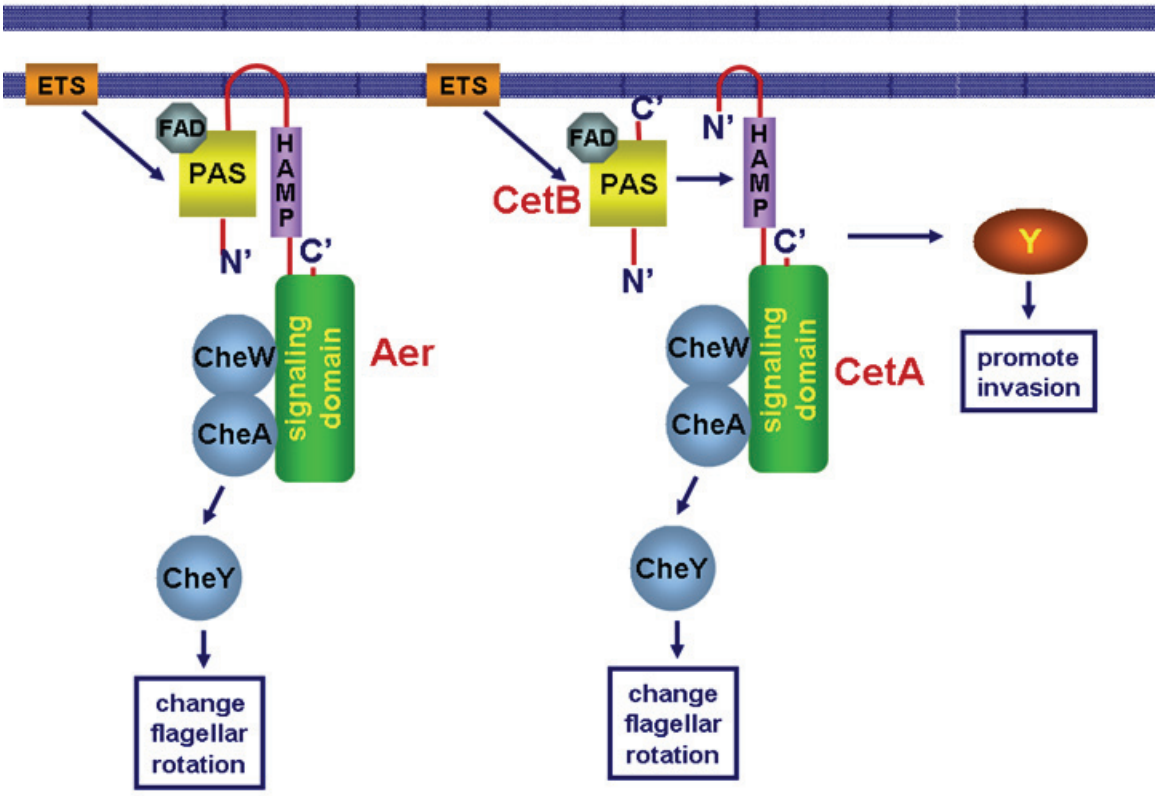

Figure 24. Proposed model for CetA/CetB function compared to Aer. CetA and CetB are proposed to transduce an energy taxis signal via a similar mechanism as Aer. However, CetA is proposed to interact with another unidentified protein to promote invasion, while CetB does not. See discussion for details.

identified (Table 4). We propose that these HAMP/PAS pairs comprise a new family of bipartite energy taxis receptors. The species containing HAMP/PAS pairs represent a broad range of bacteria, including α-proteobacteria, β-proteobacteria, ε-proteobacteria, γ-proteobacteria, and one Gram-positive actinobacterium (Table 5). The GC content of the HAMP-containing bipartite family genes generally agrees well with that of the bacterial genome in which they are found (Fig. 17A). This is true even of the sole Gram-positive with a HAMP/PAS pair, *K. radiotolerans* (circled in Fig. 17A). This suggests that these genes were not recently spread by a horizontal gene transfer. There are a few possible exceptions to this, with slightly lower GC contents in the HAMP gene relative to their genome. One of these, indicated by an arrow in Fig. 17A, occurs in a genomic island discussed below. The species containing HAMP/PAS pairs include human pathogens, animal commensals, plant symbionts, and species found in marine, aquatic and soil environments. Together, these observations suggest that these HAMP/PAS pairs have been conserved under a diverse set of selection pressures.

Other than CetA and CetB, none of the HAMP/PAS pairs has been studied beyond sequence analysis. The presence of multiple MCPs with PAS neighbors in the genome sequence of *Rhodopseudomonas palustris* CGA009 has been observed and the fact that similar sets of genes are found in *Magnetospirillum* and *Rhodospirillum* was noted (Larimer *et al.*, 2004). The genes pointed out in this study are members of the bipartite family identified here. Several of the strains containing multiple HAMP/PAS pairs, *Magnetospirillum gryphiswaldense* MSR-1, *M. magneticum* AMB-1 and *M. magneticum* MS-1, are capable of magnetoaerotaxis (also called magnetotaxis). In magnetoaerotaxis, bacteria are oriented along magnetic field lines by magnetosomes and

move along those field lines in response to an oxygen gradient (Bazylinski and Frankel, 2004). The receptor(s) responsible for the aerotaxis component of magnetoaerotaxis remain unknown, and we propose that one or more of the HAMP/PAS pairs we identified in these species may play a role. One such HAMP/PAS pair, YP_420357 (*amb0994*) and YP_420358 (*amb0995*) in *M. magneticum* AMB-1, is located in a genomic "magnetosome island" the deletion of which leads to a loss of magnetosome formation and magnetoaerotaxis (Fukuda *et al.*, 2006). This island, and this HAMP/PAS pair, has a lower GC content than the rest of the genome (arrow, Fig. 17A), indicating that it may have arrived via horizontal transfer.

In several *Campylobacter* species, there are two PAS neighbors encoded by genes flanking the gene encoding the HAMP protein. These are likely homologous to *cetB* and *cj1191c*, which flank *cetA* in the *C. jejuni* 11168 genome (Hendrixson *et al.*, 2001). The role of *cj1191c* remains unclear. Multiple attempts at constructing an in-frame deletion in this orf have been unsuccessful. The *C. lari* HAMP gene has two PAS neighbors, but rather than flank the HAMP gene, both PAS neighbors occur on the same side of the HAMP gene. The same arrangement is seen for second PAS neighbors of HAMP genes in *Magnetospirillum gryphiswaldense* MSR-1 and *Magnetospirillum magneticum* MS-1. In these last two cases, however, the PAS neighbor further from the HAMP protein possesses additional functional domains, as predicted by SMART. In *M. gryphiswaldense* MSR-1, CAM78135 is predicted to possess a PAS domain, a transmembrane region, an histidine kinase domain and an ATPase domain. In *M. magneticum* MS-1, ZP_00051415 is predicted to possess a PAS domain, a transmembrane region and a HAMP domain, which was not identified in the initial

BLASTP search. Whether or not the PAS domains of these proteins interact with their HAMP neighbors remains an open question.

The various classes of CetA-like HAMP-containing proteins (Fig. 16) present some novel functional possibilities. In Class IV, there is an apparent NAD-dependent glycerol-3-phosphate dehydrogenase domain (GPDH) at the C-terminus of the protein. GPDH is a key glycolytic enzyme. Beyond its role in glycolysis, however, various eukaryotic GPDH homologues have been implicated in an osmotic stress response, resistance to reactive oxygen species and redox regulation (Ansell *et al.*, 1997; Jeong *et al.*, 2004; Shen *et al.*, 2006). These last two functions are accomplished via regulation of the NADH/NAD+ ratio (Ansell *et al.*, 1997; Jeong *et al.*, 2004; Shen *et al.*, 2006). We speculate that the PAS domain signal may modulate the activity of the GPDH domain in order to maintain a proper redox environment in the cell. If so, this PAS domain may bind NAD(H), as opposed to FAD(H). It is difficult, however, to envision how this signal might be propagated to the GPDH domain from the HAMP domain, when there is an intervening HCD domain.

In Class V of HAMP-containing CetA-like proteins, there is a C-terminal PilZ domain. PilZ domains are thought to be cyclic diguanylate (c-di-GMP) effector domains, with the binding of this second messenger resulting in an altered confirmation (Benach *et al.*, 2007). This leads to the hypothesis that the Class V domain arrangement may allow this MCP-like protein to alter flagellar rotation in response to both PAS and c-di-GMP signals. Class VI has the same domains as CetA, but with a larger periplasmic loop. We propose that this domain arrangement may allow this MCP-like protein to sense an extracellular signal, as well as the PAS domain signal. This would be somewhat

analogous to the alternate energy taxis receptor in *E. coli*, Tsr, which senses changes in extracellular serine, as well as changes in proton motive force (Edwards *et al.*, 2006).

Classes VII and VIII contain no apparent output domains. It is unclear whether these "orphan" HAMP domains could function without being covalently linked to an output domain. It should be noted that the first HAMP domain structure to be solved was that of the *Archaeoglobus fulgidus* protein Af1503, which contains a transmembrane domain and HAMP domain, but no C-terminal output domain (Hulko *et al.*, 2006). This HAMP domain structure has since been supported by cysteine cross-linking studies of Tar and Aer (Swain and Falke, 2007; Watts *et al.*, 2008a), indicating that the Af1503 HAMP domain folds similarly to known functional HAMP domains. HAMP domains have been proposed to signal via both *cis* and *trans* mechanisms (Hulko *et al.*, 2006). A *trans* mechanism would be necessary for Af1503 and the Class VII and VIII proteins to function in signal transduction. A *trans* signaling mechanism might also explain how the PAS signal in Class IV could be relayed to the C-terminal GPDH domain discussed above.

Within the HAMP and proximal signaling domain of the bipartite family members, we identified nine highly conserved residues that are not conserved in a canonical HAMP domain (Fig. 18). These residues occur in the connector between AS-1 and AS-2, in AS-2 and in the proximal signaling region. We examined the effect of alanine substitutions at each of these positions in CetA. Only three of the point mutations (R71A, Y99A and K118A) retained the growth kinetics and CetA expression levels of cells expressing the wildtype sequence (Fig. 21). Each of these point mutants was unable to restore motility when expressed in the Δ*cetAB* mutant (Fig. 20), prompting our

conclusion that these residues are required for wildtype function of CetA in motility. Complementation tests with these mutant plasmids for the invasion phenotype of the Δ*cetA* mutant have been difficult to interpret (Young and DiRita, data not shown). To test these residues for their role in *C. jejuni* invasion may require that we cross these mutations onto the chromosome, which works with varying efficiency in *C. jejuni*. We cannot draw any conclusions about the role of the other six conserved residues in CetA function. Other substitutions may be required to probe the role of these residues.

The current model of signal transduction through Aer includes a direct interaction between the PAS and HAMP domains, allowing the FAD redox signal to be transmitted parallel to the inner membrane (Taylor, 2007). Current evidence for such an interaction is thus far indirect. Deletion of, or mutations in, the Aer HAMP domain disrupt Aer maturation and FAD binding (Bibikov *et al.*, 2000; Buron-Barral *et al.*, 2006; Ma *et al.*, 2005). A point mutation in the HAMP domain that abrogated aerotaxis by Aer could be specifically suppressed by a second-site mutation in the PAS domain (Watts *et al.*, 2004). We propose that the CetA HAMP domain and CetB interact, similarly to the proposed PAS-HAMP interaction in Aer. Studies to investigate this proposed interaction are currently under way. Further, we predict that the other HAMP-PAS pairs in the bipartite family identified in this study also interact with one another.

Modeling the structure of the Aer HAMP domain onto that previously determined for Af1503 led to the observation that point mutations resulting in a constant "signal on" state of Aer cluster together at the base of the four-helix bundle formed by the HAMP dimer (Watts *et al.*, 2008b). These point mutations may strengthen the proposed PAS-HAMP interaction and define the PAS-HAMP interaction surface (Taylor, 2007; Watts *et*

al., 2008b). Most of the conserved residues within the HAMP domains of the bipartite family members are predicted to be located at the base of the HAMP dimer four-helix bundle, near one another on the surface of this dimer (Fig. 19B). We hypothesize that this region of the HAMP domain dimer plays a role in HAMP-PAS interactions between members of the HAMP/PAS pairs in this family of proteins.

The one residue in the CetA HAMP domain model that does not fall on the same surface as the others is Y99 (Fig. 19B). While the role of this tyrosine in HAMP domain function remains unclear, the location of these tyrosines in our model lends support to a recently proposed model of HAMP domain signaling (Hulko *et al.*, 2006). Specifically, if the helices of the HAMP domain four-helix bundle do rotate relative to one another, they must do so in the direction proposed by Hulko *et al.* (Hulko *et al.*, 2006); rotation in the opposite direction would be prevented by steric hindrance by Y99.

The HAMP domain of CetA is a polar structure, with a positively charged N-terminus and negatively charged C-terminus (Fig. 19C). This dipole moment is apparent, but less pronounced, in the Af1503 structure (Fig. 19D), and may be a previously unrecognized feature of HAMP domains. As the N-termini of HAMP domains are generally proximal to the inner membrane, it may be that the net positive charge in this region acts as an attractive force, further tethering the HAMP domain to the membrane. The role of the net negative charge of the base of the HAMP domain is more speculative. As this region has been implicated in Aer in the PAS-HAMP interaction, we propose that there may be a cognate positive surface on the CetB PAS domain facilitating interaction between CetA and CetB. As the AS-2 helix of Aer is hydrophobic, we would predict that the equivalent surface of the Aer PAS domain would comprise a hydrophobic patch.

C. jejuni is one of the most prevalent causes of bacterial gastroenteritis in the US (Foodnet, 2007). While not considered a highly invasive organism, compared to bacteria such as *Salmonella* and *Shigella*, *C. jejuni* has been seen to actively invade non-phagocytic human epithelial cells in tissue culture models (Konkel and Joens, 1989; Oelschlaeger *et al.*, 1993). Our studies indicate that the Δ*cetA* mutant and the Δ*cetAB* mutant have an approximately 5-fold defect in invasion compared to wildtype (Fig. 22A). Compared to some other known invasion mutants in *C. jejuni*, the magnitude of the invasion defect of the Δ*cetA* mutant is a relatively small (Goon *et al.*, 2006; Konkel *et al.*, 2004; Szymanski *et al.*, 2002). What is striking about our observations regarding invasion is not the magnitude of the Δ*cetA* effect, but rather that a *cetB* mutation shows no defect (Fig. 22A). If CetA and CetB function solely as partners to transduce an energy taxis signal, we would expect that both the Δ*cetA* and Δ*cetB* mutants would have similar phenotypes. It should be noted that CetB levels are quite low in the Δ*cetA* mutant (see Chapter II). However, the lack of an invasion defect by the Δ*cetB* mutant rules out a role for CetB in invasion. We conclude that CetA and CetB function independently of one another to regulate invasion. A previous study found that a transposon insertion in *cetB* led to an increase in adherence to INT 407 cells and a decrease in invasion of INT 407 cells (Golden and Acheson, 2002). These results clearly differ from our findings that the Δ*cetB* mutant is unaffected in adherence (Fig. 23A) or invasion (Fig. 22A). This difference is likely attributable to the use of a transposon insertion mutant in the previous study, as opposed to the in-frame deletion used in our experiments.

One explanation for the invasion defect of the Δ*cetA* mutant is that this results from the motility defect of this mutant. To reduce the contribution of motility to invasion

in these experiments, the bacteria are brought into contact with the INT 407 cells by a low speed centrifugation at the beginning of the assay. However, this may not completely eliminate motility effects on invasion. In any event, we would expect a motility defect to manifest itself as a decrease in the number of adherent bacteria. This should be reflected in both the number of total cell-associated bacteria and, proportionally, the number of intracellular bacteria. We eliminated this potential contribution of motility to our results by determining the percentage of total cell-associated bacteria that are intracellular. When calculated this way, the Δ*cetA* and Δ*cetAB* mutants still have an approximately 5-fold defect in invasion (Fig. 22A). Finally, it should be noted that the Δ*cetB* mutant is actually slightly, but reproducibly, less motile than the Δ*cetA* mutant (Fig. 23B). Accordingly, if the invasion defect of the Δ*cetA* mutant were due to its motility defect, the Δ*cetB* mutant should have an invasion defect that is equal to or greater than that of the Δ*cetA* mutant. As this is not the case, we conclude that the invasion defect of the Δ*cetA* mutant cannot be attributed solely to that strain's motility defect.

We have determined that the invasion defect of the Δ*cetA* mutant results from an initial lag in the rate of invasion. By 2-4 hours post-infection, the Δ*cetA* mutant invades at rates near or at wildtype levels (Fig. 22B). The mechanism of *C. jejuni* invasion is still being dissected, but appears to be mainly microtubule-dependent (Kopecko *et al.*, 2001), which differentiates the *C. jejuni* invasion process from that of many invasive pathogens that use host cell actin for internalization. Also, proteins secreted from the flagellum are known to be required for *C. jejuni* invasion (Konkel *et al.*, 1999a; Konkel *et al.*, 2004; Song *et al.*, 2004). Metabolic labeling experiments showed no significant changes in the

ability of the Δ*cetA* mutant to secrete proteins associated with invasion (Fig. 23C). Additionally, *C. jejuni* invasion involves host cell protein kinase activity as well as a subset of small Rho GTPases (Biswas *et al.*, 2004; Hu *et al.*, 2006; Krause-Gruszczynska *et al.*, 2007), and we speculate that the Δ*cetA* mutant has a defect in its ability to initiate these signaling events. A recent study observed that *C. jejuni* can migrate beneath ("subvade") epithelial cells in tissue culture prior to invasion (van Alphen *et al.*, 2008). However, it was observed that increased subvasion efficiency correlated with decreased CheW expression and decreased motility in soft agar (van Alphen *et al.*, 2008). If CetA contributes to subvasion, it would appear that it must do so independently of CetB and the chemotactic machinery. Until more mechanistic details about both subvasion and the initiation of epithelial cell signaling events are known, the molecular mechanisms behind the invasion defect of the Δ*cetA* mutants will remain to be elucidated.

We suggest that the finding that the Δ*cetA* mutant has an invasion defect, while the Δ*cetB* mutant does not, indicates that CetA may interact with another protein to contribute to invasion in a CetB-independent manner. However, we have not yet ruled out the fact that CetA may have an inherent CetB-independent function that does not require an additional interaction partner. For example, it is possible that CetA senses a signal directly and independently of CetB. CetA contains a histidine residue in its short periplasmic loop (Chapter II), which could provide a mechanism for pH-sensing, although there is no evidence as yet to this effect. Such a sensory mechanism, or any other that requires regions of CetA alone, would allow CetA to regulate CetB-independent behaviors, in addition to CetB-dependent energy taxis.

In summary, we identified a new family of proposed bipartite energy taxis receptors, similar to the CetA/CetB system in *C. jejuni*. Although we suggest that the HAMP/PAS pairs in this family transduce and energy taxis signal via a similar mechanism as Aer, there are clear departures from the Aer model. Differences from the Aer HAMP domain primary and secondary structure, as well as the presence of highly conserved residues within the HAMP and proximal domains of these family members, suggest that the nature of the PAS-HAMP interaction within this family is mechanistically different from that in Aer. Finally, the involvement of CetA, but not CetB, in epithelial cell invasion supports our hypothesis that the members of HAMP/PAS pairs may act independently of each other to control phenotypes other than energy taxis. Further studies are needed to determine if these bipartite family members are in fact energy taxis receptors, to further investigate the nature of the putative HAMP-PAS interaction and to determine those cellular processes in which these proteins may be involved outside of energy taxis. Such studies will both expand our knowledge of these bipartite family members as well as provide insight regarding potential mechanisms for the function of other HAMP domains that may sense intracellular signals.

CHAPTER IV

CONCLUSION

This work centers on the CetA/CetB energy taxis system in *C. jejuni*. When these studies were initiated, *cetA* and *cetB* had been identified and found to be required for energy taxis. Based on similarity to Aer, we predicted that CetA and CetB interact, likely at the CetA HAMP domain. Further, we hypothesized that this interaction mediates the transduction of an energy taxis signal from CetB to CetA and, accordingly, to the CheA histidine kinase. We made one additional prediction – that CetA and CetB, by virtue of being separate proteins (and unlike Aer), might be able to act independently of each other. Specifically, we predicted that CetA and/or CetB might have other interaction partners through which they could influence processes other than energy taxis. The broad aim of this dissertation was to characterize the CetA/CetB energy taxis system. Specifically, this work aimed to test two key hypotheses: 1) CetA and CetB interact directly to transduce an energy taxis signal; 2) CetA and CetB function independently to regulate responses other than energy taxis.

In Chapter II, we initiated the molecular and biochemical characterization of CetA and CetB. We determined that *cetA* and *cetB* are co-transcribed independently of the flagellar σ-factors, σ^{54} and σ^{28}. As there are only three known σ-factors in *C. jejuni*, this suggests that *cetA* and *cetB* are transcribed in a σ^{70}-dependent fashion. This implies that CetA and CetB may be present when there are no flagella to power energy taxis, consistent with the possibility that one or both may be involved in non-energy taxis

responses. We also determined that both CetA and CetB are membrane proteins. CetA contains a helical hairpin membrane anchor, similar in topology to that of Aer. CetB, on the other hand, is a peripheral membrane protein, associated with the membrane with an avidity suggestive of a protein-protein interaction.

In work described in Chapter II, we determined that both CetA and CetB participate in larger protein complexes. CetB forms a homodimer, as well as participating in larger complexes. CetA is involved in complexes lacking CetB, one of which is present at higher levels in the Δ*cetB* mutant than wildtype. Most pertinent to our hypotheses, however, CetA and CetB appear to participate in a complex together. This finding, along with the fact that CetB levels are CetA dependent, supports our hypothesis that CetA and CetB interact.

As described in Chapter III, we determined that the CetA and Aer HAMP domains differ significantly from one another in secondary structure. This implies that if CetA and CetB interact, as do the Aer HAMP and PAS domains, the molecular nature of these interactions must differ significantly. Based upon similarity to the HAMP domain of CetA, we identified several pairs of adjacent genes encoding proteins with similarity to CetA and CetB. We propose that these genes represent a new family of bipartite energy taxis transducers.

Within this family, there are nine HAMP domain residues that are highly conserved. In an *in silico* model of the CetA HAMP domain, several of these residues are present on the same surface, indicating that they may define an interaction surface. As these residues are conserved within the bipartite family, and the location of this cluster is similar to a proposed PAS domain interaction surface on the Aer HAMP

domain, we propose that these conserved HAMP domain residues define a CetB interaction surface on CetA.

Also as described in Chapter III, we determined that CetA, but not CetB, contributes to human epithelial cell invasion by *C. jejuni*. This finding supports our hypothesis that CetA and/or CetB act independently of one other to participate in traits other than energy taxis. While we have not yet defined the precise role played by CetA in invasion, we did determine that the invasion defect of the Δ*cetA* mutant lies in the initiation of invasion. The initiation process involves interactions with host-cell receptors, likely in caveolae, followed by host cell signaling events including protein kinases and small Rho GTPases (Krause-Gruszczynska *et al.*, 2007). Additionally, *C. jejuni* may "subvade" epithelial cells prior to invasion, although this is less well-established (van Alphen *et al.*, 2008). It is not yet clear which of these aspects of the initiation of invasion is affected by the presence or absence of CetA.

Emerging questions and future directions

While this work has provided support for key hypotheses regarding the function of the *C. jejuni* CetA/CetB energy taxis system, many questions remain and several more have emerged as a result of our findings. Although my experiments were limited to CetA and CetB, this work has implications beyond these two proteins and beyond *C. jejuni*. I will conclude by addressing potential directions of future study with respect to CetA and CetB function, as well as suggesting implications of our findings beyond these two proteins.

A central remaining question regarding the CetA/CetB energy taxis system is the nature of the proposed CetA-CetB interaction. Our data thus far are consistent with such

an interaction and suggest candidates for an interaction surface. Particularly, we propose that the conserved HAMP and proximal signaling domain residues in the bipartite family define a CetB interaction surface. However, alanine substitutions at only three of these could be tested for motility phenotypes due to growth or stability affects of the others. These three alanine substitutions reduced or eliminated CetA/CetB-mediated motility. In order to study the rest of these conserved residues, other substitutions may be required. I suggest the generation of random substitutions at each position using degenerate primers, and subsequent screening for motility defects. Additionally, none of these point mutants affected CetB levels or membrane localization, except in the cases where CetA stability was also affected. I propose that, as several residues are present at this predicted interaction surface, a combination of multiple mutations may be necessary to disrupt the CetA-CetB interaction to the point where CetB levels or localization are affected.

The corresponding interaction surface on CetB remains completely undefined. The dipole moment of the predicted CetA HAMP domain structure, with a general negative charge at the base of the HAMP domain, might suggest a corresponding positive patch on the surface of CetB. Pseudoreversion analysis of the type used with Aer may be quite helpful here. Specifically, random mutagenesis of CetB in the context of mutations in the conserved CetA HAMP and proximal signaling domains, followed by screening for increased motility, may allow the identification of both specific and non-specific suppressors. Specific CetB suppressors of CetA HAMP point mutations would provide strong evidence for a direct interaction between the two, as well as the location of such an interaction surface on CetB.

A much more daunting approach to the study of CetA and CetB interactions could be potentially quite valuable. Studies of Aer and other MCPs in *E. coli* have benefited tremendously from the combination of cysteine-scanning mutagenesis and *in vivo* disulfide cross-linking analysis (Amin *et al.*, 2006, 2007; Swain and Falke, 2007; Taylor *et al.*, 2007; Watts *et al.*, 2006b; Watts *et al.*, 2008b). While the application of this approach to CetA and CetB would be tedious and logistically challenging, it could result in significant advances. Within CetB, whole-protein cysteine-scanning and *in vivo* disulfide cross-linking could identify the CetB dimerization surface. Once identified, these residues could be targeted for further mutagenesis to disrupt CetB dimerization. This would allow us to determine whether CetB dimerization is required for energy taxis, for membrane localization or for interaction with CetA. Further, once these residues are identified, we could determine if they are conserved in Aer, which would indicated whether the PAS domain of Aer also dimerizes and provide the ability to potentially disrupt this dimerization.

Cysteine-scanning and *in vivo* disulfide cross-linking analysis of the entire CetA protein would be more difficult and I would hesitate to start with a completely undirected approach, as the protein consists of 459 amino acids, compared to 165 in CetB. Rather, I would begin with cysteine-scanning mutagenesis of the HAMP and proximal signaling domains of CetA. These could be used for *in vivo* disulfide cross-linking analysis to test the validity of the *in silico* model of the CetA HAMP domain structure, as was done with Aer (Watts *et al.*, 2008b). Additionally, pairwise combinations of CetA and CetB cysteine mutants could be co-expressed and analyzed by *in vivo* disulfide cross-linking to

probe for interacting residues on both proteins. Again, this suggestion entails a tremendous amount of work, but could provide a wealth of new information.

CetA and CetB were both identified in large complexes other than the one that appears to include both proteins. It would be very instructive to identify the components of all of these complexes by LC-MS/MS. In Chapter II, we make some predictions about potential interaction partners of CetA, including Che proteins. We also predict that CetB might interact directly with elements of the electron transport system. Further, we predict that one or more of CetB's interaction partners are involved in the association of CetB with the membrane. Identification of the proteins within CetB complexes may provide targets for mutagenesis to test these predictions. Further, as mentioned above, CetA participates in a CetB-independent complex that is present at higher levels in the Δ*cetB* mutant than wildtype. Identification of the members of this complex may lead to some insight into CetB-independent functions of CetA.

Several experiments that we would like to perform are hampered by the low levels of CetB in the absence of CetA. We suspect that this is due to decreased stability of CetB in the absence of CetA, but that is not yet definitive. However, based on the finding that the Aer N-terminal cap is important for stability (Watts *et al.*, 2006b), and CetB contains no homology to this part of the Aer PAS domain, I suggest that fusion of the Aer N-terminal cap to CetB may result in increased stability of CetB. This fusion would then provide a tool to answer some questions that currently elude us. For example, a more stable variant of CetB might allow us to determine whether CetB membrane localization is CetA dependent. Also, increased CetB stability might allow us to determine whether the high molecular weight complexes in which CetB participates are

present in the Δ*cetA* mutant. Additionally, such a variant might be necessary to determine whether multiple CetA HAMP point mutations affect the localization of CetB, if wildtype CetB is less stable in such a background.

Studies with Aer indicate that the PAS-HAMP interactions required for FAD binding by the HAMP domain may not be identical to the interactions resulting in signal transduction. Specifically, signal transduction within an Aer dimer occurs from PAS domain to HCD domain of the same monomer, but FAD binding requires the HAMP domain on the cognate monomer (Watts *et al.*, 2006a). It would be interesting to test the route of signal transduction within CetA/CetB. Can mutations in the conserved HAMP residues be tolerated in the same CetA monomer as an HCD mutation? Or must they also be in cognate monomers? If we identify CetA point mutations in the HAMP domain that abrogate the proposed FAD binding by CetB, can those mutations be tolerated in the same monomer as an HCD mutation? Or, like equivalent mutations in the Aer HAMP domain, must they be in the cognate monomer? Experiments such as these will aid our understanding of the molecular mechanism of signal transduction within CetA and between CetA and CetB.

Another broad set of remaining questions relates to the *cetB* paralogue located upstream of *cetA*, *cj1191c*. In Chapter II, I demonstrated that levels of a tagged version of *cj1191c* are not CetA-dependent. I have also observed that overexpression of *cj1191c* leads to a severe growth defect (data not shown). These data indicate that there are functional differences between CetB and Cj1191c. However, that is extent of our conclusions regarding Cj1191c at this point. Constructing an in-frame deletion mutant of *cj1191c*, as well as a double deletion strain lacking both *cj1191c* and *cetB* would allow us

to ask some crucial questions. Is *cj1191c* involved in energy taxis? Is *cj1191c* involved in human epithelial cell invasion? If so, this might explain why invasion is CetB-independent, as perhaps CetA functions with Cj1191c for this trait. Production of antibodies to Cj1191c would allow us to determine whether this protein dimerizes, as does CetB, and whether Cj1191c and CetB can form heterodimers. Additionally, we could use such antibodies to ask whether Cj1191c interacts with CetA and whether the levels of the native protein, expressed from the chromosome, are CetA-dependent.

Several other questions remain regarding CetA/CetB function. Does CetB bind FAD, as sequence conservation would suggest? Likely the answer to this question awaits purification of CetB, a non-trivial undertaking due to the protein's avid association with the membrane and tendency to form inclusion bodies when overexpressed. Regarding CetA, what is the mechanism underlying the invasion defect of the Δ*cetA* mutant? Answering this question may be complicated by the small magnitude of the invasion defect, only 5-fold. As the initial events in *C. jejuni* invasion become clearer, more tools may be available to dissect this phenotype. For now, experiments determining the effect of the Δ*cetA* mutant on host cell protein phosphorylation would be enlightening, as would experiments to determine the effects of small Rho GTPase inhibitors on the Δ*cetA* mutant compared to wildtype. As more becomes known about the relevance and mechanism of "subvasion," it may be possible to determine if there are steps in this process in which the Δ*cetA* mutant is impaired.

Other questions less central to our main hypotheses, but important for a more complete understanding of CetA and CetB also remain. Is CetA methylated? If so, is methylation required for energy taxis? A corollary to this is the question of how

adaptation occurs in *C. jejuni* generally. As the *C. jejuni* CheR is pentapeptide-independent (Perez and Stock, 2007), and CheB lacks a response regulator domain (Marchant *et al.*, 2002), the system clearly deviates from the *E. coli* and *B. subtilis* paradigms. Are any *C. jejuni* MCPs methylated? If so, is this methylation required for chemotaxis, and how is methylation regulated so that it leads to appropriate adaptation? If not, is CheV involved in adaptation? And is this required for energy taxis by *C. jejuni*? Or is energy taxis by CetA/CetB independent of adaptation mechanisms, as is Aer-mediated energy taxis in *E. coli*? Mutants lacking CheB, CheR and CheV would be instructive here.

Also, while not mentioned in the *Campylobacter* literature, my sequence analysis indicates that there is a cytoplasmic *aer* homologue in *C. jejuni*, *cj1110c*. While an insertion in *cj1110c* does not lead to a motility defect similar to the Δ*cetA* and Δ*cetB* mutant (Hendrixson and DiRita, 2004), the possibility for redundancy is clear. Can *cj1110c* complement the Δ*cetAB* mutant? This may seem unlikely due to the phenotypes of a Δ*cetAB* mutant, where *cj1110c* is present, but it is possible that *cj1110c* is not expressed under our culture conditions or is not expressed to high enough levels to compensate for the loss of *cetA* and *cetB*. Can the Cj1110c PAS domain interact with the CetA HAMP domain? Alternatively, can CetB interact with the Cj1110c HAMP domain? The Cj1110c HAMP domain was not identified as being similar to that of CetA, which leads me to predict that interactions of this sort between these energy taxis systems are unlikely, but this prediction should be tested. If there is not cross-talk between Cj1110c and CetA/CetB, do they sense different signals? Are they expressed under different conditions? Work on other species harboring multiple Aer homologues

suggests that these systems are not necessarily redundant in function (Boin and Hase, 2007; Sarand *et al.*, 2008).

cetA and *cetB* appear to be expressed independently of the flagellar regulon, which is a departure from the regulation of MCPs in *E. coli*. Are *cetA* and *cetB* unique in this regard, or are other MCPs also expressed independently of the flagellar regulon in *C. jejuni*? Gene expression in wildtype has been compared with that of *fliA* and *flhA* mutants by microarray analysis (Carrillo *et al.*, 2004). These experiments did not identify any MCPs as being expressed at lower levels in these mutants (Carrillo *et al.*, 2004). In fact, the only chemotaxis gene affected by either mutation is *cheY* (Carrillo *et al.*, 2004). FlhA acts upstream of both σ^{54} and σ^{28} regulated flagellar genes in *C. jejuni* (Carrillo *et al.*, 2004; Hendrixson and DiRita, 2003). If MCP and *che* gene expression is unaffected in *flhA* and *fliA* mutants, then MCPs and *che* genes are not co-regulated with flagella in this bacterium. If MCPs and Che proteins are present in the absence of flagella, do they have a function other than regulation of flagellar rotation? In other organisms, discrete sets of MCPs and Che proteins are involved in gene regulation (or regulation of macromolecular structure assembly) and do not participate in chemotaxis. Perhaps in *C. jejuni*, one set of MCPs and Che proteins is involved in both chemotaxis and gene regulation. This concept is entirely speculative at this point, but intriguing nonetheless.

In Chapter III, I identified a family of proteins with similarity to CetA and CetB and suggested that they also interact to regulate energy taxis. However, our knowledge about these proteins is entirely limited to their sequences. Are these proteins in fact energy taxis transducers? Do they interact with one another? Many of these genes were identified in species lacking in genetic tools. Some of these species also encode

unusually high numbers of MCPs, including multiple sets of bipartite family members, Aer homologues and cytoplasmic Aer homologues. Studying these proteins in their native background may not be practical. While cross-species complementation does not always work with MCPs, including with apparent Aer homologues (Nichols and Harwood, 2000), attempts to use bipartite family members to complement Δ*cetAB* may prove more successful than attempts to study them by knock-out and complementation in their native background. If such cross-species complementation experiments prove fruitful, then the Δ*cetAB* mutant could be used to study other family members in more detail. In particular, in those strains expressing multiple HAMP/PAS pairs, I am curious as to whether there is any specificity within these pairs. Or can HAMP-containing proteins have multiple PAS partners and vice versa? Is there a difference in affinity between different HAMP/PAS proteins? Characterization of other bipartite family members would help us more fully understand the nature of the proposed HAMP/PAS interaction.

Some HAMP-containing members of the bipartite family represent compelling targets for further study because of additional functional domains. The *M. magneticum* protein ZP_00055894 contains an additional GPDH domain. Does this alter the NAD+/NADH ratio? If so, does this occur in concert with an energy taxis response? The *M. gryphiswaldense* protein CAM75032 contains a PilZ domain. Is energy taxis by this protein affected by c-di-GMP levels? Does the PilZ domain interact with the HAMP domain of this protein? There are HAMP-containing proteins in the bipartite family that lack apparent output domains. Are these also involved in energy taxis?

Beyond the bipartite family members, our studies raise intriguing possibilities for MCPs and other HAMP-containing proteins. If HAMP domains can bind and respond to signals from separate proteins containing sensory domains, then might MCP sensing be more flexible than previously thought? Is it possible that a given MCP could have multiple sensory partners, some signaling through the transmembrane helices and some directly through the HAMP domain? If so, then might these partners change during different growth conditions, as well? Additionally, if HAMP domain signaling is bidirectional, an intracellular signal might alter the conformation of an MCP such that it is insensitive to an extracellular signal or vice versa. These possibilities are certainly raised by the *M. gryphiswaldense* protein CAM78133, which contains a large periplasmic domain in addition to the CetA-like HAMP domain. Finally, if such sensory flexibility is possible with MCPs, might it also be possible with other HAMP-containing signal transduction proteins? The possibility for these sorts of additional interactions with MCPs and other HAMP-containing proteins is compelling.

At first glance, the CetA/CetB system may appear to be a slight variation on the energy taxis transducer Aer. However, the CetA/CetB system diverges significantly from Aer. Differences between the Aer and CetA HAMP domains are clear and, based on them, we identified a family of CetA/CetB-like proteins, indicating that this system may be a widespread alternative to Aer. Understanding the mechanism of CetA/CetB signal transduction will ultimately help us to understand energy taxis in other species containing these bipartite family members, many of which are of environmental or biotechnological import. Additionally, new knowledge gained regarding CetA/CetB function may be applicable to other MCPs and, potentially, other HAMP-containing proteins, which are

numerous. My studies and others of chemotaxis and energy taxis in a wide variety of microorganisms demonstrate an extensive capacity for variation within microbes. The only organisms that appear to conform completely to model systems (*E. coli* and *B. subtilis*) are themselves or their close relatives. Other microbes continually reveal novel and complex ways to regulate chemotaxis and energy taxis responses. The CetA/CetB system represents just one such variation.

APPENDIX

Effect of Δ*cetA* and Δ*cetB* mutations on *C. jejuni* gene expression

As described in Chapter I, multiple instances of MCPs and Che proteins regulating gene expression or macromolecular structure assembly have been described. In most cases, these MCPs and Che proteins are dedicated to their regulatory role and do not participate in chemotaxis. However, one report indicated that Aer, the energy taxis transducer of *E. coli*, also plays a role in gene expression (Pruss *et al.*, 2003). Specifically, Aer was found to be involved in activating transcription of several genes encoding enzymes involved in anaerobic respiration, as well as the Entner-Doudoroff pathway, the major route of degradation of sugar acids (Pruss *et al.*, 2003). The authors of this study assert that this regulation by Aer is independent of its role in chemotaxis, however the data supporting this result was not published (Pruss *et al.*, 2003).

We sought to determine whether CetA and/or CetB might play a role in regulating gene expression in *C. jejuni* and, if so, whether this regulation is independent of their roles in energy taxis. As a first approach to these questions, we used microarrays to examine the affect of the Δ*cetA* and Δ*cetB* mutations on gene expression, when compared to wildtype. For these experiments, wildtype (DRH212), Δ*cetA* and Δ*cetB* were grown biphasically in MH media under microaerophilic conditions to an OD_{600} of 1.0. Cells were collected by centrifugation and RNA isolated as described in Chapter II. RNA

quality was assessed using the Agilent 2100 Bioanalyzer with the RNA 6000 Nano Lapchip® kit (Agilent Technologies).

For each experiment, RNA was converted to labelled cDNA and genomic DNA labelled using a direct labelling method. Genomic DNA labelled-Cy3 and cDNA from the RNA sample labelled with Cy5 were combined and mixed, then purified using the MinElute PCR purification kit from QIAGEN. After purification the sample was hybridized against a *C. jejuni* array. The *C. jejuni* array was constructed using PCR products from primers designed to reduce cross-hybridization. The array contains all of the open reading frames in the *C. jejuni* 11168 genome, as well as additional open reading frames identified in several other strains, including 81-176, our background strain. After hybridization, the slides were washed and dried.

Microarray slides were scanned using a GMS 418 Array Scanner on Cy3 and Cy5 channels. BlueFuse For Microarrays (BlueGnome, Version 2.0), was used to quantify microarray images. Bayesian statistical models were used to automatically generate a confidence estimate in each result. These estimates are used to assign a color coded confidence flag to each spot and to combine replicate data. Image alignment was carried out using BlueFuse Image Aligner (BlueGnome, Version 1.0). These arrays contained duplicate genes on an array, thus an additional option of data 'Fusing' was carried out where averaging out occurs. This function aims to ignore data that are highly skewed, thus lessening the effect of that particular spot on the final signal intensity ratio. GeneSpring analysis software (Silicon Genetics, Version 7.1), was used to analyze microarray data. Each experiment had a normalization procedure carried out, dividing each gene in the selected sample(s) by the mean of that gene's measurement in the

control sample. Using this data set, a t-test was carried out with a 5% null hypothesis. Genes whose expression levels were significantly different between samples according to this t-test, and whose fold-induction or fold-decrease is greater than or equal to a cut-off value of 1.5 are listed.

The results of these experiments are presented in Tables 5-10. 217 and 144 genes are downregulated in the Δ*cetA* and Δ*cetB* mutants, respectively, compared to wildtype (Tables 5 and 7). The largest class of genes downregulated in these mutants compared to wildtype are known or predicted to be involved in membrane transport, including iron transport. Both mutants also downregulate three predicted transcriptional regulators, providing a potential mechanism for the effects of gene expression observed. Several components of the natural transformation apparatus are also downregulated in the Δ*cetA* mutant. 77 and 86 genes are upregulated in the Δ*cetA* and Δ*cetB* mutants, respectively, compared to wildtype (Tables 6 and 8). Most of these genes are involved in metabolism, electron transport and biosynthetic processes. Notably, several cytochromes are upregulated in both mutants compared to wildtype.

Differences in gene expression between the Δ*cetA* and Δ*cetB* mutants were observed, but these gene sets were smaller. 50 genes were downregulated in the Δ*cetB* mutant compared to the Δ*cetA* mutant (Table 10). These included several flagella-associated genes, although the Δ*cetB* mutant is fully motile. Only 23 genes were upregulated in the Δ*cetB* mutant compared to the Δ*cetA* mutant, with transport proteins the largest class represented here (Table 11).

In order to verify the effects on gene expression observed by microarray analysis, we used qRT-PCR to test the expression of several representative genes. This also

Table 6. Genes downregulated in the Δ*cetA* mutant compared to wildtype

orf id[a]	gene name	fold-decrease	annotation/updated functional information[b]
cj1190c	*cetA*	17.54385965	probable MCP-domain signal transduction protein
cj0975		9.523809524	probable outer-membrane protein; similar to OM proteins involved in specific protein secretion/activation
cj1615	*chuB*	6.993006993	probable hemin uptake system permease protein
cj1614	*chuA*	5.988023952	hemin uptake system outer membrane receptor
cj1617	*chuD*	5	probable hemin uptake system periplasmic hemin-binding protein
cj0246c		4.901960784	probable MCP-domain signal transduction protein
cj0291c	*glpT'*	4.405286344	glycerol-3-phosphate transporter, possible pseudogene
cj1582c		4.166666667	probable peptide ABC-transport system permease protein
cj0613	*pstS*	4.032258065	possible periplasmic phosphate binding protein
cj0517	*crcB*	3.816793893	probable integral membrane protein
cj0057		3.802281369	possible periplasmic protein
cj1470c	*ctsF*	3.731343284	probable type II protein secretion system F protein pseudogene/involved in natural transformation (Wiesner *et al.*, 2003)
cj0044c		3.6900369	unknown
cj1471c	*ctsE*	3.424657534	probable type II protein secretion system E protein/involved in natural transformation (Wiesner *et al.*, 2003)
cj0300c	*modC*	3.389830508	probable molybdenum transport ATP-binding protein
cj0174c		3.322259136	possible iron-uptake ABC transport system permease protein
cj0046		3.236245955	probable transmembrane transport protein pseudogene
cj1211		3.144654088	probable integral membrane protein, 33.9% identity to HP1361 (called competence locus E (comE3))
cj0614	*pstC*	3.115264798	probable phosphate transport system permease protein
cj1385	*katA*	3.03030303	catalase
cj1555c		2.985074627	unknown
cj0999c		2.88184438	probable integral membrane protein
cj1616	*chuC*	2.873563218	probable hemin uptake system ATP-binding protein
cj1283	*ktrB*	2.857142857	probable K+ uptake protein
cj1613c	*chuZ*	2.801120448	unknown/heme oxygenase (Ridley *et al.*, 2006)
cj1590c		2.762430939	probable peptide ABC-transport system ATP-binding protein
cj0741		2.680965147	unknown
cj0571		2.645502646	possible transcriptional regulator; similar in C-terminus to two hypothetical DeoR family transcriptional regulators from E. coli
cj1436c		2.645502646	probable aminotransferase/located in capsule biosynthesis locus (Karlyshev *et al.*, 2000)
cj1330		2.631578947	unknown, some similarity to predicted oxidoreductases
cj0580c		2.610966057	probable oxidoreductase
cj0616	*pstB*	2.597402597	probable phosphate transport ATP-binding protein
cj0263	*zupT*	2.590673575	probable integral membrane protein/metal permease (Weingarten *et al.*, 2008)
cj1453c		2.570694087	unknown
cj0563		2.557544757	unknown
cj0793	*flgS*	2.551020408	probable signal transduction histidine kinase/σ^{54}-dependent

			two-component system kinase (Hendrixson and DiRita, 2003; Wosten *et al.*, 2004)
cj1587c		2.551020408	probable ABC transporter
cj0241c		2.544529262	possible iron-binding protein
cj1254		2.481389578	unknown
cj1530		2.469135802	probable ATP/GTP-binding protein
cj1586	*cgb*	2.421307506	probable bacterial hemoglobin/single domain globin involved in nitrosative stress response (Elvers *et al.*, 2004)
cj0304c	*bioC*	2.403846154	possible biotin synthesis protein
cj0058		2.398081535	possible periplasmic protein
cj1669c		2.398081535	probable ATP-dependent DNA ligase
cj0262c	*docC*	2.375296912	probable methyl-accepting chemotaxis signal transduction protein
cj0865	*dsbB*	2.341920375	possible disulfide oxidoreductase
cj1268c		2.325581395	unknown
cj1040c		2.314814815	probable transmembrane transport protein
cj1212c		2.257336343	possible polysaccharide modification protein
cj0430		2.252252252	probable integral membrane protein
cj1538c		2.242152466	possible anion-uptake ABC-transport system ATP-binding protein
cj0341c		2.232142857	possible integral membrane protein
cj1622	*ribD*	2.232142857	probable riboflavin-specific deaminase
cj1647	*iamA*	2.227171492	probable ABC transport system ATP-binding protein
cj1583c		2.222222222	probable peptide ABC-transport system permease protein
cj0340		2.222222222	possible nucleoside hydrolase
cj1187c	*arsB*	2.212389381	possible arsenical pump membrane protein
cj1551c		2.202643172	probable type I restriction enzyme S protein
cj0680c	*uvrB*	2.188183807	probable excinuclease ABC subunit B
cj0937		2.169197397	probable integral membrane protein
cj0836	*ogt*	2.164502165	probable methylated-DNA--protein-cysteine methyltransferase
cj0444		2.150537634	probable tonB-denpendent outer membrane receptor
cj0082	*cioB*	2.145922747	probable cytochrome bd oxidase subunit II/cyanide independent oxidase, not cytochrome bd type (Jackson *et al.*, 2007)
cj1179c	*fliR*	2.136752137	probable flagellar biosynthetis protein
cj1549c		2.127659574	probable type I restriction enzyme R protein
cj1588c		2.127659574	probable transmembrane transport protein
cj0523		2.118644068	Cj0523, possible membrane protein, may be fragment of pseudogene
cj1389	*dcuC*	2.114164905	probable transmembrane transport protein pseudogene/involved in efflux of succinate (Hofreuter *et al.*, 2006)
cj1713		2.114164905	unknown
cj0727		2.114164905	probable periplasmic solute-binding protein
cj1241		2.114164905	probable transmembrane transport protein
cj0301c	*modB*	2.109704641	probable molybdenum transport system permease protein
cj1000		2.096436059	probable transcriptional regulator, LysR family
cj1581c		2.092050209	probable peptide ABC-transport system ATP-binding protein
cj1276c		2.087682672	probable integral membrane protein
cj1467		2.083333333	unknown

cj0692c		2.083333333	possible membrane protein
cj1544c		2.074688797	probable integral membrane protein
cj1628	*exbB2*	2.036659878	probable exbB/tolQ family transport protein
cj1113		2.012072435	unknown
cj1716c	*leuD*	2.008032129	probable 3-isopropylmalate dehydratase small subunit
cj1039	*murG*	2	possible UDP-N-acetylglucosamine--N-acetylmuramyl-(pentapeptide) pyrophosphoryl-undecaprenol N-acetylglucosamine transferase
cj0888c		1.996007984	ABC transport system ATP-binding protein
cj1630	*tonB2*	1.988071571	probable tonB transport protein
cj0289c	*peb3*	1.976284585	major antigenic peptide
cj0920c		1.968503937	probable ABC-type amino-acid transporter permease protein/involved in aspartate and glutamate transport (Reid *et al.*, 2008b)
cj0308c	*bioD*	1.968503937	possible dethiobiotin synthetase
cj1584c		1.960784314	probable peptide ABC-transport system periplasmic peptide-binding protein
cj0620		1.953125	unknown
cj1556		1.945525292	unknown
cj0175c		1.926782274	possible iron-uptake ABC transport system periplasmic iron-binding protein
cj1383c		1.915708812	unknown
cj0017c	*dsbI*	1.915708812	probable ATP/GTP binding protein/involved in disulfide bond formation (Raczko *et al.*, 2005)
cj0862	*pabB*	1.915708812	probable para-aminobenzoate synthase component I
cj1384c		1.901140684	unknown
cj1472c	*ctsX*	1.890359168	probable membrane protein/involved in natural transformation (Wiesner *et al.*, 2003)
cj1676	*murB*	1.886792453	possible UDP-N-acetylenolpyruvoylglucosamine reductase
cj1146c	*waaV*	1.883239171	possible glucosyltransferase/los biosynthesis (Parker *et al.*, 2005)
cj1275c		1.865671642	probable periplasmic protein
cj1095		1.865671642	probable integral membrane protein
cj0684	*priA*	1.865671642	probable primosomal protein N'
cj0849c		1.865671642	unknown
cj0850c		1.862197393	transmembrane transport protein
cj0606		1.862197393	probable periplasmic protein
cj0323		1.858736059	unknown
cj0302c		1.858736059	unknown
cj1218c	*ribA*	1.858736059	probable riboflavin synthase alpha chain
cj1646	*iamB*	1.85528757	possible ABC transport system permease protein
cj0464	*recG*	1.848428835	probable ATP-dependent DNA helicase
cj0690c		1.834862385	possible restriction/modification enzyme
cj0377		1.834862385	probable ATPase
cj0198c		1.818181818	unknown
cj0825		1.818181818	possible processing peptidase
cj0495		1.818181818	unknown
cj1722c		1.814882033	unknown
cj0247c		1.814882033	unknown
cj0033		1.811594203	probable integral membrane protein

cj0826		1.798561151	probable integral membrane protein
cj0792		1.798561151	unknown
cj1068		1.798561151	probable integral membrane protein
cj1651c	*map*	1.792114695	probable methionine aminopeptidase
cj0951c		1.792114695	probable MCP-domain signal transduction protein
cj0313		1.782531194	probable integral membrane protein
cj1257c		1.773049645	possible efflux pump
cj0335	*flhB*	1.769911504	probable flagellar biosynthetic protein
cj0524		1.745200698	unknown
cj1560		1.739130435	probable membrane protein
cj1661		1.730103806	possible ABC transport system permease protein
cj0546		1.727115717	unknown
cj0339		1.724137931	probable transmembrane transport protein
cj1634c	*aroC*	1.709401709	probable chorismate synthase
cj1547		1.700680272	unknown
cj1712		1.686340641	unknown, 40.9% identity to HP1530 (called purine nucleoside phosphorylase (punB))
cj1452		1.686340641	possible integral membrane protein
cj0651		1.680672269	possible integral membrane protein
cj0634	*dprA*	1.677852349	Unknown/ involved in natural transformation (Takata *et al.*, 2005)
cj1225		1.675041876	unknown
cj0904c		1.675041876	probable RNA methylase
cj0295		1.672240803	possible acetyltransferase
cj0486	*fucP*	1.672240803	probable sugar transporter/involved in fucose transport (Saidijam *et al.*, 2005)
cj0312	*pth*	1.669449082	probable peptidyl-tRNA hydrolase
cj1285c		1.669449082	unknown
cj1442c		1.669449082	unknown
cj1731c	*ruvC*	1.666666667	probable crossover junction endodeoxyribonuclease
cj0238		1.663893511	probable integral membrane protein/putative mechanosensitive ion channel (Reid *et al.*, 2008b)
cj1237c		1.661129568	possible phosphatase
cj0733		1.652892562	unknown
cj1562		1.650165017	unknown
cj0728		1.650165017	probable periplasmic protein
cj1663		1.647446458	probable ABC transport system ATP-binding protein
cj1352	*ceuB*	1.644736842	probable enterochelin uptake permease
cj0863c	*xerD*	1.642036125	probable DNA recombinase
cj1664		1.642036125	possible periplasmic thioredoxin
cj1263	*recR*	1.639344262	probable recombination protein
cj1246c	*uvrC*	1.639344262	probable excinuclease ABC subunit C
cj0390		1.639344262	possible transmembrane protein
cj1042c		1.62601626	probable transcriptional regulatory protein, AraC family
cj1038		1.62601626	probable cell division/peptidoglycan biosynthesis protein
cj1239	*pdxA*	1.623376623	probable pyridoxal phosphate biosynthetic protein
cj0325	*xseA*	1.620745543	probable exodeoxyribonuclease VII large subunit
cj0376		1.620745543	possible periplasmic protein
cj1393	*metC'*	1.618122977	probable cystathionine beta-lyase

cj1648		1.618122977	possible ABC transport system periplasmic substrate-binding protein
cj0593c		1.615508885	probable integral membrane protein
cj0081	*cioA*	1.615508885	probable cytochrome bd oxidase subunit I/ cyanide independent oxidase, not cytochrome bd type (Jackson *et al.*, 2007)
cj1633		1.615508885	unknown
cj0860		1.607717042	probable integral membrane protein
cj1474c	*ctsD*	1.602564103	probable type II protein secretion system D protein/involved in natural transformation (Wiesner *et al.*, 2003)
cj0272		1.6	unknown
cj0031		1.597444089	probable DNA restriction/modification enzyme, N-terminal half
cj1532		1.592356688	possible periplasmic protein
cj0861c	*pabA*	1.592356688	probable para-aminobenzoate synthase glutamine amidotransferase component II
cj1311	*pseF*	1.592356688	probable acylneuraminate cytidylyltransferase (CMP-N-acetylneuraminic acid synthetase)/involved in flagella glycosylation (McNally *et al.*, 2006a)
cj1687		1.592356688	possible efflux protein
cj0580c		1.587301587	probable integral membrane protein
cj1563c		1.582278481	probable transcriptional regulator, MerR family
cj0451	*rep*	1.582278481	probable ribulose-phosphate 3-epimerase
cj0654c		1.57480315	probable transmembrane transport protein pseudogene
cj0179	*exbB1*	1.569858713	biopolymer transport protein
cj0820c	*fliP*	1.567398119	probable flagellar biosynthesis protein
cj1684c		1.567398119	probable transmembrane transport protein
cj0309c		1.564945227	probable efflux protein
cj1169c		1.560062402	probable periplasmic protein
cj0500		1.560062402	probable ATP/GTP binding protein
cj0837c		1.560062402	unknown
cj1028c	*ctsW*	1.557632399	possible purine/pyrimidine phosphoribosyltransferase/involved in natural transformation (Wiesner *et al.*, 2003)
cj1552c		1.557632399	unknown
cj0453	*thiC*	1.557632399	probable thiamin biosynthesis protein
cj0852c		1.557632399	possible integral membrane protein
cj0005c		1.550387597	possible molybdenum containing oxidoreductase
cj1089c		1.550387597	unknown
cj0253		1.547987616	unknown
cj0890c		1.545595054	probable sensory transduction transcriptional regulator, response regulator receiver domain/response regulator involved in oxidative stress resistance (reviewed in (Murphy *et al.*, 2006))
cj0851c		1.543209877	probable integral membrane protein
cj0827	*truA*	1.543209877	probable tRNA pseudouridine synthase
cj1379	*selB*	1.543209877	probable selenocysteine-specific elongation factor
cj1278c		1.540832049	unknown
cj1629	*exbD2*	1.538461538	probable exbD/tolR family transport protein
cj0305c		1.529051988	unknown
cj1032	*cmeE*	1.529051988	possible membrane fusion component of efflux system
cj0560		1.526717557	probable integral membrane protein

cj0889c		1.526717557	probable sensory transduction histidine kinase/histidine kinase involved in oxidative stress resistance (reviewed in (Murphy *et al.*, 2006))
cj1649		1.526717557	probable lipoprotein
cj1717c	*leuC*	1.522070015	probable 3-isopropylmalate dehydratase large subunit
cj1277c		1.522070015	probable ABC transporter ATP-binding protein
cj0353c		1.522070015	probable phosphatase
cj0736		1.519756839	unknown
cj0905c	*alr*	1.519756839	probable alanine racemase
cj0243c		1.517450683	unknown
cj0378c		1.515151515	probable integral membrane protein
cj1546		1.515151515	unknown
cj0619		1.515151515	probable integral membrane protein
cj0250c		1.510574018	probable transmembrane transport protein
cj0585	*folP*	1.510574018	probable dihydropteroate synthase
cj1260c	*dnaJ*	1.503759398	probable chaperone
cj0099	*birA*	1.503759398	possible biotin--[acetyl-CoA-carboxylase] synthetase
cj1457c		1.501501502	unknown

[a]orf id's in this table and all subsequent tables are taken from *C. jejuni* 11168 genome sequence (Parkhill *et al.*, 2000).
[b]*C. jejuni* 11168 gene annotations are given (Parkhill *et al.*, 2000). If more recent functional information is available, that is provided with references. This applies to this table and all subsequent microarray tables.

Table 7. Genes upregulated in the Δ*cetA* mutant compared to wildtype

orf id	gene name	fold-induction	annotation/updated functional information
cj1199		3.494	probable iron/ascorbate-dependent oxidoreductase
cj1200		3.446	probable periplasmic protein
cj0569		3.16	unknown
cj0681		2.89	unknown
cj1201	*metE*	2.757	probable 5-methyltetrahydropteroyltriglutamate--homocysteine methyltransferase
cj0491	*rpsL*	2.092	30S ribosomal protein S12
cj0425		2.042	probable periplasmic protein
cj0781	*napG*	2.032	probable ferredoxin
cj1611	*rpsT*	2.024	probable 30S ribosomal protein S20
cj0347	*trpF*	2.003	probable N-(5'-phosphoribosyl)anthranilate isomerase
cj0225		1.989	probable acetyltransferase
cj0348	*trpB*	1.964	probable tryptophan synthase beta chain
cj0739		1.945	unknown
cj0482	*uxaA'*	1.898	possible altronate hydrolase N-terminus
cj0331c		1.895	unknown
cj0156c		1.887	unknown
cj1513c		1.868	possible periplasmic protein
cj0748		1.862	unknown
cj0180	*exbD1*	1.859	biopolymer transport protein
cj0913c	*hupB*	1.858	DNA-binding protein HU homologue
cj1083c		1.84	possible nuclease
cj0771c		1.798	probable periplasmic protein
cj1727c	*metY*	1.797	possible O-acetylhomoserine (thiol)-lyase
cj1520		1.766	unknown/removed from new annotation due to presence of CRISPR sequences (Gundogdu *et al.*, 2007)
cj1138		1.764	probable galactosyltransferase
cj0926		1.762	possible membrane protein
cj1265c	*hydC*	1.762	probable Ni/Fe-hydrogenase B-type cytochrome subunit
cj0874c		1.749	possible cytochrome C
cj0073c		1.734	unknown
cj0876c		1.723	probable periplasmic protein
cj1186c	*petA*	1.715	probable ubiquinol-cytochrome C reductase iron-sulfur subunit
cj0922c	*pebC*	1.694	probable ABC-type amino-acid transporter ATP-binding protein/component of PEB1 aspartate and glutamate ABC transporter (Leon-Kempis Mdel *et al.*, 2006)
cj1488c	*ccoQ*	1.687	cb-type cytochrome C oxidase subunit IV
cj0450c	*rpmB*	1.686	50S ribosomal protein L28
cj0770c		1.679	probable periplasmic protein
cj0345	*trpE*	1.671	possible anthranilate synthase component I
cj1115c		1.668	probable membrane protein
cj0346	*trpD*	1.664	probable anthranilate synthase component II
cj1294	*pseC*	1.662	probable aminotransferase/involved in flagella glycosylation (Obhi and Creuzenet, 2005)
cj0095	*rpmA*	1.662	50S ribosomal protein L27
cj0537	*oorB*	1.655	probable OORB subunit of 2-oxoglutarate:acceptor

			oxidoreductase
cj0226	*argB*	1.647	probable acetylglutamate kinase
cj1185c	*petB*	1.638	probable ubiquinol-cytochrome C reductase cytochrome B subunit
cj1339c	*flaA*	1.632	flagellin A
cj0512	*purC*	1.631	probable phosphoribosylaminoimidazole-succinocarboxamide synthase
cj1267c	*hydA*	1.627	probable Ni/Fe-hydrogenase small subunit
cj1087c		1.626	possible periplasmic protein
cj0448c		1.625	probable MCP-type signal transduction protein
cj1056c		1.609	unknown
cj0536	*oorA*	1.608	probable OORA subunit of 2-oxoglutarate:acceptor oxidoreductase
cj0526c	*fliE*	1.604	probable flagellar hook-basal body complex protein
cj0265c		1.603	probable cytochrome C-type heme-binding periplasmic protein
cj0459c		1.585	unknown
cj0274	*lpxA*	1.581	probable acyl-[acyl-carrier-protein]--UDP-N-acetylglucosamine O-acyltransferase
cj1337		1.58	unknown
cj1500		1.57	probable integral membrane protein
cj1063		1.562	possible acetyltransferase
cj0422c		1.561	unknown
cj1690c	*rpsE*	1.558	30S ribosomal protein S5
cj1505c		1.556	unknown
cj0621		1.549	unknown
cj0476	*rplJ*	1.544	probable 50S ribosomal protein L10
cj1290c	*accC*	1.543	probable biotin carboxylase (subunit of acetyl-CoA carboxylase (EC 6.4.1.2))
cj1338c	*flaB*	1.542	flagellin B
cj0588	*tlyA*	1.54	possible hemolysin
cj1595	*rpoA*	1.54	probable DNA-directed RNA polymerase alpha chain
cj0012c		1.54	non-heme iron protein
cj0933c	*pycB*	1.536	possible pyruvate carboxylase B subunit
cj1696c	*rplX*	1.529	50S ribosomal protein L24
cj0409	*frdA*	1.528	probable fumarate reductase flavoprotein subunit
cj0980		1.523	possible peptidase,
cj0437	*sdhA*	1.523	probable succinate dehydrogenase flavoprotein subunit
cj0408	*frdC*	1.519	probable fumarate reductase cytochrome B subunit
cj1639		1.517	unknown/involved in iron-sulfur cluster biogenesis (Reid *et al.*, 2008a)
cj1698	*rpsQ*	1.507	30S ribosomal protein S17
cj0566		1.505	unknown
cj1668		1.502	probable periplasmic protein

Table 8. Genes downregulated in the Δ*cetB* mutant compared to wildtype

orf id	gene name	fold-decrease	annotation/updated functional information
cj0975		7.462686567	probable outer-membrane protein
cj1614	*chuA*	5.376344086	hemin uptake system outer membrane receptor
cj0046		5.208333333	probable transmembrane transport protein pseudogene
cj1615	*chuB*	4.95049505	probable hemin uptake system permease protein
cj0793	*flgS*	4.608294931	probable signal transduction histidine kinase/σ^{54}-dependent two-component system kinase (Hendrixson and DiRita, 2003; Wosten *et al.*, 2004)
cj0999c		4.081632653	probable integral membrane protein
cj0246c		3.521126761	probable MCP-domain signal transduction protein
cj1385	*katA*	3.460207612	catalase
cj0741		3.367003367	unknown
cj1582c		3.095975232	probable peptide ABC-transport system permease protein
cj0580c		3.039513678	probable oxidoreductase
cj0727		3.03030303	probable periplasmic solute-binding protein
cj1211		2.93255132	probable integral membrane protein, 33.9% identity to HP1361 (called competence locus E (comE3))
cj0291c	*glpT'*	2.93255132	glycerol-3-phosphate transporter, possible pseudogene
cj1467		2.915451895	unknown
cj0041	*fliK*	2.865329513	unknown/flagella hook length control gene (Kamal *et al.*, 2007)
cj1471c	*ctsE*	2.857142857	probable type II protein secretion system E protein/involved in natural transformation (Wiesner *et al.*, 2003)
cj0243c		2.824858757	unknown
cj0937		2.645502646	probable integral membrane protein
cj0613	*pstS*	2.564102564	possible periplasmic phosphate binding protein
cj1669c		2.557544757	probable ATP-dependent DNA ligase
cj0334	*ahpC*	2.469135802	probable alkyl hydroperoxide reductase
cj1613c	*chuZ*	2.469135802	unknown/heme oxygenase (Ridley *et al.*, 2006)
cj1389	*dcuC*	2.444987775	probable transmembrane transport protein pseudogene/involved in efflux of succinate (Hofreuter *et al.*, 2006)
cj1039	*murG*	2.433090024	possible UDP-N-acetylglucosamine--N-acetylmuramyl-(pentapeptide) pyrophosphoryl-undecaprenol N-acetylglucosamine transferase
cj1555c		2.415458937	unknown
cj1453c		2.398081535	unknown
cj1586	*cgb*	2.392344498	probable bacterial hemoglobin/single domain globin involved in nitrosative stress response (Elvers *et al.*, 2004)
cj1581c		2.386634845	probable peptide ABC-transport system ATP-binding protein
cj0174c		2.358490566	possible iron-uptake ABC transport system permease protein
cj0792		2.352941176	unknown
cj1617	*chuD*	2.352941176	probable hemin uptake system periplasmic hemin-binding protein
cj0428		2.331002331	unknown
cj0563		2.325581395	unknown
cj0616	*pstB*	2.325581395	probable phosphate transport ATP-binding protein
cj1530		2.320185615	probable ATP/GTP-binding protein
cj1393	*metC'*	2.304147465	probable cystathionine beta-lyase
cj0058		2.304147465	possible periplasmic protein

cj1000		2.288329519	probable transcriptional regulator, LysR family
cj0571		2.283105023	possible transcriptional regulator, DeoR family
cj1283	*ktrB*	2.283105023	probable K+ uptake protein
cj0629	*capA*	2.232142857	possible lipoprotein/autotransporter involved in adherence (Ashgar *et al.*, 2007)
cj1551c		2.222222222	probable type I restriction enzyme S protein
cj1676	*murB*	2.222222222	possible UDP-N-acetylenolpyruvoylglucosamine reductase
cj0057		2.197802198	possible periplasmic protein
cj0262c	*docC*	2.197802198	probable methyl-accepting chemotaxis signal transduction protein
cj1040c		2.192982456	probable transmembrane transport protein
cj0716		2.178649237	probable phospho-2-dehydro-3-deoxyheptonate aldolase
cj1169c		2.178649237	probable periplasmic protein
cj1618c		2.164502165	unknown
cj0849c		2.164502165	unknown
cj0263	*zupT*	2.127659574	probable integral membrane protein/metal permease (Weingarten *et al.*, 2008)
cj1275c		2.118644068	probable periplasmic protein
cj0523		2.114164905	possible membrane protein, may be fragment of pseudogene
cj0861c	*pabA*	2.109704641	probable para-aminobenzoate synthase glutamine amidotransferase component II
cj0850c		2.074688797	transmembrane transport protein
cj1587c		2.057613169	probable ABC transporter
cj1394		2.057613169	probable fumarate lyase
cj1268c		2.040816327	unknown
cj0495		2.036659878	unknown
cj0692c		2.032520325	possible membrane protein
cj0620		2.008032129	unknown
cj0715		1.976284585	transthyretin-like periplasmic protein
cj1622	*ribD*	1.968503937	probable riboflavin-specific deaminase
cj1254		1.960784314	unknown
cj0289c	*peb3*	1.953125	major antigenic peptide
cj1095		1.949317739	probable integral membrane protein
cj0524		1.937984496	unknown
cj0593		1.915708812	probable integral membrane protein
cj1729c	*flgE2*	1.912045889	probable flagellar hook subunit protein
cj1113		1.908396947	unknown
cj0736		1.883239171	unknown
cj1373		1.872659176	probable integral membrane protein
cj0353c		1.834862385	probable phosphatase
cj0198c		1.824817518	unknown
cj0175c		1.821493625	possible iron-uptake ABC transport system periplasmic iron-binding protein
cj0340		1.811594203	possible nucleoside hydrolase
cj1025c	*flgQ*	1.811594203	Unknown/flagella-associated protein with unknown function (Sommerlad and Hendrixson, 2007)
cj1263	*recR*	1.805054152	probable recombination protein
cj1381		1.798561151	probable lipoprotein
cj0500		1.788908766	probable ATP/GTP binding protein
cj0762c	*aspB*	1.788908766	probable aspartate aminotransferase

cj1650		1.776198934	unknown
cj1344c		1.773049645	probable glycoprotease
cj1646	*iamB*	1.766784452	possible ABC transport system permease protein
cj0557c		1.757469244	probable integral membrane protein
cj1548c		1.754385965	probable type I restriction enzyme R protein
cj0888c		1.754385965	ABC transport system ATP-binding protein
cj1716c	*leuD*	1.751313485	probable 3-isopropylmalate dehydratase small subunit
cj0464	*recG*	1.742160279	probable ATP-dependent DNA helicase
cj1382c	*fldA*	1.736111111	flavodoxin
cj0323		1.724137931	unknown
cj0826		1.715265866	probable integral membrane protein
cj1563c		1.694915254	probable transcriptional regulator, MerR family
cj1560		1.683501684	probable membrane protein
cj1660		1.675041876	probable integral membrane protein
cj0444		1.669449082	probable tonB-denpendent outer membrane receptor pseudogene
cj1538c		1.666666667	possible anion-uptake ABC-transport system ATP-binding protein
cj1630	*tonB2*	1.661129568	probable tonB transport protein
cj1259	*porA*	1.658374793	major outer membrane protein (MOMP)
cj1556		1.655629139	unknown
cj1547		1.652892562	unknown
cj1509c	*fdhC*	1.650165017	probable formate dehydrogenase, cytochrome B subunit
cj1634c	*aroC*	1.650165017	probable chorismate synthase
cj1544c		1.647446458	probable integral membrane protein
cj0003	*gyrB*	1.63132137	probable DNA gyrase subunit B
cj0600		1.63132137	unknown
cj525c	*pbpB*	1.628664495	probable penicillin-binding protein
cj0043	*flgE*	1.62601626	probable flagellar hook protein
cj1651c		1.618122977	probable methionine aminopeptidase
cj1341c		1.615508885	unknown
cj0938c	*aas*	1.612903226	probable 2-acylglycerophosphoethanolamine acyltransferase / acyl-acyl carrier protein synthetase
cj0453	*thiC*	1.612903226	probable thiamin biosynthesis protein
cj1276c		1.610305958	probable integral membrane protein
cj1295		1.610305958	unknown
cj0113	*pal*	1.607717042	peptidoglycan associated lipoprotein
cj1466	*flgK*	1.607717042	possible flagellar hook-associated protein
cj0599		1.607717042	probable periplasmic protein
cj0067		1.605136437	unknown
cj1187c	*arsB*	1.602564103	possible arsenical pump membrane protein
cj1242		1.594896332	unknown
cj0548	*fliD*	1.592356688	probable flagellar hook-associated protein
cj0002	*dnaN*	1.584786054	probable DNA polymerase III
cj1369		1.582278481	probable transmembrane transport protein
cj1648		1.577287066	possible ABC transport system periplasmic substrate-binding protein
cj0698	*flgG*	1.57480315	probable flagellar basal-body rod protein
cj0946		1.572327044	probable lipoprotein

cj0313		1.572327044	probable integral membrane protein
cj1284	*ktrA*	1.569858713	probable K+ uptake protein
cj0680c	*uvrB*	1.569858713	probable excinuclease ABC subunit B
cj0082	*cioB*	1.567398119	probable cytochrome bd oxidase subunit II/cyanide independent oxidase, not cytochrome bd type (Jackson *et al.*, 2007)
cj1713		1.557632399	unknown
cj1474c	*ctsD*	1.552795031	probable type II protein secretion system D protein/involved in natural transformation (Wiesner *et al.*, 2003)
cj1532		1.547987616	possible periplasmic protein
cj0862c	*pabB*	1.547987616	probable para-aminobenzoate synthase component I
cj0024	*nrdA*	1.547987616	ribonucleoside-diphosphate reductase alpha chain
cj0948c		1.547987616	possible transmembrane transport protein
cj1481c		1.545595054	possible helicase
cj0099	*birA*	1.538461538	possible biotin--[acetyl-CoA-carboxylase] synthetase
cj1285c		1.53609831	unknown
cj1588c		1.53609831	probable transmembrane transport protein
cj0956c	*thdF*	1.506024096	probable thiophene and furan oxidation protein
cj1663		1.503759398	probable ABC transport system ATP-binding protein
cj0589	*ribF*	1.501501502	possible riboflavin kinase/FMN adenylyltransferase

Table 9. Genes upregulated in the Δ*cetB* mutant compared to wildtype

orf id	gene name	fold-induction	annotation/updated functional information
cj1422c		4.76	possible sugar transferase
cj1199		3.65	probable iron/ascorbate-dependent oxidoreductase
cj1200		3.55	probable periplasmic protein
cj1201	*metE*	2.792	probable 5-methyltetrahydropteroyltriglutamate--homocysteine methyltransferase
cj0181	*tonB1*	2.65	possible tonB transport protein
cj0681		2.545	unknown
cj0225		2.49	probable acetyltransferase
cj0347	*trpF*	2.483	probable N-(5'-phosphoribosyl)anthranilate isomerase
cj0566		2.389	unknown
cj0007	*gltB*	2.293	probable glutamate synthase (NADPH) large subunit
cj0348	*trpB*	2.271	probable tryptophan synthase beta chain
cj0874c		2.155	possible cytochrome C
cj0987c		2.151	probable integral membrane protein
cj1727c	*metY*	2.136	possible O-acetylhomoserine (thiol)-lyase
cj1087c		2.132	possible periplasmic protein
cj1004		2.052	probable periplasmic protein
cj0425		2.046	probable periplasmic protein
cj0818		2.013	probable lipoprotein
cj0226	*argB*	1.881	probable acetylglutamate kinase
cj1188c	*gidA*	1.879	glucose inhibited division protein A homologue
cj1229	*cbpA*	1.874	probable curved-DNA binding protein
cj0770c		1.871	probable periplasmic protein
cj0922c	*pebC*	1.869	probable ABC-type amino-acid transporter ATP-binding protein/component of PEB1 aspartate and glutamate ABC transporter (Leon-Kempis Mdel *et al.*, 2006)
cj0345	*trpE*	1.858	possible anthranilate synthase component I
cj1265c	*hydC*	1.805	probable Ni/Fe-hydrogenase B-type cytochrome subunit
cj1138		1.791	probable galactosyltransferase
cj1726c	*metA*	1.787	probable homoserine O-succinyltransferase
cj1139c	*wlaN*	1.772	probable galactosyltransferase/involved in los biosynthesis, phase variable (Linton *et al.*, 2000)
cj1600	*hisH*	1.757	probable amidotransferase
cj0423		1.747	probable integral membrane protein
cj1029c	*mapA*	1.746	probable lipoprotein
cj0264c		1.735	probable molybdopterin-containing oxidoreductase/TMAO and DMSO reductase (Hofreuter *et al.*, 2006)
cj0685c		1.725	possible sugar transferase
cj0346	*trpD*	1.716	probable anthranilate synthase component II
cj0576	*lpxD*	1.709	probable UDP-3-O-[3-hydroxymyristoyl] glucosamine N-acyltransferase
cj0239c	*nifU*	1.68	nifU protein homologue/scaffold for iron-sulphur cluster assembly (Reid *et al.*, 2008a)
cj1682c	*gltA*	1.677	probable citrate synthase
cj0757	*hrcA*	1.676	possible heat shock regulator
cj0552		1.67	unknown

cj0771c		1.663	probable periplasmic protein
cj0491	*rpsL*	1.658	30S ribosomal protein S12
cj0448c		1.651	probable MCP-type signal transduction protein
cj0511		1.649	probable secreted protease
cj1294	*pseC*	1.642	probable aminotransferase/involved in flagella glycosylation (Obhi and Creuzenet, 2005)
cj1488c	*ccoQ*	1.64	cb-type cytochrome C oxidase subunit IV
cj1513c		1.64	possible periplasmic protein
cj0265c		1.636	probable cytochrome C-type heme-binding periplasmic protein
cj0883c		1.633	unknown
cj0626	*hypE*	1.63	probable hydrogenase isoenzymes formation protein
cj0251c		1.629	highly acidic protein
cj1680c		1.628	probable periplasmic protein
cj0169	*sodB*	1.623	superoxide dismutase (Fe)
cj1267c	*hydA*	1.622	probable Ni/Fe-hydrogenase small subunit
cj0330c	*rpmF*	1.619	probable 50S ribosomal protein L32
cj0781	*napG*	1.597	probable ferredoxin
cj0873c		1.593	unknown
cj1342c		1.593	unknown
cj1690c	*rpsE*	1.593	30S ribosomal protein S5
cj0369c		1.588	ferredoxin domain-containing integral membrane protein
cj0140		1.585	unknown
cj0536	*oorA*	1.579	probable OORA subunit of 2-oxoglutarate:acceptor oxidoreductase
cj1122c	*wlaJ*	1.572	possible integral membrane protein
cj0935c		1.572	probable transmembrane transport protein
cj0496		1.572	unknown
cj0854c		1.567	probable periplasmic protein/cytochrome c signature motif (Reid *et al.*, 2008b)
cj1008c	*aroB*	1.566	probable 3-dehydroquinate synthase
cj1424c	*gmhA2*	1.562	probable phosphoheptose isomerase/involved in capsule biosynthesis (Karlyshev *et al.*, 2005a)
cj0157c		1.562	probable integral membrane protein
cj1674		1.561	unknown
cj0252	*moaC*	1.561	probable molybdenum cofactor biosynthesis protein C
cj1115c		1.559	probable membrane protein
cj0766c	*tmk*	1.55	probable thymidylate kinase
cj0408	*frdC*	1.547	probable fumarate reductase cytochrome B subunit
cj0274	*lpxA*	1.54	probable acyl-[acyl-carrier-protein]--UDP-N-acetylglucosamine O-acyltransferase
cj0224	*argC*	1.539	probable N-acetyl-gamma-glutamyl-phosphate reductase
cj1116c	*ftsH*	1.534	probable membrane bound zinc metallopeptidase
cj1266c	*hydB*	1.531	probable Ni/Fe-hydrogenase large subunit
cj1132c	*wlaA*	1.52	unknown/los biosynthesis (Bernatchez *et al.*, 2005)
cj1245c		1.515	possible membrane protein
cj0944c		1.514	probable periplasmic protein
cj0782	*napH*	1.512	probable ferredoxin
cj0066c	*aroQ*	1.51	probable 3-dehydroquinate dehydratase
cj1274c	*pyrH*	1.506	probable uridylate kinase

cj0128c		1.506	unknown
cj0689	*ackA*	1.505	probable acetate kinase
cj0839c		1.504	unknown

Table 10. Genes downregulated in the Δ*cetB* mutant compared to the Δ*cetA* mutant

orf id	gene name	fold-decrease	annotation/updated functional information
cj0113	*pal*	3.496503497	peptidoglycan associated lipoprotein
cj1189c	*cetB*	3.194888179	possible signal-transduction sensor protein
cj0569		2.72479564	unknown
cj1448c	*kpsM*	2.34741784	probable capsule polysaccharide export system inner membrane protein
cj1522c		2.34741784	unknown
cj0041	*fliK*	2.277904328	unknown/flagella hook length control gene (Kamal *et al.*, 2007)
cj1380		2.267573696	probable periplasmic protein
cj0043	*flgE*	2.247191011	probable flagellar hook protein
cj0698	*flgG*	2.2172949	probable flagellar basal-body rod protein
cj1331	*ptmB/neuA3*	2.183406114	probable acylneuraminate cytidylyltransferase (CMP-N-acetylneuraminic acid synthetase)/involved in flagella glycosylation (Karlyshev *et al.*, 2002)
cj0716		2.145922747	probable phospho-2-dehydro-3-deoxyheptonate aldolase
cj1650		2.123142251	unknown
cj1729c	*flgE2*	2.087682672	probable flagellar hook subunit protein
cj1463		2.079002079	unknown
cj0428		2.036659878	unknown
cj0334	*ahpC*	1.984126984	probable alkyl hydroperoxide reductase
cj1242		1.949317739	unknown
cj1462	*flgI*	1.904761905	probable flagellar P-ring protein
cj0887c	*flaD*	1.901140684	possible flagellin
cj0793	*flgS*	1.879699248	probable signal transduction histidine kinase/σ^{54}-dependent two-component system kinase (Hendrixson and DiRita, 2003; Wosten *et al.*, 2004)
cj1466	*flgK*	1.876172608	possible flagellar hook-associated protein
cj0243c		1.872659176	unknown
cj0095	*rpmA*	1.848428835	50S ribosomal protein L27
cj1656c		1.779359431	unknown
cj1184c	*petC*	1.748251748	possible ubiquinol-cytochrome C reductase cytochrome C subunit
cj0589	*ribF*	1.745200698	possible riboflavin kinase/FMN adenylyltransferase
cj0913c	*hupB*	1.736111111	DNA-binding protein HU homologue
cj1357c	*nrfA*	1.733102253	probable periplasmic cytochrome C/putative nitrate reductase (Pittman *et al.*, 2007)
cj1259	*porA*	1.703577513	major outer membrane protein (MOMP)
cj0697	*flgG2*	1.694915254	probable flagellar basal-body rod protein
cj1056c		1.655629139	unknown
cj0331c		1.650165017	unknown
cj0577c	*queA*	1.647446458	probable S-adenosylmethionine:tRNA ribosyltransferase-isomerase
cj0002	*dnaN*	1.628664495	probable DNA polymerase III
cj0584		1.62601626	unknown
cj0223		1.615508885	probable pseudogene, similar to several members of the IgA protease/hemaglutinin/sepA family
cj0727		1.577287066	probable periplasmic solute-binding protein

cj0118		1.567398119	unknown
cj0147c	*trxA*	1.5625	thioredoxin
cj0687c	*flgH*	1.555209953	probable flagellar L-ring protein precursor
cj1369		1.540832049	probable transmembrane transport protein
cj1344c		1.533742331	probable glycoprotease
cj0391c		1.529051988	unknown
cj0578c	*tatC*	1.524390244	probable sec-independent protein translocase/component of twin-arginine translocase system (Hofreuter *et al.*, 2006)
cj0982c		1.510574018	probable amino-acid transporter periplasmic solute-binding protein
cj0547	*flaG*	1.508295626	possible flagellar protein

Table 11. Genes upregulated in the Δ*cetB* mutant compared to the Δ*cetA* mutant

orf id	gene name	fold-induction	annotation/updated functional information
cj1190c	*cetA*	16.07	probable MCP-domain signal transduction protein
cj1422c		3.312	possible sugar transferase
cj1722c		3.142	unknown
cj0618		2.259	unknown
cj0987c		2.216	probable integral membrane protein
cj1617	*chuD*	2.098	probable hemin uptake system periplasmic hemin-binding protein
cj0007	*gltB*	1.964	probable glutamate synthase (NADPH) large subunit
cj0181	*tonB1*	1.956	possible tonB transport protein
cj0370	*rpsU*	1.873	30S ribosomal protein S21
cj0699c	*glnA*	1.833	probable glutamine synthetase
cj1678	*capB*	1.804	possible lipoprotein/putative autotransporter (Ashgar *et al.*, 2007)
cj1188c	*gidA*	1.801	glucose inhibited division protein A homologue
cj1472c	*ctsX*	1.743	probable membrane protein/involved in natural transformation (Wiesner *et al.*, 2003)
cj0301c	*modB*	1.726	probable molybdenum transport system permease protein
cj1004		1.704	probable periplasmic protein
cj1584c		1.663	probable peptide ABC-transport system periplasmic peptide-binding protein
cj0818		1.639	probable lipoprotein
cj0566		1.565	unknown
cj1583c		1.542	probable peptide ABC-transport system permease protein
cj0496		1.536	unknown
cj1413c		1.532	possible polysaccharide modification protein/located in capsule biosynthesis locus (Gundogdu *et al.*, 2007)
cj1679		1.521	unknown
cj0239	*nifU*	1.52	nifU protein homologue

allowed us to test whether the changes in gene expression we saw in the Δ*cetA* and Δ*cetB* mutants were present in other motility and chemotaxis mutants. For these experiments, cultures of wildtype, Δ*cetA*, Δ*cetB*, Δ*cetAB*, *cheY::solo* (non-chemotactic) and Δ*rpoN* (non-motile) were grown biphasically in MH media under microaerophilic conditions for 48 hours. The cells were collected by centrifugation and RNA isolated as described in Chapter II. cDNA was generated using random primers (Invitrogen) and MMLV reverse transcriptase (Invitrogen). Primers 19-21bp in length were designed for qPCR to have a Tm of 56°C ± 1.07°C and to produce 200bp fragments of the gene of interest (Table 12). Amounts of PCR product produced after each cycle during qPCR were monitored using SYBR green (Stratagene). *rpoA*, which encodes the housekeeping σ-factor σ^{70}, was used to normalize qPCR data for each gene and fold-expression compared to wildtype was calculated for each mutant strain. qPCR reactions were preformed in triplicate with the mean and (where indicated) standard deviation reported.

We chose to test the expression of two genes involved in iron transport, *chuA* and *chuD*, which were downregulated in Δ*cetA* and Δ*cetB* compared to wildtype, according to our microarray data. *chuD* was also upregulated in the Δ*cetB* mutant compared to the Δ*cetA* mutant, according to our microarray data. Additionally, we tested the expression of two transcriptional regulators, *cj0571* and *cj1000*, as well as a single domain globin, *cgb*, all of which were downregulated in both the Δ*cetA* and Δ*cetB* mutants compared to wildtype in our microarray experiments. Finally, we tested the expression of *pal*, which encodes a peptidoglycan-associated lipoprotein, as this gene was the most highly downregulated in the Δ*cetB* mutant compared to the Δ*cetA* mutant in our microarray experiments. The results of these experiments are shown in Figure 25.

Table 12. Primers used for qRT-PCR

Primer #	Gene target	Sequence
AB001	*chuA*	GGA TTC AAA TTT ACG CAA TG
AB002	*chuA*	TAA TAG CAT GCC CAT CAA TC
AB003	*cgb*	AGC AAT GGC GAT TTT AAT G
AB004	*cgb*	AAG CAA CTT CCC AAG CTT TA
AB005	*cj1000*	ATT TTT GGC AAG ATG ATG AAC
AB006	*cj1000*	CGC AGC CAT TCT ATC AAG T
AB007	*pal*	TTC AAA TCG TGG TTC AGG T
AB008	*pal*	CGC AGT TTC CTT CAA CAG TA
AB011	*cj0571*	GCC AAA TCA AAC CTT ACA AAC
AB012	*cj0571*	CAC TTC TTT GCT TTC TCC AA
AB013	*rpoA*	TGC TTA TAC GCC AAC AGA AT
AB014	*rpoA*	TAC CAC GCA TGC TAT CAA AT
AB027	*chuD*	AAC CTC AAA ACT TAC AAG CGT A
AB028	*chuD*	TTT GGC CTA AGG TTG TGA TA

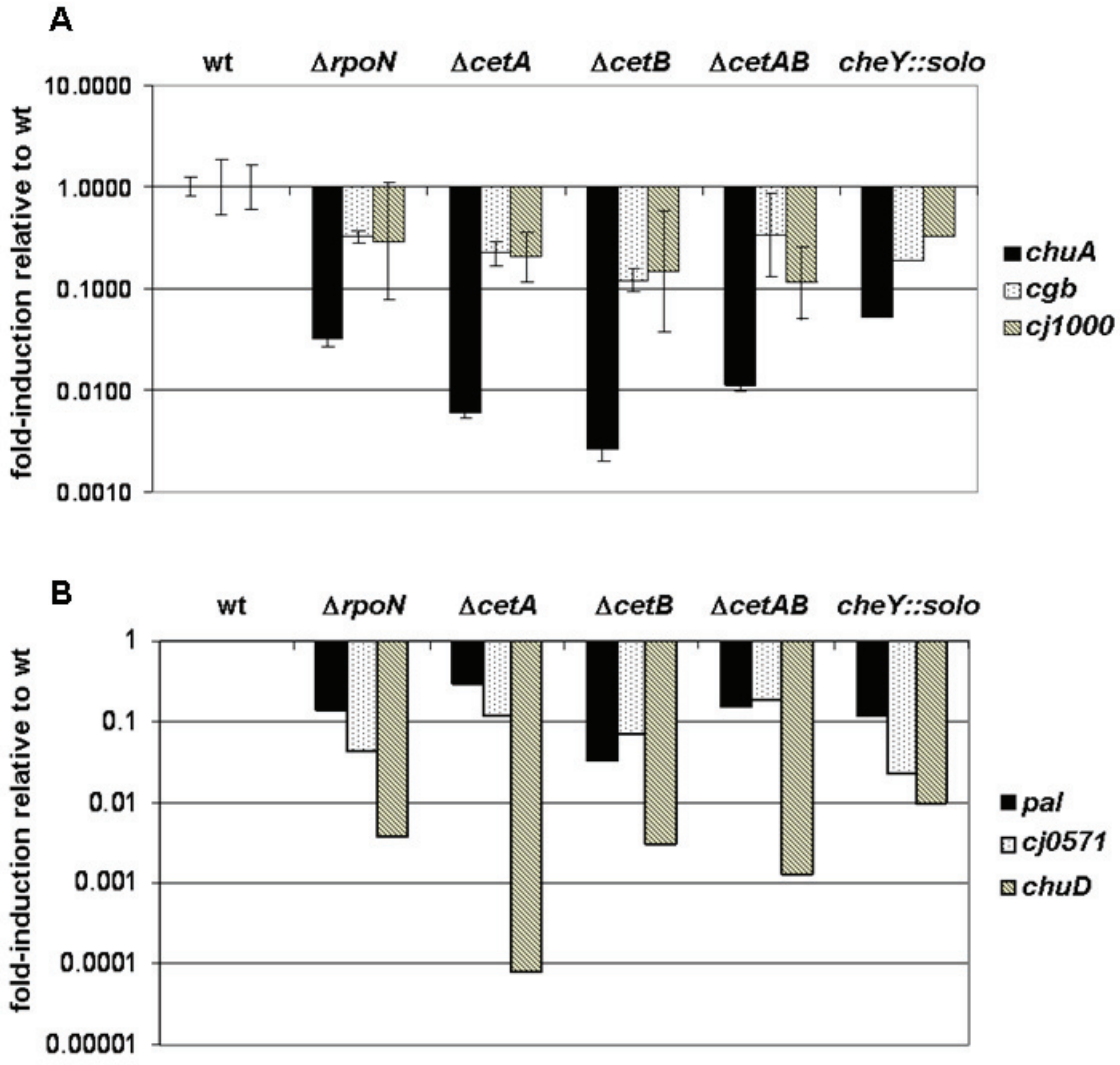

Figure 25. qRT-PCR analysis of gene expression in energy taxis, chemotaxis and motility mutants. qRT-PCR was used to assess the expression of genes found to be up- or down-regulated in the Δ*cetA* or Δ*cetB* mutants by microarray analysis. Fold-induction relative to wildtype in Δ*rpoN* (non-motile), Δ*cetA*, Δ*cetB*, Δ*cetAB* and *cheY::solo* (non-chemotactic) is reported. **A.** qRT-PCR analysis of *chuA*, *cgb* and *cj1000* expression. **B.** qRT-PCR analysis of *pal*, *cj0571* and *chuD* expression.

As expected from our microarray data, all of these genes were downregulated in the Δ*cetA* and Δ*cetB* mutants, as well as the Δ*cetAB* mutant compared to wildtype. In addition, *chuD* expression was higher in the Δ*cetB* mutant than the Δ*cetA* mutant, also supporting our microarray observations. The difference in pal expression between Δ*cetA* and Δ*cetB*, however, is small and likely insignificant. All of the genes tested were also downregulated in the *cheY::solo* mutant (non-chemotactic) and the Δ*rpoN* mutant (non-motile). While there are some differences in the extent of downregulation of these genes in each of the mutants tested, it is clear that the same trends predominate in the non-chemotactic and non-motile mutants tested as in the Δ*cetA* and Δ*cetB* mutants.

These data led us to conclude that many, if not all, of the changes in gene expression observed in the Δ*cetA* and Δ*cetB* mutants in our microarray experiments are likely due to the mutants' defects in energy taxis, as opposed to more direct changes in gene regulation. Specifically, cells lacking the ability to swim away from an energy poor environment, whether due to a defect in the CetA/CetB system or a more general defect in chemotaxis or motility, will find themselves experiencing a similar environment and will alter their gene expression accordingly. If correct, this would imply that CetA/CetB-mediated energy taxis is a major determinant of the *C. jejuni* local environment *in vitro*. Whether this is true under other culture conditions or *in vivo* remains to be seen. While there may still be differences in gene expression observed in our microarrays that are *cetA*-specific and/or *cetB*-specific, we have no convincing evidence that this will be the case based on our qRT-PCR analysis.

REFERENCES

AbuOun, M., Manning, G., Cawthraw, S.A., Ridley, A., Ahmed, I.H., Wassenaar, T.M., and Newell, D.G. (2005) Cytolethal distending toxin (CDT)-negative Campylobacter jejuni strains and anti-CDT neutralizing antibodies are induced during human infection but not during colonization in chickens. *Infect Immun* **73**: 3053-3062.

Alexander, R.P., and Zhulin, I.B. (2007) Evolutionary genomics reveals conserved structural determinants of signaling and adaptation in microbial chemoreceptors. *Proc Natl Acad Sci U S A* **104**: 2885-2890.

Alexandre, G., Greer, S.E., and Zhulin, I.B. (2000) Energy taxis is the dominant behavior in Azospirillum brasilense. *J Bacteriol* **182**: 6042-6048.

Alexandre, G., and Zhulin, I.B. (2001) More than one way to sense chemicals. *J Bacteriol* **183**: 4681-4686.

Alexandre, G., Greer-Phillips, S., and Zhulin, I.B. (2004) Ecological role of energy taxis in microorganisms. *FEMS Microbiol Rev* **28**: 113-126.

Altschul, S.F., Madden, T.L., Schaffer, A.A., Zhang, J., Zhang, Z., Miller, W., and Lipman, D.J. (1997) Gapped BLAST and PSI-BLAST: a new generation of protein database search programs. *Nucleic Acids Res* **25**: 3389-3402.

Amin, D.N., Taylor, B.L., and Johnson, M.S. (2006) Topology and boundaries of the aerotaxis receptor Aer in the membrane of Escherichia coli. *J Bacteriol* **188**: 894-901.

Amin, D.N., Taylor, B.L., and Johnson, M.S. (2007) Organization of the aerotaxis receptor aer in the membrane of Escherichia coli. *J Bacteriol* **189**: 7206-7212.

Andersen-Nissen, E., Smith, K.D., Strobe, K.L., Barrett, S.L., Cookson, B.T., Logan, S.M., and Aderem, A. (2005) Evasion of Toll-like receptor 5 by flagellated bacteria. *Proc Natl Acad Sci U S A* **102**: 9247-9252.

Ansell, R., Granath, K., Hohmann, S., Thevelein, J.M., and Adler, L. (1997) The two isoenzymes for yeast NAD+-dependent glycerol 3-phosphate dehydrogenase encoded by GPD1 and GPD2 have distinct roles in osmoadaptation and redox regulation. *Embo J* **16**: 2179-2187.

Appleman, J.A., Chen, L.L., and Stewart, V. (2003) Probing conservation of HAMP linker structure and signal transduction mechanism through analysis of hybrid sensor kinases. *J Bacteriol* **185**: 4872-4882.

Appleman, J.A., and Stewart, V. (2003) Mutational analysis of a conserved signal-transducing element: the HAMP linker of the Escherichia coli nitrate sensor NarX. *J Bacteriol* **185**: 89-97.

Aravind, L., and Ponting, C.P. (1999) The cytoplasmic helical linker domain of receptor histidine kinase and methyl-accepting proteins is common to many prokaryotic signalling proteins. *FEMS Microbiol Lett* **176**: 111-116.

Armitage, J. (2006) Bacterial behavior. In *The prokaryotes: a handbook on the biology of bacteria*. Vol. 2: Ecophysiology and Biochemistry. Dworkin, M., Falkow, S., Rosenberg, E., Schleifer, K. and Stackebrandt, E. (eds). New York, NY: Springer Science and Business Media, LLC, pp. 102-139.

Armitage, J.P. (2003) Taxing questions in development. *Trends Microbiol* **11**: 239-242.

Ashgar, S.S., Oldfield, N.J., Wooldridge, K.G., Jones, M.A., Irving, G.J., Turner, D.P., and Ala'Aldeen, D.A. (2007) CapA, an autotransporter protein of Campylobacter jejuni, mediates association with human epithelial cells and colonization of the chicken gut. *J Bacteriol* **189**: 1856-1865.

Avrain, L., Vernozy-Rozand, C., and Kempf, I. (2004) Evidence for natural horizontal transfer of tetO gene between Campylobacter jejuni strains in chickens. *J Appl Microbiol* **97**: 134-140.

Bachtiar, B.M., Coloe, P.J., and Fry, B.N. (2007) Knockout mutagenesis of the kpsE gene of Campylobacter jejuni 81116 and its involvement in bacterium-host interactions. *FEMS Immunol Med Microbiol* **49**: 149-154.

Bacon, D.J., Alm, R.A., Burr, D.H., Hu, L., Kopecko, D.J., Ewing, C.P., Trust, T.J., and Guerry, P. (2000) Involvement of a plasmid in virulence of Campylobacter jejuni 81-176. *Infect Immun* **68**: 4384-4390.

Bacon, D.J., Szymanski, C.M., Burr, D.H., Silver, R.P., Alm, R.A., and Guerry, P. (2001) A phase-variable capsule is involved in virulence of Campylobacter jejuni 81-176. *Mol Microbiol* **40**: 769-777.

Bacon, D.J., Alm, R.A., Hu, L., Hickey, T.E., Ewing, C.P., Batchelor, R.A., Trust, T.J., and Guerry, P. (2002) DNA sequence and mutational analyses of the pVir plasmid of Campylobacter jejuni 81-176. *Infect Immun* **70**: 6242-6250.

Baker, M.D., Wolanin, P.M., and Stock, J.B. (2006) Signal transduction in bacterial chemotaxis. *Bioessays* **28**: 9-22.

Baker, N.A., Sept, D., Joseph, S., Holst, M.J., and McCammon, J.A. (2001) Electrostatics of nanosystems: application to microtubules and the ribosome. *Proc Natl Acad Sci U S A* **98**: 10037-10041.

Barak, R., Yan, J., Shainskaya, A., and Eisenbach, M. (2006) The chemotaxis response regulator CheY can catalyze its own acetylation. *J Mol Biol* **359**: 251-265.

Barnes, I.H., Bagnall, M.C., Browning, D.D., Thompson, S.A., Manning, G., and Newell, D.G. (2007) Gamma-glutamyl transpeptidase has a role in the persistent colonization of the avian gut by Campylobacter jejuni. *Microb Pathog* **43**: 198-207.

Bazylinski, D.A., and Frankel, R.B. (2004) Magnetosome formation in prokaryotes. *Nat Rev Microbiol* **2**: 217-230.

Beliaev, A.S., Klingeman, D.M., Klappenbach, J.A., Wu, L., Romine, M.F., Tiedje, J.M., Nealson, K.H., Fredrickson, J.K., and Zhou, J. (2005) Global transcriptome analysis of Shewanella oneidensis MR-1 exposed to different terminal electron acceptors. *J Bacteriol* **187**: 7138-7145.

Benach, J., Swaminathan, S.S., Tamayo, R., Handelman, S.K., Folta-Stogniew, E., Ramos, J.E., Forouhar, F., Neely, H., Seetharaman, J., Camilli, A., and Hunt, J.F.

(2007) The structural basis of cyclic diguanylate signal transduction by PilZ domains. *Embo J* **26**: 5153-5166.
Berleman, J.E., Hasselbring, B.M., and Bauer, C.E. (2004) Hypercyst mutants in Rhodospirillum centenum identify regulatory loci involved in cyst cell differentiation. *J Bacteriol* **186**: 5834-5841.
Berleman, J.E., and Bauer, C.E. (2005) A che-like signal transduction cascade involved in controlling flagella biosynthesis in Rhodospirillum centenum. *Mol Microbiol* **55**: 1390-1402.
Bernatchez, S., Szymanski, C.M., Ishiyama, N., Li, J., Jarrell, H.C., Lau, P.C., Berghuis, A.M., Young, N.M., and Wakarchuk, W.W. (2005) A single bifunctional UDP-GlcNAc/Glc 4-epimerase supports the synthesis of three cell surface glycoconjugates in Campylobacter jejuni. *J Biol Chem* **280**: 4792-4802.
Bespalov, V.A., Zhulin, I.B., and Taylor, B.L. (1996) Behavioral responses of Escherichia coli to changes in redox potential. *Proc Natl Acad Sci U S A* **93**: 10084-10089.
Bibikov, S.I., Biran, R., Rudd, K.E., and Parkinson, J.S. (1997) A signal transducer for aerotaxis in Escherichia coli. *J Bacteriol* **179**: 4075-4079.
Bibikov, S.I., Barnes, L.A., Gitin, Y., and Parkinson, J.S. (2000) Domain organization and flavin adenine dinucleotide-binding determinants in the aerotaxis signal transducer Aer of Escherichia coli. *Proc Natl Acad Sci U S A* **97**: 5830-5835.
Bibikov, S.I., Miller, A.C., Gosink, K.K., and Parkinson, J.S. (2004) Methylation-independent aerotaxis mediated by the Escherichia coli Aer protein. *J Bacteriol* **186**: 3730-3737.
Biswas, D., Itoh, K., and Sasakawa, C. (2000) Uptake pathways of clinical and healthy animal isolates of Campylobacter jejuni into INT-407 cells. *FEMS Immunol Med Microbiol* **29**: 203-211.
Biswas, D., Itoh, K., and Sasakawa, C. (2003) Role of microfilaments and microtubules in the invasion of INT-407 cells by Campylobacter jejuni. *Microbiol Immunol* **47**: 469-473.
Biswas, D., Niwa, H., and Itoh, K. (2004) Infection with Campylobacter jejuni induces tyrosine-phosphorylated proteins into INT-407 cells. *Microbiol Immunol* **48**: 221-228.
Biswas, D., Fernando, U., Reiman, C., Willson, P., Potter, A., and Allan, B. (2006) Effect of cytolethal distending toxin of Campylobacter jejuni on adhesion and internalization in cultured cells and in colonization of the chicken gut. *Avian Dis* **50**: 586-593.
Blank, T.E., and Donnenberg, M.S. (2001) Novel topology of BfpE, a cytoplasmic membrane protein required for type IV fimbrial biogenesis in enteropathogenic Escherichia coli. *J Bacteriol* **183**: 4435-4450.
Blaser, M.J., Taylor, D.N., and Feldman, R.A. (1983) Epidemiology of Campylobacter jejuni infections. *Epidemiol Rev* **5**: 157-176.
Boin, M.A., and Hase, C.C. (2007) Characterization of Vibrio cholerae aerotaxis. *FEMS Microbiol Lett* **276**: 193-201.
Borel, A.C., and Simon, S.M. (1996) Biogenesis of polytopic membrane proteins: membrane segments assemble within translocation channels prior to membrane integration. *Cell* **85**: 379-389.

Boyd, D., and Beckwith, J. (1989) Positively charged amino acid residues can act as topogenic determinants in membrane proteins. *Proc Natl Acad Sci U S A* **86**: 9446-9450.

Bras, A.M., Chatterjee, S., Wren, B.W., Newell, D.G., and Ketley, J.M. (1999) A novel Campylobacter jejuni two-component regulatory system important for temperature-dependent growth and colonization. *J Bacteriol* **181**: 3298-3302.

Brunger, A.T., Adams, P.D., Clore, G.M., DeLano, W.L., Gros, P., Grosse-Kunstleve, R.W., Jiang, J.S., Kuszewski, J., Nilges, M., Pannu, N.S., Read, R.J., Rice, L.M., Simonson, T., and Warren, G.L. (1998) Crystallography & NMR system: A new software suite for macromolecular structure determination. *Acta Crystallogr D Biol Crystallogr* **54**: 905-921.

Burkart, M., Toguchi, A., and Harshey, R.M. (1998) The chemotaxis system, but not chemotaxis, is essential for swarming motility in Escherichia coli. *Proc Natl Acad Sci U S A* **95**: 2568-2573.

Buron-Barral, M.C., Gosink, K.K., and Parkinson, J.S. (2006) Loss- and gain-of-function mutations in the F1-HAMP region of the Escherichia coli aerotaxis transducer Aer. *J Bacteriol* **188**: 3477-3486.

Butler, S.L., and Falke, J.J. (1998) Cysteine and disulfide scanning reveals two amphiphilic helices in the linker region of the aspartate chemoreceptor. *Biochemistry* **37**: 10746-10756.

Byrne, C.M., Clyne, M., and Bourke, B. (2007) Campylobacter jejuni adhere to and invade chicken intestinal epithelial cells in vitro. *Microbiology* **153**: 561-569.

Candon, H.L., Allan, B.J., Fraley, C.D., and Gaynor, E.C. (2007) Polyphosphate kinase 1 is a pathogenesis determinant in Campylobacter jejuni. *J Bacteriol* **189**: 8099-8108.

Carrillo, C.D., Taboada, E., Nash, J.H., Lanthier, P., Kelly, J., Lau, P.C., Verhulp, R., Mykytczuk, O., Sy, J., Findlay, W.A., Amoako, K., Gomis, S., Willson, P., Austin, J.W., Potter, A., Babiuk, L., Allan, B., and Szymanski, C.M. (2004) Genome-wide expression analyses of Campylobacter jejuni NCTC11168 reveals coordinate regulation of motility and virulence by flhA. *J Biol Chem* **279**: 20327-20338.

Chao, X., Muff, T.J., Park, S.Y., Zhang, S., Pollard, A.M., Ordal, G.W., Bilwes, A.M., and Crane, B.R. (2006) A receptor-modifying deamidase in complex with a signaling phosphatase reveals reciprocal regulation. *Cell* **124**: 561-571.

Chenna, R., Sugawara, H., Koike, T., Lopez, R., Gibson, T.J., Higgins, D.G., and Thompson, J.D. (2003) Multiple sequence alignment with the Clustal series of programs. *Nucleic Acids Res* **31**: 3497-3500.

Chervitz, S.A., and Falke, J.J. (1996) Molecular mechanism of transmembrane signaling by the aspartate receptor: a model. *Proc Natl Acad Sci U S A* **93**: 2545-2550.

Chou, W.K., Dick, S., Wakarchuk, W.W., and Tanner, M.E. (2005) Identification and characterization of NeuB3 from Campylobacter jejuni as a pseudaminic acid synthase. *J Biol Chem* **280**: 35922-35928.

Clancy, M., Madill, K.A., and Wood, J.M. (1981) Genetic and biochemical requirements for chemotaxis to L-proline in Escherichia coli. *J Bacteriol* **146**: 902-906.

Clayton, R.K. (1958) On the interplay of environmental factors affecting taxis and motility in Rhodospirillum rubrum. *Arch Mikrobiol* **29**: 189-212.

Cohen-Ben-Lulu, G.N., Francis, N.R., Shimoni, E., Noy, D., Davidov, Y., Prasad, K., Sagi, Y., Cecchini, G., Johnstone, R.M., and Eisenbach, M. (2008) The bacterial flagellar switch complex is getting more complex. *Embo J*.

Cohn, M.T., Ingmer, H., Mulholland, F., Jorgensen, K., Wells, J.M., and Brondsted, L. (2007) Contribution of conserved ATP-dependent proteases of Campylobacter jejuni to stress tolerance and virulence. *Appl Environ Microbiol* **73**: 7803-7813.

Colegio, O.R., Griffin, T.J.t., Grindley, N.D., and Galan, J.E. (2001) In vitro transposition system for efficient generation of random mutants of Campylobacter jejuni. *J Bacteriol* **183**: 2384-2388.

Cortes-Bratti, X., Chaves-Olarte, E., Lagergard, T., and Thelestam, M. (2000) Cellular internalization of cytolethal distending toxin from Haemophilus ducreyi. *Infect Immun* **68**: 6903-6911.

Crawford, J.A., Krukonis, E.S., and DiRita, V.J. (2003) Membrane localization of the ToxR winged-helix domain is required for TcpP-mediated virulence gene activation in Vibrio cholerae. *Mol Microbiol* **47**: 1459-1473.

Crews, S.T. (2003) *PAS proteins: regulators and sensors of development and physiology.* Boston, MA: Kluwer Academic Publishers.

Cserzo, M., Wallin, E., Simon, I., von Heijne, G., and Elofsson, A. (1997) Prediction of transmembrane alpha-helices in prokaryotic membrane proteins: the dense alignment surface method. *Protein Eng* **10**: 673-676.

Cuff, J.A., and Barton, G.J. (2000) Application of multiple sequence alignment profiles to improve protein secondary structure prediction. *Proteins* **40**: 502-511.

de Boer, P., Wagenaar, J.A., Achterberg, R.P., van Putten, J.P., Schouls, L.M., and Duim, B. (2002) Generation of Campylobacter jejuni genetic diversity in vivo. *Mol Microbiol* **44**: 351-359.

del Campo, A.M., Ballado, T., de la Mora, J., Poggio, S., Camarena, L., and Dreyfus, G. (2007) Chemotactic control of the two flagellar systems of Rhodobacter sphaeroides is mediated by different sets of CheY and FliM proteins. *J Bacteriol* **189**: 8397-8401.

DeLano, W.L. (2002) The PyMOL Molecular Graphics System

Dorrell, N., Mangan, J.A., Laing, K.G., Hinds, J., Linton, D., Al-Ghusein, H., Barrell, B.G., Parkhill, J., Stoker, N.G., Karlyshev, A.V., Butcher, P.D., and Wren, B.W. (2001) Whole genome comparison of Campylobacter jejuni human isolates using a low-cost microarray reveals extensive genetic diversity. *Genome Res* **11**: 1706-1715.

Edwards, J.C., Johnson, M.S., and Taylor, B.L. (2006) Differentiation between electron transport sensing and proton motive force sensing by the Aer and Tsr receptors for aerotaxis. *Mol Microbiol* **62**: 823-837.

Elvers, K.T., Wu, G., Gilberthorpe, N.J., Poole, R.K., and Park, S.F. (2004) Role of an inducible single-domain hemoglobin in mediating resistance to nitric oxide and nitrosative stress in Campylobacter jejuni and Campylobacter coli. *J Bacteriol* **186**: 5332-5341.

Elwell, C.A., and Dreyfus, L.A. (2000) DNase I homologous residues in CdtB are critical for cytolethal distending toxin-mediated cell cycle arrest. *Mol Microbiol* **37**: 952-963.

Falke, J.J., and Hazelbauer, G.L. (2001) Transmembrane signaling in bacterial chemoreceptors. *Trends Biochem Sci* **26**: 257-265.

Fernando, U., Biswas, D., Allan, B., Willson, P., and Potter, A.A. (2007) Influence of Campylobacter jejuni fliA, rpoN and flgK genes on colonization of the chicken gut. *Int J Food Microbiol* **118**: 194-200.

Figurski, D.H., and Helinski, D.R. (1979) Replication of an origin-containing derivative of plasmid RK2 dependent on a plasmid function provided in trans. *Proc Natl Acad Sci U S A* **76**: 1648-1652.

Finlay, B.B. (2005) Bacterial virulence strategies that utilize Rho GTPases. *Curr Top Microbiol Immunol* **291**: 1-10.

Foodnet (2007) Preliminary FoodNet data on the incidence of infection with pathogens transmitted commonly through food--10 states, 2006. *MMWR Morb Mortal Wkly Rep* **56**: 336-339.

Fouts, D.E., Mongodin, E.F., Mandrell, R.E., Miller, W.G., Rasko, D.A., Ravel, J., Brinkac, L.M., DeBoy, R.T., Parker, C.T., Daugherty, S.C., Dodson, R.J., Durkin, A.S., Madupu, R., Sullivan, S.A., Shetty, J.U., Ayodeji, M.A., Shvartsbeyn, A., Schatz, M.C., Badger, J.H., Fraser, C.M., and Nelson, K.E. (2005) Major structural differences and novel potential virulence mechanisms from the genomes of multiple campylobacter species. *PLoS Biol* **3**: e15.

Fox, J.G., Rogers, A.B., Whary, M.T., Ge, Z., Taylor, N.S., Xu, S., Horwitz, B.H., and Erdman, S.E. (2004) Gastroenteritis in NF-kappaB-deficient mice is produced with wild-type Camplyobacter jejuni but not with C. jejuni lacking cytolethal distending toxin despite persistent colonization with both strains. *Infect Immun* **72**: 1116-1125.

Froshauer, S., Green, G.N., Boyd, D., McGovern, K., and Beckwith, J. (1988) Genetic analysis of the membrane insertion and topology of MalF, a cytoplasmic membrane protein of Escherichia coli. *J Mol Biol* **200**: 501-511.

Fry, B.N., Feng, S., Chen, Y.Y., Newell, D.G., Coloe, P.J., and Korolik, V. (2000) The galE gene of Campylobacter jejuni is involved in lipopolysaccharide synthesis and virulence. *Infect Immun* **68**: 2594-2601.

Frye, J., Karlinsey, J.E., Felise, H.R., Marzolf, B., Dowidar, N., McClelland, M., and Hughes, K.T. (2006) Identification of new flagellar genes of Salmonella enterica serovar Typhimurium. *J Bacteriol* **188**: 2233-2243.

Fu, R., Wall, J.D., and Voordouw, G. (1994) DcrA, a c-type heme-containing methyl-accepting protein from Desulfovibrio vulgaris Hildenborough, senses the oxygen concentration or redox potential of the environment. *J Bacteriol* **176**: 344-350.

Fu, R., and Voordouw, G. (1997) Targeted gene-replacement mutagenesis of dcrA, encoding an oxygen sensor of the sulfate-reducing bacterium Desulfovibrio vulgaris Hildenborough. *Microbiology* **143 (Pt 6)**: 1815-1826.

Fukuda, Y., Okamura, Y., Takeyama, H., and Matsunaga, T. (2006) Dynamic analysis of a genomic island in Magnetospirillum sp. strain AMB-1 reveals how magnetosome synthesis developed. *FEBS Lett* **580**: 801-812.

Gaynor, E.C., Wells, D.H., MacKichan, J.K., and Falkow, S. (2005) The Campylobacter jejuni stringent response controls specific stress survival and virulence-associated phenotypes. *Mol Microbiol* **56**: 8-27.

Ge, Z., Feng, Y., Whary, M.T., Nambiar, P.R., Xu, S., Ng, V., Taylor, N.S., and Fox, J.G. (2005) Cytolethal distending toxin is essential for Helicobacter hepaticus colonization in outbred Swiss Webster mice. *Infect Immun* **73**: 3559-3567.

Georgiou, C.D., Dueweke, T.J., and Gennis, R.B. (1988) Beta-galactosidase gene fusions as probes for the cytoplasmic regions of subunits I and II of the membrane-bound cytochrome d terminal oxidase from Escherichia coli. *J Biol Chem* **263**: 13130-13137.

Gilbert, M., Karwaski, M.F., Bernatchez, S., Young, N.M., Taboada, E., Michniewicz, J., Cunningham, A.M., and Wakarchuk, W.W. (2002) The genetic bases for the variation in the lipo-oligosaccharide of the mucosal pathogen, Campylobacter jejuni. Biosynthesis of sialylated ganglioside mimics in the core oligosaccharide. *J Biol Chem* **277**: 327-337.

Gilbert, M., Mandrell, R.E., Parker, C.T., Li, J., and Vinogradov, E. (2007) Structural Analysis of the Capsular Polysaccharide from Campylobacter jejuni RM1221. *Chembiochem* **8**: 625-631.

Gilmore, R., and Blobel, G. (1985) Translocation of secretory proteins across the microsomal membrane occurs through an environment accessible to aqueous perturbants. *Cell* **42**: 497-505.

Glover, K.J., Weerapana, E., and Imperiali, B. (2005a) In vitro assembly of the undecaprenylpyrophosphate-linked heptasaccharide for prokaryotic N-linked glycosylation. *Proc Natl Acad Sci U S A* **102**: 14255-14259.

Glover, K.J., Weerapana, E., Numao, S., and Imperiali, B. (2005b) Chemoenzymatic synthesis of glycopeptides with PglB, a bacterial oligosaccharyl transferase from Campylobacter jejuni. *Chem Biol* **12**: 1311-1315.

Glover, K.J., Weerapana, E., Chen, M.M., and Imperiali, B. (2006) Direct biochemical evidence for the utilization of UDP-bacillosamine by PglC, an essential glycosyl-1-phosphate transferase in the Campylobacter jejuni N-linked glycosylation pathway. *Biochemistry* **45**: 5343-5350.

Golden, N.J., Camilli, A., and Acheson, D.W. (2000) Random transposon mutagenesis of Campylobacter jejuni. *Infect Immun* **68**: 5450-5453.

Golden, N.J., and Acheson, D.W. (2002) Identification of motility and autoagglutination Campylobacter jejuni mutants by random transposon mutagenesis. *Infect Immun* **70**: 1761-1771.

Goon, S., Kelly, J.F., Logan, S.M., Ewing, C.P., and Guerry, P. (2003) Pseudaminic acid, the major modification on Campylobacter flagellin, is synthesized via the Cj1293 gene. *Mol Microbiol* **50**: 659-671.

Goon, S., Ewing, C.P., Lorenzo, M., Pattarini, D., Majam, G., and Guerry, P. (2006) A sigma28-regulated nonflagella gene contributes to virulence of Campylobacter jejuni 81-176. *Infect Immun* **74**: 769-772.

Gosink, K.K., Buron-Barral, M.C., and Parkinson, J.S. (2006) Signaling interactions between the aerotaxis transducer Aer and heterologous chemoreceptors in Escherichia coli. *J Bacteriol* **188**: 3487-3493.

Gott, P., and Boos, W. (1988) The transmembrane topology of the sn-glycerol-3-phosphate permease of Escherichia coli analysed by phoA and lacZ protein fusions. *Mol Microbiol* **2**: 655-663.

Grant, A.J., Coward, C., Jones, M.A., Woodall, C.A., Barrow, P.A., and Maskell, D.J. (2005) Signature-tagged transposon mutagenesis studies demonstrate the dynamic nature of cecal colonization of 2-week-old chickens by Campylobacter jejuni. *Appl Environ Microbiol* **71**: 8031-8041.

Greer-Phillips, S.E., Alexandre, G., Taylor, B.L., and Zhulin, I.B. (2003) Aer and Tsr guide Escherichia coli in spatial gradients of oxidizable substrates. *Microbiology* **149**: 2661-2667.

Greer-Phillips, S.E., Stephens, B.B., and Alexandre, G. (2004) An energy taxis transducer promotes root colonization by Azospirillum brasilense. *J Bacteriol* **186**: 6595-6604.

Gu, R., Su, C.C., Shi, F., Li, M., McDermott, G., Zhang, Q., and Yu, E.W. (2007) Crystal structure of the transcriptional regulator CmeR from Campylobacter jejuni. *J Mol Biol* **372**: 583-593.

Guerry, P., Yao, R., Alm, R.A., Burr, D.H., and Trust, T.J. (1994) Systems of experimental genetics for Campylobacter species. *Methods Enzymol* **235**: 474-481.

Guerry, P., Szymanski, C.M., Prendergast, M.M., Hickey, T.E., Ewing, C.P., Pattarini, D.L., and Moran, A.P. (2002) Phase variation of Campylobacter jejuni 81-176 lipooligosaccharide affects ganglioside mimicry and invasiveness in vitro. *Infect Immun* **70**: 787-793.

Guerry, P., Ewing, C.P., Schirm, M., Lorenzo, M., Kelly, J., Pattarini, D., Majam, G., Thibault, P., and Logan, S. (2006) Changes in flagellin glycosylation affect Campylobacter autoagglutination and virulence. *Mol Microbiol* **60**: 299-311.

Guerry, P. (2007) Campylobacter flagella: not just for motility. *Trends Microbiol* **15**: 456-461.

Guerry, P., Ewing, C.P., Schoenhofen, I.C., and Logan, S.M. (2007) Protein glycosylation in Campylobacter jejuni: partial suppression of pglF by mutation of pseC. *J Bacteriol* **189**: 6731-6733.

Gundogdu, O., Bentley, S.D., Holden, M.T., Parkhill, J., Dorrell, N., and Wren, B.W. (2007) Re-annotation and re-analysis of the Campylobacter jejuni NCTC11168 genome sequence. *BMC Genomics* **8**: 162.

Guo, B., Wang, Y., Shi, F., Barton, Y.W., Plummer, P., Reynolds, D.L., Nettleton, D., Grinnage-Pulley, T., Lin, J., and Zhang, Q. (2008) CmeR functions as a pleiotropic regulator and is required for optimal colonization of Campylobacter jejuni in vivo. *J Bacteriol* **190**: 1879-1890.

Guvener, Z.T., Tifrea, D.F., and Harwood, C.S. (2006) Two different Pseudomonas aeruginosa chemosensory signal transduction complexes localize to cell poles and form and remould in stationary phase. *Mol Microbiol* **61**: 106-118.

Harshey, R.M. (2003) Bacterial motility on a surface: many ways to a common goal. *Annu Rev Microbiol* **57**: 249-273.

Hassane, D.C., Lee, R.B., Mendenhall, M.D., and Pickett, C.L. (2001) Cytolethal distending toxin demonstrates genotoxic activity in a yeast model. *Infect Immun* **69**: 5752-5759.

Hassane, D.C., Lee, R.B., and Pickett, C.L. (2003) Campylobacter jejuni cytolethal distending toxin promotes DNA repair responses in normal human cells. *Infect Immun* **71**: 541-545.

Hazelbauer, G.L., Falke, J.J., and Parkinson, J.S. (2008) Bacterial chemoreceptors: high-performance signaling in networked arrays. *Trends Biochem Sci* **33**: 9-19.
Hendrixson, D.R., Akerley, B.J., and DiRita, V.J. (2001) Transposon mutagenesis of Campylobacter jejuni identifies a bipartite energy taxis system required for motility. *Mol Microbiol* **40**: 214-224.
Hendrixson, D.R., and DiRita, V.J. (2003) Transcription of sigma54-dependent but not sigma28-dependent flagellar genes in Campylobacter jejuni is associated with formation of the flagellar secretory apparatus. *Mol Microbiol* **50**: 687-702.
Hendrixson, D.R., and DiRita, V.J. (2004) Identification of Campylobacter jejuni genes involved in commensal colonization of the chick gastrointestinal tract. *Mol Microbiol* **52**: 471-484.
Hendrixson, D.R. (2006) A phase-variable mechanism controlling the Campylobacter jejuni FlgR response regulator influences commensalism. *Mol Microbiol* **61**: 1646-1659.
Herrmann, S., Ma, Q., Johnson, M.S., Repik, A.V., and Taylor, B.L. (2004) PAS domain of the Aer redox sensor requires C-terminal residues for native-fold formation and flavin adenine dinucleotide binding. *J Bacteriol* **186**: 6782-6791.
Hickey, T.E., McVeigh, A.L., Scott, D.A., Michielutti, R.E., Bixby, A., Carroll, S.A., Bourgeois, A.L., and Guerry, P. (2000) Campylobacter jejuni cytolethal distending toxin mediates release of interleukin-8 from intestinal epithelial cells. *Infect Immun* **68**: 6535-6541.
Hickey, T.E., Majam, G., and Guerry, P. (2005) Intracellular survival of Campylobacter jejuni in human monocytic cells and induction of apoptotic death by cytholethal distending toxin. *Infect Immun* **73**: 5194-5197.
Hickman, J.W., Tifrea, D.F., and Harwood, C.S. (2005) A chemosensory system that regulates biofilm formation through modulation of cyclic diguanylate levels. *Proc Natl Acad Sci U S A* **102**: 14422-14427.
Hofreuter, D., Tsai, J., Watson, R.O., Novik, V., Altman, B., Benitez, M., Clark, C., Perbost, C., Jarvie, T., Du, L., and Galan, J.E. (2006) Unique features of a highly pathogenic Campylobacter jejuni strain. *Infect Immun* **74**: 4694-4707.
Hong, C.S., Kuroda, A., Ikeda, T., Takiguchi, N., Ohtake, H., and Kato, J. (2004a) The aerotaxis transducer gene aer, but not aer-2, is transcriptionally regulated by the anaerobic regulator ANR in Pseudomonas aeruginosa. *J Biosci Bioeng* **97**: 184-190.
Hong, C.S., Shitashiro, M., Kuroda, A., Ikeda, T., Takiguchi, N., Ohtake, H., and Kato, J. (2004b) Chemotaxis proteins and transducers for aerotaxis in Pseudomonas aeruginosa. *FEMS Microbiol Lett* **231**: 247-252.
Hong, C.S., Kuroda, A., Takiguchi, N., Ohtake, H., and Kato, J. (2005) Expression of Pseudomonas aeruginosa aer-2, one of two aerotaxis transducer genes, is controlled by RpoS. *J Bacteriol* **187**: 1533-1535.
Hou, S., Larsen, R.W., Boudko, D., Riley, C.W., Karatan, E., Zimmer, M., Ordal, G.W., and Alam, M. (2000) Myoglobin-like aerotaxis transducers in Archaea and Bacteria. *Nature* **403**: 540-544.
Hu, L., and Kopecko, D.J. (1999) Campylobacter jejuni 81-176 associates with microtubules and dynein during invasion of human intestinal cells. *Infect Immun* **67**: 4171-4182.

Hu, L., McDaniel, J.P., and Kopecko, D.J. (2006) Signal transduction events involved in human epithelial cell invasion by Campylobacter jejuni 81-176. *Microb Pathog* **40**: 91-100.

Hugdahl, M.B., Beery, J.T., and Doyle, M.P. (1988) Chemotactic behavior of Campylobacter jejuni. *Infect Immun* **56**: 1560-1566.

Hughes, R. (2004) Campylobacter jejuni in Guillain-Barre syndrome. *Lancet Neurol* **3**: 644.

Hugle, T., Fehrmann, F., Bieck, E., Kohara, M., Krausslich, H.G., Rice, C.M., Blum, H.E., and Moradpour, D. (2001) The hepatitis C virus nonstructural protein 4B is an integral endoplasmic reticulum membrane protein. *Virology* **284**: 70-81.

Hulko, M., Berndt, F., Gruber, M., Linder, J.U., Truffault, V., Schultz, A., Martin, J., Schultz, J.E., Lupas, A.N., and Coles, M. (2006) The HAMP domain structure implies helix rotation in transmembrane signaling. *Cell* **126**: 929-940.

Inclan, Y.F., Vlamakis, H.C., and Zusman, D.R. (2007) FrzZ, a dual CheY-like response regulator, functions as an output for the Frz chemosensory pathway of Myxococcus xanthus. *Mol Microbiol* **65**: 90-102.

Jackson, R.J., Elvers, K.T., Lee, L.J., Gidley, M.D., Wainwright, L.M., Lightfoot, J., Park, S.F., and Poole, R.K. (2007) Oxygen reactivity of both respiratory oxidases in Campylobacter jejuni: the cydAB genes encode a cyanide-resistant, low-affinity oxidase that is not of the cytochrome bd type. *J Bacteriol* **189**: 1604-1615.

Jagannathan, A., Constantinidou, C., and Penn, C.W. (2001) Roles of rpoN, fliA, and flgR in expression of flagella in Campylobacter jejuni. *J Bacteriol* **183**: 2937-2942.

Jeon, B., and Zhang, Q. (2007) Cj0011c, a periplasmic single- and double-stranded DNA-binding protein, contributes to natural transformation in Campylobacter jejuni. *J Bacteriol* **189**: 7399-7407.

Jeong, D.W., Kim, T.S., Cho, I.T., and Kim, I.Y. (2004) Modification of glycolysis affects cell sensitivity to apoptosis induced by oxidative stress and mediated by mitochondria. *Biochem Biophys Res Commun* **313**: 984-991.

Jiang, Z.Y., and Bauer, C.E. (2001) Component of the Rhodospirillum centenum photosensory apparatus with structural and functional similarity to methyl-accepting chemotaxis protein chemoreceptors. *J Bacteriol* **183**: 171-177.

Jin, S., Joe, A., Lynett, J., Hani, E.K., Sherman, P., and Chan, V.L. (2001) JlpA, a novel surface-exposed lipoprotein specific to Campylobacter jejuni, mediates adherence to host epithelial cells. *Mol Microbiol* **39**: 1225-1236.

Jin, S., Song, Y.C., Emili, A., Sherman, P.M., and Chan, V.L. (2003) JlpA of Campylobacter jejuni interacts with surface-exposed heat shock protein 90alpha and triggers signalling pathways leading to the activation of NF-kappaB and p38 MAP kinase in epithelial cells. *Cell Microbiol* **5**: 165-174.

Jones, M.A., Marston, K.L., Woodall, C.A., Maskell, D.J., Linton, D., Karlyshev, A.V., Dorrell, N., Wren, B.W., and Barrow, P.A. (2004) Adaptation of Campylobacter jejuni NCTC11168 to high-level colonization of the avian gastrointestinal tract. *Infect Immun* **72**: 3769-3776.

Jones, T.A., Zou, J.Y., Cowan, S.W., and Kjeldgaard, M. (1991) Improved methods for building protein models in electron density maps and the location of errors in these models. *Acta Crystallogr A* **47 (Pt 2)**: 110-119.

Joslin, S.N., and Hendrixson, D.R. (2008) Analysis of the Campylobacter jejuni FlgR response regulator suggests integration of diverse mechanisms to activate an NtrC-like protein. *J Bacteriol* **190**: 2422-2433.

Kakuda, T., and DiRita, V.J. (2006) Cj1496c encodes a Campylobacter jejuni glycoprotein that influences invasion of human epithelial cells and colonization of the chick gastrointestinal tract. *Infect Immun* **74**: 4715-4723.

Kalmokoff, M., Lanthier, P., Tremblay, T.L., Foss, M., Lau, P.C., Sanders, G., Austin, J., Kelly, J., and Szymanski, C.M. (2006) Proteomic analysis of Campylobacter jejuni 11168 biofilms reveals a role for the motility complex in biofilm formation. *J Bacteriol* **188**: 4312-4320.

Kamal, N., Dorrell, N., Jagannathan, A., Turner, S.M., Constantinidou, C., Studholme, D.J., Marsden, G., Hinds, J., Laing, K.G., Wren, B.W., and Penn, C.W. (2007) Deletion of a previously uncharacterized flagellar-hook-length control gene fliK modulates the sigma54-dependent regulon in Campylobacter jejuni. *Microbiology* **153**: 3099-3111.

Karatan, E., Saulmon, M.M., Bunn, M.W., and Ordal, G.W. (2001) Phosphorylation of the response regulator CheV is required for adaptation to attractants during Bacillus subtilis chemotaxis. *J Biol Chem* **276**: 43618-43626.

Karlyshev, A.V., Linton, D., Gregson, N.A., Lastovica, A.J., and Wren, B.W. (2000) Genetic and biochemical evidence of a Campylobacter jejuni capsular polysaccharide that accounts for Penner serotype specificity. *Mol Microbiol* **35**: 529-541.

Karlyshev, A.V., Linton, D., Gregson, N.A., and Wren, B.W. (2002) A novel paralogous gene family involved in phase-variable flagella-mediated motility in Campylobacter jejuni. *Microbiology* **148**: 473-480.

Karlyshev, A.V., Everest, P., Linton, D., Cawthraw, S., Newell, D.G., and Wren, B.W. (2004) The Campylobacter jejuni general glycosylation system is important for attachment to human epithelial cells and in the colonization of chicks. *Microbiology* **150**: 1957-1964.

Karlyshev, A.V., Champion, O.L., Churcher, C., Brisson, J.R., Jarrell, H.C., Gilbert, M., Brochu, D., St Michael, F., Li, J., Wakarchuk, W.W., Goodhead, I., Sanders, M., Stevens, K., White, B., Parkhill, J., Wren, B.W., and Szymanski, C.M. (2005a) Analysis of Campylobacter jejuni capsular loci reveals multiple mechanisms for the generation of structural diversity and the ability to form complex heptoses. *Mol Microbiol* **55**: 90-103.

Karlyshev, A.V., Ketley, J.M., and Wren, B.W. (2005b) The Campylobacter jejuni glycome. *FEMS Microbiol Rev* **29**: 377-390.

Kelly, J., Jarrell, H., Millar, L., Tessier, L., Fiori, L.M., Lau, P.C., Allan, B., and Szymanski, C.M. (2006) Biosynthesis of the N-linked glycan in Campylobacter jejuni and addition onto protein through block transfer. *J Bacteriol* **188**: 2427-2434.

Kentner, D., and Sourjik, V. (2006) Spatial organization of the bacterial chemotaxis system. *Curr Opin Microbiol* **9**: 619-624.

Kervella, M., Pages, J.M., Pei, Z., Grollier, G., Blaser, M.J., and Fauchere, J.L. (1993) Isolation and characterization of two Campylobacter glycine-extracted proteins that bind to HeLa cell membranes. *Infect Immun* **61**: 3440-3448.

Klare, J.P., Gordeliy, V.I., Labahn, J., Buldt, G., Steinhoff, H.J., and Engelhard, M. (2004) The archaeal sensory rhodopsin II/transducer complex: a model for transmembrane signal transfer. *FEBS Lett* **564**: 219-224.

Kojima, M., Kubo, R., Yakushi, T., Homma, M., and Kawagishi, I. (2007) The bidirectional polar and unidirectional lateral flagellar motors of Vibrio alginolyticus are controlled by a single CheY species. *Mol Microbiol* **64**: 57-67.

Komagamine, T., and Yuki, N. (2006) Ganglioside mimicry as a cause of Guillain-Barre syndrome. *CNS Neurol Disord Drug Targets* **5**: 391-400.

Konkel, M.E., and Joens, L.A. (1989) Adhesion to and invasion of HEp-2 cells by Campylobacter spp. *Infect Immun* **57**: 2984-2990.

Konkel, M.E., and Cieplak, W., Jr. (1992) Altered synthetic response of Campylobacter jejuni to cocultivation with human epithelial cells is associated with enhanced internalization. *Infect Immun* **60**: 4945-4949.

Konkel, M.E., Garvis, S.G., Tipton, S.L., Anderson, D.E., Jr., and Cieplak, W., Jr. (1997) Identification and molecular cloning of a gene encoding a fibronectin-binding protein (CadF) from Campylobacter jejuni. *Mol Microbiol* **24**: 953-963.

Konkel, M.E., Kim, B.J., Rivera-Amill, V., and Garvis, S.G. (1999a) Bacterial secreted proteins are required for the internaliztion of Campylobacter jejuni into cultured mammalian cells. *Mol Microbiol* **32**: 691-701.

Konkel, M.E., Kim, B.J., Rivera-Amill, V., and Garvis, S.G. (1999b) Identification of proteins required for the internalization of Campylobacter jejuni into cultured mammalian cells. *Adv Exp Med Biol* **473**: 215-224.

Konkel, M.E., Klena, J.D., Rivera-Amill, V., Monteville, M.R., Biswas, D., Raphael, B., and Mickelson, J. (2004) Secretion of virulence proteins from Campylobacter jejuni is dependent on a functional flagellar export apparatus. *J Bacteriol* **186**: 3296-3303.

Konkel, M.E., Christensen, J.E., Keech, A.M., Monteville, M.R., Klena, J.D., and Garvis, S.G. (2005) Identification of a fibronectin-binding domain within the Campylobacter jejuni CadF protein. *Mol Microbiol* **57**: 1022-1035.

Kopecko, D.J., Hu, L., and Zaal, K.J. (2001) Campylobacter jejuni--microtubule-dependent invasion. *Trends Microbiol* **9**: 389-396.

Kowarik, M., Numao, S., Feldman, M.F., Schulz, B.L., Callewaert, N., Kiermaier, E., Catrein, I., and Aebi, M. (2006a) N-linked glycosylation of folded proteins by the bacterial oligosaccharyltransferase. *Science* **314**: 1148-1150.

Kowarik, M., Young, N.M., Numao, S., Schulz, B.L., Hug, I., Callewaert, N., Mills, D.C., Watson, D.C., Hernandez, M., Kelly, J.F., Wacker, M., and Aebi, M. (2006b) Definition of the bacterial N-glycosylation site consensus sequence. *Embo J* **25**: 1957-1966.

Krause-Gruszczynska, M., Rohde, M., Hartig, R., Genth, H., Schmidt, G., Keo, T., Konig, W., Miller, W.G., Konkel, M.E., and Backert, S. (2007) Role of the small Rho GTPases Rac1 and Cdc42 in host cell invasion of Campylobacter jejuni. *Cell Microbiol* **9**: 2431-2444.

Kretzschmar, E., Bui, M., and Rose, J.K. (1996) Membrane association of influenza virus matrix protein does not require specific hydrophobic domains or the viral glycoproteins. *Virology* **220**: 37-45.

Kurokawa, H., Lee, D.S., Watanabe, M., Sagami, I., Mikami, B., Raman, C.S., and Shimizu, T. (2004) A redox-controlled molecular switch revealed by the crystal structure of a bacterial heme PAS sensor. *J Biol Chem* **279**: 20186-20193.

Lara-Tejero, M., and Galan, J.E. (2000) A bacterial toxin that controls cell cycle progression as a deoxyribonuclease I-like protein. *Science* **290**: 354-357.

Lara-Tejero, M., and Galan, J.E. (2001) CdtA, CdtB, and CdtC form a tripartite complex that is required for cytolethal distending toxin activity. *Infect Immun* **69**: 4358-4365.

Larimer, F.W., Chain, P., Hauser, L., Lamerdin, J., Malfatti, S., Do, L., Land, M.L., Pelletier, D.A., Beatty, J.T., Lang, A.S., Tabita, F.R., Gibson, J.L., Hanson, T.E., Bobst, C., Torres, J.L., Peres, C., Harrison, F.H., Gibson, J., and Harwood, C.S. (2004) Complete genome sequence of the metabolically versatile photosynthetic bacterium Rhodopseudomonas palustris. *Nat Biotechnol* **22**: 55-61.

Larsen, J.C., Szymanski, C., and Guerry, P. (2004) N-linked protein glycosylation is required for full competence in Campylobacter jejuni 81-176. *J Bacteriol* **186**: 6508-6514.

Laszlo, D.J., and Taylor, B.L. (1981) Aerotaxis in Salmonella typhimurium: role of electron transport. *J Bacteriol* **145**: 990-1001.

Lee, R.B., Hassane, D.C., Cottle, D.L., and Pickett, C.L. (2003) Interactions of Campylobacter jejuni cytolethal distending toxin subunits CdtA and CdtC with HeLa cells. *Infect Immun* **71**: 4883-4890.

Leon-Kempis Mdel, R., Guccione, E., Mulholland, F., Williamson, M.P., and Kelly, D.J. (2006) The Campylobacter jejuni PEB1a adhesin is an aspartate/glutamate-binding protein of an ABC transporter essential for microaerobic growth on dicarboxylic amino acids. *Mol Microbiol* **60**: 1262-1275.

Letunic, I., Copley, R.R., Schmidt, S., Ciccarelli, F.D., Doerks, T., Schultz, J., Ponting, C.P., and Bork, P. (2004) SMART 4.0: towards genomic data integration. *Nucleic Acids Res* **32**: D142-144.

Li, L., Sharipo, A., Chaves-Olarte, E., Masucci, M.G., Levitsky, V., Thelestam, M., and Frisan, T. (2002) The Haemophilus ducreyi cytolethal distending toxin activates sensors of DNA damage and repair complexes in proliferating and non-proliferating cells. *Cell Microbiol* **4**: 87-99.

Li, M., and Hazelbauer, G.L. (2004) Cellular stoichiometry of the components of the chemotaxis signaling complex. *J Bacteriol* **186**: 3687-3694.

Lin, J., Sahin, O., Michel, L.O., and Zhang, Q. (2003) Critical role of multidrug efflux pump CmeABC in bile resistance and in vivo colonization of Campylobacter jejuni. *Infect Immun* **71**: 4250-4259.

Linton, D., Gilbert, M., Hitchen, P.G., Dell, A., Morris, H.R., Wakarchuk, W.W., Gregson, N.A., and Wren, B.W. (2000) Phase variation of a beta-1,3 galactosyltransferase involved in generation of the ganglioside GM1-like lipo-oligosaccharide of Campylobacter jejuni. *Mol Microbiol* **37**: 501-514.

Linton, D., Allan, E., Karlyshev, A.V., Cronshaw, A.D., and Wren, B.W. (2002) Identification of N-acetylgalactosamine-containing glycoproteins PEB3 and CgpA in Campylobacter jejuni. *Mol Microbiol* **43**: 497-508.

Liu, X., and Parales, R.E. (2008) Chemotaxis of Escherichia coli to pyrimidines: a new role for the signal transducer tap. *J Bacteriol* **190**: 972-979.

Luo, N., Sahin, O., Lin, J., Michel, L.O., and Zhang, Q. (2003) In vivo selection of Campylobacter isolates with high levels of fluoroquinolone resistance associated with gyrA mutations and the function of the CmeABC efflux pump. *Antimicrob Agents Chemother* **47**: 390-394.

Ma, Q., Roy, F., Herrmann, S., Taylor, B.L., and Johnson, M.S. (2004) The Aer protein of Escherichia coli forms a homodimer independent of the signaling domain and flavin adenine dinucleotide binding. *J Bacteriol* **186**: 7456-7459.

Ma, Q., Johnson, M.S., and Taylor, B.L. (2005) Genetic analysis of the HAMP domain of the Aer aerotaxis sensor localizes flavin adenine dinucleotide-binding determinants to the AS-2 helix. *J Bacteriol* **187**: 193-201.

MacKichan, J.K., Gaynor, E.C., Chang, C., Cawthraw, S., Newell, D.G., Miller, J.F., and Falkow, S. (2004) The Campylobacter jejuni dccRS two-component system is required for optimal in vivo colonization but is dispensable for in vitro growth. *Mol Microbiol* **54**: 1269-1286.

Malik-Kale, P., Parker, C.T., and Konkel, M.E. (2008) Culture of Campylobacter jejuni with sodium deoxycholate induces virulence gene expression. *J Bacteriol* **190**: 2286-2297.

Mamelli, L., Pages, J.M., Konkel, M.E., and Bolla, J.M. (2006) Expression and purification of native and truncated forms of CadF, an outer membrane protein of Campylobacter. *Int J Biol Macromol* **39**: 135-140.

Manoil, C., and Beckwith, J. (1986) A genetic approach to analyzing membrane protein topology. *Science* **233**: 1403-1408.

Manoil, C. (1990) Analysis of protein localization by use of gene fusions with complementary properties. *J Bacteriol* **172**: 1035-1042.

Manoil, C. (1991) Analysis of membrane protein topology using alkaline phosphatase and beta-galactosidase gene fusions. *Methods Cell Biol* **34**: 61-75.

Mao, X., and DiRienzo, J.M. (2002) Functional studies of the recombinant subunits of a cytolethal distending holotoxin. *Cell Microbiol* **4**: 245-255.

Marchant, J., Wren, B., and Ketley, J. (2002) Exploiting genome sequence: predictions for mechanisms of Campylobacter chemotaxis. *Trends Microbiol* **10**: 155-159.

McNally, D.J., Jarrell, H.C., Li, J., Khieu, N.H., Vinogradov, E., Szymanski, C.M., and Brisson, J.R. (2005) The HS:1 serostrain of Campylobacter jejuni has a complex teichoic acid-like capsular polysaccharide with nonstoichiometric fructofuranose branches and O-methyl phosphoramidate groups. *Febs J* **272**: 4407-4422.

McNally, D.J., Hui, J.P., Aubry, A.J., Mui, K.K., Guerry, P., Brisson, J.R., Logan, S.M., and Soo, E.C. (2006a) Functional characterization of the flagellar glycosylation locus in Campylobacter jejuni 81-176 using a focused metabolomics approach. *J Biol Chem* **281**: 18489-18498.

McNally, D.J., Jarrell, H.C., Khieu, N.H., Li, J., Vinogradov, E., Whitfield, D.M., Szymanski, C.M., and Brisson, J.R. (2006b) The HS:19 serostrain of Campylobacter jejuni has a hyaluronic acid-type capsular polysaccharide with a nonstoichiometric sorbose branch and O-methyl phosphoramidate group. *Febs J* **273**: 3975-3989.

McNally, D.J., Aubry, A.J., Hui, J.P., Khieu, N.H., Whitfield, D., Ewing, C.P., Guerry, P., Brisson, J.R., Logan, S.M., and Soo, E.C. (2007) Targeted metabolomics

analysis of Campylobacter coli VC167 reveals legionaminic acid derivatives as novel flagellar glycans. *J Biol Chem* **282**: 14463-14475.
McSweeney, L.A., and Dreyfus, L.A. (2004) Nuclear localization of the Escherichia coli cytolethal distending toxin CdtB subunit. *Cell Microbiol* **6**: 447-458.
Meier, V.M., Muschler, P., and Scharf, B.E. (2007) Functional analysis of nine putative chemoreceptor proteins in Sinorhizobium meliloti. *J Bacteriol* **189**: 1816-1826.
Miller, J.B., and Koshland, D.E., Jr. (1977) Sensory electrophysiology of bacteria: relationship of the membrane potential to motility and chemotaxis in Bacillus subtilis. *Proc Natl Acad Sci U S A* **74**: 4752-4756.
Miller, J.H. (1972) *Experiments in molecular genetics*. Cold Spring Harbor, NY: Cold Spring Harbor Laboratory Press.
Minerdi, D., Fani, R., and Bonfante, P. (2002) Identification and evolutionary analysis of putative cytoplasmic mcpA-like protein in a bacterial strain living in symbiosis with a mycorrhizal fungus. *J Mol Evol* **54**: 815-824.
Monne, M., Hermansson, M., and von Heijne, G. (1999a) A turn propensity scale for transmembrane helices. *J Mol Biol* **288**: 141-145.
Monne, M., Nilsson, I., Elofsson, A., and von Heijne, G. (1999b) Turns in transmembrane helices: determination of the minimal length of a "helical hairpin" and derivation of a fine-grained turn propensity scale. *J Mol Biol* **293**: 807-814.
Monteville, M.R., and Konkel, M.E. (2002) Fibronectin-facilitated invasion of T84 eukaryotic cells by Campylobacter jejuni occurs preferentially at the basolateral cell surface. *Infect Immun* **70**: 6665-6671.
Monteville, M.R., Yoon, J.E., and Konkel, M.E. (2003) Maximal adherence and invasion of INT 407 cells by Campylobacter jejuni requires the CadF outer-membrane protein and microfilament reorganization. *Microbiology* **149**: 153-165.
Morgan, R., Kohn, S., Hwang, S.H., Hassett, D.J., and Sauer, K. (2006) BdlA, a chemotaxis regulator essential for biofilm dispersion in Pseudomonas aeruginosa. *J Bacteriol* **188**: 7335-7343.
Moukhametzianov, R., Klare, J.P., Efremov, R., Baeken, C., Goppner, A., Labahn, J., Engelhard, M., Buldt, G., and Gordeliy, V.I. (2006) Development of the signal in sensory rhodopsin and its transfer to the cognate transducer. *Nature* **440**: 115-119.
Muff, T.J., Foster, R.M., Liu, P.J., and Ordal, G.W. (2007) CheX in the three-phosphatase system of bacterial chemotaxis. *J Bacteriol* **189**: 7007-7013.
Muff, T.J., and Ordal, G.W. (2007) The CheC phosphatase regulates chemotactic adaptation through CheD. *J Biol Chem* **282**: 34120-34128.
Murphy, C., Carroll, C., and Jordan, K.N. (2006) Environmental survival mechanisms of the foodborne pathogen Campylobacter jejuni. *J Appl Microbiol* **100**: 623-632.
Myers, J.D., and Kelly, D.J. (2005) A sulphite respiration system in the chemoheterotrophic human pathogen Campylobacter jejuni. *Microbiology* **151**: 233-242.
Nachamkin, I., Yang, X.H., and Stern, N.J. (1993) Role of Campylobacter jejuni flagella as colonization factors for three-day-old chicks: analysis with flagellar mutants. *Appl Environ Microbiol* **59**: 1269-1273.
Nachamkin, I. (2002) Chronic effects of Campylobacter infection. *Microbes Infect* **4**: 399-403.

Nambu, J.R., Lewis, J.O., Wharton, K.A., Jr., and Crews, S.T. (1991) The Drosophila single-minded gene encodes a helix-loop-helix protein that acts as a master regulator of CNS midline development. *Cell* **67**: 1157-1167.

Nichols, N.N., and Harwood, C.S. (2000) An aerotaxis transducer gene from Pseudomonas putida. *FEMS Microbiol Lett* **182**: 177-183.

Nishikubo, S., Ohara, M., Ueno, Y., Ikura, M., Kurihara, H., Komatsuzawa, H., Oswald, E., and Sugai, M. (2003) An N-terminal segment of the active component of the bacterial genotoxin cytolethal distending toxin B (CDTB) directs CDTB into the nucleus. *J Biol Chem* **278**: 50671-50681.

Nita-Lazar, M., Wacker, M., Schegg, B., Amber, S., and Aebi, M. (2005) The N-X-S/T consensus sequence is required but not sufficient for bacterial N-linked protein glycosylation. *Glycobiology* **15**: 361-367.

Niwano, M., and Taylor, B.L. (1982) Novel sensory adaptation mechanism in bacterial chemotaxis to oxygen and phosphotransferase substrates. *Proc Natl Acad Sci U S A* **79**: 11-15.

Obhi, R.K., and Creuzenet, C. (2005) Biochemical characterization of the Campylobacter jejuni Cj1294, a novel UDP-4-keto-6-deoxy-GlcNAc aminotransferase that generates UDP-4-amino-4,6-dideoxy-GalNAc. *J Biol Chem* **280**: 20902-20908.

Oelschlaeger, T.A., Guerry, P., and Kopecko, D.J. (1993) Unusual microtubule-dependent endocytosis mechanisms triggered by Campylobacter jejuni and Citrobacter freundii. *Proc Natl Acad Sci U S A* **90**: 6884-6888.

Olivier, N.B., Chen, M.M., Behr, J.R., and Imperiali, B. (2006) In vitro biosynthesis of UDP-N,N'-diacetylbacillosamine by enzymes of the Campylobacter jejuni general protein glycosylation system. *Biochemistry* **45**: 13659-13669.

Oprian, D.D. (2003) Phototaxis, chemotaxis and the missing link. *Trends Biochem Sci* **28**: 167-169.

Pajaniappan, M., Hall, J.E., Cawthraw, S.A., Newell, D.G., Gaynor, E.C., Fields, J.A., Rathbun, K.M., Agee, W.A., Burns, C.M., Hall, S.J., Kelly, D.J., and Thompson, S.A. (2008) A temperature-regulated Campylobacter jejuni gluconate dehydrogenase is involved in respiration-dependent energy conservation and chicken colonization. *Mol Microbiol* **68**: 474-491.

Palyada, K., Threadgill, D., and Stintzi, A. (2004) Iron acquisition and regulation in Campylobacter jejuni. *J Bacteriol* **186**: 4714-4729.

Park, K., Choi, S., Ko, M., and Park, C. (2001) Novel sigmaF-dependent genes of Escherichia coli found using a specified promoter consensus. *FEMS Microbiol Lett* **202**: 243-250.

Parker, C.T., Horn, S.T., Gilbert, M., Miller, W.G., Woodward, D.L., and Mandrell, R.E. (2005) Comparison of Campylobacter jejuni lipooligosaccharide biosynthesis loci from a variety of sources. *J Clin Microbiol* **43**: 2771-2781.

Parkhill, J., Wren, B.W., Mungall, K., Ketley, J.M., Churcher, C., Basham, D., Chillingworth, T., Davies, R.M., Feltwell, T., Holroyd, S., Jagels, K., Karlyshev, A.V., Moule, S., Pallen, M.J., Penn, C.W., Quail, M.A., Rajandream, M.A., Rutherford, K.M., van Vliet, A.H., Whitehead, S., and Barrell, B.G. (2000) The genome sequence of the food-borne pathogen Campylobacter jejuni reveals hypervariable sequences. *Nature* **403**: 665-668.

Parkinson, J.S. (2007) Ancient chemoreceptors retain their flexibility. *Proc Natl Acad Sci U S A* **104**: 2559-2560.
Parrish, J.R., Yu, J., Liu, G., Hines, J.A., Chan, J.E., Mangiola, B.A., Zhang, H., Pacifico, S., Fotouhi, F., DiRita, V.J., Ideker, T., Andrews, P., and Finley, R.L., Jr. (2007) A proteome-wide protein interaction map for Campylobacter jejuni. *Genome Biol* **8**: R130.
Peach, M.L., Hazelbauer, G.L., and Lybrand, T.P. (2002) Modeling the transmembrane domain of bacterial chemoreceptors. *Protein Sci* **11**: 912-923.
Pei, Z., and Blaser, M.J. (1993) PEB1, the major cell-binding factor of Campylobacter jejuni, is a homolog of the binding component in gram-negative nutrient transport systems. *J Biol Chem* **268**: 18717-18725.
Pei, Z., Burucoa, C., Grignon, B., Baqar, S., Huang, X.Z., Kopecko, D.J., Bourgeois, A.L., Fauchere, J.L., and Blaser, M.J. (1998) Mutation in the peb1A locus of Campylobacter jejuni reduces interactions with epithelial cells and intestinal colonization of mice. *Infect Immun* **66**: 938-943.
Perez, E., and Stock, A.M. (2007) Characterization of the Thermotoga maritima chemotaxis methylation system that lacks pentapeptide-dependent methyltransferase CheR:MCP tethering. *Mol Microbiol* **63**: 363-378.
Pittman, M.S., Elvers, K.T., Lee, L., Jones, M.A., Poole, R.K., Park, S.F., and Kelly, D.J. (2007) Growth of Campylobacter jejuni on nitrate and nitrite: electron transport to NapA and NrfA via NrfH and distinct roles for NrfA and the globin Cgb in protection against nitrosative stress. *Mol Microbiol* **63**: 575-590.
Poly, F., Ewing, C., Goon, S., Hickey, T.E., Rockabrand, D., Majam, G., Lee, L., Phan, J., Savarino, N.J., and Guerry, P. (2007) Heterogeneity of a Campylobacter jejuni protein that is secreted through the flagellar filament. *Infect Immun* **75**: 3859-3867.
Ponting, C.P., and Aravind, L. (1997) PAS: a multifunctional domain family comes to light. *Curr Biol* **7**: R674-677.
Prasad, K., Caplan, S.R., and Eisenbach, M. (1998) Fumarate modulates bacterial flagellar rotation by lowering the free energy difference between the clockwise and counterclockwise states of the motor. *J Mol Biol* **280**: 821-828.
Pratt, J.S., Sachen, K.L., Wood, H.D., Eaton, K.A., and Young, V.B. (2006) Modulation of host immune responses by the cytolethal distending toxin of Helicobacter hepaticus. *Infect Immun* **74**: 4496-4504.
Pruss, B.M., Campbell, J.W., Van Dyk, T.K., Zhu, C., Kogan, Y., and Matsumura, P. (2003) FlhD/FlhC is a regulator of anaerobic respiration and the Entner-Doudoroff pathway through induction of the methyl-accepting chemotaxis protein Aer. *J Bacteriol* **185**: 534-543.
Purdy, D., Cawthraw, S., Dickinson, J.H., Newell, D.G., and Park, S.F. (1999) Generation of a superoxide dismutase (SOD)-deficient mutant of Campylobacter coli: evidence for the significance of SOD in Campylobacter survival and colonization. *Appl Environ Microbiol* **65**: 2540-2546.
Raczko, A.M., Bujnicki, J.M., Pawlowski, M., Godlewska, R., Lewandowska, M., and Jagusztyn-Krynicka, E.K. (2005) Characterization of new DsbB-like thiol-oxidoreductases of Campylobacter jejuni and Helicobacter pylori and

classification of the DsbB family based on phylogenomic, structural and functional criteria. *Microbiology* **151**: 219-231.
Raphael, B.H., Pereira, S., Flom, G.A., Zhang, Q., Ketley, J.M., and Konkel, M.E. (2005) The Campylobacter jejuni response regulator, CbrR, modulates sodium deoxycholate resistance and chicken colonization. *J Bacteriol* **187**: 3662-3670.
Rebbapragada, A., Johnson, M.S., Harding, G.P., Zuccarelli, A.J., Fletcher, H.M., Zhulin, I.B., and Taylor, B.L. (1997) The Aer protein and the serine chemoreceptor Tsr independently sense intracellular energy levels and transduce oxygen, redox, and energy signals for Escherichia coli behavior. *Proc Natl Acad Sci U S A* **94**: 10541-10546.
Reeser, R.J., Medler, R.T., Billington, S.J., Jost, B.H., and Joens, L.A. (2007) Characterization of Campylobacter jejuni biofilms under defined growth conditions. *Appl Environ Microbiol* **73**: 1908-1913.
Reid, A.N., Pandey, R., Palyada, K., Naikare, H., and Stintzi, A. (2008a) Identification of Campylobacter jejuni genes involved in the response to acidic pH and stomach transit. *Appl Environ Microbiol* **74**: 1583-1597.
Reid, A.N., Pandey, R., Palyada, K., Whitworth, L., Doukhanine, E., and Stintzi, A. (2008b) Identification of Campylobacter jejuni genes contributing to acid adaptation by transcriptional profiling and genome-wide mutagenesis. *Appl Environ Microbiol* **74**: 1598-1612.
Repik, A., Rebbapragada, A., Johnson, M.S., Haznedar, J.O., Zhulin, I.B., and Taylor, B.L. (2000) PAS domain residues involved in signal transduction by the Aer redox sensor of Escherichia coli. *Mol Microbiol* **36**: 806-816.
Ridley, K.A., Rock, J.D., Li, Y., and Ketley, J.M. (2006) Heme utilization in Campylobacter jejuni. *J Bacteriol* **188**: 7862-7875.
Rivera-Amill, V., Kim, B.J., Seshu, J., and Konkel, M.E. (2001) Secretion of the virulence-associated Campylobacter invasion antigens from Campylobacter jejuni requires a stimulatory signal. *J Infect Dis* **183**: 1607-1616.
Rowsell, E.H., Smith, J.M., Wolfe, A., and Taylor, B.L. (1995) CheA, CheW, and CheY are required for chemotaxis to oxygen and sugars of the phosphotransferase system in Escherichia coli. *J Bacteriol* **177**: 6011-6014.
Saidijam, M., Bettaney, K.E., Szakonyi, G., Psakis, G., Shibayama, K., Suzuki, S., Clough, J.L., Blessie, V., Abu-Bakr, A., Baumberg, S., Meuller, J., Hoyle, C.K., Palmer, S.L., Butaye, P., Walravens, K., Patching, S.G., O'Reilly, J., Rutherford, N.G., Bill, R.M., Roper, D.I., Phillips-Jones, M.K., and Henderson, P.J. (2005) Active membrane transport and receptor proteins from bacteria. *Biochem Soc Trans* **33**: 867-872.
Sambrook, J., Fritsch, E.F., and Maniatis, T. (1989) *Molecular cloning: A laboratory manual.* Cold Spring Harbor, NY: Cold Spring Harbor Laboratory Press.
Sarand, I., Osterberg, S., Holmqvist, S., Holmfeldt, P., Skarfstad, E., Parales, R.E., and Shingler, V. (2008) Metabolism-dependent taxis towards (methyl)phenols is coupled through the most abundant of three polar localized Aer-like proteins of Pseudomonas putida. *Environ Microbiol*.
Schweinitzer, T., Mizote, T., Ishikawa, N., Dudnik, A., Inatsu, S., Schreiber, S., Suerbaum, S., Aizawa, S.I., and Josenhans, C. (2008) Functional characterization

and mutagenesis of the proposed behavioral sensor TlpD of Helicobacter pylori. *J Bacteriol*.

Selbach, M., and Backert, S. (2005) Cortactin: an Achilles' heel of the actin cytoskeleton targeted by pathogens. *Trends Microbiol* **13**: 181-189.

Sert, V., Cans, C., Tasca, C., Bret-Bennis, L., Oswald, E., Ducommun, B., and De Rycke, J. (1999) The bacterial cytolethal distending toxin (CDT) triggers a G2 cell cycle checkpoint in mammalian cells without preliminary induction of DNA strand breaks. *Oncogene* **18**: 6296-6304.

Shen, W., Wei, Y., Dauk, M., Tan, Y., Taylor, D.C., Selvaraj, G., and Zou, J. (2006) Involvement of a glycerol-3-phosphate dehydrogenase in modulating the NADH/NAD+ ratio provides evidence of a mitochondrial glycerol-3-phosphate shuttle in Arabidopsis. *Plant Cell* **18**: 422-441.

Shioi, J., Tribhuwan, R.C., Berg, S.T., and Taylor, B.L. (1988) Signal transduction in chemotaxis to oxygen in Escherichia coli and Salmonella typhimurium. *J Bacteriol* **170**: 5507-5511.

Silhavy, T.J., and Beckwith, J.R. (1985) Uses of lac fusions for the study of biological problems. *Microbiol Rev* **49**: 398-418.

Singh, M., Berger, B., Kim, P.S., Berger, J.M., and Cochran, A.G. (1998) Computational learning reveals coiled coil-like motifs in histidine kinase linker domains. *Proc Natl Acad Sci U S A* **95**: 2738-2743.

Sommerlad, S.M., and Hendrixson, D.R. (2007) Analysis of the roles of FlgP and FlgQ in flagellar motility of Campylobacter jejuni. *J Bacteriol* **189**: 179-186.

Song, Y.C., Jin, S., Louie, H., Ng, D., Lau, R., Zhang, Y., Weerasekera, R., Al Rashid, S., Ward, L.A., Der, S.D., and Chan, V.L. (2004) FlaC, a protein of Campylobacter jejuni TGH9011 (ATCC43431) secreted through the flagellar apparatus, binds epithelial cells and influences cell invasion. *Mol Microbiol* **53**: 541-553.

St Michael, F., Szymanski, C.M., Li, J., Chan, K.H., Khieu, N.H., Larocque, S., Wakarchuk, W.W., Brisson, J.R., and Monteiro, M.A. (2002) The structures of the lipooligosaccharide and capsule polysaccharide of Campylobacter jejuni genome sequenced strain NCTC 11168. *Eur J Biochem* **269**: 5119-5136.

Stephens, B.B., Loar, S.N., and Alexandre, G. (2006) Role of CheB and CheR in the complex chemotactic and aerotactic pathway of Azospirillum brasilense. *J Bacteriol* **188**: 4759-4768.

Stintzi, A. (2003) Gene expression profile of Campylobacter jejuni in response to growth temperature variation. *J Bacteriol* **185**: 2009-2016.

Studdert, C.A., and Parkinson, J.S. (2005) Insights into the organization and dynamics of bacterial chemoreceptor clusters through in vivo crosslinking studies. *Proc Natl Acad Sci U S A* **102**: 15623-15628.

Swain, K.E., and Falke, J.J. (2007) Structure of the conserved HAMP domain in an intact, membrane-bound chemoreceptor: a disulfide mapping study. *Biochemistry* **46**: 13684-13695.

Szurmant, H., and Ordal, G.W. (2004) Diversity in chemotaxis mechanisms among the bacteria and archaea. *Microbiol Mol Biol Rev* **68**: 301-319.

Szymanski, C.M., King, M., Haardt, M., and Armstrong, G.D. (1995) Campylobacter jejuni motility and invasion of Caco-2 cells. *Infect Immun* **63**: 4295-4300.

Szymanski, C.M., Yao, R., Ewing, C.P., Trust, T.J., and Guerry, P. (1999) Evidence for a system of general protein glycosylation in Campylobacter jejuni. *Mol Microbiol* **32**: 1022-1030.

Szymanski, C.M., Burr, D.H., and Guerry, P. (2002) Campylobacter protein glycosylation affects host cell interactions. *Infect Immun* **70**: 2242-2244.

Szymanski, C.M., Michael, F.S., Jarrell, H.C., Li, J., Gilbert, M., Larocque, S., Vinogradov, E., and Brisson, J.R. (2003) Detection of conserved N-linked glycans and phase-variable lipooligosaccharides and capsules from campylobacter cells by mass spectrometry and high resolution magic angle spinning NMR spectroscopy. *J Biol Chem* **278**: 24509-24520.

Takata, T., Ando, T., Israel, D.A., Wassenaar, T.M., and Blaser, M.J. (2005) Role of dprA in transformation of Campylobacter jejuni. *FEMS Microbiol Lett* **252**: 161-168.

Taylor, B.L., Miller, J.B., Warrick, H.M., and Koshland, D.E., Jr. (1979) Electron acceptor taxis and blue light effect on bacterial chemotaxis. *J Bacteriol* **140**: 567-573.

Taylor, B.L. (1983) Role of proton motive force in sensory transduction in bacteria. *Annu Rev Microbiol* **37**: 551-573.

Taylor, B.L., and Zhulin, I.B. (1998) In search of higher energy: metabolism-dependent behaviour in bacteria. *Mol Microbiol* **28**: 683-690.

Taylor, B.L., and Zhulin, I.B. (1999) PAS domains: internal sensors of oxygen, redox potential, and light. *Microbiol Mol Biol Rev* **63**: 479-506.

Taylor, B.L., Zhulin, I.B., and Johnson, M.S. (1999) Aerotaxis and other energy-sensing behavior in bacteria. *Annu Rev Microbiol* **53**: 103-128.

Taylor, B.L., Rebbapragada, A., and Johnson, M.S. (2001) The FAD-PAS domain as a sensor for behavioral responses in Escherichia coli. *Antioxid Redox Signal* **3**: 867-879.

Taylor, B.L., Johnson, M.S., and Watts, K.J. (2003) Signal transduction in prokaryotic PAS domains. In *PAS proteins: regulators and sensors of development and physiology*. Crews, S.T. (ed). Boston, MA: Kluwer Academic Publishers, pp. 17-50.

Taylor, B.L. (2004) An alternative strategy for adaptation in bacterial behavior. *J Bacteriol* **186**: 3671-3673.

Taylor, B.L. (2007) Aer on the inside looking out: paradigm for a PAS-HAMP role in sensing oxygen, redox and energy. *Mol Microbiol* **65**: 1415-1424.

Taylor, B.L., Watts, K.J., and Johnson, M.S. (2007) Oxygen and redox sensing by two-component systems that regulate behavioral responses: behavioral assays and structural studies of aer using in vivo disulfide cross-linking. *Methods Enzymol* **422**: 190-232.

Terry, K., Go, A.C., and Ottemann, K.M. (2006) Proteomic mapping of a suppressor of non-chemotactic cheW mutants reveals that Helicobacter pylori contains a new chemotaxis protein. *Mol Microbiol* **61**: 871-882.

Thar, R., and Kuhl, M. (2003) Bacteria are not too small for spatial sensing of chemical gradients: an experimental evidence. *Proc Natl Acad Sci U S A* **100**: 5748-5753.

Thibault, P., Logan, S.M., Kelly, J.F., Brisson, J.R., Ewing, C.P., Trust, T.J., and Guerry, P. (2001) Identification of the carbohydrate moieties and glycosylation motifs in Campylobacter jejuni flagellin. *J Biol Chem* **276**: 34862-34870.

Thiem, S., Kentner, D., and Sourjik, V. (2007) Positioning of chemosensory clusters in E. coli and its relation to cell division. *Embo J* **26**: 1615-1623.

Thompson, J.D., Gibson, T.J., Plewniak, F., Jeanmougin, F., and Higgins, D.G. (1997) The CLUSTAL_X windows interface: flexible strategies for multiple sequence alignment aided by quality analysis tools. *Nucleic Acids Res* **25**: 4876-4882.

van Alphen, L.B., Bleumink-Pluym, N.M., Rochat, K.D., van Balkom, B.W., Wosten, M.M., and van Putten, J.P. (2008) Active migration into the subcellular space precedes Campylobacter jejuni invasion of epithelial cells. *Cell Microbiol* **10**: 53-66.

Van Deun, K., Pasmans, F., Ducatelle, R., Flahou, B., Vissenberg, K., Martel, A., Van den Broeck, W., Van Immerseel, F., and Haesebrouck, F. (2007) Colonization strategy of Campylobacter jejuni results in persistent infection of the chicken gut. *Vet Microbiol*.

Velayudhan, J., Jones, M.A., Barrow, P.A., and Kelly, D.J. (2004) L-serine catabolism via an oxygen-labile L-serine dehydratase is essential for colonization of the avian gut by Campylobacter jejuni. *Infect Immun* **72**: 260-268.

Wacker, M., Linton, D., Hitchen, P.G., Nita-Lazar, M., Haslam, S.M., North, S.J., Panico, M., Morris, H.R., Dell, A., Wren, B.W., and Aebi, M. (2002) N-linked glycosylation in Campylobacter jejuni and its functional transfer into E. coli. *Science* **298**: 1790-1793.

Wadhams, G.H., and Armitage, J.P. (2004) Making sense of it all: bacterial chemotaxis. *Nat Rev Mol Cell Biol* **5**: 1024-1037.

Wassenaar, T.M., van der Zeijst, B.A., Ayling, R., and Newell, D.G. (1993) Colonization of chicks by motility mutants of Campylobacter jejuni demonstrates the importance of flagellin A expression. *J Gen Microbiol* **139 Pt 6**: 1171-1175.

Watson, R.O., and Galan, J.E. (2008) Campylobacter jejuni survives within epithelial cells by avoiding delivery to lysosomes. *PLoS Pathog* **4**: e14.

Watts, K.J., Ma, Q., Johnson, M.S., and Taylor, B.L. (2004) Interactions between the PAS and HAMP domains of the Escherichia coli aerotaxis receptor Aer. *J Bacteriol* **186**: 7440-7449.

Watts, K.J., Johnson, M.S., and Taylor, B.L. (2006a) Minimal requirements for oxygen sensing by the aerotaxis receptor Aer. *Mol Microbiol* **59**: 1317-1326.

Watts, K.J., Sommer, K., Fry, S.L., Johnson, M.S., and Taylor, B.L. (2006b) Function of the N-terminal cap of the PAS domain in signaling by the aerotaxis receptor Aer. *J Bacteriol* **188**: 2154-2162.

Watts, K.J., Johnson, M.S., and Taylor, B.L. (2008a) Structure-Function Relationships in the HAMP and Proximal Signaling Domains of the Aerotaxis Receptor Aer. *J Bacteriol*.

Watts, K.J., Johnson, M.S., and Taylor, B.L. (2008b) Structure-Function Relationships in the HAMP and Proximal Signaling Domains of the Aerotaxis Receptor Aer. *J Bacteriol* **190**: 2118-2127.

Weerapana, E., Glover, K.J., Chen, M.M., and Imperiali, B. (2005) Investigating bacterial N-linked glycosylation: synthesis and glycosyl acceptor activity of the

undecaprenyl pyrophosphate-linked bacillosamine. *J Am Chem Soc* **127**: 13766-13767.

Weiner, M.P., Costa, G.L., Schoettlin, W., Cline, J., Mathur, E., and Bauer, J.C. (1994) Site-directed mutagenesis of double-stranded DNA by the polymerase chain reaction. *Gene* **151**: 119-123.

Weingarten, R.A., Grimes, J.L., and Olson, J.W. (2008) Role of Campylobacter jejuni respiratory oxidases and reductases in host colonization. *Appl Environ Microbiol* **74**: 1367-1375.

Whitchurch, C.B., Leech, A.J., Young, M.D., Kennedy, D., Sargent, J.L., Bertrand, J.J., Semmler, A.B., Mellick, A.S., Martin, P.R., Alm, R.A., Hobbs, M., Beatson, S.A., Huang, B., Nguyen, L., Commolli, J.C., Engel, J.N., Darzins, A., and Mattick, J.S. (2004) Characterization of a complex chemosensory signal transduction system which controls twitching motility in Pseudomonas aeruginosa. *Mol Microbiol* **52**: 873-893.

Whitehouse, C.A., Balbo, P.B., Pesci, E.C., Cottle, D.L., Mirabito, P.M., and Pickett, C.L. (1998) Campylobacter jejuni cytolethal distending toxin causes a G2-phase cell cycle block. *Infect Immun* **66**: 1934-1940.

Wiesner, R.S., Hendrixson, D.R., and DiRita, V.J. (2003) Natural transformation of Campylobacter jejuni requires components of a type II secretion system. *J Bacteriol* **185**: 5408-5418.

Wilson, D.L., Bell, J.A., Young, V.B., Wilder, S.R., Mansfield, L.S., and Linz, J.E. (2003) Variation of the natural transformation frequency of Campylobacter jejuni in liquid shake culture. *Microbiology* **149**: 3603-3615.

Woodall, C.A., Jones, M.A., Barrow, P.A., Hinds, J., Marsden, G.L., Kelly, D.J., Dorrell, N., Wren, B.W., and Maskell, D.J. (2005) Campylobacter jejuni gene expression in the chick cecum: evidence for adaptation to a low-oxygen environment. *Infect Immun* **73**: 5278-5285.

Woodmansee, A.N., and Imlay, J.A. (2002) Reduced flavins promote oxidative DNA damage in non-respiring Escherichia coli by delivering electrons to intracellular free iron. *J Biol Chem* **277**: 34055-34066.

Wosten, M.M., Wagenaar, J.A., and van Putten, J.P. (2004) The FlgS/FlgR two-component signal transduction system regulates the fla regulon in Campylobacter jejuni. *J Biol Chem* **279**: 16214-16222.

Wright, S., Walia, B., Parkinson, J.S., and Khan, S. (2006) Differential activation of Escherichia coli chemoreceptors by blue-light stimuli. *J Bacteriol* **188**: 3962-3971.

Yan, J., Barak, R., Liarzi, O., Shainskaya, A., and Eisenbach, M. (2008) In vivo acetylation of CheY, a response regulator in chemotaxis of Escherichia coli. *J Mol Biol* **376**: 1260-1271.

Yao, J., and Allen, C. (2007) The plant pathogen Ralstonia solanacearum needs aerotaxis for normal biofilm formation and interactions with its tomato host. *J Bacteriol* **189**: 6415-6424.

Yao, R., Alm, R.A., Trust, T.J., and Guerry, P. (1993) Construction of new Campylobacter cloning vectors and a new mutational cat cassette. *Gene* **130**: 127-130.

Yao, R., Burr, D.H., and Guerry, P. (1997) CheY-mediated modulation of Campylobacter jejuni virulence. *Mol Microbiol* **23**: 1021-1031.
Yoshioka, S., Kobayashi, K., Yoshimura, H., Uchida, T., Kitagawa, T., and Aono, S. (2005) Biophysical properties of a c-type heme in chemotaxis signal transducer protein DcrA. *Biochemistry* **44**: 15406-15413.
Young, G.M., Schmiel, D.H., and Miller, V.L. (1999) A new pathway for the secretion of virulence factors by bacteria: the flagellar export apparatus functions as a protein-secretion system. *Proc Natl Acad Sci U S A* **96**: 6456-6461.
Young, K.T., Davis, L.M., and DiRita, V.J. (2007) Campylobacter jejuni: molecular biology and pathogenesis. *Nat Rev Microbiol* **5**: 665-679.
Young, N.M., Brisson, J.R., Kelly, J., Watson, D.C., Tessier, L., Lanthier, P.H., Jarrell, H.C., Cadotte, N., St Michael, F., Aberg, E., and Szymanski, C.M. (2002) Structure of the N-linked glycan present on multiple glycoproteins in the Gram-negative bacterium, Campylobacter jejuni. *J Biol Chem* **277**: 42530-42539.
Yuki, N., and Koga, M. (2006) Bacterial infections in Guillain-Barre and Fisher syndromes. *Curr Opin Neurol* **19**: 451-457.
Yuki, N. (2007a) Campylobacter sialyltransferase gene polymorphism directs clinical features of Guillain-Barre syndrome. *J Neurochem* **103 Suppl 1**: 150-158.
Yuki, N. (2007b) Ganglioside mimicry and peripheral nerve disease. *Muscle Nerve* **35**: 691-711.
Zhong, X., Hao, B., and Chan, M.K. (2003) Structure of the PAS fold and signal transduction mechanisms. In *PAS proteins: regulators and sensors of development and physiology.* Crews, S.T. (ed). Boston, MA: Kluwer Academic Publishers, pp. 1-16.
Zhulin, I.B., Rowsell, E.H., Johnson, M.S., and Taylor, B.L. (1997) Glycerol elicits energy taxis of Escherichia coli and Salmonella typhimurium. *J Bacteriol* **179**: 3196-3201.
Ziprin, R.L., Young, C.R., Stanker, L.H., Hume, M.E., and Konkel, M.E. (1999) The absence of cecal colonization of chicks by a mutant of Campylobacter jejuni not expressing bacterial fibronectin-binding protein. *Avian Dis* **43**: 586-589.
Ziprin, R.L., Young, C.R., Byrd, J.A., Stanker, L.H., Hume, M.E., Gray, S.A., Kim, B.J., and Konkel, M.E. (2001) Role of Campylobacter jejuni potential virulence genes in cecal colonization. *Avian Dis* **45**: 549-557.
Zusman, D.R., Scott, A.E., Yang, Z., and Kirby, J.R. (2007) Chemosensory pathways, motility and development in Myxococcus xanthus. *Nat Rev Microbiol* **5**: 862-872.